Universitatea
Politehnica
Timișoara

ACTA TECHNICA CORVINIENSIS – Bulletin of Engineering

15 years ANNIVERSARY

Fascicule 2
[April–June]
Tome XV [2022]

ASSOCIATE EDITORS and
REGIONAL COLLABORATORS

The Editor and editorial board members do not receive any remuneration. These positions are voluntary. The members of the Editorial Board may serve as scientific reviewers.

We are very pleased to inform that our journal **ACTA TECHNICA CORVINIENSIS – Bulletin of Engineering** is going to complete its ten years of publication successfully. In a very short period it has acquired global presence and scholars from all over the world have taken it with great enthusiasm. We are extremely grateful and heartily acknowledge the kind of support and encouragement from you.

ACTA TECHNICA CORVINIENSIS – Bulletin of Engineering seeking qualified researchers as members of the editorial team. Like our other journals, **ACTA TECHNICA CORVINIENSIS – Bulletin of Engineering** will serve as a great resource for researchers and students across the globe. We ask you to support this initiative by joining our editorial team.

If you are interested in serving as a member of the editorial team, kindly send us your resume to redactie@fih.upt.ro.

INTERNATIONAL SCIENTIFIC COMMITTEE MEMBERS
and SCIENTIFIC REVIEWERS

MANAGER & CHAIRMAN

ROMANIA — **Imre KISS**, University Politehnica TIMISOARA, Faculty of Engineering HUNEDOARA

INTERNATIONAL SCIENTIFIC COMMITTEE MEMBERS & SCIENTIFIC REVIEWERS from:

ROMANIA
- **Viorel–Aurel ŞERBAN**, University Politehnica TIMIŞOARA – TIMIŞOARA
- **Teodor HEPUŢ**, University Politehnica TIMIŞOARA – HUNEDOARA
- **Ilare BORDEAŞU**, University Politehnica TIMIŞOARA – TIMIŞOARA
- **Liviu MARŞAVIA**, University Politehnica TIMIŞOARA – TIMIŞOARA
- **Ioan VIDA-SIMITI**, Technical University of CLUJ-NAPOCA – CLUJ-NAPOCA
- **Sorin VLASE**, "Transilvania" University of BRASOV – BRASOV
- **Horatiu TEODORESCU DRĂGHICESCU**, "Transilvania" University of BRASOV – BRASOV
- **Maria Luminiţa SCUTARU**, "Transilvania" University of BRASOV – BRASOV
- **Carmen ALIC**, University Politehnica TIMIŞOARA – HUNEDOARA
- **Sorin DEACONU**, University Politehnica TIMIŞOARA – HUNEDOARA
- **Liviu MIHON**, University Politehnica TIMIŞOARA – TIMIŞOARA

SLOVAKIA
- **Ervin LUMNITZER**, Technical University of KOŠICE – KOŠICE
- **Miroslav BADIDA**, Technical University of KOŠICE – KOŠICE
- **Karol VELIŠEK**, Slovak University of Technology BRATISLAVA – TRNAVA
- **Imrich KISS**, Institute of Economic & Environmental Security – KOŠICE
- **Vladimir MODRAK**, Technical University of KOSICE – PRESOV

CROATIA
- **Drazan KOZAK**, Josip Juraj Strossmayer University of OSIJEK – SLAVONKI BROD
- **Predrag COSIC**, University of ZAGREB – ZAGREB
- **Milan KLJAJIN**, Josip Juraj Strossmayer University of OSIJEK – SLAVONKI BROD
- **Antun STOIĆ**, Josip Juraj Strossmayer University of OSIJEK – SLAVONKI BROD
- **Ivo ALFIREVIĆ**, University of ZAGREB – ZAGREB

HUNGARY
- **Imre DEKÁNY**, University of SZEGED – SZEGED
- **Cecilia HODÚR**, University of SZEGED – SZEGED
- **Béla ILLÉS**, University of MISKOLC – MISKOLC
- **Imre RUDAS**, Óbuda University of BUDAPEST – BUDAPEST
- **István BIRÓ**, University of SZEGED – SZEGED
- **Tamás KISS**, University of SZEGED – SZEGED
- **Imre TIMÁR**, University of Pannonia – VESZPRÉM
- **Károly JÁRMAI**, University of MISKOLC – MISKOLC
- **Ádám DÖBRÖCZÖNI**, University of MISKOLC – MISKOLC
- **György SZEIDL**, University of MISKOLC – MISKOLC
- **Miklós TISZA**, University of MISKOLC – MISKOLC
- **József GÁL**, University of SZEGED – SZEGED
- **Ferenc FARKAS**, University of SZEGED – SZEGED
- **Géza HUSI**, University of DEBRECEN – DEBRECEN

SERBIA
- **Sinisa KUZMANOVIC**, University of NOVI SAD – NOVI SAD
- **Mirjana VOJINOVIĆ MILORADOV**, University of NOVI SAD – NOVI SAD
- **Miroslav PLANČAK**, University of NOVI SAD – NOVI SAD

ITALY
- **Alessandro GASPARETTO**, University of UDINE – UDINE
- **Alessandro RUGGIERO**, University of SALERNO– SALERNO
- **Adolfo SENATORE**, University of SALERNO– SALERNO
- **Enrico LORENZINI**, University of BOLOGNA – BOLOGNA

FINLAND   Antti Samuli KORHONEN, University of Technology – HELSINKI
           Pentti KARJALAINEN, University of OULU – OULU

UKRAINE   Sergiy G. DZHURA, Donetsk National Technical University – DONETSK
           Heorhiy SULYM, Ivan Franko National University of LVIV – LVIV
           Yevhen CHAPLYA, Ukrainian National Academy of Sciences – LVIV
           Vitalii IVANOV, Sumy State University – SUMY

The Scientific Committee members and Reviewers do not receive any remuneration. These positions are voluntary.

We are extremely grateful and heartily acknowledge the kind of support and encouragement from all contributors and all collaborators!

ACTA TECHNICA CORVINIENSIS – Bulletin of Engineering is dedicated to publishing material of the highest engineering interest, and to this end we have assembled a distinguished Editorial Board and Scientific Committee of academics, professors and researchers.

ACTA TECHNICA CORVINIENSIS – Bulletin of Engineering publishes invited review papers covering the full spectrum of engineering. The reviews, both experimental and theoretical, provide general background information as well as a critical assessment on topics in a state of flux. We are primarily interested in those contributions which bring new insights, and papers will be selected on the basis of the importance of the new knowledge they provide.

ACTA TECHNICA CORVINIENSIS – Bulletin of Engineering encourages the submission of comments on papers published particularly in our journal. The journal publishes articles focused on topics of current interest within the scope of the journal and coordinated by invited guest editors. Interested authors are invited to contact one of the Editors for further details.

ACTA TECHNICA CORVINIENSIS – Bulletin of Engineering accept for publication unpublished manuscripts on the understanding that the same manuscript is not under simultaneous consideration of other journals. Publication of a part of the data as the abstract of conference proceedings is exempted.

Manuscripts submitted (original articles, technical notes, brief communications and case studies) will be subject to peer review by the members of the Editorial Board or by qualified outside reviewers. Only papers of high scientific quality will be accepted for publication. Manuscripts are accepted for review only when they report unpublished work that is not being considered for publication elsewhere.

The evaluated paper may be recommended for:

— **Acceptance without any changes** – in that case the authors will be asked to send the paper electronically in the required .doc format according to authors' instructions;

— **Acceptance with minor changes** – if the authors follow the conditions imposed by referees the paper will be sent in the required .doc format;

— **Acceptance with major changes** – if the authors follow completely the conditions imposed by referees the paper will be sent in the required .doc format;

— **Rejection** – in that case the reasons for rejection will be transmitted to authors along with some suggestions for future improvements (if that will be considered necessary).

The manuscript accepted for publication will be published in the next issue of ACTA TECHNICA CORVINIENSIS – Bulletin of Engineering after the acceptance date.

All the authors and the corresponding author in particular take the responsibility to ensure that the text of the article does not contain portions copied from any other published material which amounts to plagiarism. We also request the authors to familiarize themselves with the good publication ethics principles before finalizing their manuscripts.

Fascicule 2
[April – June]
t o m e [2022] XV

ACTA Technica CORVINIENSIS
BULLETIN OF ENGINEERING

15 YEAR ANNIVERSARY

ACTA TECHNICA CORVINIENSIS
Bulletin of Engineering

TABLE of CONTENTS
ACTA TECHNICA CORVINIENSIS – Bulletin of Engineering
Tome XV [2022],
Fascicule 2 [April – June]

The **ACTA TECHNICA CORVINIENSIS – Bulletin of Engineering, Tome XV [2022], Fascicule 2 [April–June]** includes original papers submitted to the Editorial Board, directly by authors or by the regional collaborators of the Journal.

Also, the **ACTA TECHNICA CORVINIENSIS – Bulletin of Engineering, Tome XV [2022], Fascicule 2 [April–June]**, includes scientific papers presented in the sections of:

⎯ **International Conference on Science, Technology, Engineering and Economy – ICOSTEE 2022**, organized by University of Szeged, Faculty of Engineering (HUNGARY) and Hungarian Academy of Sciencies – Commettee on Bio– and Agricultural Engineering – Regional Commettee in Szeged (HUNGARY), in Szeged, HUNGARY, in 24th of March, 2022, in a hybrid mode (on site & online). The current identification numbers of the selected papers are the **#9–10**, according to the present contents list.

⎯ **International Conference on Applied Sciences – ICAS 2021**, organized by University Politehnica Timisoara – Faculty of Engineering Hunedoara (ROMANIA) and University of Banja Luka, Faculty of Mechanical Engineering Banja Luka (BOSNIA & HERZEGOVINA), in cooperation with Academy of Romanian Scientists (ROMANIA), Ministry for Scientific and Technological Development, Higher Education and Information Society of the Republic of Srpska (BOSNIA & HERZEGOVINA), Academy of Sciences and Arts of the Republic of Srpska (BOSNIA & HERZEGOVINA), Academy of Technical Sciences of Romania – Timisoara Branch (ROMANIA), General Association of Romanian Engineers – Hunedoara Branch (ROMANIA) and Association Universitaria Hunedoara (ROMANIA), in Hunedoara, ROMANIA, 12–14 May, 2021. The current identification numbers of the selected papers is the **#12**, according to the present contents list.

⎯ **International Symposium (Agricultural and Mechanical Engineering) – ISB–INMA TEH' 2021**, organized by Politehnica University of Bucharest – Faculty of Biotechnical Systems Engineering (ISB), National Institute of Research–Development for Machines and Installations Designed to Agriculture and Food Industry (INMA Bucharest), Romanian Agricultural Mechanical Engineers Society (SIMAR), National Research & Development Institute for Food Bioresources (IBA Bucharest), National Institute for Research and Development in Environmental Protection (INCDPM), Research–Development Institute for Plant Protection (ICDPP), Research and Development Institute for Processing and Marketing of the Horticultural Products (HORTING), Hydraulics and Pneumatics Research Institute (INOE 2000 IHP) and "Food for Life Technological Platform", in Bucharest, ROMANIA, between 31 October – 1 November, 2021. The current identification numbers of the selected papers are the **#1–4** and **#17–20**, according to the present contents list.

CELEBRATING 15 YEARS OF EXCELLENCE
A milestone moment for ACTA TECHNICA CORVINIENSIS – Bulletin of Engineering!

ACTA TECHNICA CORVINIENSIS – Bulletin of Engineering is an international and interdisciplinary journal which reports on scientific and technical contributions and publishes invited review papers covering the full spectrum of engineering.

We are very pleased to inform that our journal ACTA TECHNICA CORVINIENSIS – Bulletin of Engineering completed its 14 years of publication successfully [2008–2021, Tome I–XIV]. In a very short period it has acquired global presence and scholars from all over the world have taken it with great enthusiasm. This year, 2022, marks ACTA TECHNICA CORVINIENSIS – Bulletin of Engineering' 15th year in scientific publishing! Our ability to adapt has allowed us to prosper over the years. I look forward to new challenges, new technology and to seeing what the next 15 years will bring. We look forward to the next 15 years of service excellence!

We are extremely grateful and heartily acknowledge the kind of support and encouragement from all contributors and all collaborators! Our ongoing success would be impossible without you! And thank you to all of our readers and partners who continue to believe in our services and people, and who have helped us endure and thrive throughout the years.

Every year, in four online issues (fascicules 1 – 4), ACTA TECHNICA CORVINIENSIS – Bulletin of Engineering [e–ISSN: 2067–3809] publishes a series of reviews covering the most exciting and developing areas of engineering. Each issue contains papers reviewed by international researchers who are experts in their fields. The result is a journal that gives the scientists and engineers the opportunity to keep informed of all the current developments in their own, and related, areas of research, ensuring the new ideas across an increasingly the interdisciplinary field.

ACTA TECHNICA CORVINIENSIS – Bulletin of Engineering is a good opportunity for the researchers to exchange information and to present the results of their research activity. Scientists and engineers with an interest in the respective interfaces of engineering fields, technology and materials, information processes, research in various industrial applications are the target and audience of ACTA TECHNICA CORVINIENSIS – Bulletin of Engineering. It publishes articles of interest to researchers and engineers and to other scientists involved with materials phenomena and computational modeling.

The journal's coverage will reflect the increasingly interdisciplinary nature of engineering, recognizing wide–ranging contributions to the development of methods, tools and evaluation strategies relevant to the field. Numerical modeling or simulation, as well as theoretical and experimental approaches to engineering will form the core of ACTA TECHNICA CORVINIENSIS – Bulletin of Engineering's content, however approaches from a range of environmental science and economics are strongly encouraged.

Publishing in ACTA TECHNICA CORVINIENSIS – Bulletin of Engineering is free of charge. There are no author fees. All services including peer review, copy editing, typesetting, production of web pages and reproduction of color images are included. The journal is free of charge to access, read and download. All costs associated with publishing and hosting this journal are funded by ACTA TECHNICA CORVINIENSIS – Bulletin of Engineering as part of its investment in global research and development.

Fascicule 2
[April – June]
t o m e [2022] XV

ACTA Technica CORVINIENSIS
BULLETIN OF ENGINEERING

[1.]Andreea–Catalina CRISTESCU, [1.]Ilie FILIP, [2.]Vasilica STEFAN,
[2.]Lucretia POPA, [1.]George IPATE, [1.]Gheorghe VOICU

IMPORTANCE OF MATERIALS USED IN CAR BREAKING SYSTEMS – REVIEW

[1.]Faculty of Biotechnical Engineering, University Politehnica of Bucharest, ROMANIA
[2.]National Institute for Research–Development of Machines and Installations designed for Agriculture and Food Industry, ROMANIA

Abstract: Tribological conditions of the brake components during operation have a dominant effect on brake wear. Tribological analysis is one of the most important mechanical fields in the industry. The tribological properties of two contact surfaces of engines and machines generally depend on factors such as load, speed, temperature, slip time, lubricant and additives. The individual friction mechanisms depend on the temperature, normal load and sliding speed, so the coefficient of friction is dependent on these parameters. High temperature values during braking cause brake degradation, premature wear, brake fluid vaporization, bearing failure, thermal cracking and thermal vibration. The ideal brake pads must ensure a uniform and stable friction in all working conditions, without causing brake degradation, regardless of temperature. Brake friction materials consist of at least 10 components, required to achieve the desired braking performance, including stable coefficients of friction, reduced wear and low noise, in a wide range of braking conditions.
Keywords: car breaking system, cast iron, ceramic breaks, brake pads

INTRODUCTION

The safety of the steering wheel depends on the braking parameters of the car. Braking is the ability of the car to decelerate quickly and stop completely at a minimum distance. When braking, the kinetic energy of the car is converted into thermal energy in the braking mechanisms and in the contact area of the tires with the road surface.

The key braking parameters of the car are the braking force and deceleration, however, in practice, the braking time and distance are mostly used. The grip parameters of the car could be changed, e.g. driving the car on various road surfaces and equipping it with new tires with good tread, as well as varying the weight of the car, e.g. driving it loaded or unloaded. If the car is loaded, the axle load distribution, the center of mass height and the area of contact of the tire with the road surface may change. According to the physical laws, the braking factor does not change if the load on the tire varies. (Vinodkumar, Jairaman, Anvesh, & Viswanath, 2017; Denimalab, Sinouac, & Nacivetb, 2019; Denimal, Sinou, Nacivet, & Nechak, 2019))

During braking, the temperature of the interface between the disc and the pad, and the change in speed have a significant impact on the coefficient of friction. The coefficient of friction decreases with increasing temperature and sliding speed. Brake wear is an event that occurs for any vehicle equipped with a brake braking system, when the coefficient of friction decreases significantly with temperature

Mathematical models are frequently used which are intended for the analysis of vehicle braking parameters. However, the values of the deceleration and braking distance parameters are random values in practice. (Borivoj & S., 2016)

Tribological conditions of the brake components during operation have a dominant effect on brake wear. Tribological analysis is one of the most important mechanical fields in the industry. The tribological properties of two contact surfaces of engines and machines generally depend on factors such as load, speed, temperature, slip time, lubricant and additives. The individual friction mechanisms depend on the temperature, normal load and sliding speed, so the coefficient of friction is dependent on these parameters. Numerous studies have shown the dependence of the coefficient of friction on temperature, braking force and braking speed. In most of these studies, the coefficient of friction is inversely proportional to the speed of travel, while showing a mixed trend depending on the mass of the vehicle. In recent decades, more and more sophisticated models have been developed. The most common model is the static model. An analytical wording was proposed taking into account only the speed dependence. A very simple analytical formulation was evaluated based on experimental tests at steady state that correlate the dependence of pressure, speed and temperature of friction and wear, thermal effects due to increasing temperature of friction materials [(Borivoj & S., 2016).

MATERIALS AND METHODS

— Gray cast iron brake disc

Gray cast iron is a widely used material for brake discs. The advantages of using cast iron as a material for brake discs are: easy processing, high thermal conductivity and heat capacity, high coefficient of friction, reliability and lower costs.

The goal is represented by using the materials that are as light as possible for the brake discs, so that it contributes as little as possible to the total weight of the vehicle and, finally, to improve fuel consumption and increase comfort while driving.

One way to reduce the weight of the brake disc is to use an aluminium and cast iron mounting bowl (hub), which is called a hybrid brake disc. These two parts can be connected to either (Rashid, 2014)

The brake disc, made of cast iron, cast with an aluminium bell, or fastened by means of screws or bolts, has a friction ring made of cast iron to take advantage of superior abrasion resistance and good thermal properties, while mounting the bell is made of aluminium to reduce overall weight (Rashid, 2014).

To reduce the mass, lightweight materials with suitable properties are required in the construction of the brake disc. Since heat is generated at the surface of a disk due to frictional forces, it is desired that for a given heat input, the temperature rise of the material be minimal, ie to have the maximum possible volumetric heat capacity (ie density × specific heat capacity). During short braking, this is very important as a significant amount of heat is stored (Rashid, 2014).

Other desired properties are frictional stability, corrosion resistance and wear, lower coefficient of thermal expansion.

Aluminium metal matrix composites are an alternative to braking. They offer good wear and corrosion resistance and a comparatively lower mass with cast iron. They also have higher thermal conductivity and diffusivity. A disadvantage is the higher coefficient of thermal expansion compared to cast iron. Another major disadvantage is the limited temperature resistance and therefore did not gain widespread acceptance (Rashid, 2014).

As seen above, the two main functions of a brake disc are transmitting a considerable mechanical force and dissipating the heat produced in operation. The working temperature for breaking systems, depending on the mass and the number of bursts, can be placed between room temperature and, in some cases, up to 700º C (Maluf, et al., 2004).

The disc is also exposed to the action of a cyclic mechanical load applied by the pads during a break, which contributes to component wear. Therefore, under real working conditions, the disk is exposed to a thermal fatigue load condition instead of thermal load (Maluf, et al., 2004).

Theoretically, several materials could meet the requirements for good performance. However, due to better metallurgical stability, lower costs and light production, cast iron is the most widely used.

Other types of materials are used for high performance braking conditions, in which the disc is subjected to very high temperatures. For example, carbon matrix composites are used to produce brake discs for racing cars and aircraft, but also for high–tech cars. They have excellent heat performance, but the manufacturing cost is relatively higher. Another example is the titanium cast iron brake disc, which increases the strength of the components but reduces the coefficient of friction, which can be a major problem when there is a short braking distance. (Maluf, et al., 2004).

Aluminium alloys containing silicon carbide can also be used because they have a low density. However, despite their lower weight, these alloys do not dissipate heat, like cast iron.

Cast iron alloys are considered cheap by the manufacture of car brake discs. For the production of several types of cast iron, the molten metal is usually composed of low iron ore, scrap iron and alloys such as iron–silicon, iron–manganese, iron–chromium, nickel and others. All the elements in the alloy tend to increase the mechanical strength, and the most effective are vanadium, molybdenum and chromium. For example, the most commonly used alloys for the production of General Motors brake discs in Brazil are cast iron, with or without other chemical elements, as shown in Table 1 (Maluf, et al., 2004).

Table 1. Chemical composition (% by mass) of cast iron used by General Motors Brazil (Maluf, et al., 2004).

Element	Metal Alloy			
	A	B	C	D
%C	3.20 3.60	3.20 3.60	3.60 3.80	3.70 3.90
%Si	1.90 2.40	1.90 2.40	1.80 2.20	1.75 1.95
%Mn	0.60 0.90	0.60 0.90	0.60 0.80	0.50 0.80
%P	Max 0.20	Max 0.10	Max 0.12	Max 0.13
%S	Max 0.20	Max 0.10	Max 0.12	Max 0.13
%Cr	–	0.25 0.40	0.10 0.25	Max 0.20
%Mo	–	0.40 0.50	0.30 0.60	Max 0.10
%Cu	–	–	0.30 0.45	Max 0.40

— Ceramic brake disc

Ceramic matrix (CMC) compositions, based on carbon fibers and carbon–silicon matrix are another choice for brake discs, due to their superior tribological properties compared to cast iron. Their key features are:

≡ low density
≡ high thermal expansion coefficient compared to cast iron
≡ constant coefficients of friction and high stability

A disadvantage of CMCs is their smaller volumetric heat capacity, which is offset by larger diameter discs. They are used in high performance cars, but their prices are currently very high compared to cast iron discs. They are connected to the wheel by the mounting bowl. (Rashid, 2014)

Ceramic brakes offer excellent braking performance, wear well over time and are very light. They are made of ceramic fibers, fillers, gluing agents and may even contain small amounts of copper fibers inside them. Due to the ceramic properties, these brake parts dissipate heat well, which maintains strong performance, even after hard, repeated stops. They also produce less dust than other types of brakes, and the dust they produce has a smaller mass and does not stick to the wheels. However, they are very expensive, so ceramic brakes are not for every type of vehicle. Formula 1 sports cars can benefit from ceramic brakes. Almost all other

vehicles perform excellently with other brake pad materials (Rancsó, 2015)

A special feature of the carbon–ceramic brake discs is the ceramic composite material from which they are made. The carbon–ceramic brake disc body and the friction layers applied on each side are made of silicon carbide reinforced with carbon fiber. Silicon carbides (SiC) and elemental silicon (Si) are the main components of the matrix (Rancsó, 2015).

The reinforcement of the material is provided by carbon fibers (C). Silicon carbide, the main component of the matrix, provides high hardness for the composite material. Carbon fibers provide high mechanical strength and provide the fracture strength required in technical applications.

The quasi–ductile properties resulting from the ceramic composite material ensure its resistance to high thermal and mechanical load. Carbon fiber–reinforced silicon carbide materials, therefore combine the useful properties of carbon fiber reinforced carbon (C / C) and polycrystalline silicon carbide ceramics.

The elongation at break of C / SiC materials is between 0.1 and 0.3%. The characteristic profile of the fiber–reinforced silicon carbide makes it a material of choice for high–performance braking systems.

The low weight, hardness, stable characteristics, as well as the high pressure and temperature, not to mention the thermal shock resistance and quasi–ductility properties, offer a long life of the brake disk and avoid all problems resulting from loading, which are typical of classic cast iron brake discs.

Table 2. Differences between cast iron disc and ceramic disk (Rancsó, 2015)

	Carbon–ceramic brake discs (C/SiC)	Gray cast iron brake discs
Density (g cm^{-3})	2.45	7.25
Tensile strength	20–40	200–250
Modulus of elasticity (MPa)	30	90–110
Bending strength (MPa)	50–80	150–250
Elongation at break (%)	0.3	0.3–0.8
Thermal shock resistance (second thermal coefficient K') (Wm^{-1})	>27.000	<5.400
Thermal stability (°C)	1350	Aprox. 700
Maximum operating temperature (°C)	900	700
Linear coefficient of thermal expansion (K^{-1})	2.6–3.0	9–12
Thermal conductivity (W m^{-1}K^{-1})	40	54
Specific heat capacity (c_p) (kJkg^{-1}K^{-1})	0.8	0.5

Table 2 shows the characteristic properties and differences between carbon–carbon ceramic discs and cast iron discs (Rancsó, 2015)

⸺ Brake pad materials

The modern brake pad has a history of the last 100 years. Herbert Frood was the first to invent brake pad materials in 1897. This pad had a cotton–based material, which was used for wagon wheels as well as early cars and was watered with bitumen solution (Abutu, 2018)

Bertha Benz, Carl Benz's wife, was the first to invent automatic friction pads. This invention appeared during his first long–distance car journey in 1888.

In the 1950s, metal pads that were glued to the resin were introduced, and in the 1960s semi–metals containing a larger amount of metal additives were developed.

The material of the brake pad is a heterogeneous substance composed of various elements. Each component has its own functions, which include improving the friction properties at low and high temperatures, reducing noise, prolonging life, increasing strength and stiffness, and reducing porosity (Abutu, 2018)

Changes in the mass percentage or types of elements in the composition can lead to changes in the chemical, mechanical and physical properties of the friction materials developed. Early researchers concluded that there is no simple correlation between wear and friction properties of friction materials with mechanical and physical properties. As a result, each new formulation developed must be subjected to several tests to assess its wear and friction properties, using the road braking performance test, as well as an abrasion testing mechanism, to ensure that the developed material of the friction plate meets the minimum requirements for use. Figureure 1 shows the construction of the brake pads

Figure 1 – Brake pad construction (Stefan–Ionescu, 2019)
1–friction material; 2–thermal material; 3–adhesive layer; 4–metal plate; 5–shock absorber

From a functional and safety point of view, the following friction material requirements are required:

≡ High coefficient of friction
≡ Stable coefficient of friction regardless of temperature, speed, pressure, humidity, wear, corrosion and water spray
≡ Low wear rate of the friction material and long service life
≡ Low disc wear rate
≡ Smooth braking without noise and vibration
≡ Regeneration of original properties after severe braking and aging
≡ Ecological raw materials
≡ Reduced cost

These are essential requirements in the selection of material. To meet so many requirements, friction materials are made of

several compounds and are therefore called compounds. There can be up to 25 different materials (Rashid, 2014).

Materials are usually classified into the following four categories:

≡ Binders

A binder "binds" different component materials of a friction material. Phenolic thermoregulatory resins are usually used as binders, with the addition of rubber for enhanced properties. The resin strongly affects the wear resistance of the friction material (Rashid, 2014)

≡ Reinforcing fibers

Reinforcing fibers ensure mechanical strength. Asbestos fibers have been widely used as a reinforcing material, but have been replaced by other materials for environmental reasons. Other materials used as reinforcing fibers are copper, aramid fiber, ceramic and various metals, for example copper, steel, iron, brass, bronze and aluminium. The fibers are arranged in the tangential or radial direction of the plate, and not in the axial direction. This is to keep the heat away from the metal fixing plate, as the fibers, especially the metal ones, usually have a high thermal conductivity. If the pad overheats in the axial direction, it may eventually reach the brake fluid and may cause the brake to lose its efficiency (Rashid, 2014)

The following table (Table 3) shows the classification of friction materials

Table 3. Classification of friction materials (Rashid, 2014)

Type of friction material	Metal content	Metal Type
Semi–metal	≥40	Steel
Low steel content, low metal content	≤15	Steel and no–steel
No steel content, Low metal content	≤15	No–steel
Metallic European	15–40	Steel and no–steel

RESULTS

— Breaking pads wear

In addition to normal wear and tear caused by long–term use of the pads, there are a number of factors that can lead to wear and tear of the brake pads, such as: thermal deformation, frictional detachment, defective assembly, manufacturing defects, damage related to use, damage caused by environmental influences.

☐ Thermal deformation of the plate

The overall thermal deformation of the plate called the convex bend results in a reduced contact surface in the middle of the plate, as shown in Figure 2. The generation of frictional heat at the interface between the disc and the plate results in a higher plate temperature. Surface, in a short period of time, in the inner region of the support plate. As a result, the surface expands more than the inner region of the plate and the support plate, leading to a convex bend. (Rashid, 2014)
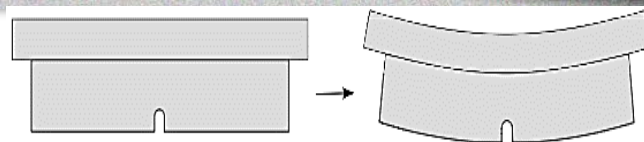
Figure 1 – Thermal deformation of brake pads (Rashid, 2014)

☐ Detachment of the friction material from the fixing plate

❖ Detachment of friction material caused by corrosion

This phenomenon has as causes:

≡ Use of pads on extremely worn brake discs.

≡ Inadequate compression spring force (off–centre displacement).

≡ Mechanical overloads

≡ High and constant thermal stress on the disc brake pads.

≡ The friction material became porous (in whole or in points).

≡ Friction material is loose due to corrosion.

≡ The mounting plate shows obvious signs of corrosion.

≡ Adhesive residues

≡ The substrate and friction material are visible on the mounting plate (TEXTAR, n.d.).

An example with a plate showing such defects can be found in Figure 2

Figure 2. – Corrosion damage (TEXTAR, n.d.)

❖ Detachment of friction material caused by thermal decomposition

This phenomenon occurs when the maximum allowable temperature has been exceeded at the level of the plates, for more than 15–20 minutes. Thus, the compounds that contribute to the stability of the material were destroyed. As a result, the friction material of the brake pad decomposes, may crack, the substrate and the adhesive are damaged (TEXTAR, n.d.). The friction material becomes solid, showing a reddish–brown colour (Figure 3)

Figure 3 – Thermally damaged friction material (TEXTAR, n.d.)

❖ **Detachment of friction material caused by mechanical influences**

These occur when the brake pads are tilted or the mounting has been made incorrectly in an inclined position. Another cause may be a deformity caused by the "shaking" of the calliper. As a result, the friction material can come off the metal plate. Thus, exfoliation occurs (TEXTAR, n.d.). An example of such a fault is found in Figure 4. Table 4 shows the causes, effects and detachments of the friction material.

Figure 4 – Brake pad deformations caused by mechanical influences (TEXTAR, n.d.)

Table 4. Causes, effects and characteristics
of friction material detachment (TEXTAR, n.d.)

Detachment caused by	Cause	Effect	Characteristics
Corrosion	1. Damage to the edges due to extreme wear of the brake disc; inadequate compression spring (off–center displacement) 2. Constant high thermal stress on plate	The friction material became porous (in whole or in parts), the detachment of the friction material as a result of corrosion	The mounting plate shows obvious signs of corrosion; adhesive residue, the substrate and the friction material are visible on the fixing plate
Manufacturing defect	Wrong adhesive. Improperly distributed substrate.	The friction material has come off since it was subjected to low stress	Fine fixing plate or substrate and adhesive only partially visible
Thermal decomposition of adhesive, substrate and friction material	Disc brake pads have exceeded the maximum allowable temperature for more than 15–20 minutes; During this period, components that contribute significantly to stability were destroyed.	The friction material decomposes, breaks in certain places and / or the substrate and adhesive are damaged, the plates show complete detachment	The coating exfoliates, the fixing plate is colored blue in some places, the friction material has solidified, has a hard ring, reddish–brown coloration of the friction material, white ash in some places
Mechanical destruction	For example, the disc brake pads have tilted	Friction material comes off the mounting plate, exfoliation occurs	Disc brake pads are new; separation above the adhesive / substrate. Visible damage to the mounting plate.

☐ **Damage related to use**

These can be caused by:
≡ Worn or non–compliant brake disc
≡ Brake defective or contaminated
≡ Insufficient brake load
≡ Assembly defect (Figure 4) / Manufacturing defect
≡ Destruction of frictional material caused by mechanical or thermal overload at some points on the surface.
≡ Improper spacing of the pads caused by a defective brake.
≡ Use of new brake pads on worn or scratched brake disc (TEXTAR, n.d.)

Figure 5 – Damage caused by manufacturing defects (TEXTAR, n.d.)

☐ **Damage caused by environmental influences**

These can be caused by the following factors:
≡ Inadequate contact structure, no cleaning of the brake after thermal loading.
≡ Often the operating temperature is not reached; no self–cleaning takes place
≡ Contamination of the friction surface, i.e. by corrosion, due to dirt, paint or salt.
≡ Using the scratched brake disc.
≡ Penetration of foreign objects, such as dirt, salt or corrosion. (Figure 6)
≡ Inadequate distribution of friction particles in the friction material.
≡ Transfer of material from the brake disc to the brake pad due to, for example, different load, climate and / or material incompatibility (TEXTAR, n.d.)

Figure 6 – Penetration of metal chips on the plate surface (TEXTAR, n.d.)

CONCLUSIONS

Further studies with different braking systems are needed to fully validate the model and other friction materials can be

tested to generate a database with maps for friction centres (Gabriele RIVA, 2020).

Friction materials are a vital part of car and vehicle brakes. System designers need to understand the characteristics of the friction and wear behaviour and the causes of the variation of their properties (Dante, 2016).

Specifications for commercially available friction materials include mechanical properties, friction and wear characteristics, and an indication of the effects of temperature and recommended operating conditions. The coefficient of friction of these materials depends on their composition, and vehicle manufacturers can select friction materials that meet their requirements; for example, for cars they can use friction materials with a nominal value of the coefficient of friction in the range 0.38 <m <0.45, while commercial vehicles often emphasize durability above m high and use a lower nominal range of the coefficient friction, e.g. 0.35 <m <0.40. They are a starting point for the design of the braking system (Dante, 2016).

A friction torque practically complies with Amontons' friction laws, but when the braking load increases and the temperatures generated at the friction interface increase significantly, the coefficient of friction will change. Most changes in the coefficient of friction are related to temperature. How much it changes depends on the specification of the friction material. The coefficient of friction of any friction material can only be accurately assessed by testing (Dante, 2016).

Note: This paper was presented at ISB–INMA TEH' 2021 – International Symposium, organized by University "POLITEHNICA" of Bucuresti, Faculty of Biotechnical Systems Engineering, National Institute for Research-Development of Machines and Installations designed for Agriculture and Food Industry (INMA Bucuresti), National Research & Development Institute for Food Bioresources (IBA Bucuresti), University of Agronomic Sciences and Veterinary Medicine of Bucuresti (UASVMB), Research-Development Institute for Plant Protection – (ICDPP Bucuresti), Research and Development Institute for Processing and Marketing of the Horticultural Products (HORTING), Hydraulics and Pneumatics Research Institute (INOE 2000 IHP) and Romanian Agricultural Mechanical Engineers Society (SIMAR), in Bucuresti, ROMANIA, in 29 October, 2021

References

[1] (NHTSA), N. H. (2003). Consumer Braking Information.
[2] Abutu, J. &.–A. (2018). An overview of brake pad production using non–hazardous reinforcement materials. Acta Technica Corviniensis – Bulletin of Engineering ,, 3.
[3] Borivoj, N., & S., M. K. (2016). The Importance of Application and Maintenance of Braking System in Modern Automobile. VI International Conference Industrial Engineering and Environmental Protection.
[4] Cimpeanu, C. I., & Cimpeanu, I. S. (2019). Automobilul: Siguranţa Rutieră Şi Poluarea. Resita: Editura Tim.
[5] Dante, R. C. (2016). Types of friction material formula. Woodhead Publishing.
[6] Denimal, E., Sinou, J.–J., Nacivet, S., & Nechak, L. (2019). Squeal analysis based on the effect and determination of the most influential contacts between the different components of an automotive brake system. International Journal of Mechanical Sciences, 151, 192–2013.
[7] Denimalab, E., Sinouac, J.–J., & Nacivetb, S. (2019). Influence of structural modifications of automotive brake systems for squeal events with kriging meta–modelling method. Journal of Sound and Vibration, 463.
[8] Gabriele RIVA, F. V. (2020). finite element analysis (FEA) approach to simulate the coefficient of friction of a brake system starting from material friction characterization.
[9] Greibe, p. (2007). Braking distance, friction and behaviour. Findings, analyses and rec–ommendations based on braking trials. Lyngby.
[10] Kemmer, H. (2002). nvestigation of the Friction Behavior of Automotive BrakesThrough Experiments and Tribological Modeling. Universitat Paderborn.
[11] Maluf, O., Milan, M., Spinelli, M., Wladimir, D., Filho, W., Bose. (2004). Development of materials for automotive disc brakes. Pesquisa Technol Minerva, 2.
[12] Österle, W., Dörfel, I., Prietzel, C., Rooch, H., Cristol–Bulthé, A.–H., Degallaix, G., & Desplanques, Y. (2008). A comprehensive microscopic study of third body formationat the interface between a brake pad and brake disc during thefinal stage of apin–on–disc test. Wear(268), 781–788.
[13] Parczewski, K. (fără an). Effect of tyre inflation preassure on the vehicle dynamics. Eksploatacja i Niezawodnosc –Maintenance and Reliability, 2(15), 134–139.
[14] Rancsó, B. (2015). Manufacture and examination of carbon ceramic brakes.
[15] Rashid, A. (2014). Overview of disc brakes and related phenomena – A review. International Journal of Vehicle Noise and Vibration, 10(4), 257.
[16] Reif, K. (2019). Antilock braking system (ABS). În K. Reif, Car braking–system components. Function, Regulation and Components (pg. 74–93). Wiesbaden,: Springer Vieweg.
[17] Reif, K. (2019). Car braking–system components. În K. Reif, Brakes, Brake Control and Driver Assistance Systems. Function, Regulation and Components (pg. 28–39). Wiesbaden: Springer Vieweg.
[18] Stefan–Ionescu, R. (2019). Optimizarea constructiva si ecologica a componentelor sistemului de franare al autoturismelor. Brasov: Universitatea Transilvania din Brasov.
[19] TEXTAR. https://textar.com/
[20] Tretsiak, D. V., Kliauzovich, S. V., Augsburg, K., Sendler, J., & Ivanov, V. G. (fără an). Research in hyraulic components and operational factors influencing the hysteresis losses. Journal of Automobile Engineering, Procediings of the Institution of Mechanical Engineers, 1633–1645.
[21] Vinodkumar, S., Jairaman, S., Anvesh, P., & Viswanath, G. (2017). Improvement of braking efficiency in vehicle by using fusion braking system. International Research Journal of Engineering and Technology (IRJET), 04(08), 527–529.
[22] W., P. (2019). Car braking systems (Vol. Car braking–system components. Function, Regulation and Components). Wiesbaden: Springer Vieweg.

1.Florin NENCIU

INTERLABORATORY TESTING PRACTICES BENEFITS AND THEIR IMPLEMENTATION

1. National Institute of R&D for Machines and Installations Designed to Agriculture and Food Industry (INMA), Bucharest, ROMANIA

Abstract: Proficiency testing (PT) and inter–laboratory comparison schemes (ILC) provide laboratories with a useful tool for increasing their testing and calibration standards. These two interlaboratory testing practices are often neglected since they are regarded just as a requirement to fulfill and not an approach for continuous development. Proficiency testing provides for an independent assessment of laboratory findings, in comparison to reference values or the performance of other laboratories. A positive evaluation is a confirmation of the laboratory ability to show high technical competence and provide credibility in the accuracy, reliability, and security of the test data it delivers. This paper aims to analyze Inter–laboratory testing practices, focusing on their benefits and their implementation process.

Keywords: proficiency testing, laboratory performance, quality control tools

INTRODUCTION

Analytical data is used today to make economic, legal, or environmental management choices, therefore the results of analytical determinations are considered highly significant. It's critical that these metrics to be precise, reliable, cost–effective, and reasonable. Experimental laboratories play an essential role, since they are involved in the generation of scientific information, which in many situations leads to critical decisions or other broader evaluations. It is fundamental to assure the quality of the data supplied from each laboratory since scientific findings must be based on reliable and internationally comparable data (Voiculescu et al., 2013).

The need for a high level of confidence in laboratory performance is critical not only for laboratory practices and for their customers, but also for other interested parties such as regulators, laboratory accreditation bodies, and other organizations. As a result, proficiency testing is becoming increasingly important. In the domain of quality assurance of laboratory results, proficiency testing is an essential technique to achieve the legal performance standards (Boley, 2000).

Proficiency testing (PT) is a method for measuring the correctness of analytical data provided by laboratories for specific measures on a regular basis. It is the laboratories responsibility to select the most appropriate scheme and to check and evaluate the quality of the PT provider. The time and effort required can be costly, especially for laboratories performing many different tests, so selecting the most appropriate PT scheme is very important.

Laboratory analysis are performed for a variety of purposes, but most commonly used reason is to ensure that a product has been made in accordance with standards and regulations and it is safe to be distributed to the market. It is therefore critical that the analysis results to be trusted in terms of both accuracy and repeatability.

Using effective Quality Control Tools to monitor the classification of the data regarding foods can aid prevent acceptable products from being destroyed and non–conforming product from being distributed on the market. Quality Control tools that can be implemented in the laboratory practices should contain an external reference point over which the lab has no direct control. External quality controls may include proficiency testing (PT) and reference materials (RM) supplied from an external and independent quality source. The level of performance of laboratory measurements must be monitored as part of the national and international regulations for the competence of testing and calibration laboratories and accreditation process.

In order to remove the trading barriers worldwide it is necessary to establish foundations for free commerce throughout the world.

Therefore, agreements promoting the growth of mutual acceptance of international conformity assessment systems must be implemented. These agreements are based on mutual trust and are the result of a long–term collaborative partnership. They consist of three major elements: harmonization of accreditation criteria and operating procedures, a comprehensive program of inter–laboratory comparisons, and assessments by international team of accredited experts (Basic et al., 2010). The most important elements that must be defined in the case of establishing such procedures are: the concepts for designing a laboratory calibration system, the calibration processes and operating instructions required, the choice of traceable values to be calibrated, the calibration precision to be used, and the calibration intervals to be determined (Koch et al., 2001).

MATERIALS AND METHODS

Inter–laboratory investigations are useful for a variety of reasons in terms of determining measurement quality. They enable the validation of measuring techniques, the assessment of individual laboratories' competency, the estimation of measurement uncertainty, and the certification of reference materials in a wide range of application sectors.

Inter–laboratory comparisons (ILCs) also known Measurement comparisons, are the most common method of determining the compatibility of testing across various laboratories or measurement systems. As a result, they serve

as a tool for determining the alignment with national and international standards. These techniques clarify important elements in the operation of laboratories such as the measurement traceability when transferring the information from National laboratories to secondary laboratories, the effectiveness of their accreditation processes (when accrediting laboratories for new types of analyzes), and the operators competence and equipment (Galliana et al., 2019).

RESULTS

Inter–laboratory tests have the benefit of allowing measurements previously only possible with the technology and competence of a national extremely sophisticated laboratory to be regularly expected in private industrial laboratories. Inter–laboratory studies have been employed as an independent quality control by the laboratory community for many years.

Many of chemical measurements are taken to inform both consumers and decision makers about food safety, health, and environmental protection. The global market, requires precise and trustworthy actions in order to reduce technological trade obstacles. Reliable laboratory analysis depends to a large extent on several elements such as: qualified personnel approved and validated procedures, extensive quality systems, and traceability to appropriate measurement standards. In addition the increasing in the use of standards and standardized methods, as well as laboratory accreditation, demonstrates that the minimum quality requirements are ensured. At the regional and international levels, using comparability between is a useful technique that helps improving the measurement standards.

— Proficiency testing

Inter–laboratory studies, or collaborative studies, are more elaborated studies where several laboratories analyses the same material with a specific purpose.

There are three basic categories that may be recognized depending on the study's focus (Hogan, 2019; ISO 5725–2:2019):

≡ Collaborative trials or method–performance studies evaluate a method's performance characteristics. These are known as accuracy experiments, and they take into account the precision and correctness evaluations from the inter–laboratory testing. Precision experiments for the evaluation of repeatability and reproducibility are described in the ISO 5725–2 guideline. The second component of accuracy is trueness, which quantifies the measurement method bias in an inter–laboratory environment.

≡ Laboratory–performance (proficiency studies) orient towards the laboratory with the goal of determining the laboratory's level of proficiency. Test samples that are known or have been allocated, are assessed by a group of laboratories in certain investigations, also known as round robin studies. The laboratories utilize the approach that is currently in use.

≡ Material–certification studies have the goal of providing (certified) reference materials. A consortium of laboratories analyzes a sample, preferably using multiple methods, to estimate the most likely concentration of a certain substance with the least amount of uncertainty.

Proficiency testing is a technique used for inter–laboratory evaluation that verifies laboratory testing performance. Participation in proficiency testing schemes and programs offers laboratories the possibility of evaluating and demonstrating the reliability of the results they provide.

In addition, these requirements are mandatory for all certified and applicant (for accreditation) laboratories. They have to successfully complete a proficiency testing program in their specific area of testing. Inter–laboratory comparisons are frequently utilized for a variety of applications and are becoming more popular across the world.

A Proficiency Testing (PT) scheme is a technique for objectively reviewing laboratory findings by external means, which involves comparing a laboratory results with those of other laboratories, at regular time intervals. This is accomplished by providing homogenous test samples to participating laboratories on a regular basis for data analysis and reporting. A Proficiency Testing scheme has the main goal is to assist the participating laboratory in assessing the correctness of its test results.

The material under testing, the testing method that is being used, and the number of testing laboratories participating to the Proficiency Testing all influence the testing methodologies. These methodologies must all have the ability to compare the results produced by one testing laboratory with those provided by other testing laboratories. One of the participating laboratories may responsible for supervising and coordinating certain programs.

— Benefits Inter–Laboratory Comparisons/Proficiency Testing (ILC/PT)

As earlier discussed inter–laboratory comparisons (ILC) need two or more laboratories to organize, conduct, and evaluate tests on the same or comparable samples under pre–determined conditions, while Proficiency testing (PT) is a method of evaluating participant performance by comparing results from different laboratories. Participation in PT activities provides laboratories with several benefits in addition to achieving ISO/IEC standards.

Besides the accreditation requirements, different parties, such as regulators, direct customers, indirect customers, and professional bodies, have a strong interest in the laboratory Proficiency Testing. In addition, external stakeholders, as well as laboratory employees and management, gain trust as a result of successful involvement in ILC/PT operations. Achievement of proficiency testing provides an external assessment of the laboratory testing or measuring skills, which complements the laboratory's internal quality control operations. When a laboratory agrees to have its testing or measurement performance reviewed using PT, it gives interested parties more credibility and respect.

Another important advantage is that laboratories can compare their performance to that of other participating facilities using Inter–Laboratory Comparisons and Proficiency Testing data. Furthermore, ILC / PT may be used to compare analytical data gathered using various methodologies, contributing to the quality of services in the long–term. The laboratory may compare new methods to current procedures or conduct a trial run of a new or irregularly executed process in the laboratory. ILC / PT findings can also help validate a method by proving its precision and accuracy and giving useful information for estimating measurement uncertainty.

LC and PT efforts can be employed to demonstrate laboratory advanced capabilities, validating competent technique performance, or to compare operator capabilities, supplying operator repeatability data, for the measurement of uncertainty estimations. Confirming competent performance offers confidence to laboratory management with assurance that the laboratory's performance is adequate, or notifies the management to possible difficulties in certain areas of the laboratory.

Participation in ILC and PT offers management with external monitoring of the management system's continued effectiveness in regard to key tests or metrics. The review and analysis of proficiency testing results might also result in additional people education, training, and competence monitoring. Participation in specific ILC and PT may also be utilized to assign the certified value and to assess the uncertainty of this value for certified reference materials. A well–designed PT strategy helps guarantee that the laboratory gets the most out of PT involvement and the data provided by PT activities.

When novel measurement technologies are developed, that are based on new concepts with application in the field of environmental protection or agriculture, it is needed a testing methodology performed with the proper equipment in several conditions and for several laboratories. There is a need for research organizations to adopt quality management system in research testing laboratories as an asset, to improve not also the management, but also the technical and scientific competence (Nenciu et al., 2021; Mircea et al 2020).

If a laboratory is required to participate in an inter–laboratory comparison of a calibration "type" that covers a wide range of instruments / quantities there should be a four–year plan that addresses a different calibration each time (Softic et al., 2012).

Only in the event that a calibration service from a certified laboratory is unavailable, services provided by an external calibration laboratory without certification are permitted. When no accredited calibration laboratory services are available for highly specialized test equipment, the equipment may be calibrated by the manufacturer as long as the used calibration standards are traceable to national or international units of measurement, the traceability chain is recognized, and an estimate of measurement uncertainty is included on the calibration certificate (Walczak–Zlotkowska et al., 2016; Nenciu et al., 2014).

For quality testing, measuring equipment accuracy and constraints/tolerances and traceability are critical matters. Measurement traceability refers to the value of measurement findings or the value of a standard in relation to existing references, which is maintained by an unbroken chain of comparison of all these uncertainties. Traceability exists only when properly scientific records indicate that the measurement is continuous and validated by findings, for which entire measurement uncertainty has been determined (Zaimovic–Uzunovic, 1999). The rank of the operations carried on the apparatus, as well as the variable metrological parameters and rankings for the laboratory to which the traceability requirement applies, must be specified during the procedure. Because all measurements are time–dependent, traceability identifies the measurement method and related measurement uncertainties for the present measurement result, which must be preserved in the traceability documentation. Because measurement uncertainty is the core of creating traceability, it is very important for building methodologies for assessing measurement uncertainty under various measurement settings (Ehrlich, 1998).

There is widespread agreement on the significance and benefit of testing laboratories implementing a Quality Management System (QMS) to support their work, whether it is industrial or research–based. Due to the unique nature of their work, laboratories involved in R&D testing have unique challenges in implementing a QMS. Researchers and professionals have long debated whether or not a Quality Management System (QMS) should be implemented in research testing facilities (Martinez–Perales et. al., 2021; Lemes et al., 2012).

— Elements to be followed by the parties participating to the tests

There are a few key principles that all of the parties involved must follow (Boley, 2000):

≡ The Proficiency testing scheme in which a laboratory participates should resemble as closely as possible the laboratory's routine work in terms of test samples, substances and levels; any variations should be noted and accounted for;

≡ Performance in a PT scheme should be placed in the correct context and in the proper perspective;

≡ Wherever feasible, the performance of a laboratory across numerous rounds of a PT scheme should be examined.

≡ The documentation and statistical protocol should always be read, in order to better understand how the scheme operates

≡ If needed, should communicate with the scheme coordinator to get a better understanding of the scheme and how it works.

CONCLUSIONS

The correct use and interpretation of Proficiency testing (PT) scheme results is complex and requires the evaluation of a large amount of data. As a result developing a good understanding of proficiency testing, in order to use the

information in a more sophisticated and suitable manner is sometimes difficult for laboratory operators, particularly for those with a relatively limited technical background. It is therefore essential that interpretation of proficiency testing scheme to be carried out and interpreted in an appropriate manner. This is important not only for laboratory personnel and management, but also for the entities who use their results, including accreditation bodies, public institutions, partners and the laboratory customers.

As part of an overall quality plan, a frequent independent examination of a laboratory technical performance is advised as an important way of verifying the validity of analytical measurements. Independent proficiency testing (PT) programs are a typical way to this evaluation. A PT scheme is a technique for objectively reviewing laboratory findings by external sources, which includes comparing a laboratory's results with those of other laboratories at regular intervals.

However, as a quality assurance technique for laboratories, proficiency testing is becoming increasingly important. The performance of laboratories evaluated in Proficiency Testing systems is increasingly being applied as a measure of laboratory competence and quality, especially by accreditation agencies. It is critical for laboratories to have detailed knowledge of the scope, range and availability of proficiency testing programs in the regions they operate. As a result, they will be capable of making appropriate decisions about the scheme where they should participate, in order to obtain the best results. As a result, laboratories must establish a solid understanding of proficiency testing, including what the goal are and how the evidence from proficiency testing schemes must be reviewed and used. This is essential not just for scientific employees and management, but also for those who employ the laboratory's results, such as accreditation authorities and customers.

Acknowledgement

References

[1] Basic, H. Softic, A. (2010). The Importance of Interlaboratory Comparison in Length Measurement as a Prerequisite for Raising the Accuracy of Measurement and Development of Measurement Traceability, 14th International Research/Expert Conference "Trends in the Development of Machinery and Associated Technology" TMT 2010, Mediterranean Cruise, 2010, 185–188.

[2] Boley, N. (2000). EURACHEM: Selection, Use and Interpretation of Proficiency Testing (PT) Schemes by Laboratories, Testing Mirror Group LGC, Queens Road, Teddington, Middlesex, TW11 0LY, United Kingdom, English Edition 1.0, 2000.

[3] Ehrlich, C. Rasbery, S. (1998). Metrological Timelines in Traceability, I.Res. Just. Stand.Technol., 103, 93.

[4] Galliana F., (2019). Measurement Comparisons: A Tool to Guarantee the Reliability of Measurement Systems and of High–Tech Industry, IEEE Instrumentation & Measurement Magazine, 62–66.

[5] Ghernaout, D., Aichouni, M., Alghamdi, A. (2018). Overlapping ISO/IEC 17025:2017 into Big Data: A Review and Perspectives, International Journal of Science and Qualitative Analysis, 4(3), 83–92.

[6] Hogan, R., (2019). Proficiency Testing and Interlaboratory Comparisons: The Ultimate Guide to ISO/IEC 17025, https://www.isobudgets.com/proficiency–testing–and–interlaboratory–comparisons/

[7] ISO 5725–2:2019, Accuracy (trueness and precision) of measurement methods and results — Part 2: Basic method for the determination of repeatability and reproducibility of a standard measurement method.

[8] Koch, M., Metzger, J. (2001) Definition of assigned values for proficiency tests in water analysis. Accred Qual Assur, 6, 181–185

[9] Lemes, S., Zaimovic–Uzunovic, N, Alisic S., Memic, H. (2012). Development of Competences of National Reference laboratory for mass measurement, %th international Symposium of Industrial Engineering, 273–276.

[10] Martinez‑Perales, S., Ortiz‑Marcos, I., Ruiz, J.J. (2021). A proposal of model for a quality management system in research testing laboratories, Accreditation and Quality Assurance, 26, 237–248

[11] Mircea C., Nenciu F., Vlăduţ V., Voicu G., Cujbescu D., Gageanu I., Voicea I., Increasing the performance of cylindrical separators for cereal cleaning, by using an inner helical coil, INMATEH Agricultural Engineering, 62 /3 (2020), 249–258.

[12] Nenciu, F. Vaireanu, D.I. (2014). A Versatile System for Indoor Monitoring Of Some Volatile Organic Compounds, Revista de Chimie, 65, 5, 565–569.

[13] Nenciu, F., Vladut, V., (2021). Studies on the perspectives of replacing the classic energy plants with Jerusalem artichoke and Sweet Sorghum, analyzing the impact on the conservation of ecosystems, IOP Conference Series: Earth and Environmental Science, 635, 012002

[14] Softic, A. Zaimovic–Uzunovic, N. Basic, H. (2012). Proficiency testing and interlaboratory comparisons in laboratory for dimensional measurement, Journal of Trends in the Development of Machinery and Associated Technology 16, 1, 2012, 15–118

[15] Voiculescu, R.M., Olteanu, M.C., Nistor V.M. (2013). Design and operation of an interlaboratory comparison scheme, nuclear – 2013, 95–103.

[16] Walczak–Zlotkowska, J. Starczewski, M., Lysko, J.M. (2016). Appropriate calibration intervals of laboratory test equipment in accordance with the international iecee regulations and ite predom division activity, IAPGOŚ 3/2016, 16–19

[17] Zaimovic–Uzunovic, N., (1999). Influence of time on traceability in national institutes, Zenica, 11 (12), 253–260.

[1.]Ana–Maria TĂBĂRAŞU, [2.]Sorin Ştefan BIRIŞ, [1.]Iuliana GĂGEANU,
[1.]Dragos ANGHELACHE, [1.]Carmen BĂLŢATU, [1.]Cătălin PERSU

METHODS OF EXTRACTING THE ACTIVE PRINCIPLES FROM MEDICINAL AND AROMATIC PLANTS – A REVIEW

[1.]National Institute of R&D for Machines and Installations Designed to Agriculture and Food Industry (INMA), Bucharest, ROMANIA
[2.]University Politehnica of Bucharest, ROMANIA

Abstract: Medicinal plants are gaining much interest recently because their use in ethno–medicine treating in common disease such as cold, fever and other medicinal claims are now supported with sound scientific evidences. A wide range of technologies is available for the extraction of active components and essential oils from medicinal and aromatic plants. The choice depends on the economic feasibility and suitability of the process to each particular situation. Bioactive compounds from medicinal plants were synthesized using effective extraction methods which have important roles in the pharmaceutical product development. In this paper will be presented some methods of extraction of active principles from medicinal and aromatic plants.
Keywords: medicinal plants, active components, bioactive compounds, extraction methods

INTRODUCTION

Plants were once considered as a daily food. Now, plants are popular used as a common source in medicinal agents, food additives, cosmeceuticals and nutraceuticals. Although, the medicinal properties of plants have gained attention, many research studies are still conducted to discover their values because the utilisation of synthetic drugs to heal or control most chronic diseases have caused several long–term effects. There is rising approach regarding the application of herbal medicinal plants in treating diseases with minimal or no aftereffects. Therefore, the extraction of bioactive compounds from herbal medicinal plants offers great potentials for new drug discoveries (Nur Amanina Abd Aziz et al., 2021).

These therapeutically useful medicinal compounds in plants are extracted or separated by using selective solvents through a standard procedure. Generally, the extraction techniques can be divided into two categories, namely classical technique and modern technique. The former technique faces several limitations, such as the use of excess solvents, time–consuming and a long heating time which could risk the degradation of bioactive compounds. In most cases, extraction by using these solvents was hazardous and toxic to human health and the environment.

Organic solvents release greenhouse gases into the environment, threatening humans, agriculture and microorganisms. Moreover, the usage of excess solvent produces a large amount of waste by–products. Contrary to the hazardous classical techniques, environmentally friendly extraction approaches like 'green solvents', 'green processing' and 'green product' are favoured.

Green extraction methods should be applied to encourage efficient and safe extraction method. Green extraction methods reduce energy consumption which allow the use of alternative solvents and renewable natural sources to produce a safe and high–quality product. Therefore, these modern extraction techniques are considered as green processing. These techniques reduce the usage of organic solvents, minimise bioactive compounds degradation in the sample and improve extraction efficiency (Nur Amanina Abd Aziz et al., 2021; Antigoni Oreopoulou et al., 2019).

The increased population led to a higher utilization of these plants, so their residues are proportional, with a huge amount of biomass generated as by–products, representing a growing market in the natural–based products. The general use of MAPs all over the world is not homogenic, due to different factors:

≡ in developed countries, even if the demand for natural treatments is high, profits of the growers and producers remain low because of the existing intermediaries which increase the price, as well as the lack of organization and networking by the poor collectors of medicinal plants from the wild;

≡ rigorous regulations and documentations requirements; and

≡ in less developed countries, there are poor traceability mechanisms from plant to population (Pruteanu A et al., 2014).

In addition to traditional medical applications of medicinal and aromatic plants, there is the possibility of using them in cosmetic products, feed or food additives and preservatives, or as a viable tool for biotechnological applications, such as the enhancement of secondary metabolites by genetic engineering (Radu Claudiu Fierascu et al., 2021).

Extraction, as the term is used pharmaceutically, involves the separation of medicinally active portions of plant or animal tissues from the inactive or inert components by using selective solvents in standard extraction procedures. The products so obtained from plants are relatively impure liquids, semisolids or powders intended only for oral or external use. These include classes of preparations known as

decoctions, infusions, fluid extracts, tinctures, pilular (semisolid) extracts and powdered extracts. Such preparations popularly have been called galenicals, named after Galen, the second century Greek physician.
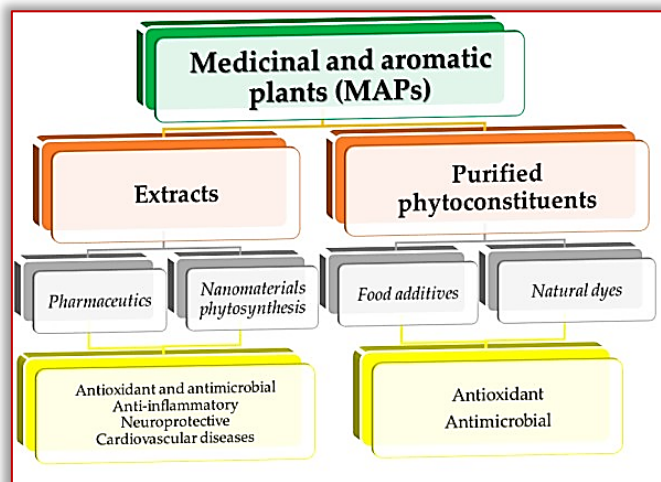
Figure 1. Some of the potential applications of medicinal and aromatic plants (Radu Claudiu Fierascu et al., 2021)

The purposes of standardized extraction procedures for crude drugs are to attain the therapeutically desired portion and to eliminate the inert material by treatment with a selective solvent known as menstruum. The extract thus obtained may be ready for use as a medicinal agent in the form of tinctures and fluid extracts, it may be further processed to be incorporated in any dosage form such as tablets or capsules, or it may be fractionated to isolate individual chemical entities such as ajmalicine, hyoscine and vincristine, which are modem drugs. Thus, standardization of extraction procedures contributes signifi cantly to the final quality of the herbal drug (S. S. Handa et al., 2008; Romulus Gruia, 2015).

An overview of the results recorded in recent years in the field of medicinal and aromatic plants and the analysis of statistical data show a clear increase in the interest of consumers and businesses to the green pharmacy.

The activity of production and marketing of medicinal plants grown from spontaneous flora has become a large economic activity, being a source of income for producers, traders, but also for various processors.

In Romania, the general framework for the production, processing and organization of the market for medicinal and aromatic plants, the relations between producers, processors and traders is established by the Law on Medicinal and Aromatic Plants (Law 491/2003), and Order 244/2005 regulates the processing, processing and the marketing of medicinal and aromatic plants used as such, partially processed or processed in the form of pre–dosed food supplements.

In the production of medicinal and aromatic plants the quality of the products is given by the content in active principles. The amount of active principles in the plant is conditioned by ecological factors, the zoning of the species, the cultivation technology, the biological value of the cultivar (population, variety, hybrid, etc.) and last but not least, the processing (processing) (Romulus Gruia, 2015; Țuia Steluța, 2021).

MATERIALS AND METHODS

Plant extracts are fluid soft or dry pharmaceutical / phytopharmaceutical preparations obtained by extracting plant products with different solvents. In recent years, emphasis has been placed on the pharmaceutical and therapeutic revaluation of herbal preparations through a good knowledge of the physico–chemical and therapeutic properties of the active principles in medicinal plants and by the development of extraction techniques and quality control means.

Extracts obtained from medicinal plants can be classified according to several criteria, as can be seen in the table below (Țuia Steluța, 2021).

Table 1. Extracts obtained from medicinal plants (Țuia Steluța, 2021)

Classification criterion	The name of the extract	Remarks
By the nature of the solvent	Extract aqueous Hydroalcoholic extract Extract oils Medicinal vinegars Medicinal wines	–
According to the method of obtaining	Selective extract Non–selective extract Extract obtained by pressing or centrifugation	Selective extracts cannot be considered to be entirely natural preparations, as they are hyperconcentrated and without identical patterns in nature.
After the preparation operation	Simple extract Successive extract Multiple extract	–
After the parts of the plant subjected to extraction	Partial extract Total extract	–
According to the humidity of the plant	Extract obtained from the dried plant Extract obtained from fresh plant	–

Solvent extraction is the most widely used type of extraction for bioactive plant compounds. This separation technique involves the extraction of components from a solid or semi–solid sample in a suitable solvent. In the extraction operation, the choice of solvent is made depending on the nature of the substance to be extracted and the nature of the raw material. The actual solubilization of bioactive compounds is achieved by treating the finely chopped plant with water, saline solutions, hydroalcoholic solutions, etc. The chemical nature of the optimal extraction medium, its molarity and pH, as well as the time required for optimal extraction are determined experimentally (Țuia Steluța, 2021).

In the preparation of extracts, in particular, the influence of the following factors must be taken into account:

≡ Nature of the solvent: solvents must dissolve and extract most of the active components in a high yield and contain as few inert materials as possible without therapeutic value; the most used solvents used in the plant extract industry are: water (for alkaloid salts, glycosides, sugars, proteins, enzymes, tannins, etc.), 50% or 70% alcohol (for biofertilizers, hydrocarbons, tannins, base alkaloids and salts of glycosides, resins, chlorophyll, etc.), ethyl ether (for base alkaloids, resins, biofertilizers, etc.), oil, wine, vinegar;

≡ Degree of crushing of the plant: the more advanced the plant product is brought to a degree of crushing, the larger the contact surface, so the extraction is complete; for aqueous extractive solutions it is recommended to grind according to the plant product;

≡ The ratio between the amount of plant and solvent: the Romanian Pharmacopoeia provides concentrations of up to 6% for aqueous extracts, 20% for most tinctures and 10% for tinctures prepared from plant products containing highly active substances;

≡ Contact time between plant and solvent: differs depending on the extraction technique applied, but also on the type of extract; for aqueous extracts it is 5–6 hours, and for alcoholic ones 6–10 days;

≡ Shaking effect: shaking shortens the time to obtain the extract;

≡ The temperature at which it is worked: it positively influences the extraction efficiency, due to the increased solubility of the hot active principles; The Romanian Pharmacopoeia provides for the extraction of thermostable principles, at a temperature of 90 – 100 ° C, in the case of infusions and decoctions;

≡ Separation of the mixture and how to recover the active compounds from the solid residue.

In the case of preparation of aqueous or hydroalcoholic extractive solutions by maceration, the degree of crushing plays a very important role. This correlated with the nature of the solvent used and the intensity of stirring determines the contact time for the extraction of soluble components until the concentration balance between the solid phase and the liquid phase is reached (Sukhdev Swami Handa, 2008; Ţuia Steluţa, 2021).

RESULTS

Extraction can be performed by batch processes (maceration, percolation, infusion, decoction, as well as new high–performance methods: accelerated solvent extraction, microwave–assisted extraction, supercritical fluid extraction) and continuous processes (continuous extraction with organic solvents, continuous percolation, Soxhlet extraction) (Ţuia Steluţa, 2021; Popova A, 2018).

— **Maceration**: consists in treating the crushed vegetable product with a required amount of solvent, keeping in contact for a certain period (macerated in water 8–12 hours), simultaneously with continuous or intermittent stirring and then separating the extractive solution from the residue by filtration or settling; in the case of macerations in other solutions (alcohol, oil, wine, vinegar), the maceration time increases, reaching a few weeks.

Maceration is applied especially in the case of extraction of easily cold–soluble and thermolabile principles. Maceration can be done:

≡ in the cold (17–22 ° C).
≡ hot (called digestion) at 40–60 ° C (Popova A, 2018; Ţuia Steluţa, 2021).
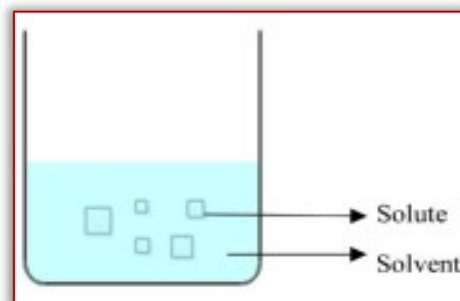
Figure 2. Example of maceration extraction method
(Nur Amanina Abd Aziz et al., 2021)

— **Percolation**: the process by which the active principles are extracted from plants, cold, using solvent in countercurrent. The process takes place as follows: before the solvent becomes saturated in the extracted active ingredients, it is displaced by another layer of solvent in which the plant product undergoes a short maceration and yields another part of the active ingredients. This phenomenon is continuous, each portion of solvent added coming into contact with the plant product until its complete depletion (Ţuia Steluţa, 2021).

Soxhlet extraction is a common conventional method used for extracting heat–stable compounds. The advantage of this method is that large amounts of drug can be extracted with a much smaller quantity of solvent. This is tremendously economic in terms of time, energy, and consequently financial inputs. The Soxhlet extractor consists of a distillation flask, an extractor, and a condenser. The solvent in the distillation flask is heated and the resulting vapor is condensed in the condenser. The condensed solvent from the condenser fills into the thimble holder containing the sample that needs to be extracted.

When the solution in the extractor reaches the overflow level, a siphon aspirates the solution of the thimble holder and unloads it back into the distillation flask, carrying dissolved solute into the bulk liquid. The solute is left in the distillation

flask while the solvent is evaporated, condensed, and passed back into the sample solid bed.

This process is repeated 3–5 times or until a complete extraction is achieved (Popova A., 2018).
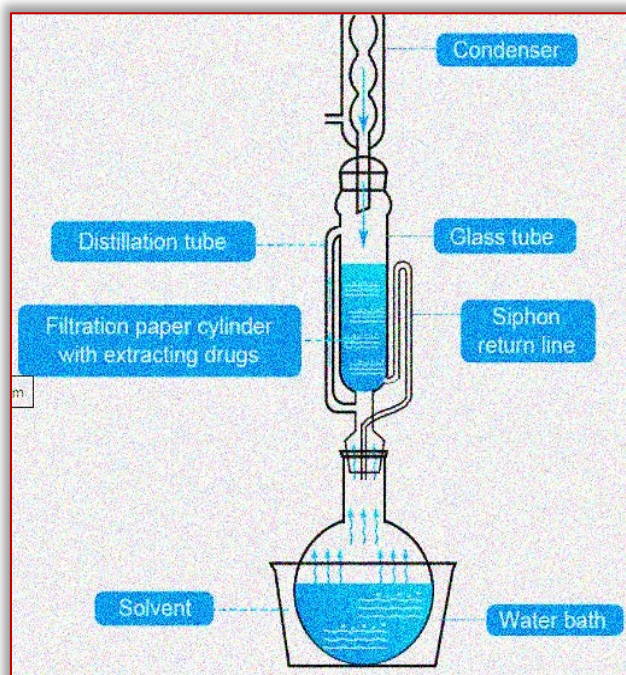
Figure 3. Soxhlet extractor (Ţuia Steluţa, 2021; Popova A., 2018)

— **Infusion**: consists in wetting the crushed plant product with water, except for plant products containing biofertilizers which are moistened with a dilute alcohol solution; after about 5 minutes add the mass of water provided, heated to boiling and leave in contact for 30 minutes [5]. After the infusion time has elapsed, the solution is filtered. In general, the infusion is used in the case of plant parts that have thinner cell walls (flowers, leaves, herbaceous parts) (Ţuia Steluţa, 2021).

Infusion and decoction use the same principle as maceration; both are soaked in the cold/boiled water. The maceration period for infusion is shorter, and the sample is boiled in specified volume of water (e.g., 1:4 or 1:16) for a defined time for decoction, however. An infusion is a dilute solution that contains readily soluble constituents prepared by short period of sample maceration (steeping) in cold/boiling water. Heat–sensitive compounds are recommended to be extracted by cold water.

Infusion (the folk method) is made using tablespoon of fresh/dried herbs per cup of boiled water. The aerial parts are mainly used and steeped for 2–10 min, covered. Common herbal infusions are aromatic plants, including mint, chamomile, lavender, and ginger. Nourishing herbal infusion (folk method) is produced for a minimum of 4 hours of steeping dried herbs in a 1:10 herb: water ratio. This should extract most of the minerals contained in the plant. Popular nourishing herbal infusions are made from U. dioica, Avena sativa, and Trifolium pretense (Danciu A et al., 2011; Popova A, 2018).

— **Decoction**: the preparation technique is similar to that of infusions: the chopped vegetable product will be soaked in 5 parts cold water; soak for 5 minutes and then add the remaining hot water to the required proportion (1% or 5%) after which it is heated on the water bath for 30 minutes (boiling). At the end, strain and wash the residue to the prescribed volume (medicinal plants with a high content of essential oils will be moistened with 50 ° C alcohol, then hot water will be added). In phytotherapy, the decoction is made in the case of plant organs (roots, rhizomes, bark, etc.) from which the principles are more difficult to extract (Ţuia Steluţa, 2021; Popova A, 2018).

— **Alcoholic extraction by fermentation**: The active principles contained in some medicinal preparations are obtained by extraction in a fermentation process. The extraction procedure involves soaking the plant material either in the form of a decoction or in a ground state, for a certain period of time, during which the fermentation and generation of alcohol takes place in situ; this facilitates the extraction of the active substances contained in the plant material. The alcohol thus generated also has a preservative role. On an industrial scale, wooden vats, porcelain vessels or food grade stainless steel vessels are used (Ţuia Steluţa, 2021; Popova A, 2018).

— **Continuous extraction with organic solvents**: The principle of extraction is simple. The components present in the crude raw material are extracted by dissolving in the liquid–solvent. The raw material is placed in a specially built extractor, and the solvent must be continuously recycled through the mass of plant material (Ţuia Steluta, 2021; Popova A, 2018).

— **Accelerated solvent extraction (ASE)** is a new extraction method, based on the use of high temperature and pressure to accelerate the dissolution kinetics and break the analytical interaction bonds (Ţuia Steluţa, 2021; Popova A, 2018).
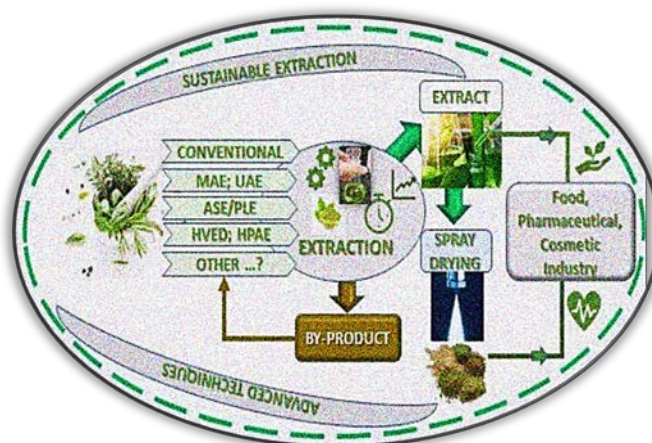
Figure 4. Sustainable extraction with advanced techniques (Popova A., 2018)

— **Microwave assisted extraction (MAE)** is suitable for the recovery of a vast array of compounds and is recognized as a versatile and efficient extraction technique of secondary plant metabolites. A lot of examples suggested

that MAE has some considerable merits such as shorter extraction time, higher extraction yield, and less solvent consumption compared to conventional extraction methods. MAE utilizes microwave energy to facilitate partition of analytes from the sample matrix into the solvent. Microwave radiation interacts with dipoles of polar and polarizable materials (e.g., solvents and sample) causes heating near the surface of the materials and heat is transferred by conduction.

Dipole rotation of the molecules induced by microwave electromagnetic disrupts hydrogen bonding; enhances the migration of dissolved ions, and promotes solvent penetration into the matrix. In non–polar solvents, poor heating occurs as the energy is transferred by dielectric absorption only. MAE of plant secondary metabolites may be affected by a large variety of factors, such as power and frequency of microwave, duration of microwave radiation, moisture content and particle size of plant samples, type and concentration of solvent, ratio of solid to liquid, extraction temperature, extraction pressure, and number of extraction cycles. MAE was currently regarded as a robust alternative to traditional extraction techniques (Popova A, 2018; Azwanida NN, 2015).

Figure 5. Extraction of phytocompounds from the medicinal plant Clinacanthus nutans Lindau by microwave–assisted extraction and supercritical carbon dioxide extraction (Popova A., 2018)

Figure 6. Microwave–assisted extraction (Nur Amanina Abd Aziz et al., 2021)

— **Ultrasound–assisted extraction (UAE)** is one of the most important techniques used for the extraction of valuable compounds from plant materials and is quite adaptable on a small or large scale (eg in the laboratory or on an industrial scale). Comparing this technique with others, such as microwave assisted extraction (MFA), the ultrasound device is cheaper and easier to handle (Ţuia Steluţa, 2021; Popova A, 2018).
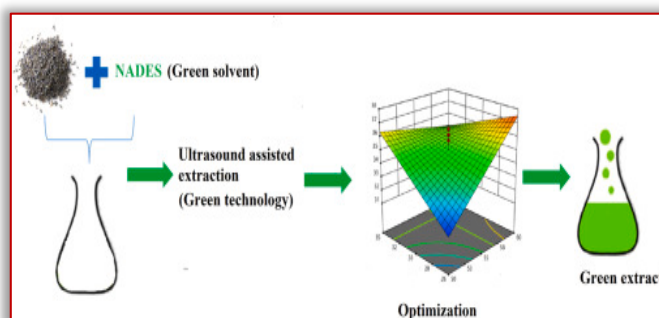
Figure 7. Ultrasound–assisted extraction of antioxidant phenolic compounds from Lavandula angustifolia flowers using natural deep eutectic solvents (Popova A., 2018)

— **Supercritical fluid extraction** has been developed in recent years for analytical use, as an alternative to conventional solvent extraction. In practice, more than 90% of supercritical fluid extractions are performed with CO_2 for several practical reasons (Ţuia Steluţa, 2021; Popova A, 2018).
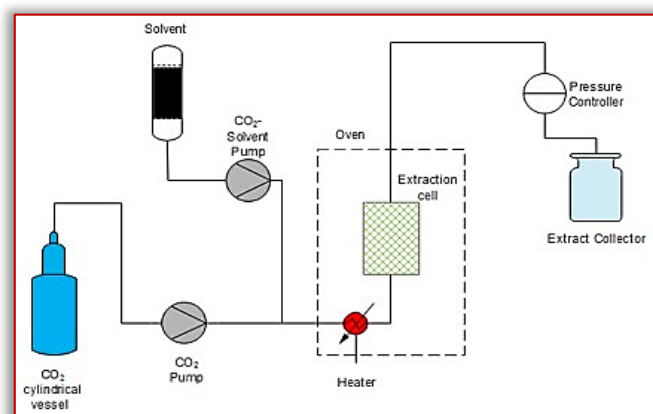
Figure 8. Supercritical fluid extraction (SFE) (Nur Amanina Abd Aziz et al., 2021)

CONCLUSIONS

All stages of extractions, from the pre–extraction and extraction are equally important in the study of medicinal plants. The sample preparation such as grinding and drying affected the efficiency and phytochemical constituents of the final extractions; that eventually have an effect on the final extracts. It can be concluded that, no universal extraction methods is the ideal method and each extraction procedures is unique to the plants.

The improvement of the extraction methods is essential for the most comprehensive obtaining of the compounds of bioactive substances from the vegetal resources, simultaneously with the isolation and standardization of each component substance of the extract.

The technologies regarding the extraction of the active principles and of conditioning of the vegetal extracts will allow to raise the qualitative level of the processing, with the possibility of obtaining innovative foods.

Advanced techniques for obtaining extracts of bioactive plant compounds offer wide applicability in the food,

pharmaceutical, textile or cosmetic industries, meaning, lead to innovative foods such as functional foods, nutraceuticals, composite foods of excellence, and, can be used in the manufacturing process of certain drugs, natural food or industrial pigments, food or cosmetic flavors, etc.

References
[1]   Antigoni Oreopoulou, Dimitrios Tsimogiannis and Vassiliki Oreopoulou, 2019 – Extraction of polyphenols from aromatic and medicinal plants: An overview of the methods and the effect of extraction parameters;

[2]   Azwanida NN, 2015 – A review on the extraction methods use in medicinal plants, principle, strength and limitation;

[3]   Danciu A., Postelnicu E., Vladut V., Voicea I., Matache M., Ludig M., Martinov M., Atanasov A., Florea C., 2011 – Testing the manufacturing technology and equipment for medicinal and aromatic plant processing. Obtaining the active–principle extracts out of medicinal plants, vol. 34, no.2, INMATEH;

[4]   Nur Amanina Abd Aziz, Rosnani Hasham, Mohamad Roji Sarmidi, Siti Hasyimah Suhaimi, Mohamad Khairul Hafiz Idris, 2021 – A review on extraction techniques and therapeutic value of polar bioactives from Asian medicinal herbs: Case study on Orthosiphon aristatus, Eurycoma longifolia and Andrographis paniculate;

[5]   Pruteanu A., Muscalu A., Ferdeş M., Efficiently extraction of bioactive compounds from medicinal plants using organic and sustainable techniques, 3nd International Conference on Thermal Equipment, Renewable Energy and Rural Development, TE–RE–RD, 12–14 iunie, 2014, Mamaia, România, p. 297–302.

[6]   Popova A., Mihaylova D., 2018 – A review of the medicinal plants in Bulgaria – collection, storage, and extraction techniques;

[7]   Radu Claudiu Fierascu, Irina Fierascu, Anda Maria Baroi, Alina Ortan, 2021 – Selected aspects related to medicinal and aromatic plants as alternative sources of bioactive compounds;

[8]   Romulus Gruia, Dumitru Lazurca, 2015 – Research on improving methods for extracting bioactive compounds from plant products / Cercetări privind perfecţionarea metodelor de extracţie a compuşilor bioactivi din produse vegetale;

[9]   S. S. Handa, Suman P.S. Khanuja, Giuseppe Longo, D.D. Rakesh, 2008 – An overview of extraction techniques for medicinal and aromatic plants;

[10]   Sukhdev Swami Handa, Suman Preet Singh Khanuja, Gennaro Longo, Dev Dutt Rakesh, 2008 – Extraction technologies for medicinal and aromatic plants;

[11]   Ţuia Steluta – 2021, Research on obtaining biofertilizers through the percolation process, Dissertation, Polytechnic University of Bucharest / Cercetări privind obţinerea biofertilizanţilor prin procesul de percolare, Lucrare de disertaţie, Universitatea Politehnica din Bucureşti.

[1.]Gabriela MATACHE, [1.]Valentin BARBU, [1.]Ioan PAVEL, [2.]Mihai IONEL, [3.]Mihai OLAN

INTELLIGENT DRIVE INSTALLATION FOR BIOMASS CONVEYOR

[1.]INOE 2000 – Subsidiary Hydraulics and Pneumatics Research Institute (INOE 2000–IHP) Bucharest, ROMANIA
[2.]S.C. CORNER PROD S.R.L., ROMANIA
[3.]National Institute of Research – Development for Machines and Installations Designed to Agriculture and Food Industry – INMA, Bucharest, ROMANIA

Abstract: On the market there are biomass conveyor solutions where the electric drive installation does not notice the imminent blockage in the conveyor piping, ensures only its stopping when overcoming an overload. The work presents the way in which the functioning of the motor reducer can be improved by operating it by means of a converter, with speed adjustment and anti–locking system, but without a monitoring based on a warning and parameter recording system during operation it is not known where the problems arise, what is actually the necessary torque, why the peak torque appears, how long does a peak last. It is necessary to perform predictive maintenance and eventually to integrate into a fully automatic system. This installation has been developed by INOE 2000–IHP together with S.C. CORNER PROD S.R.L. The solution can be applied both for individual equipment and for a large number of machines that can be monitored remotely on a smart phone or computer. The results are based on models developed by manufacturers of engines and reducers. All information is recorded and can be available in an easy–to–use way on the smart phone or computer app.
Keywords: intelligent drive, biomass, conveyor, automation

INTRODUCTION

Due to the dimensional inequality of the biomass passed through a conveyor, it can get stuck in its piping. This locking leads to excessive heating of the reducer, burning of the drive motor, destruction of the reducer seals, loss of lubricant, destruction of the gear reducer and breakage of its housing. Of course, a problem is the insufficient torque in the engine for the current mode of use, the time capable and the service factor too small at the reducer, but there may be other problems related to improper use, wear, lack of alignment, voltage variations, unbalanced phases or insufficient installed power. In case of such failures, the technological flow is interrupted, with major economic effects. To reduce the risk of blockages, the drives are greatly oversized. This solution is totally uneconomic, and when the blockage of the material occurs, the time required for weave is much longer.

In general, at low power, at this moment the problem is solved by oversizing the engines and reducers, but in the conditions in which it is necessary to use engines with premium efficiency (increased) to decrease the energy consumption, the oversizing approach is a matter of the past, especially as the energy is expensive and the reactive energy charges the bills even more. For this reason, it is necessary to monitor and optimize these drives.

Big problems occur in medium and large drives, where powers of over 3kW–4kW are common (Narayan, S., 2015). Depending on the type of conveyor, molten reducers are generally used for low power and especially for screw or inclined strips, pendulum reducers (cylindrical with parallel axes) for screw, conical–cylindrical reducers for strips, orthogonal reducers for operating biomass blenders (it actually has the role of bringing it to the biomass evacuation area at the same time as mixing).

In the working process of agricultural equipment, the supervision of their operation in optimal operating parameters is a complex process and requires for the operators extended working time, increased attention, concentration and knowledge in the field (Gandjbakhch, E. et al., 2020). However, they cannot notice the sensitive functioning problems (Caixal, G. et al., 2021) by which major defects can be avoided. Meeting the needs of reliable equipment with active assisted operation based on intelligent supervision (Hassan, M.M. et al., 2020) is a priority for researchers.

Luz E. et al. (2021) introduced an intelligent algorithm in the management of agricultural equipment. The monitoring system surveys the status of use and lease of the equipment. Good results have been achieved and work efficiency has been improved (Luz, E. et al., 2021).

MATERIALS AND METHODS

On the market there are biomass conveyor solutions where the electric drive installation does not notice the imminent blockage in the conveyor piping, ensures only its stopping when overcoming an overload. Researching the current situation of the market, we found that there is room for improvement which meets the needs of users (Stojanovic, N. et al., 2018)

There are extremely expensive general solutions. An example is the monitoring system using the vibration and temperature sensor QM42VT1. It is designed for monitoring pumps, compressors and engines of different sizes. Data can be collected from multiple engines, evaluated, centrally displayed and, if necessary, related to alarm actions for timely warning of imminent damage. Users can use radio technology to connect the vibration and temperature sensor QM42VT1 with the high–performance HMI TX700 device for this purpose.

The sensor, figure 1, detects vibration and temperature values. Changes in temperature or vibrations occur when in that transmission the screws through which the engine is

fixed have been loosened, causing the wrong alignment of the shaft, it is a blocked bearing or an imbalance has occurred, mechanical vibrations can signal problems such as these.
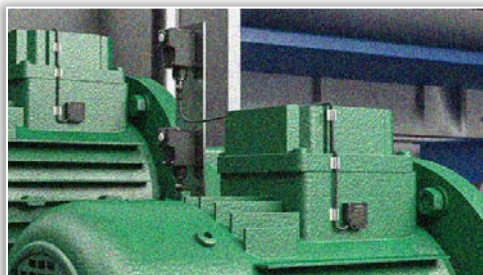
Figure 1 – Sensor mounting mode and data display

The QM42VT1 vibration and temperature sensor detects vibrations with a high level of accuracy. For this purpose, the compact sensor based on MEMS (micro–electromechanical system) is simply mounted directly on the engine block through a magnetic support. From there, it offers data on speed and acceleration on two dimensions in different frequency ranges. Changes to the measurement data can then be used to identify different problems in operation (Lacatus, P. et al., 2021).

Figure 2 – Optimal Schaeffler System

Measuring the temperature of the engines is also vital, since a significant increase in temperature could be an indication of insufficient wear or lubrication for the bearing. The IP67 sensor also detects working temperatures in the measurement range from –40°C to +105°C. Another very new system is Schaeffler OPTIME, which is now under testing at the Schaeffler factory in Brasov.

The Schaeffler OPTIME solution developed by the bearing manufacturer Schaeffler in collaboration with Siemens, monitors the behavior of the bearings in the machines by measuring vibrations and temperature at a distance of up to 500mm from the bearing, then transmits the data and its interpretation, taking into account the existing database for bearings.

THE CONSTRUCTIVE SOLUTION OF THE INTELLIGENT DRIVE INSTALLATION FOR BIOMASS CONVEYER

The solution developed and realized by INOE 2000 together with the partner company CORNER PROD aims to continuously monitor the state of the system (voltage, absorbed current, temperature, and power), developed for biomass conveyers of different types, recommended for a range of gear motors and reducers with speed between 2 rpm and 1400 rpm. The solution can be applied both for individual equipment and for a large number of machines that can be monitored remotely on a smart phone or computer.

The data collecting is done through sensors for monitoring the absorbed currents and temperature sensors, the wireless transmission of the collected data to the Gateway. The gateway receives the data sent by the sensors and transmits it to the cloud. In the cloud, data is continuously and automatically analyzed based on predetermined models and if it is necessary warnings or messages of imminent failuret are sent.

The results are based on models developed by manufacturers of engines and reducers. All information is recorded and can be available in an easy–to–use way on the smart phone or computer app.
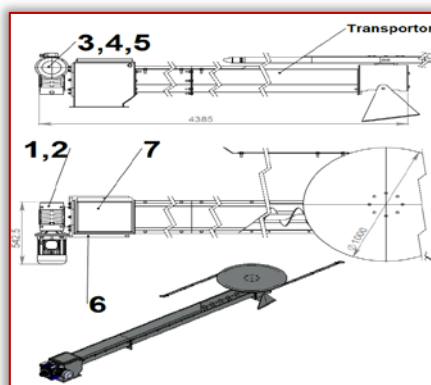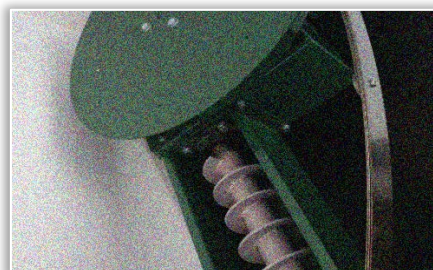
Figure 3 – Type of screw conveyor with additional action for homogenization and loading; 1,2 – reducers; 3 – temperature sensor; 4,5– engines; 6– Raspberry Pi4; 7 – Monitoring block

SENSOR SYSTEM

For the realization of the sensor module and the transmission of wi–fi to the gateway, the mounting below, Figure 4, is used.
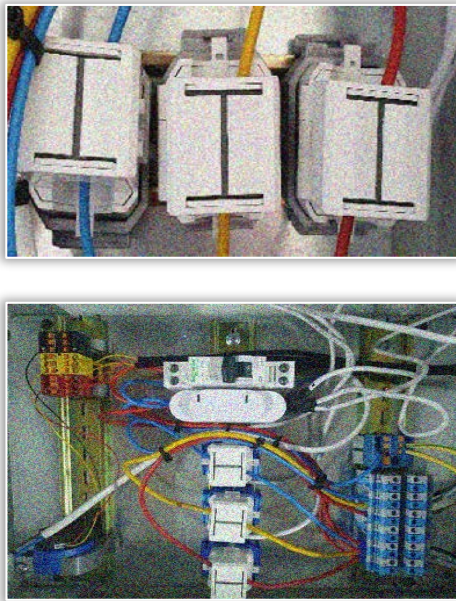
Figure 4 – Sensor module mounting

The sensors used in this application are sensors with WiFi communication produced by Shelly Cloud Bulgaria. In this application, two sensors are used. The first sensor, electrical, allows measuring the voltage in the three–phase network and the current consumed by each phase of the motor. The sensor acquires all six of these parameters with a cadence of one measurement per minute. The electrical sensor also makes calculations to indicate the power consumed on each phase and the power factor. The second sensor, thermally, is Shelly 1 with temperature measuring mode that allows the acquisition of three temperatures, in three points with semiconductor sensors of type 18S20 in cases with IP67 degree of protection. Temperatures are read with a cadence of one measurement per minute.

COMMUNICATION NETWORK

In order to achieve the data processing mode and the communication network, the assembly below, figure 5, is used. High–performance equipment for solar installations such as solar chargers or inverters have Serial, Ethernet, CAN or Modbus communication ports. These devices can be connected to the internet through gateways (Radoi, R.–I. et al, 2021)

The communication network used in the application is a local WiFi network, used only by the application components.

The network is controlled by the microtik Hap Lite RB941 Access Point swarm that ensures the management of network functions:

≡ Authentication of clients in the Wi–Fi network
≡ Automatic allocation of addresses in the local network through DHCP protocol
≡ Network Address Translation function to connect the local network to the internet
≡ Firewall function to protect the internal network from attacks from the internet
≡ Port forwarding function to make available resources from the local network to the Internet to allow access to data

collected and processed by the system from the Internet. All sensors connect to the WiFi network and automatically receive IP addresses from the Microtik router.
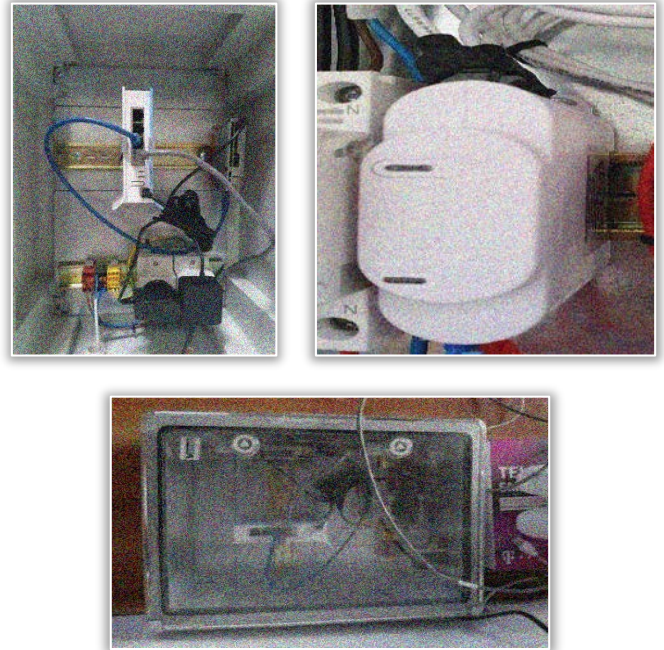
Figure 5 – Communication network assembly

Applying the Internet of Things (IoT) can improve the efficiency of the technology for monitoring the operation of agricultural equipment (Pi, J. et al., 2021).

DATA PROCESSING MODULE

The data processing module is implemented with a Raspberry Pi 4 with 4GB of RAM that provides all the necessary functions for the application:

≡ Data collection
≡ Storage
≡ Data processing.

On the Raspberry Pi runs the Raspbian operating system along with the applications necessary to ensure the above functions. In order to ensure a slight replication of the system, a solution was chosen to use docker containers with the necessary applications. Under these conditions, only a compose file for the Docker Compose application is required to replicate the application. The compose file that was written specifically for this application has the YAML format. It allows downloading from the internet the necessary Docker containers and linking them to ensure the operation of the application. The management of the installed containers can be done through the web interface of the Portainer–CE application.

The data collection function allows retrieving data from sensors with the cadence of one measurement per minute. Each sensor is programmed to transmit once a minute the data measured by MQTT protocol.

In order to use the MQTT protocol, it is necessary to use a Broker that takes the data published by the sensors and transmits it to the applications that have subscribed for receiving the data in question. The MQTT broker is provided

by the open source Mosquitto application that runs in a Docker container.

Within the data collection function is also the node–red open source application that allows the graphic realization and running of Node JS applications. The function of the Node Red module is to connect to the MQTT Broker and process the primary data received from the sensors in order to be stored in a database in a unitary way (Lacatus, P. et al., 2021).
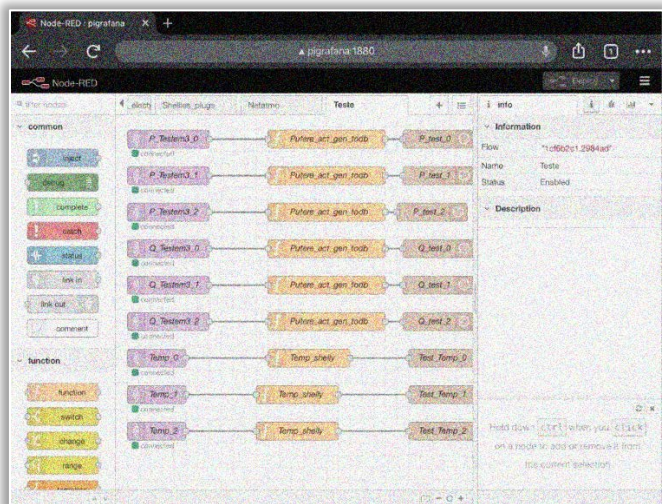
Figure 6 – Node–Red graphics application

INTELLIGENT DRIVE INSTALLATION TEST

For testing the prototype of the intelligent drive installation used for biomass conveyors, the conveyor belt equipment from the experimental model was used; the validated tests to the experimental model were repeated and the transmission of data and warnings of damage on the computer and mobile phone was followed.
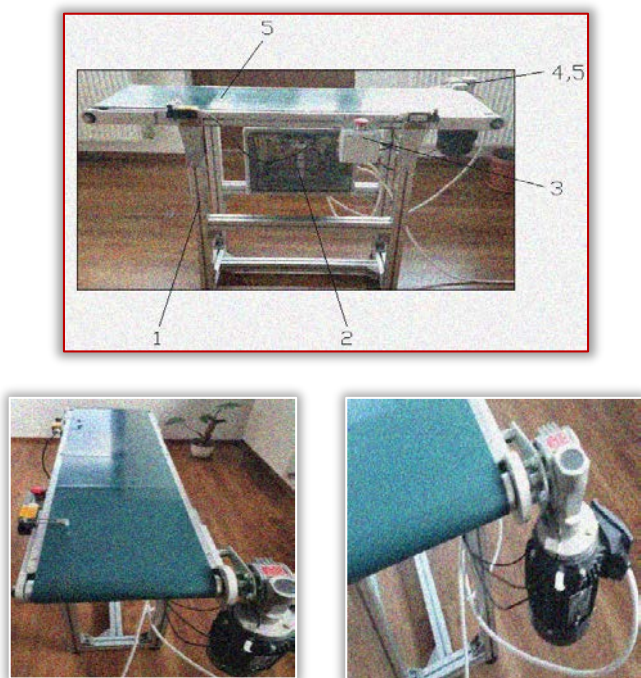
Figure 7 – Prototype testing installation
1–frame; 2– the way of recording and transmitting data; 3– crash button;
4– moto–reducer; 5– temperature sensors; 6– conveyor belt

The installation for prototype testing consists of a frame (1), a module for recording and transmitting data (2), a hazard button (3) the moto–reducer (4) with temperature sensors (5) and the conveyor belt (6) for simulating the load variation.

The monitoring module is located near the monitored motor assembly, and the connection of the motor is made through it to take over the electrical voltage current sizes necessary for the analysis.

The control module contains the router that ensures wi–fi communication with the rest of the monitoring modules and the Raspberry Pi 4 single board computer that stores the data and processes it according to the processing levels described above (Russell T., 2017).

The equipment monitors the behavior of the operation throughout the period of use and follows the following parameters:

≡ The current absorbed on each phase of the motor;
≡ The power absorbed on each phase;
≡ Voltage on each phase;
≡ The power factor on each phase;
≡ The temperature recorded in correlation with the other parameters in 3 strategic points on the engine and on the reducer (a sensor is also used to measure the ambient temperature)

These parameters are transmitted through the recording system, via wireless to the reception system that is connected to a computer. Thus, the intelligent drive installation stores the data recorded during operation and provides in real time error messages in case of exceeding the predetermined warning or damage values, so that the user can make decisions in the shortest time or establish the necessary changes to optimize the operation of the conveyor.

After the empty start of the installation, the loading of the conveyor belt is simulated by pressing with the hand.
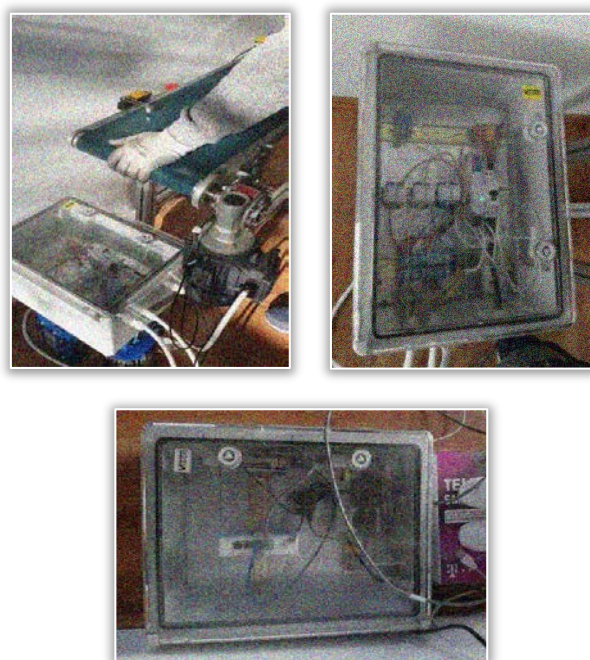
Figure 8 – Mounting of the automatic control module

The data is automatically recorded every 5 sec and is transmitted via Wi–Fi by the monitoring module located near the conveyor belt to the control module located in another room that is connected to the central computer for data acquisition and interpretation in order to optimize the operation of the monitored system.

RESULTS

At the same time, this data is displayed on the mobile phone:

Figure 9 – Displaying the results on the mobile phone screen and on the computer screen

Data monitoring is displayed independently on both devices. The data is automatically recorded every 5 sec and is transmitted wirelessly by the monitoring module located near the conveyor belt to the control module connected to the central computer for data interpretation and establishing the decisions to be taken. The power outage was simulated and the installation sent an alert to the mobile phone.
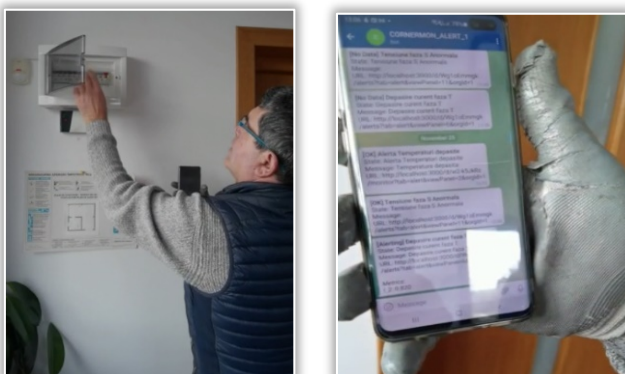
Figure 10 – Displaying the results

At the reboot, a new status change alert was sent. Higher load charges were simulated at the conveyor belt and the intelligent installation transmitted again on the monitor and on the phone alerts of exceeding the current and of the phase voltages at the monitored electric motor.

Figure 11 – Simulation at the conveyor belt

CONCLUSIONS

The prototype of "Intelligent drive installation for biomass conveyor" was tested in operating conditions in the laboratory, for monitoring, acquisition and data transfer of monitored parameters, via Wi–Fi from the conveyor belt equipment to the mobile phone and to the central computer where a dedicated program monitors and stores data for warning in case of failures or for the subsequent analysis of the monitored system.

It has been proven that it is possible to improve the operation of the motor by operating it by means of a converter, with speed adjustment and anti–locking system, but without a monitoring with a warning system and recording the parameters in the type of operation it is not known where the problems arise, what is actually the necessary moment, why the peaks appear, how long the peaks last. It is necessary to perform predictive maintenance and eventually to integrate into a fully automatic system. The same problems are encountered not only in the tracks but also in other types of conveyors, especially where the personnel using the installations do not check and do not comply with the conditions listed in the technical book, but where they can't be checked if the normal operating conditions have been observed.

Competitiveness Operational Programme 2014–2020, Priority Axis 1: Research, technological development and innovation (RD&I) to support economic competitiveness and business development, Action 1.2.3 – Partnerships for knowledge transfer, project title: Eco–innovative technologies for recovery of biomass wastes, project acronym: ECOVALDES, SMIS code: 105693–594, Financial agreement no. 129/23.09.2016.

Note: This paper was presented at ISB–INMA TEH' 2021 – International Symposium, organized by University "POLITEHNICA" of Bucuresti, Faculty of Biotechnical Systems Engineering, National Institute for Research–Development of Machines and Installations designed for Agriculture and Food Industry (INMA Bucuresti), National Research & Development Institute for Food Bioresources (IBA Bucuresti), University of Agronomic Sciences and Veterinary Medicine of Bucuresti (UASVMB), Research–Development Institute for Plant Protection – (ICDPP Bucuresti), Research and Development Institute for Processing and Marketing of the Horticultural Products (HORTING), Hydraulics and Pneumatics Research Institute (INOE 2000 IHP) and Romanian Agricultural Mechanical Engineers Society (SIMAR), in Bucuresti, ROMANIA, in 29 October, 2021

References

[1] Caixal, G., Alarcón, F., & Althoff, T. F. (2021). Accuracy of left atrial fibrosis detection with cardiac magnetic resonance: correlation of late gadolinium enhancement with endocardial voltage and conduction velocity. EP Europace 23(3), pp. 380–388, England

[2] Gandjbakhch, E., Dacher, J. N., & Taieb, J. (2020). Joint Position Paper of the Working Group of Pacing and Electrophysiology of the French Society of Cardiology and the French Society of Diagnostic and Interventional Cardiac and Vascular Imaging on magnetic resonance imaging in patients with cardiac electronic implantable devices. Archives of Cardiovascular Diseases 113(6–7), pp. 473–484, France

[3] Ionel, M., & Miloiu, Gh. (2011). Aspecte energetice la alegerea unei antrenări electromecanice A XI–a Conferinţă Naţională multidisciplinară "Profesorul Dorin Pavel –fondatorul hidroenergeticii româneşti"

[4] Hassan, M.M., Gumaei, A., & Alsanad, A. (2020). A hybrid deep learning model for efficient intrusion detection in big data environment. Information Sciences, 513, pp. 386–396, United States

[5] Lacatus, P., Ionel, M., Matache, G., & Barbu, V. (2021). Strategy for Implementation und use of monitoring systems for gear–motors. Hidraulica Magazine (3), pp. 86–93

[6] Luz, E., Silva, P., & Silva, R. (2021). Towards an effective and efficient deep learning model for covid–19 patterns detection in x–ray images. Research on Biomedical Engineering, pp. 1–14, United States

[7] Narayan, S. (2015). Effects of Various Parameters on Piston Secondary Motion. SAE Technical Paper 2015– 01–0709

[8] Pi, J., Wang, W., & Ji, M. (2021). YTHDF1 promotes gastric carcinogenesis by controlling translation of FZD7. Cancer Research 81(10), pp. 2651–2665, United States

[9] Rădoi, R.–I., Dumitrescu, L., Chiriţă, A–P, & Vlăduţ, N–V. (2021). Remote monitoring of energy production and efficiency of an off–grid photovoltaic system / Monitorizarea de la distanta a productiei de energie si a eficientei unui sistem fotovoltaic off–grid. INMATEH–Agricultural Engineering 64(2), pp. 131–140

[10] Crawford, R.T. (2017). Condition Monitoring & Dynamic Control Systems. Technology, Applications & Research. Nova Science Publishers Inc.

[11] Stojanovic, N., Glisovic, J., Grujic, I., Narayan, S., Vasiljevic, S., & Boskovic, B. (2018). Experimental and numerical modal analysis of brake squeal noise. Mobility & Vehicle Mechanics 44(4), pp. 73–85

[12] Au, Y.H.J., Griffiths, B., & Rao, B.K. (2012). Condition Monitoring and Diagnostic Engineering Management. Proceeding of COMADEM 90: The Second International Congress on Condition Monitoring and Diagnostic Engineering Management

[13] *** https://wematik.de/wematik–gmbh/

[1.]Jelena VUKOVIĆ, [1.]Milomirka OBRENOVIĆ, [2.]Jelena GARIĆ, [3.]Una MARČETA

REMOVAL OF SULFIDE FROM WATER USING ALUMINA

[1.]Faculty of technology Zvornik, University of East Sarajevo, Zvornik, BOSNIA & HERZEGOVINA
[2.]Alumina Ltd Zvornik, BOSNIA & HERZEGOVINA
[3.]Technical faculty "Mihajlo Pupin", University of Novi Sad, Zrenjanin, SERBIA

Abstract: Sulfides can cause the corrosion of pipes and the appearance of unpleasant odors. In drinking water sulfides affect organoleptic properties. Investigation of the adsorption onto various materials is increasing because this process gives the possibility for the use of low–cost adsorbents and it is a relatively simple technique for water treatment. Materials considered as adsorbents should primarily meet conditions such as particle size, porosity, and specific surface area. Due to their characteristics, alumina nanoparticles (Al_2O_3) have wide application in the ceramics industry, as abrasive material, in heterogeneous catalysis, and as sorbents. As an adsorbent, alumina nanoparticles have extensive application in the removal of undesirable compounds and contaminants from drinking water and wastewater. Alumina with a high content of aluminum oxide was used as an adsorbent to remove sulfides from aqueous solutions. This paper aims to examine the possibility of adsorption of sulfide ions onto alumina with a very high content of aluminum oxide (Al_2O_3). The results of the paper can serve as a starting point for further investigation of the adsorption characteristics of alumina, as well as the behavior of sulfides during adsorption on various adsorbents. Experiments in a column packed with alumina were conducted at room temperature. The effect of different initial concentrations and contact time on the sulfide removal efficiency was investigated. The best efficiency is achieved at low initial concentration and short contact time.
Keywords: sulfides, hydrogen sulfide, alumina, adsorption

INTRODUCTION

The presence of sulfides in the environment can be the result of natural processes and anthropogenic activities. Naturally, they are found in minerals, ores, and fossil fuels (oil and coal). Hydrogen sulfide (H_2S) in normal conditions is in the gaseous phase, present in ores and minerals, and as a product of volcanic activities (Clarisse et al, 2011; Ma et al., 2019). Gaseous hydrogen sulfide is toxic, flammable, colorless, with a recognizable odor of rotten eggs, so it is easy for detection in the air (Wu et al., 2018).

Hydrogen sulfide and sulfides of alkali and alkaline earth metals are soluble in water (Li and Lancaster, 2013). In groundwater, sulfides are naturally present due to the dissolution of mineral deposits in the aquifer. Hydrogen sulfide, which is a product of bacterial reduction of sulfate under anaerobic conditions, is very common in groundwater (Miao et al., 2012).

Conditions for sulfate reduction to sulfide are the following: the presence of sulfate source, the presence of reducing bacterias and their energy source, and the anaerobic environment (Fanning et al., 2002). Sulfides are present in both municipal and industrial wastewater. Dominant industrial sources are tanneries, paper mills, the petrochemical industry, and the textile industry (Vaiopoulou et al., 2005; Dutta et al., 2010; Pikaar et al., 2011).

Sulfides affect organoleptic properties of the drinking water. The odor and taste threshold for hydrogen sulfide in water is estimated to be between 0.05 and 0.1 mg/L. The health effects of hydrogen sulfide have not been proven yet, and therefore the maximum limit value of H_2S in water has not been officially defined (WHO, 2011). However, researches show that sulfides are very toxic for aquatic life, and they have a direct negative impact on the human central nervous system and respiratory system (Abdollahi & Hosseini, 2014; Huang et al., 2020). In addition, excessive intake of hydrogen sulfide through potable water can cause headaches, dizziness, fatigue, blurred vision, and other symptoms (Verma and Ratan, 2020).

Dissolved hydrogen sulfide and sulfide ions are undesirable primarily because they can lead to corrosion of the pipes, and the occurrence of unpleasant odors in the close environment (Dutta et al., 2010; Vaiopoulou et al., 2005). The most commonly used methods for removing sulfides from water are chemical and biological oxidation (Nielsen, & Vollertsen, 2021; Wilson et al., 2020). In addition to the above, other investigated techniques are adsorption, anaerobic digestion, precipitation, ion exchange, and electrochemical removal (Lito et al., 2012).

Investigation of the adsorption onto various materials is increasing because this process gives the possibility for the use of low–cost adsorbents and it is a relatively simple technique for water treatment. Materials considered as adsorbents should primarily meet conditions such as particle size, porosity, and specific surface area. Due to their characteristics, alumina nanoparticles (Al_2O_3) have wide application in the ceramics industry, as abrasive material, in heterogeneous catalysis, and as sorbents (Farahmandjou and Golabiyan, 2016). As an adsorbent, alumina nanoparticles have extensive application in the removal of undesirable compounds and contaminants from drinking water and wastewater. It is possible to use alumina for the removal of heavy metals, fluoride and nitrate adsorption, biological remediation, color degradation, desalination, etc. (Ghorai and Pant, 2004; Tripathy et al., 2006; Ravindhranath and Ramamoorty, 2017; Younssi et al., 2018).

This paper aims to examine the possibility of adsorption of sulfide ions onto alumina with a very high content of aluminum oxide (Al_2O_3). The results of the paper can serve as a starting point for further investigation of the adsorption characteristics of alumina, as well as the behavior of sulfides during adsorption on various adsorbents.

MATERIALS AND METHODS

The study of the potential of S^{2-} ions adsorption from aqueous solutions was performed in the laboratory of the Faculty of Technology Zvornik. Synthetic aqueous solutions of defined composition, similar to the composition of oligomineral natural waters, were used for the experimentation. Granular sodium sulfide (Na_2S) of analytical grade was used for the sulfide solution of known concentration. For each experiment, a new solution of sodium sulfide with double–distilled water was made. Solutions were prepared with initial sulfide concentrations ranging from 2.4802 mg/dm^3 to 40.9931 mg/dm^3, which were determined by the iodometric method (Clesceri et al., 1999).

Alumina, from the factory "Alumina" Ltd Zvornik, was used as an adsorbent for the adsorption of the sulfide ions. Determination of the chemical composition of the alumina sample was performed in the Alumina Research Laboratory using the ICP – OES SPECTRO GENESIS device, according to the standard method (BS EN ISO 11885, 2016). The loss on ignition was also determined according to the ISO standard method. (ISO 6606: 1986). Preparation of alumina for the adsorption included thermal treatment, where the sample was dried at a temperature of 300°C for 3 hours.

The adsorption was performed in an adsorption column with a diameter of 5cm and a length of 34cm. The filter paper was placed at the bottom of the column to prevent small granules from passing into the leaked solution. The experiment was conducted at room temperature. During the experiment, the variable parameters were the initial concentration of sulfide ions, and the contact time of the sulfide solution and the adsorbent.

The contact time between the sulfide solution and the alumina was 10, 20, and 30 minutes, with the volume of the leaked sulfide solution of 50 cm^3. The concentration of sulfide ions remaining in the solution, which was passed through the adsorbent, was monitored by spectrophotometric method (ISO 10530: 1992), using *UV–VIS 1800 Shimadzu* spectrophotometer, and measuring the absorbance at a wavelength $\lambda = 665$ nm. A 1 cm cuvette was used for analysis.

RESULTS AND DISCUSSION

⸺ Chemical composition of the alumina sample

Alumina is anhydrous aluminum (III) oxide, which is confirmed with the low value obtained by loss on ignition (0.82%). Based on the results of the chemical analysis of alumina presented in Table 1, it can be seen that Al_2O_3 constitutes 98.80 wt.% of alumina, which is in accordance with the data presented in the studies (Hart & Lense, 1990; Morris et al., 2008).

Table 1. Chemical composition of the alumina sample

Chemical component	Weight percentage (wt. %)
Al_2O_3	98.80
Na_2O_{total}	0.33
CaO	0.02
Fe_2O_3	0.011
ZnO	0.01
SiO_2	0.006
Loss on ignition (1000 °C)	0.82

RESULTS OF SULFIDE ION ADSORPTION ON ALUMINA

As can be seen from the data shown in Tables 2 – 4 and Figure 1, the initial concentration of sulfide in the solution affects the adsorption efficiency. Regardless of the contact time of the alumina and the sulfide solution, at initial sulfide concentrations up to 20 mg/dm^3, a significant adsorption efficiency, over 80%, was achieved. An important decrease in the adsorption efficiency of sulfide ions is observed at initial sulfide concentrations higher than 30 mg/dm^3, at all examined contact times.

Increasing the initial concentration of sulfide, with approximately the same amount of adsorbent, leads to a decrease in the adsorption efficiency. The reason for this is the fact that the alumina surface is saturated faster with sulfide ions at a higher initial sulfide concentration.

Table 2. Sulfide adsorption on alumina at a contact time of 10 minutes

Initial sulfide concentration, c_0 [mg/dm^3]	Sulfide concentration after adsorption, c_1 [mg/dm^3]	Adsorbent dosage, m [g]	Adsorption efficiency [%]
2.4802	0.0223	108.70	99.10
10.0791	0.6350	109.01	93.70
20.4558	2.6572	107.98	87.01
31.1298	9.8962	109.00	68.21
40.9931	15.5815	107.70	61.99

Table 3. Sulfide adsorption on alumina at a contact time of 20 minutes

Initial sulfide concentration, c_0 [mg/dm^3]	Sulfide concentration after adsorption, c_1 [mg/dm^3]	Adsorbent dosage, m [g]	Adsorption efficiency [%]
2.4802	0.0295	108.70	98.81
10.0791	0.9374	109.01	90.69
20.4558	3.0663	107.43	85.01
31.1298	10.8301	109.03	65.21
40.9931	19.6808	107.98	51.99

Table 4. Sulfide adsorption on alumina at a contact time of 30 minutes

Initial sulfide concentration, c_0 [mg/dm^3]	Sulfide concentration after adsorption, c_1 [mg/dm^3]	Adsorbent dosage, m [g]	Adsorption efficiency [%]
2.4802	0.0374	108.95	98.49
10.0791	1.0458	108.81	89.62
20.4558	3.3149	107.98	83.79
31.1298	11.1149	109.02	64.29
40.9931	19.9875	109.01	51.24

Figure 1 shows that the contact time of the sulfide solution and alumina slightly affects the adsorption efficiency, at initial sulfide concentrations less than 30 mg/dm^3.

At initial sulfide concentrations higher than 30 mg/dm^3, the adsorption efficiency achieved at a contact time of 10 minutes (61.99%) is about 10% higher than the adsorption efficiency at a contact time of 20 minutes (51.99%) and 30 minutes (51.24 %).
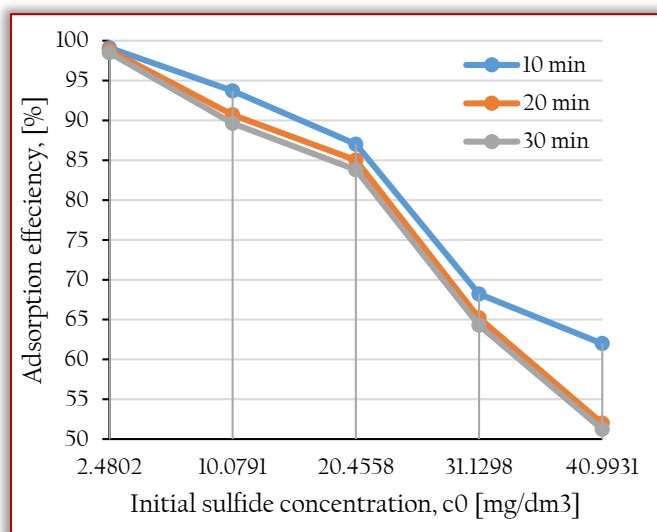
Figure 1. Adsorption efficiency at different initial sulfide concentrations and different contact times

CONCLUSION

Alumina with a very high content of aluminum oxide (Al$_2$O$_3$) was examined as an adsorbent for the removal of sulfide ions from aqueous solutions.

The experiment was conducted in a column (5x34cm), loaded with sufficient amounts of the adsorbent. The impact of contact time and the initial sulfide concentration was monitored. When initial concentrations are less than 30 mg/dm^3, the influence of the contact time is minor. Increasing the initial concentration negatively affects the adsorbent efficiency.

From above it can be concluded that alumina can be used as an efficient adsorbent for the removal of sulfide from water, in the conditions of low initial concentration and short contact time.

Further research should be focused on examining the influence of pH, temperature, and other relevant parameters.

References

[1] Abdollahi, M., & Hosseini, A. (2014). Hydrogen sulfide. Encyclopedia of Toxicology, 3, 971–974

[2] BS EN ISO 11885, 9th Edition, July 11, 2016 – Water quality – Determination of selected elements by inductively coupled plasma optical emission spectrometry (ICP–OES)

[3] Clarisse, L., Coheur, P. F., Chefdeville, S., Lacour, J. L., Hurtmans, D., & Clerbaux, C. (2011). Infrared satellite observations of hydrogen sulfide in the volcanic plume of the August 2008 Kasatochi eruption. Geophysical research letters, 38(10)

[4] Clesceri, L. S., Greenberg, A. E., Eaton, A. D. (1999). APHA. AWWA, WEF, Standard methods for the examination of water and wastewater. 20th edn, Washington, DC, USA.

[5] Dutta, P. K., Rabaey, K., Yuan, Z., Rozendal, R. A., & Keller, J. (2010). Electrochemical sulfide removal and recovery from paper mill anaerobic treatment effluent. Water research, 44(8), 2563–2571.

[6] Fanning, D. S., Rabenhorst, M. C., Burch, S. N., Islam, K. R., & Tangren, S. A. (2002). Sulfides and sulfates. Soil mineralogy with environmental applications, 7, 229–260.

[7] Farahmandjou, M., & Golabiyan, N. (2016). Synthesis and characterization of Alumina (Al. Int. J. Bio–Inorg. Hybr. Nanomater, 5(1), 73–77.

[8] Ghorai, S., & Pant, K. K. (2004). Investigations on the column performance of fluoride adsorption by activated alumina in a fixed–bed. Chemical Engineering Journal, 98(1–2), 165–173.

[9] Hart, L. D., & Lense, E. (Eds.). (1990). Alumina chemicals: science and technology handbook. John Wiley & Sons.

[10] Huang, Y., Liu, Z., Guo, Y., Lin, Q., Liao, X., & Qi, H. (2020). A comparative study on sulfide removal by HClO and KMnO$_4$ in drinking water. Environmental Science: Water Research & Technology, 6(10), 2871–2880.

[11] ISO 10530:1992 Water quality — Determination of dissolved sulfide — Photometric method using methylene blue.

[12] ISO 6606:1986 Water quality — Determination of loss of mass at 1075 °C — Gravimetric method.

[13] Li, Q., & Lancaster Jr, J. R. (2013). Chemical foundations of hydrogen sulfide biology. Nitric oxide, 35, 21–34.

[14] Lito, P. F., Cardoso, S. P., Loureiro, J. M., & Silva, C. M. (2012). Ion exchange equilibria and kinetics. In Ion Exchange Technology I (pp. 51–120). Springer, Dordrecht.

[15] Ma, X., Zheng, G., Liang, M., Xie, D., Martinelli, G., Sajjad, W., Xu, W., Fan, Q., Li L., Du L, & Zhao, Y. (2019). Occurrence and origin of H$_2$S from volcanic reservoirs in Niudong area of the Santanghu Basin, NW China. Geofluids, 2019.

[16] Miao, Z., Brusseau, M. L., Carroll, K. C., Carreón–Diazconti, C., & Johnson, B. (2012). Sulfate reduction in groundwater: characterization and applications for remediation. Environmental geochemistry and health, 34(4), 539–550.

[17] Morris, S. M., Fulvio, P. F., & Jaroniec, M. (2008). Ordered mesoporous alumina–supported metal oxides. Journal of the American Chemical Society, 130(45), 15210–15216.

[18] Nielsen, A. H., & Vollertsen, J. (2021). Model parameters for aerobic biological sulfide oxidation in sewer wastewater. Water, 13(7), 981.

[19] Pikaar, I., Rozendal, R. A., Yuan, Z., Keller, J., & Rabaey, K. (2011). Electrochemical sulfide removal from synthetic and real domestic wastewater at high current densities. Water research, 45(6), 2281–2289

[20] Ravindhranath, K., & Ramamoorty, M. (2017). Nano aluminum oxides as adsorbents in waterremediation methods: a review. Rasayan J. Chem, 10, 716–722.

[21] Tripathy, S. S., Bersillon, J. L., & Gopal, K. (2006). Removal of fluoride from drinking water by adsorption onto alum–impregnated activated alumina. Separation and purification technology, 50(3), 310–317.

[22] Vaiopoulou, E., Melidis, P., & Aivasidis, A. (2005). Sulfide removal in wastewater from petrochemical industries by autotrophic denitrification. Water Research, 39(17), 4101–4109.

[23] Verma, P., & Ratan, J. K. (2020). Assessment of the negative effects of various inorganic water pollutants on the biosphere—an overview. Inorganic Pollutants in Water, 73–96.

[24] WHO, (2011). Edition, F., Guidelines for drinking–water quality. WHO chronicle, 38(4), 104–108.

[25] Wilson, E. V., Litvinenko, V. A., & Obukhov, D. I. (2020, August). Methods for removing reduced sulfur compounds from groundwater. In IOP Conference Series: Materials Science and Engineering (Vol. 913, No. 4, p. 042045). IOP Publishing.

[26] Wu, H., Zhu, Y., Bian, S., Ko, J. H., Li, S. F. Y., & Xu, Q. (2018). H_2S adsorption by municipal solid waste incineration (MSWI) fly ash with heavy metals immobilization. Chemosphere, 195, 40–47

[27] Younssi, S. A., Breida, M., & Achiou, B. (2018). Alumina membranes for desalination and Water treatment. InTech.

¹·C.I. MADUEKE, ²·M.M. OGUEJIOFOR, ¹·R. UMUNAKWE

REVIEW ON HEAT TREATMENT OF NATURAL FIBRES FOR USE AS REINFORCEMENT IN COMPOSITES

[1.]Department of Materials and Metallurgical Engineering, Faculty of Engineering, Federal University Oye–Ekiti, Ekiti State, NIGERIA
[2.]Department of Mechanical engineering, Faculty of Engineering, Federal university Oye–Ekiti, NIGERIA

Abstract: Heat treatment of natural fibres is important for their use as reinforcements in composites. Heat treatment of natural fibres has been reported to reduce moisture and improve mechanical properties both in the fibre and in the manufactured composites. Therefore such factors as the specimen gauge length, number of specimens tested, average diameter of each specimen taken at various points along the gauge length and mode of fracture of the specimen after heat treatment should be fully reported as they affect the outcome of the mechanical properties of heat treated fibres. Others include the type of oven (vacuum or air oven), pre and post processing as well as storage conditions of the fibres after heat treatment prior to testing should be taken care of. These factors and their implications with respect to heat treatments were addressed with a view of improving the mechanical properties of natural fibres for use in composites for advanced applications.

Keywords: heat treatment, natural fibres, reinforcement, properties

INTRODUCTION

A classification for natural fibres is displayed in Figure 1 showing that such fibres are derived from natural resources such as mineral, plants animal. Mineral–based fibres are often associated with extractive and manufacturing industries whilst plants and animal–based fibres are associated with agriculture.
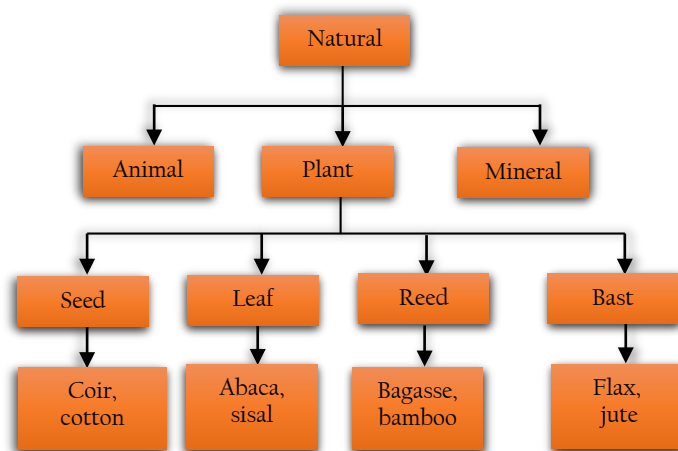
Figure 1. Basic classifications of natural fibres

Several approaches have been sought in other to reduce the use of conventional synthetic fibres such as glass and carbon via the use of natural fibres as reinforcements in composites. Apart from sustainability factor, natural fibres possess several relevant properties and advantages as shown in Tables 1 and 2. Biofibres from plants and other natural materials have been exploited for use as reinforcements in composites (Rao, Rao and Prasad, 2010; Agunsoye et al., 2015; Edoziuno et al., 2020). Unlike synthetic fibres, bio fibres are not dependent on petroleum based precursors. In addition, utilization of natural fibres as composites reinforcements promotes the use of local natural resources and subsequently adds to the socioeconomic development, local content and sustainability of those products (Araújo and Godoy, 2018). They are abundantly available (Jawaid and Khalil, 2015) and require much less energy to produce than synthetic fibres (Joshi et al., 2004).

Table1. Advantages and limitations of natural fibre

Advantages of natural fibre	– Low–cost – Relatively low density – Non–toxic – Sustainable – Renewability – Environmentally–friendly
Limitations of natural fibre	– Poor resistance to moisture ingress – Variability in fibre length and diameter – Relatively high porosity – Significantly lower mechanical properties when compared to synthetic fibres – Low degradation temperatures limit the options for selecting the matrix

(N Mahato", 1995; Fujiura et al., 2010; Gourier et al., 2014).

Table 2. Relevant properties of coir fibre in comparison with other natural fibres and with E–glass fibre

Fibre	Tensile Strength (MPa)	Tensile Modulus (GPa)	Elongation at break (%)	Density (kg/m³)
Coir	131–175	4–6	30.0–45.0	1150
Sisal	468–640	9.4–22	2.0–2.5	1450
Jute	393–1316	13–91.9	1.3–1.8	1300
Hemp	514–2140	24.8–143.2	1.6–1.8	1480
E–Glass	400	1.0	2.5	1900–2500

Sources: (Carl and Brook, 1985; Ticoalu, Aravinthan and Cardona, 1997; Gassan and Bledzki, 1999; Alves Fidelis et al., 2013; Latif et al., 2019; Park 2006; ; Ferreira, Cruz and Fangueiro, 2018; Brígida et al., 2010b; Sanjay, Arpitha and Yogesha, 2015)

HEAT TREATMENT OF NATURAL FIBRES

Natural fibres are made up of different chemical constituents; as a result, heat treatment at increased temperature can give

rise to varying degrees of changes in the fibre. Such changes include change in colour and appearance, weight, fibre orientation, decomposition of the chemicals that make up the fibres. Natural fibres have showed different decomposition temperatures and different levels of changes in physical properties.

Investigations from many researchers confirm that natural fibres undergo thermal degradation in two stages:

(a) at lower temperatures (150–300°C) and

(b) at higher temperatures (300–400°C).

(a) has been linked with the degradation of cellulose and includes hydrolysis, oxidation, dehydration among others while (b) has been mainly associated with degradation of both cellulose and lignin with formation of charred product (Varma, Varma and Varma, 1986; Silva et al., 1999; Dam et al., 2006).

In one study, coir fibres were subjected to heat treatment in an air–circulating oven at a temperature of 150°C for 10 minutes; a drop in tensile strength by 0.58% and increase in Young's modulus by 20% were recorded, however, at 200°C for the same duration, a drop in the tensile strength and increase in modulus by 40% and 20% respectively were recorded (Ezekiel et al., 2011), however, the storage conditions after the treatment prior to tensile testing was not revealed.

In a similar way, at heat treatment temperatures of 100, 140 and 180°C, a drop in the tensile strength by 14, 24 and 29% and a drop in the value of the degree of polymerization by 5, 12 and 19% respectively were observed (Khan, Alam and Terano, 2012). An improvement in dimensional stability has been recorded for heat treated fibres. At 170°C and duration of 2 hours for Eucalypt wood, a 60% anti shrinkage efficiency in radial direction was recorded (Esteves, Domingos and Pereira, 2007).

Esteves, Domingos and Pereira, (2007) carried out an oven heat treatment on eucalypt wood in the presence of oxygen at 170–200°C for 2 to 24 hours and observed an increase in the dimensional stability whereas the bending strength decreased and a mass loss of 9.5% was observed at 190°C. After heat treatment of hemp and bamboo fibres, a 60% decrease in the tensile strength was recorded for both fibres (Ochi, Takagi and Niki, 2002), the gauge length and strain rate were not mentioned, besides only 10 specimens were tested. (Shahzad, 2013) subjected hemp fibres to oven temperatures for 30, 100, 150 and 200°C, however it was not specified if it was a vacuum or air oven.

Cao, Sakamoto and Goda, (2007) subjected kenaf fibres to vacuum heat treatment at temperatures of 130°C, 140°C and 160°C and observed maximum increase in strength at 140°C but the diameter, stiffness and elongation were not mentioned (Varma, Varma and Varma, 1986) subjected coir fibres to air oven heat treatment Aprt temperatures of 150, 200 and 250 for 1 hour, however, the number of fibres, fibre origin and specie as well as gauge length used were not stated.

Kenaf and bamboo fibres were subjected to an oven heat treatment temperature of 140°C, an increase in tensile strength, fracture strain, crystallinity index and in the length to width ratio were observed (Y. Cao, Sakamoto and Goda, 2007; Yun et al., 2016).

Dixit and Verma, (2012) recorded a reduction in moisture content, increase in crystallinity index, increase in elastic modulus and increase in fracture strain at 140–150°C for 4 hours of oven heat treatment.

Gassan and Bledzki, (1999) subjected jute and flax fibres to a maximum temperature of 170°C and observed a change in the mechanical properties.

The tensile properties of untreated sisal fibres were evaluated by Luz et al., (2017) for varying gauge lengths but at a constant strain rate, no effect on the tensile strength was observed rather a 35% decrease in Weibull modulus was observed with increase in gauge length.

DISCUSSIONS

The Issues with heat treatment of natural fibres in preparation for use in composites are that several factors were not reported by the authors in other to validate their findings. For example, in the case of coir fibres, the number of fibres used were either not mentioned or below the minimum number stipulated for natural fibres in order to achieve meaningful result.

Several other factors such as gauge length, diameter of the fibre, fibre specie and origin, strain rate, method of extraction, age, specie and origin of the fibres, porosity and pore size distribution were missing in the literature. These factors have been identified among other factors to influence the tensile strength of natural fibres and their applications in composites. Besides, several authors have used different diameters for the same type of natural fiber such as coir resulting in significant inconsistency in the tensile properties. The failure traces and changes in failure pattern of heat treated fibres were not discussed.

Investigations into the tensile properties coir fibres of different varieties and different ages but of Philippine origin and extracted manually were carried out (van Dam et al., 2006). It was discovered that the tensile strength of the Indian retted coir fibre was 248 MPa while the strongest fibre of all the species of the manually extracted Philippine coir fibre was 114 MPa. Therefore, information such as fibre origin, specie and maturity ought to be provided.

For lignocellulosic fibres such as natural fibers, an inverse relationship between the tensile strength and the fibre diameter has been reported by several authors (Mukherjee and Satyanarayana, 1984; Tomczak, Sydenstricker and Satyanarayana, 2007; Fiore et al., 2016).

The gauge length used for tensile testing has been reported by Mukherjee and Satyanarayana, (1984); Defoirdt et al., (2010); Fidelis et al., (2013) and Mathura and Cree, (2016) to significantly influence the results of such tests, see Figures 2 and 3.
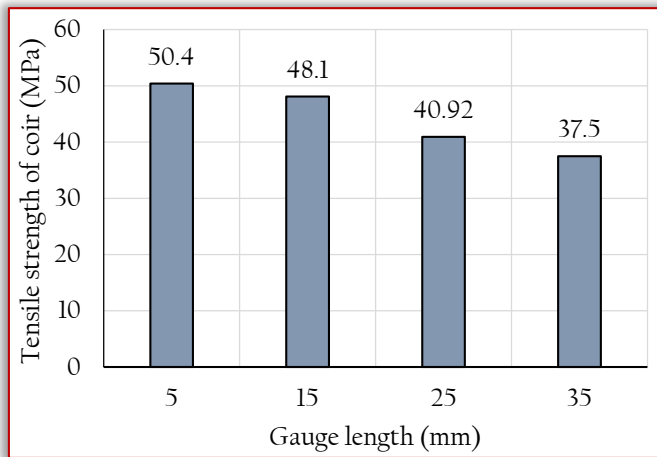
Figure 2. Effect of gauge length on tensile strength of coir fibre
adapted from (Mir et al., 2012)
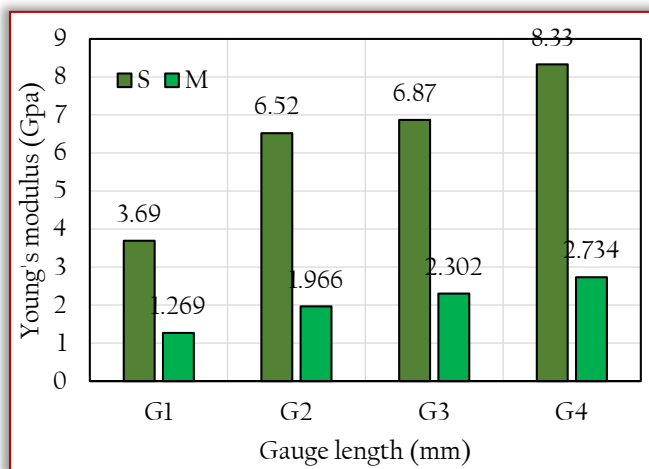
Figure 3. Effect of gauge length on the Young's modulus of coir fibre adapted from
(Tomczak, Sydenstricker and Satyanarayana, 2007; Mir et al., 2012) {T for: G1=5;
G2=10; G3=20;G4= 25. M for: G1=5; G2=15;G3=25;G4=35}

Mukherjee and Satyanarayana, (1984) observed that increase in the test length of coir fibres from15–65mm brought about decrease in UTS and elongation at break while Young's modulus increased, moreover, increase in strain rate from 1 to 50mm/minute led to increase in the UTS signifying tearing of the cell wall.

The Young's modulus of raw treated coir fiber increased with increase in span length, while the tensile strength and strain to failure of the same decreased with increase in span length (Mir et al., 2012). (Defoirdt et al., 2010) reported that strain to failure depends on the specimen gauge length and that this value varies with a factor of 1.62 for coir fibres.

The longer the gauge length, the lower the strength and vice versa. This can be attributed to the increase in the degree of flaws for natural fibres or as a result of the number of defects and so the weak links present in the fibre.

The incremental change in strength $d\sigma$ of the fibre with a corresponding change in gauge length dL according to Mukherjee and Satyanarayana, (1984) is represented by Equation [1];

$$d\sigma = \propto \frac{dL}{L} \qquad [1]$$

≡ σ represents the fibre strength
≡ $\propto$ represents a measure of the frequency of occurrence of weak links; and
≡ L represents the gauge length of the fibre.
≡ The change in strength with respect to change in gauge length is obtained by integrating Equation [1];
≡ The strength of the fibre of length L is represented by σ_o

$$\sigma_L = \sigma_o + \alpha \ln \frac{L}{L_o} \qquad [2]$$

The properties of natural fibres have been reported to depend on the type of fibre, specie, age or maturity and method of extraction (van Dam et al., 2006; Tomczak, Sydenstricker and Satyanarayana, 2007; Mathura and Cree, 2016; Dhaliwal, 2019). Therefore these information ought to be provided for a better characterization of the effects of heat treatment of natural fibres for their use in composites.

CONCLUSION
Heat treatment of natural fibres is important for composite applications. Therefore such factors as the specimen gauge length, number of specimens tested after heat treatment, average diameter of each specimen taken from various points along the gauge length before and after heat treatment and mode of fracture of the specimen should be fully reported. Others include the type of oven (vacuum or air oven) pre and post processing as well as storage conditions of the fibres after heat treatment prior to testing.

References
[1] Agunsoye, J.O; Bello, S.A; Talabi, I.S; Yekinni, A.A; Raheem, I.A and Oderinde, A.D: Tribology in Industry Recycled Aluminium Cans / Eggshell Composites : Evaluation of Mechanical and Wear Resistance Properties, Tribology in Industry, 37(1), pp. 107–116 2015.
[2] Alves, M.E; Pereira, T.V.C; Gomes, O.D.F.M; De Andrade, F andToledo, R: 'The effect of fiber morphology on the tensile strength of natural fibers', Journal of Materials Research and Technology. Korea Institute of Oriental Medicine, 2(2), pp. 149–157 2013.
[3] Araújo, A and Godoy, M. C: 'Polypropylene / chemically treated coir composites : optimizing coir delignification conditions using central composite design', Cellulose. Springer Netherlands, 25(2), pp. 1159–1170 2018.
[4] Arifuzzaman, G.M; Alam, M.S and Terano, M: 'Thermal characterization of chemically treated coconut husk fibre', Indian Journal of Fibre and Textile Research, 37(1), pp. 20–26 2012.
[5] Brígida, A. I. S; Calada V.M,A; Goncalves, LRB; Coelho, MAZ: 'Effect of chemical treatments on properties of green coconut fiber', Carbohydrate Polymers, 79(4), pp. 832–838 2010.
[6] Cao, Y; Sakamoto, S and Goda, K: 'Effects of heat and Alkali treatment on mechanical properties of kenaf fibres', 16th International Conference on Composite Materials, pp. 1–4 2007.
[7] Carl, B. and Brook, S: 'United States patent', Geothermics, 14(4), pp. 595–599 1985.
[8] Jan, J.E.G; van Dan; Martien, J.A et al:'Process for production of high density/high performance binderless boards from whole coconut husk. Part 2: Coconut husk morphology, composition and properties', Industrial Crops and Products, 24(2), pp. 96–104 2006.
[9] Defoirdt, N; Biswas, S;Vriese, L; De Tran et al: 'Assessment of the tensile properties of coir, bamboo and jute fibre', Composites Part A: Applied Science and Manufacturing. 41(5), pp. 588–595 2010..

[10] Dhaliwal, J: (2019) 'Natural Fibers: Applications', Intech, i(tourism), p. 13. 2019

[11] Dixit, S and Verma, P: 'The effect of surface modification on the water absorption behavior of coir fibers', Adv. Appl. Sci. Res. 3(3), pp. 1463–1465 2012.

[12] Edoziuno, F.O; Akaluzia, R.O; Odoni, B.U; Edibo, S: 'Experimental study on tribological (dry sliding wear) behaviour of polyester matrix hybrid composite reinforced with particulate wood charcoal and periwinkle shell', Journal of King Saud University – Engineering Sciences. King Saud University 05.007.2020.

[13] Esteves, B; Domingos, I and Pereira, H: 'Improvement of technological quality of eucalypt wood by heat treatment in air at 170–200°C', Forest Products Journal, 57(1–2), pp. 47–52 2007.

[14] Ezekiel,N; Ndazi, B; Nyahumwa, C and Karlsson, S: 'Effect of temperature and durations of heating on coir fibers', Industrial Crops & Products. 33(3), pp. 638–643, 2011.

[15] Ferreira, D.P; Cruz, J and Fangueiro, R: Surface modification of natural fibers in polymer composites, Green Composites for Automotive Applications. 2018

[16] Fiore, V; Scalici, T; Nicoletti, F; Vitale, G; Prestipino, M and Valenza, A: 'A new eco–friendly chemical treatment of natural fibres: Effect of sodium bicarbonate on properties of sisal fibre and its epoxy composites', Composites Part B: Engineering 85, pp. 150–160,. 2016

[17] Gassan, J and Bledzki, A K: 'Possibilities for improving the mechanical properties of jute/epoxy composites by alkali treatment of fibres', Composites Science and Technology, 59(9), pp. 1303–1309. 1999.

[18] Gourier, C; Antoine, D; Bourmaud, A; Baley, C: 'Mechanical analysis of elementary flax fibre tensile properties after different thermal cycles', Composites: Part A, 64, pp. 159–166. 2014.

[19] Jawaid, M and Khalil, H. P. S. A: 'Cellulosic / synthetic fibre reinforced polymer hybrid composites : A review', Carbohydrate Polymers 86(1), pp. 1–18, 2015

[20] Joshi, S.V; Drzal, L.T; Mohanty, A.K and Arora,S: 'Are natural fiber composites environmentally superior to glass fiber reinforced composites?', Composites Part A: Applied Science and Manufacturing, 35(3), pp. 371–376, 2004

[21] Latif, R; Wakeel,S; Khan,NZ et al: 'Surface treatments of plant fibers and their effects on mechanical properties of fiber–reinforced composites: A review', Journal of Reinforced Plastics and Composites, 38(1), pp. 15–30. 2019..

[22] Luz, F.S; Paciornik, S; Monteiro, S.N; Silva, L.C and Tommasini, V.I.O.J: 'Porosity Assessment for Different Diameters of Coir Lignocellulosic Fibers', The Minerals, Metals & Materials Society Porosity, 69(10), pp. 2045–2051, 2017.

[23] Mathura, N and Cree, D: 'Characterization and mechanical property of Trinidad coir fibers', Journal of Applied Polymer Science, 133(29), pp. 1–9. 2016

[24] Mir, S.S; Syed, M.N; Hassan, Md; Hossain, J and Hassan, M: 'Chemical modification effect on the mechanical properties of coir fiber', Engineering Journal, 16(2), pp. 73–83, 2012.

[25] Mukherjee, P.S. and Satyanarayana, K.G: 'Structure and properties of some vegetable fibres – Part 1 Sisal fibre', Journal of Materials Science, 19(12), pp. 3925–3934, 1984

[26] N Mahato, D; Mathur,BK and Bhattacherjee,S: 'Effect of alkali treatment on thermal stability and moisture retention of coir fibre', D, 20, pp. 202–205, 1995

[27] Ochi, S; Takagi, H and Niki, R: 'Mechanical properties of heat–treated natural fibers', High Performance Structures and Materials, 4, pp. 117–125, 2002

[28] Rao, K.M; Rao, K.M and Prasad, A.V.R: 'Fabrication and testing of natural fibre composites : Vakka , sisal , bamboo and banana', Materials and Design 31(1), pp. 508–513, 2010

[29] Saheb, N and Jog, J: 'Natural Fiber Polymer Composites : A Review', Advances in polymer technology, 2329(July), pp. 351–363, 2015

[30] Sanjay, M.R; Arpitha, G.R and Yogesha, B: 'Study on Mechanical Properties of Natural – Glass Fibre Reinforced Polymer Hybrid Composites: A Review', Materials Today: Proceedings. 2(4–5), pp. 2959–2967, 2015

[31] Shahzad, A: 'A Study in Physical and Mechanical Properties of Hemp Fibres', Advances in Materials Science and Engineering, 2013.

[32] Silva, G.G; Souza, D.A; Machado, J.C and Hourston, D.J: 'Mechanical and Thermal Characterization of Native', Journal of Applied Polymer Science, 76, pp. 1197–1206, 1999.

[33] Ticoalu, A; Aravinthan, T and Cardona, F: 'A review of current development in natural fiber composites for structural and infrastructure applications', in Southern Region Engineering Conference 2010, pp. 13–X1, 1997.

[34] Tomczak, F; Sydenstricker, T.H.D and Satyanarayana, K.G: 'Studies on lignocellulosic fibers of Brazil. Part II: Morphology and properties of Brazilian coconut fibers', Composites Part A: Applied Science and Manufacturing, 38(7), pp. 1710–1721, 2007

[35] Varma, D.S; Varma, M and Varma, I.K: 'Thermal behaviour of coir fibres', Thermochimica Acta, 108(C), pp. 199–210, 1986.

[36] Yun, H; Li, K; Tu, D and Hu, C; 'Effect of heat treatment on bamboo fiber morphology crystallinity and mechanical', 61(2), pp. 227–234, 2016.

[1.]V. VENKATESWARA REDDY, [1.]P.M. HADALGI

DESIGN FINITE ARRAY WITH NON–LINEAR ELEMENT SPACING

[1.] DOAE, Gulbarga University, Kalaburagi, Karnataka, INDIA

Abstract: Antenna arrays have positioned a large style of signal processing applications due to their multitude of offerings which include prolonged familiar benefit, range benefit, interference cancellation, beam steering, and direction–of–arrival (DOA) estimation among others. Generally speaking, the general overall performance of an antenna array improves with growing elements with inside the array. Several non–uniform array configurations have been reported in the literature including minimum redundancy arrays, minimum hole arrays, nested arrays, and co–prime arrays, among many others. Each of these configurations provides certain advantages and few drawbacks over the others. In this paper, the analysis and design of non–linear element spacing were investigated for direction–of–arrival estimation. Various methods were proposed to resolve the different challenges that are encountered by non–linear element spacing. The final matrix presented here consists of identical matrix elements, located at random. The fixed patch antenna serves as the base element for the grille. Arrays are created by randomly placing a base element. Arrays of this type are difficult to model and can be resource–intensive. It will show you how you can construct matrices using the available finite matrix tools. When the array is built in this way, DFM (Domain Green Function Method) acceleration can be applied to reduce the required resources: 20 mV, 20 dB general orientation, 0 dB axis ratio.
Keywords: Microstrip antenna, Ultra–wideband (UWB), Gain, Directivity, finite array, DGFM, CADFEKO

INTRODUCTION

An antenna array is a collection of or more spatially separated antennas prepared in a particular structure. The signs transmitted or received via the ones antennas are blended or processed definitely as a way to benefit a sophisticated normal overall performance over what is probably obtained via using the man or woman elements. An antenna array can develop the overall benefit, provide a selection benefit, cancel out interference from a hard and fast of directions, steer the beam in a particular direction, determine the DOA of incoming signs, and maximize the signal–to–interference–plus noise ratio.

Antenna arrays have positioned a large style of signal processing applications due to their multitude of offerings which include prolonged familiar benefit, range benefit, interference cancellation, beam steering, and direction–of–arrival (DOA) estimation among others [1]. Generally speaking, the general overall performance of an antenna array improves with growing elements with inside the array [2]. This is due to the fact that the prolonged range of things produces more levels of freedom (DOFs). For example, the overall benefit of an antenna array with the equal elements is the crafted from the element benefit with the array difficulty [3].

For a non–linear detail spacing, the array difficulty is similar to the range of things with inside the array. This approach that a larger range of things produce a larger benefit. Another example is the style of resolvable reasserts in DOA estimation using a ULA[4]. This range is tied to the range of things with inside the array, and as such, for a larger range of things more reasserts can be estimated. The Figure 1 represents the 3D far field pattern for the array.

A radio wire cluster is an assortment of or all the more spatially isolated receiving wires ready in a specific design. The signs communicated or got through one's receiving wires are mixed or prepared unquestionably as an approach to help a complex ordinary generally execution over what is most likely gotten by means of utilizing the man or lady components.
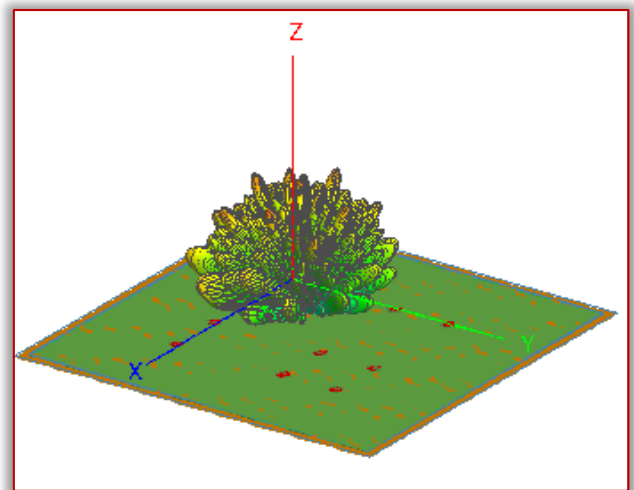
Figure 1. The 3D far field pattern for the array

A radio wire exhibit can foster the general advantage, give a choice advantage, offset impedance from immovable headings, steer the pillar a specific way, decide the DOA of approaching signs, and expand the sign to–obstruction in addition to clamor proportion. Receiving wire exhibits have situated a huge style of sign preparing applications because of their large number of contributions which incorporate delayed natural advantage, range advantage, impedance scratch–off, bar guiding, and course of–appearance (DOA) assessment among others [1]. As a rule, the overall generally speaking presentation of a receiving wire cluster improves with developing components with inside the exhibit [2]. This is on the grounds that the drawn out scope of things creates more degrees of opportunity (DOFs). For instance, the general advantage of a radio wire exhibit with equivalent components is created from the component advantage with the cluster trouble [3]. For a non–direct detail dispersing, the exhibit

trouble is like the scope of things with inside the cluster. This methodology that a bigger scope of things delivers a bigger advantage. Another model is the style of resolvable reasserts in DOA assessment utilizing a ULA[4]. This reach is attached to the scope of things with inside the exhibit, and thusly, for a bigger scope of things, more reasserts can be assessed.

LITERATURE SURVEY

≡ John Colaco et al: The creator talked about the rectangular fix having a dielectric consistent of 2.2 and dielectric mishap deviation of 0.0010. The plan is reflect and explored utilizing FEKO. Along these lines, after age creators have tracked down a decent return loss of – 33.4 dB, incredible data move breaking point of 3.56 GHz, VSWR <2, high rate increment of 10 dB and receiving wire radiation practicality of 99.5%. [1]

≡ J. Jasika Fa et al: The creator has talked about the radio wire has been organized at a repeat in the degree of 2.65GHz–3GHz. The radio wire is displayed with three novel layers of substrate, for delineation, FR–4, BAKELITE and ROGER (RO3010) without a ground plane and moreover showed up for a biomedical layer, for outline skin which has its relative permittivity (εr) as 46.6 and conductivity (σ) as 0.64. The age results are crossed CADFEKO programming [30]".

≡ Pei Cheng Ooi.et al "This paper shows a significant and lacking CPWfed T–formed printed receiving wire for WiMAX 3.5 GHz applications. A model has been all together, contorted and endeavor. The conscious outcomes show that the execution rehash of the radio wire is from 3.26 GHz to 4.28 GHz for a return loss of better than – 10 dB. Acceptable radiation plans have what's more been crossed proliferation. [32]

≡ Rashmi Gyawali et al: The planar receiving wire development has a lessened size of 30mm×25mm when cut on a substrate of dielectric steady 4.4 and tallness 1.6mm. The regular results show incredible single–rehash development with 10dB impedance all together transmission of 1.3 GHz and the reverberating rehash of 5.62GHz. The proposed radio wire conveys as Omni directional in azimuth plane and steady high getting wire acquire over the working band has been gotten. It additionally gives stable radiation plans, low return risk, high sending and radio wire helpfulness all through the WLAN band. The uniplanar nature, clear managing method and inconsequential improvement work on it for isolated plan. [33]

≡ Satya Kumar V. et al: In this paper the thoughtful and execution of an unadventurous T – molded space radio wire for ultra wideband (UWB) affiliation frameworks is introduced. different reverberating group are convey and bound together to outline a more wide trade speed from 2.9 to 11.7 GHz for S11 < – 10dB by making open ended changed T–outlined space radio wire and by along with a little piece of the microstrip feed line. The recreate result shows that it has stable unidirectional radiation models

and heartbeat managing limits inside the band of interest. [34]

DESIGN METHODOLOGY

Pin–took care of fix exhibit Creating the form The means for placing in the variant are as per the following:

Characterize the resulting factors: freq = 2.4e9 (Operating recurrence of the fix), lam0 = c0/freq*1000 (Free region frequency in millimeters), epsr = 2.08 (Relative dielectric reliable of fix substrate), patchLength = 41 (Length of the fix radio wire) , patchWidth = 35 (Width of the fix receiving wire), h = 3.5 (The highest point of the substrate), pinOffset = – 11 (Distance of feed pin from fix focus), wire Radius = 0.1 (Radius of the feed pin line), Set the adaptation unit to milli meters .

Make a square shape designated on the establishment with a width of patchWidth and a power of patchLength. Make a line area between (0, pinOffset,–h) and (0, pinOffset,0). Association the parts together. Make a dielectric medium with a permittivity of EPSR and name it substrate. Make a planar multi–facet substrate with a top of h. The medium must be substrate. Guarantee that a story airplane is portrayed at the most minimal of the dielectric layer. Add a port to the line area. Add a voltage supply to the port with the default esteems. Set the recurrence to freq. The figure 2 represents the array layout that will be analyzed.
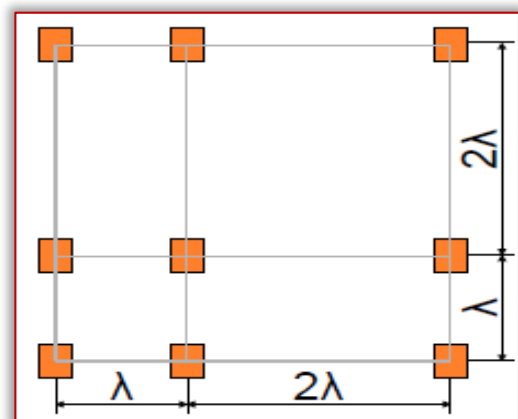
Figure 2. The array layout that will be analyzed

The math above addresses the base detail, which isn't constantly covered with inside the cluster estimations through method of way of default. Make the cluster portrayed in decide 2 through method of way of playing out the ensuing advances: Create a planar exhibit: Request 4 variables in each measurements Space the elements lam0 separated. Convert the planar exhibit right legitimate solidly into a custom cluster. This makes it conceivable to erase, reposition or turn character elements of the exhibit.

Erase all components similar as the 1/3 line and section. There need to now be 9 factors left. Note that everything about can have a particular direction. Components are orbited through method of way of altering the organization workplace of the custom receiving wire cluster factors. No components need to be orbited for this model, anyway the benefactor in prescribed to turn some of the variables after the recreation has completed to research the effect at the cluster design. Cross

section Use Standard lattice to work the calculation. Set the stage range to wireRadius. Solicitations Request a 3–D an extended way adventure that covers the apex 1/2 of space. An inspecting addition of θ = 1.5∘ and φ = 1.5∘ is needed to acquire a significantly less lavish goal. Set the start of an extended way adventure (Workplane tab) to 1.5*lam0 for each the X and the Y segments. This does now not substitute an extended way adventure design (this could affect the stage), anyway areas the demonstration of an extended way adventure at the 3–D view with inside the focal point of the fix exhibit.

Note that an alert can be experienced simultaneously as strolling the arrangement. This is because of reality misfortunes cannot be determined in a boundlessly enormous medium, as is required for the extraction of receiving wire directivity data (acquire is processed by means of method of way of default). This alert might be deflected by means of method of way of ensuring that an extended way adventure acquire be determined in inclination to the directivity. This is prepared at the prevalent tab of the an extended way adventure demand with inside the tree

ANTENNA PARAMETERS
— Directivity
It is described as the extent of the radiation power in a given direction from the getting wire to the radiation power showed up at the midpoint of generally speaking orientation.

— Gain
Gain is portrayed as the extent of the power in a gave direction to the radiation power that would be gotten if the power recognized by the getting wire were sent isotropically

— Radiation pattern
It is described as the assortment of the power radiated by an accepting wire as a component of the bearing away from the radio wire this power assortment as a segment of the appearance point is found in radio wires for fields

— Axial Ratio or Pivotal Proportion
The Pivotal Proportion or Axial Ratio of a receiving wire is characterized as the proportion between the major and minor hub of a circularly captivated radio wire design. On the off chance that a radio wire has amazing roundabout polarization, this proportion would be 1 (0 dB). Thusly, it is consistently bigger than 1 (>0 dB) in an oval.

SIMULATION RESULTS
Arrays of this kind are hard to version and might bring about excessive aid requirements. It could be proven how the array may be built the use of to be had finite array tools. When arrays are built on this way, the DGFM (area Green's characteristic method) acceleration may be implemented to decrease the sources which are wished. The Figure 3 indicates the 3D far field pattern for the array.

— Total Directivity (dB)
It is defined because the quantity of the radiation energy in a given path from the getting twine to the radiation energy confirmed up on the midpoint of usually talking orientation.

The Figure 4 shows the total directivity is 20 dB for the frequency of 5.875 GHz
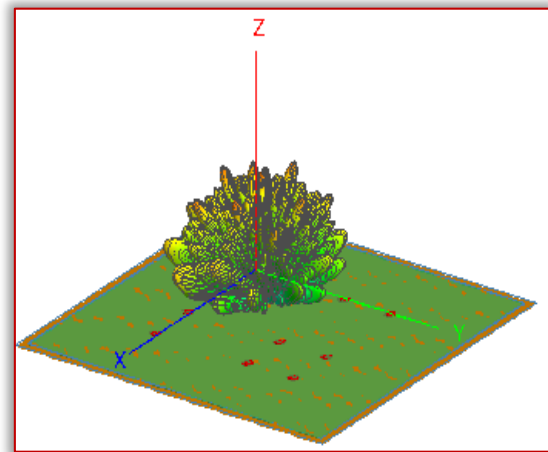
Figure 3. The 3D far field pattern for the array
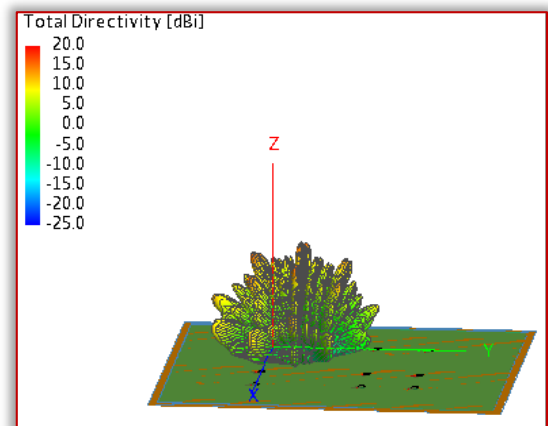
Figure 4. Total directivity in dB

— Total E–Field Magnitude (dB)
The value and course of the electrical discipline are expressed with the aid of using the price of E, known as electric powered discipline energy or electric powered discipline depth or truely the electrical discipline. The price of the electrical discipline at a factor in space, for example, equals the pressure that could be exerted. The figure 5 shows the Total E–Field Magnitude (dBV) is –20 dB for the frequency of 5.875 GHz
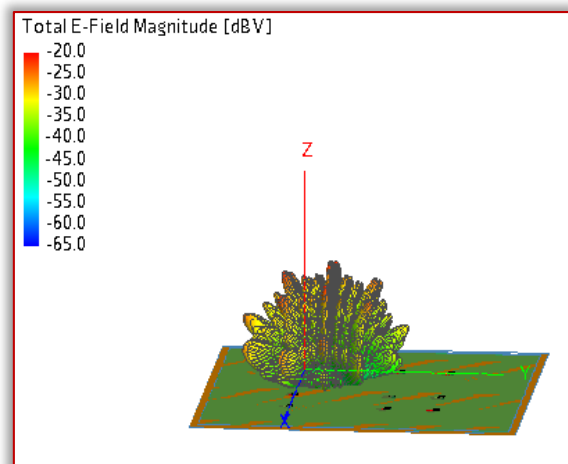
Figure 5. Total E–Field Magnitude (dB)

⎯ Axial Ratio or Pivotal Proportion

It is defined because the quantity of the radiation energy in a given path from the getting twine to the radiation energy confirmed up on the midpoint of usually talking orientation. The figure 6 shows the Axial Ratio is less than 0dB for the frequency of 5.875 GHz.
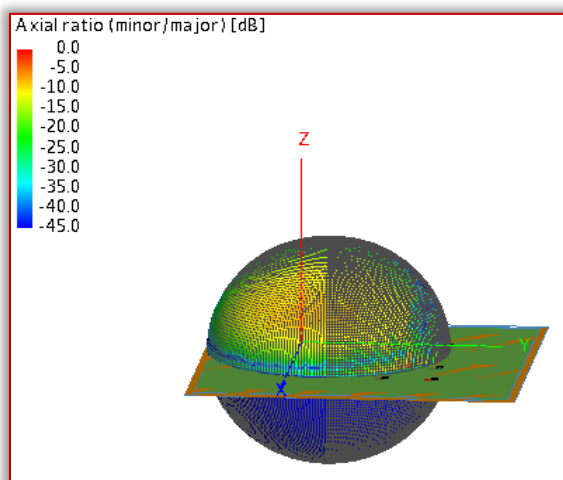
Figure 6. Axial Ratio less than 0dB for the frequency of 5.875 GHz

⎯ Handedness

The figure 7 shows the handedness with left and right for the frequency of 5.875 GHz
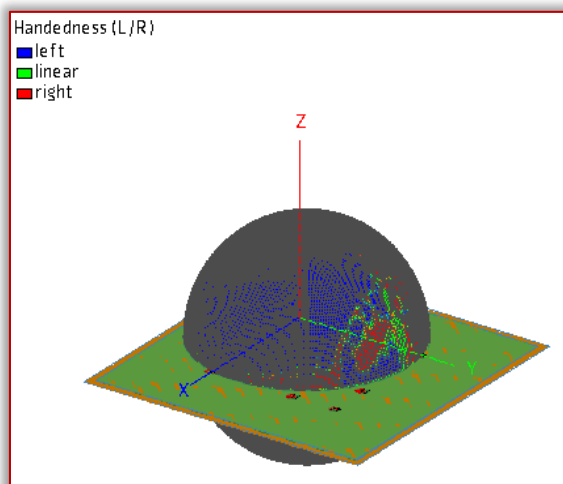
Figure 7. Handedness with left and right for the frequency of 5.875 GHz

⎯ Total Realized Gain (dB)

Actual profit is the difference between costs and gains from the sale or redemption of a security. Profit arises when a product is sold at a price that is higher than its original price. The Figure 8 represents the overall gain of 1.0 dB for frequency of 5.875 GHz.

⎯ Total Gain

This is the whole advantage on a portfolio role including unrealized profits on modern holdings, realized profits from income and dividends obtained expressed with inside the selected portfolio currency. The figure 9 shows 3D radiation pattern of Total Gain. The total advantage is 50 for the frequency of 5.875 GHz.
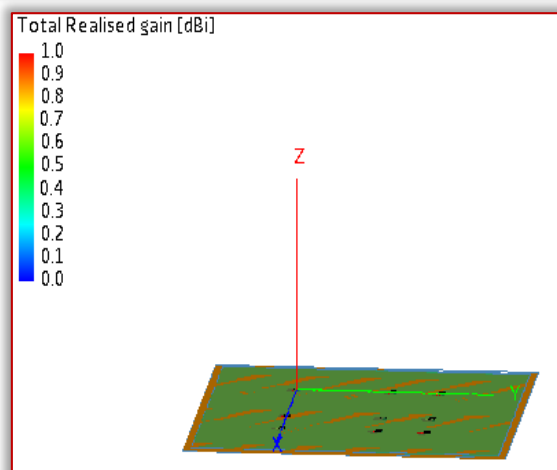
Figure 8. Plot of 3D radiation pattern of Total Realized Gain with the frequency 5.875 GHz
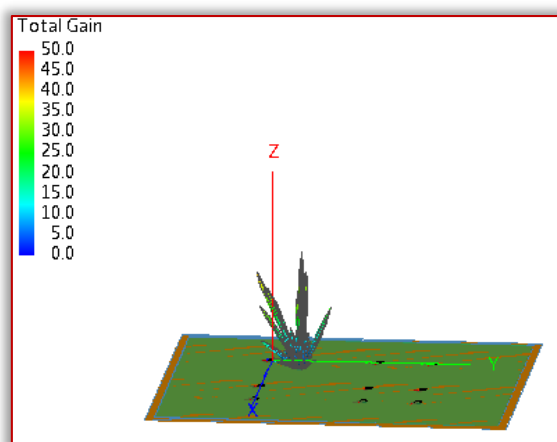
Figure 9. Plot of 3D radiation pattern of Total Gain

⎯ Total gain (dB)

The gain is defined as the ratio of the output power to the input power in dB. The Figure 10 shows 3D radiation pattern of Total Gain (dB). The total gain is 20 dB at 5.875 GHz.
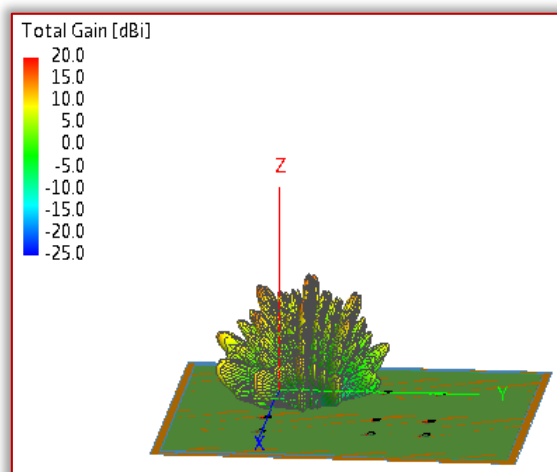
Figure 10. Plot of 3D radiation pattern of Total Gain (dB)

THE FAR FIELD GAIN PATTERN FOR THE ARRAY

The Figure 11 shows the far field gain pattern for the array and suggests the assessment of theta cuts of the array approximation with the outcomes acquired the usage of an

equal complete MoM model. The outcomes evaluate favourably. The Table I alternate of frequencies and parameters values tabulated for the frequency of 5.875 GHz
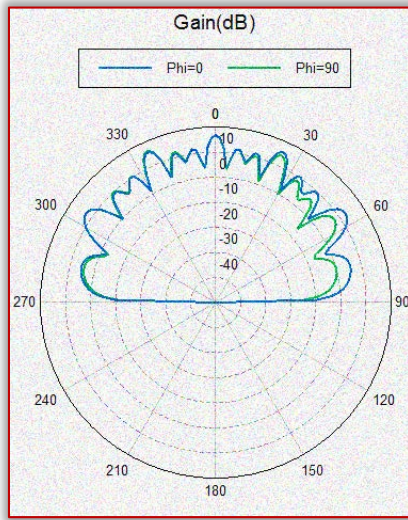
Figure 11. The far field gain pattern for the array

Table 1. Frequency and parameters values

S.No	Freq (GHz)	Gain dB	Total Relaised Gain dB	Total E–field Magnitude	Total Directivity	Axial ratio [minor/ major] dB
1	5.875	20	17.5	−20mV	20dB	0

CONCLUSION

Antenna arrays are widely used in signal processing applications due to their multiple offerings non–linear element spacing provide an effective way to deal with the issue of increased hardware cost and complexity in large antenna arrays. These arrays deliver a similar performance to that of a uniform array with a reduced number of elements. Several non–uniform array configurations have been reported in the literature including minimum redundancy arrays, minimum hole arrays, nested arrays, and co–prime arrays, among many others.

Each of these configurations provides certain advantages and few drawbacks over the others. In this paper, the analysis and design of non–linear element spacing were investigated for direction–of–arrival estimation. Various methods were proposed to resolve the different challenges that are encountered by non–linear element spacing. For the frequency 5.875GHz the gain is 20db and the total realized gain is 17.5 dB, the total E field Magnitude is −20mV, the total directivity is 20 dB and the axial ratio is 0 dB The challenges include the reduction of the available degrees–of–freedom due to the presence of missing elements in the difference coarray, the mutual coupling effect in practical antenna arrays, and the presence of correlated or coherent targets in the field of view.

References

[1] D. H. Johnson and D. E. Dudgeon, Array Signal Processing: Concepts and Techniques. Englewood, NJ: Prentice Hall, 1993.

[2] A. Moffet, "Least repetition direct gatherings," IEEE Trans. Radio wires Propag., vol. AP16, no. 2, pp. 172–175, Mar. 1968.

[3] G. S. Juvenile then S. W. Golomb, "Utilization of numbered undirected layouts," Proc. IEEE, vol. 65, no. 4, pp. 562–570, Apr. 1977.

[4] P. Mate and P. P. Vaidyanathan, "Settled showcases: a totally surprising strategy in emulate of mastermind managing along better levels concerning opportunity," IEEE Trans. Signal Process., vol. 58, no. 8, pp. 4167–4181, Aug. 2010.

[5] P. P. Vaidyanathan then P. Buddy, "Inadequate recognizing including co–prime samplers then, at that point gatherings," IEEE Trans. Signal Process., vol. 59, no. 2, pp. 573–586, 2011.

[6] P. Buddy then P. P. Vaidyanathan, "Coprime model or in like way the MUSIC assessment,'' into IEEE Digital Signal Process. Studio then IEEE Signal Process. Show Workshop, Sedona, AZ, 2011, pp. 289–294.

[7] C.– L. Liu then P. P. Vaidyanathan, "Cramér–Rao field considering the way that coprime then despicable sprase shows, who find more prominent sources than sensors," Digital Signal Processing Special Issue of Co–prime Sampling and Arrays (in press).

[8] R. T. Hoctor then S. A. Kassam, "The restricting together situation on the coarray among opening change thinking about the way that unquestionable and mutilated imaging," Proc. IEEE, vol. 78, no. 4, pp. 735–752, Apr. 1990.

[9] H. L. Van Trees, Optimum Array Processing: Part IV as for Detection, Estimation, yet Modulation Theory. New York, NY: John Wiley yet Sons, 2002.

[10] S. Chandran, Advances into Direction–of–Arrival Estimation. Norwood, MA: Artech House, 2006. 167

[11] T. E. Tuncer then B. Friedlander, Classical and Modern Direction–of–Arrival Estimation. Boston, MA: Academic Press (Elsevier), 2009.

[12] R. Schmidt, "Diverse creator area yet signal cutoff assessment," IEEE Trans. Receiving wires Propag., vol. 34, no. 3, pp. 276–280, Mar. 1986.

[13] S. U. Pillai, Y. Bar–Ness, and F. Haber, "A subsequent technique to oversee change calculation on account of extra made spatial arrive at evaluation," Proc. IEEE, vol. 73, pp. 1522–1524, Oct. 1985.

[14] Y. I. Abramovich, D. A. Weak, A. Y. Gorokhov, then, at that point N. K. Spencer, "Positive–unequivocal Toeplitz completing inside DOA augmentation for nonuniform straight radio wire shows. I. Absolutely augmentable shows," IEEE Trans. Signal Process., vol. 46, pp. 2458–2471, Sep. 1998.

[15] Y. I. Abramovich, N. K. Spencer, yet A. Y. Gorokhov, "Positive–clear Toeplitz finish inside DOA assessment considering the way that nonuniform straight radio wire packs. II. Fairly augmentable bundles," IEEE Trans. Signal Process., vol. 47, pp. 1502–1521, Jun. 1999.

[16] T. J. Shan, M. Wax, yet T. Kailath, "On spatial smoothing on account obviously of–appearance understanding about clear signals," IEEE Trans. Acoust., Speech, Signal Process., vol. 33 no. 4, pp. 806–811, Aug. 1985.

[17] Q. Wu or Q. Liang, "Coprime model for nonstationary sign among radar signal arranging," EURASIP J. on Wireless Commun. Netw., 2013:58, 2013.

[18] K. Adhikari, J. R. Buck, then, at that point K. E. Pay, "Beamforming with extended co–prime sensor gatherings," among IEEE Int. Conf. Acoustics, Speech and Signal Process., Vancouver, BC, Canada, 2013, pp. 4183–4186.

[19] Y. Zhang, M. Amin, F. Ahmad, or B. Himed, "DOA assessment a few tantamount direct changes close by two CW signals concerning co–prime frequencies," in IEEE fifth Int. Studio Computational Advances in Multi–

Sensor Adaptive Process., Saint Martin, French West Indies, France, 2013, pp. 404–407.

[20] Z. Tan or A. Nehorai, "Lacking technique for essence assessment utilizing co–prime bundles including off–structure targets," IEEE Signal Process. Lett., vol. 21, no. 1, pp. 26–29, Jan. 2014. 168

[21] A. T. Pyzdek and R. L. Culver, "Arranging strategies on the grounds that coprime shows inside complex shallow lotus conditions," J. Acoust. Soc. Am., vol. 135, no. 4, pp. 2392–2392, Apr. 2014.

[22] J. Chen or Q. Liang, "Rate mutilation execution assessment on settled duplicate yet coprime examining," EURASIP J. Adv. Signal Process., 2014:18, 2014.

[23] J. Ramirez, J. Odom, and J. Krolik, "Taking advantage of sort out advancement thinking about join of co–prime shows," into IEEE eighth Int. Sensor Array then Multichannel Signal Process. Studio, A Coruna, Spain, 2014, pp. 525–528.

[24] R. Roy or T. Kailath, "ESPRIT–Estimation on sign cutoff points with the assistant of rotational invariance frameworks," IEEE Trans. Acoust., Speech, Signal Process., vol. 37, no. 7, pp. 984–995, Jul. 1989.

[25] A. J. Barabell, "Further encouraging the target all things considered execution of eigenstructure–based directionfinding calculations," inside IEEE Int. Conf. Acoustics, Speech yet Signal Process., Boston, MA, 1983, pp. 336–339.

[26] C. El Kassis, J. Picheral, yet C. Mokbel, "Benefits concerning nonuniform gatherings utilizing rootMUSIC," Signal Processing, vol. 90, no. 2, pp. 689–695, Feb. 2010.

[27] D. Malioutov, M. Cetin, yet A. Willsky, "Little sign delight perspective since source limitation including sensor shows," IEEE Trans. Signal Process., vol. 53, no. 8, pp. 3010–3022, Aug. 2005.

[28] C.– Y. Hung and M. Kaveh, "Heading discovering kept up with the thought about super–objective of forlorn reference assessments," between IEEE Int. Conf. Acoustics, Speech or Signal Process., Brisbane, Australia, 2015, pp. 2404–2408.

[29] Y. D. Zhang, M. G. Amin, or B. Himed, "Sparsity–based DOA consistency the utilization of co–prime gatherings," of IEEE Int. Conf. Acoustics, Speech then, at that point Signal Process., Vancouver, BC, Canada, 2013, pp. 3967–3971. 169

[30] J. Jasika Fairy, M.Nesasudha "Low Profile receiving join plan considering the way that biomedical applications" International Conference over Signal Processing then Correspondence"(ICSPC'17) – twenty eighth or twenty 10th July 2017

[31] Pei Cheng Ooi then Krishnasamy T. Selvan "More moderate T–Shaped CPW–Fed Printed Antenna for 3.5 GHz WiMAX Applications" 2009

[32] Rashmi Gyawali, Praveen Kumar Penta, V.Sudha "CPW–FED S–Shaped Single Band WLAN Antenna" PROCEEDINGS OF ICETECT 2011

[33] Satya Kumar. V, Anup Kumar Gogoi "Plan on T–Shaped Slot Antenna by prudence of UWB Communications Systems" 2011 International Conference about Broadband Furthermore, Wireless Computing, Communication yet Applications.

[34] Mohamed Tarbouch, Hanae Terchoune, Abdelkebir El Amri "Restricted CPW–Fed Microstrip Octagonal adjusting radio wire with H house for WLAN yet WIMAX Applications" 2017

[1.]O.C. OKOYE, [2.]C. I. MADUEKE, [2.]R. UMUNAKWE, [1.]D.O. KOMOLAFE

EFFECTS OF ADDITION OF CARBON BLACK TO PALM KERNEL SHELL AS CARBURIZER ON THE MECHANICAL PROPERTIES AND CASE STRUCTURE OF LOW CARBON STEEL

[1.]Department of Mechanical Engineering, Faculty of Engineering, Federal University Oye-Ekiti, Ekiti State, NIGERIA
[2.]Department of Materials and Metallurgical Engineering, Faculty of Engineering, Federal University Oye-Ekiti, Ekiti state, NIGERIA

Abstract: This study investigated the influence of the addition of carbon black to palm kernel shell, as the carburizing media, on the mechanical properties and case structure of low carbon steel. The particle size of the carburizers used was 150 μm. Various compositions of the carburizing media were used, and carbon black was added to palm kernel shell to a maximum of 10 wt% of the total weight of the carburizer. For each composition, 20 wt% of calcium carbonate was added as energizer. Samples for tensile test, hardness test and microstructural examination were carburized at 950^{0}C for 3 hours. The samples were then tempered at 450^{0}C for forty minutes. The best combination of mechanical properties was obtained for the sample carburized with 95 wt% palm kernel shell and 5 wt% carbon black.
Keywords: low carbon steel, carburization, palm kernel shell, carbon black, mechanical properties

INTRODUCTION

Low carbon steel, also known as mild steel, has carbon content of less than 0.30% [1]Typical applications of low carbon steel are in: rivets, seam welded pipes, structural steels, plates, nuts, screws, bolts, sheets, and parts of machines which do not demand high – strength requirement [2, 1]. When the carbon content in a steel is varied, in conjunction with using a suitable heat-treatment method adequate for that particular amount of carbon, a myriad of mechanical properties can be obtained. No other metallic alloy has this unique feature of carbon steel. In addition, carbon steel in comparison with non-ferrous alloys, is not expensive, thus steel is largely the most important engineering alloy [2].

Steel undergoes heat treatment in order to harden it, and to increase its strength, ductility and toughness. The carbon content and the intended use of the steel determine the kind of heat treatment the steel will undergo (Higgins, 1993). The types of heat treatment are as follows: normalising, tempering, annealing, isothermal transformations and hardening [2, 3].

Carburization is the process of adding carbon to the exterior of low-carbon steels mainly at temperatures of between 850^{0}C and 980^{0}C [4]. Within this temperature range, austenite which has high solubility for carbon, is the crystal structure which is stable. Hardening is obtained by quenching the high-carbon exterior of the steel to form martensite. Thus, the martensitic case which has high carbon content (having good wear and fatigue resistance) is laid over a tough core that is low in carbon content [5, 4] .The carburizing method used may be solid, liquid or gaseous [5, 2, 4]. These methods have their merits and demerits [5, 4], and the kind and extent of the work to be done by the metal will determine the best carburizing method to be used [2]. The most frequently used method for high-volume production is gas carburizing, since it is precisely regulated and needs much reduced special handling [5, 4] .

Researchers have investigated the use of cheap and locally available carbonaceous materials as carburizing agents in pack carburization.

[6] experimentally studied the effect of coal, bone charcoal and wood charcoal on the hardness, tensile strength and impact strength of mild steel. He found out that each carburizing medium increased the hardness and tensile strength of mild steel with carburizing time, while each medium decreased the impact strength of mild steel with carburizing time. The results of the hardness tests he obtained had reasonable agreement with those available in literature. He suggested that with the addition of energizers to the local carburizing media, better results could be obtained in less time. He further reported that wood charcoal gave the highest values of mean hardness and mean tensile strength, while coal gave the least values. [7] studied the effect of the variation in carburizing temperature and time on the mechanical properties of mild steel quenched in oil, and tempered at 550^{0}C for one hour. For their experimental conditions, they reported that the best blend of mechanical properties was obtained at carburizing temperature and time of 900^{0}C and 30 minutes respectively, with quenching in oil and tempering for an hour at 550^{0}C following the carburization process.

[8] studied the effect of varying carburizing temperature and carburizing time on the mechanical properties of mild steel using pulverized bone as carburizer. They reported a strong connection between the properties and carburization process, carburization temperature and soaking time at a particular temperature. In particular, they noted that the best results were obtained for the samples carburized at 900^{0}C and 15 minutes, and at 850^{0}C and 30 minutes, as they both had a hard case with a softer core.

[9] investigated the effects of using graphite, charcoal, palm kernel shell and mixed carburizer on the case hardness of low carbon steel. Impact tests and microstructural examination were also conducted on the steel samples. The sample

carburized with palm kernel shell had the highest hardness value, while that carburized with graphite had the highest impact energy. [10] investigated pack carburization of mild steel using seashell, palm kernel shell and animal (cow) bone in the temperature range of 700 to 1100⁰C. They reported that palm kernel shell and animal (cow) bone were better carburizing media compared to seashell. [11] studied pack carburization of mild steel using charcoal with bone as energizer. The compositions of the carburizing compounds that were used were 100 wt% charcoal, 75 wt% charcoal/25 wt% cowbone, 70 wt% charcoal/30 wt% cowbone and 60 wt% charcoal/40 wt% cowbone. The best hardness value reported was for the 60 wt% charcoal/40 wt% cowbone composition. [11] set out to determine whether egg shell waste could be used as an energizer using sugar case waste, aracaceae flower droppings and melon shell as the carburizing media. They concluded that egg shell waste was a good energizer as it increased the hardness values of the samples, as compared to when the samples were carburized without it. [12] conducted experimental investigation on the effectiveness of locally available carbonate minerals as energizers in pack carburization of mild steel using charcoal as the carburizing medium. The minerals they studied were marble, limestone and dolomite, and they compared the efficacy of these minerals with that of barium carbonate. They reported that marble or limestone is a suitable replacement for most of the barium carbonate used as energizer in pack carburization of mild steel. They showed that the best result, in terms of effective case depth and relative efficacy of the energizer, was obtained using 15% marble and 5% barium carbonate. They noted that this composition of energizer seems to be more effective than using 20% barium carbonate. They reported that dolomite is not an energizer and that in fact, it seems to slow down carburizing action.

More research work is needed, especially in the comparative analysis of carburizing media, to determine suitable local carburizing media for pack carburization of mild steel. Palm kernel shell is a readily available waste product in Nigeria, and it has been shown to have a high carbon potential. However, its efficacy as a carburizing medium has not been extensively investigated. In this work, mild steel will be carburized using palm kernel shell with the addition of carbon black to a maximum of 10 wt% carbon black. 20 wt% calcium carbonate was used as energizer, since it has been shown in the literature to be effective, and is in abundant supply in Nigeria. The effects of various compositions of the carburizing media on the hardness, tensile properties and microstructure of mild steel will be studied

Table1. Chemical composition of the low carbon steel

Element	Al	Si	P	S	Ti	V	Cr
Composition (%)	0.1478	0.3113	0.0369	0.0025	0.9355	0.0097	0.1808
Element	Mn	C	Fe	Ni	Cu	As	Mo
Composition (%)	0.5071	0.14	97.4118	0.0865	0.1806	0.0032	0.0463
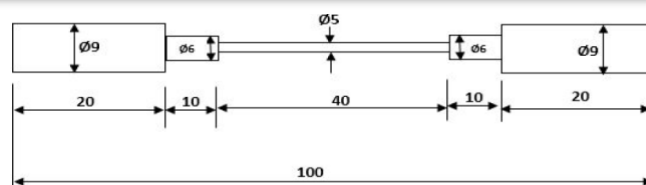
Figure 1. Dimensions of tensile test sample

MATERIALS AND METHODS
— Preparation of Samples
Palm kernel shells were obtained, washed and dried. Thereafter they were crushed with hammer mill, and pulverized using a ball mill. The powder was then sieved to particle size of 150 μm. Grade 330 carbon black was purchased and used for the work. A 10 mm mild steel rod was used for the work.

The chemical composition of the rod is presented in Table 1. Specimens for the tensile test were machined from the rod according to ASTM E8 (refer to Figure 1).

The samples for the hardness test and microstructural examination were also cut out. Four boxes measuring 120 x 30 x 30 mm were constructed using 5 mm thick steel plate. The composition of the carburizing media was measured out for each sample as shown in Table 2. For each composition of carburizer, 20 wt% of calcium carbonate, that is 20 wt% of the carburizer's total compositon, was included as energizer. The samples for the tensile and hardness tests and those for microstructural examination were buried in the carburizer and then the boxes were properly sealed.

Table 2: Compositions of the carburizing media used

Sample	Palm kernel shell powder (wt%)	Carbon black (wt%)	Calcium Carbonate ($CaCO_3$) wt%
1	100	0	20
2	90	10	20
3	95	5	20
4	99	1	20
5 (control sample)	0	0	0

— Carburization of the Samples
The sealed boxes were then placed in an electric heat treatment furnace and the temperature of the furnace was set to 950⁰C. When the temperature of the furnace attained 950⁰C, the time was taken. The samples were then held in the furnace on attainment of 950⁰C for 3 hours. After this time, the samples were quenched in water at room temperature. Afterwards, the samples were tempered in the furnace at 450⁰C for forty minutes, and were cooled in air at room temperature. The control sample (Sample 5) did not undergo heat treatment.

TESTS CONDUCTED
— Tensile Test
Uniaxial tensile tests were conducted on the tensile specimen according to ASTM E8 using an Instron Universal Testing Machine, at a strain rate of 10 mm/mm. Before beginning the tests, the gauge length and initial diameter of the specimens were entered into the software. The ultimate tensile strength,

fracture strength, modulus of elasticity, percentage elongation and fracture load were determined for each of the specimens.

—— Hardness Test

Hardness tests were performed using a digital Brinell hardness testing machine.

—— Microstructural Examination

The microstructures of the cases of samples 1, 2 and 5 (control sample) were examined using a Phenom scanning electron microscope.

RESULTS AND DISCUSSION

The tensile test results of the samples are presented in Figures 2 to 6, while the hardness test results are presented in Figure 7.
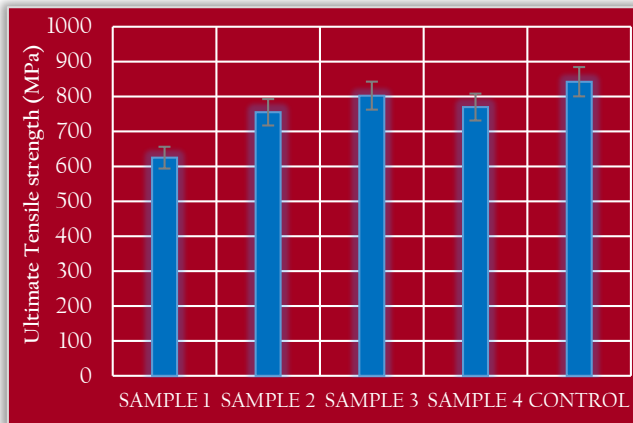
Figure 2: Ultimate tensile strength of the samples
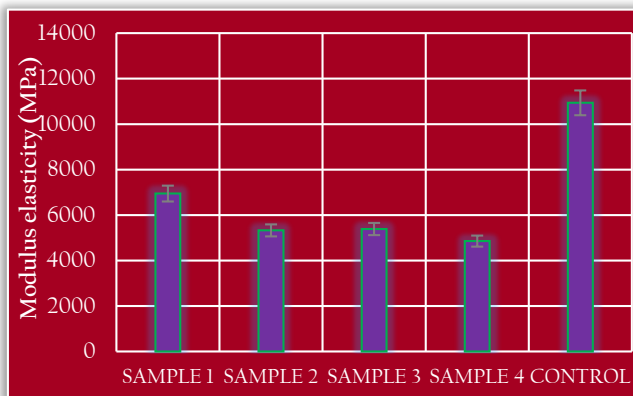
Figure 3: Modulus of elasticity of the samples
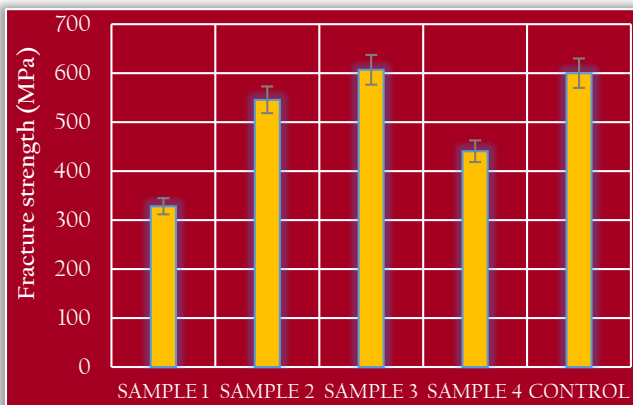
Figure 4: Fracture strength of the samples
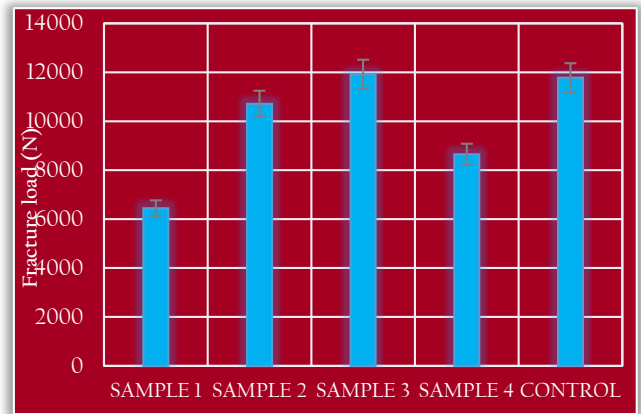
Figure 5: Fracture load of the samples
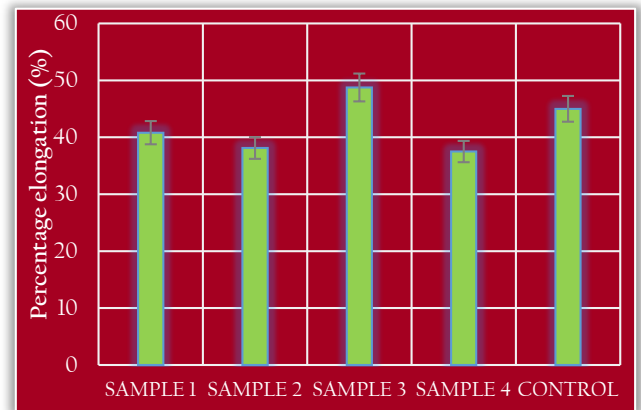
Figure 6: Percentage elongation of the samples
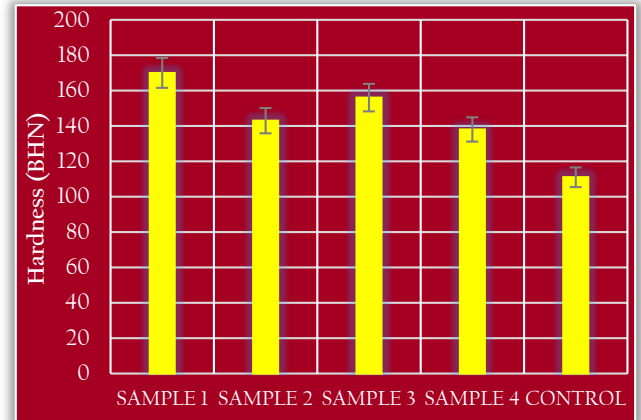
Figure 7: Hardness of the samples

From the results of the tensile test, it can be seen that generally there is a reduction in the values of the ultimate tensile strength and the modulus of elasticity of the heat-treated samples. This is due to the fact that the hardened steel was tempered [2, 1].

From Figure 2, there is a reduction in the ultimate tensile strength of the heat-treated samples. Also, there was a reduction in the modulus of elasticity of the heat-treated samples as shown in Figure 3. As expected, there was an increase in the fracture strength, the fracture load and the percentage elongation of the samples that were subjected to heat treatment. This is because tempering improves the toughness and the ductility of carbon steels [2, 13].

From Figure 7 it can be seen that the hardness values of the heat-treated samples increased significantly as compared to the control sample. This suggests that palm kernel shell is indeed a good carburizing medium as can be seen from sample 1 (Figure 7). From Figures 2 to 7, it can be seen that sample 3 had the highest values, compared to other heat-treated samples, of ultimate tensile strength, fracture strength, fracture load and percentage elongation. However, its modulus of elasticity and hardness values are lower than those of sample 1. Thus sample 3 has the best combination of tensile properties and hardness value.

The photomicrographs of samples 5, 1 and 2 are presented in Figures 8, 9 and 10.
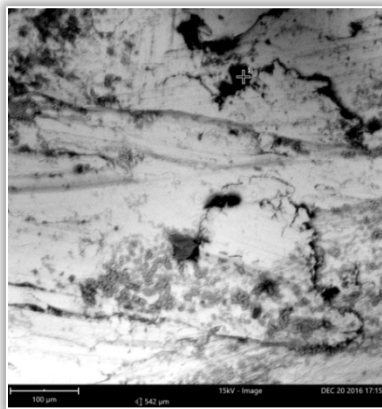
Figure 8: Photomicrograph of the case of sample 5 (control sample)
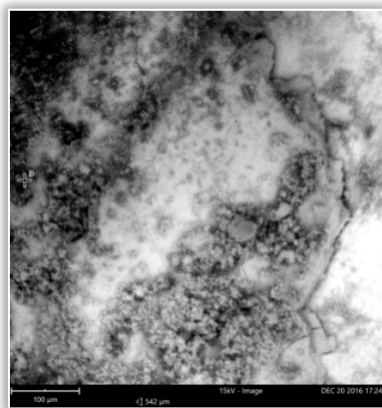
Figure 9: Photomicrograph of the case of sample 1
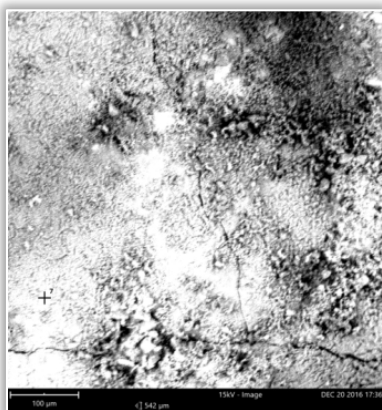
Figure 10: Photomicrograph of the case of sample 2

The photomicrograph of the control sample (Figure 8) shows the typical structure of mild steel, that is ferrite (light areas) and pearlite (black areas) [13, 14].

In Figure 9, coalesced globules of cementite can be seen in the ferrite matrix. Cementite was precipitated from the martensitic structure on tempering [2]; while Figure 10 shows a more even distribution of spheroid cementite in the matrix of ferrite.

The presence of cementite in Figures 9 and 10 indicates carbon enrichment of the steel surface. The ultimate tensile strength, fracture strength and fracture load of sample 2 are greater than those of sample 1 as seen from Figures 2, 4 and 5 respectively.

The modulus of elasticity and hardness of sample 2 are lower than that of sample 1 (Figures 3 and 7) while the percentage elongation of sample 2 is slightly lower than that for sample 1 (Figure 6). It appears that the addition of 10 wt% of carbon black to palm kernel shell increased its toughness.

From the results of this study, sample 3 gave the best combination of mechanical properties. This suggests that carbon black has some effects on the improvement of the mechanical properties of steels carburized with palm kernel shell.

CONCLUSIONS

The following conclusions can be drawn from this study:

— Palm kernel shell is a good carburizing agent as it has very high carbon potential, and gave the highest case hardness value.

— The addition of carbon black to palm kernel shell as carburizing media helps to improve the toughness of low carbon steel.

— The best combination of mechanical properties was obtained with a composition of the carburizing media containing 95 wt% palm kernel shell and 5 wt% carbon black.

— The findings of this work will be useful to the following companies in Nigeria: Integrated Steel PLC, Osogbo; Nigeria Machine Tools Limited, Osogbo; Ajaokuta Steel Company Limited, Ajaokuta; Delta Steel Company, Ovwian – Aladja as well as similar companies in Nigeria and across the world.

References

[1]   K. Serope, S. R. Steven and M. Hamidon, Manufacturing Engineering and Technology, Pearson Publications, Singapore, 2009

[2]   A.R. Higgins, "Engineering Metallurgy-Part 1-Applied Physical Metallurgy. Edward Arnold," 1993

[3]   S. M. A. Al-Qawabah, N. Alshabatat and U. F. Al-Qawabeha, "Effect of annealing temperature on the microstructure, microhardness, mechanical behavior and impact toughness of low carbon steel, grade 45," International Journal of Engineering Research and Applications, vol. 2, p. 1550–1553, 2012.

[4]   M. J. Schneider, "The Timken Company, and Madhu S. Chatterjee, bodycote introduction to surface hardening of steels," ASM handbook, steel heat-treating fundamentals and processes, vol. 4, 2013.

[5]   S. Lampman, "Introduction to surface hardening of steels," ASM International, ASM Handbook., vol. 4, p. 259–267, 1991.

[6]   E. J. Ohize, "Effects of local carbonaceous materials on the mechanical properties of mild steel," Assumption University Journal of Technology, vol. 13, p. 107–113, 2009.

[7]   F. O. Aramide, S. A. Ibitoye, I. O. Oladele and J. O. Borode, "Effects of carburization time and temperature on the mechanical properties of carburized mild steel, using activated carbon as carburizer," Materials research, vol. 12, p. 483–487, 2009.

[8]   F. O. Aramide, S. A. Ibitoye, I. O. Oladele and J. O. Borode, "Pack carburization of mild steel, using pulverized bone as carburizer: Optimizing process parameters," Leonardo Electronic Journal of Practices and Technologies, vol. 16, p. 1–12, 2010.

[9]   M. Alagbe, "Effects of some carburizing media on surface hardening of low carbon steel," Journal of Sciences and Multidisciplinary Research, vol. 3, p. 31–37, 2011

[10]   A. Oyetunji and S. O. Adeosun, "Effects of carburizing process variables on mechanical and chemical properties of carburized mild steel," Journal of basic & Applied Sciences, vol. 8, 2012

[11]   A. Paul, N. G. Bem, N. I. Justine and O. N. Joy, "Investigation of egg shell waste as an enhancer in the carburization of mild steel," American Journal of Materials Science and Engineering, vol. 1, p. 29–33, 2013.

[12]   D. A. Okongwu and V. Paranthaman, "Assessment of the Efficacy of Some Carbonate Minerals as Energizers in Pack Carburisation of Mild Steel," Nigerian Journal of Technology, vol. 11, p. 28–43, 1987.

[13]   W. A. J. Chapman, Workshop technology: Part I An introductory course, Routledge, 2019

[14]   R. S. Khurmi and J. K. Gupta, A Textbook of Workshop Technology, S. Chand Publishing, 2008.

Fascicule 2
[April – June]
t o m e [2022] XV

ACTA Technica CORVINIENSIS
BULLETIN OF ENGINEERING

[1.]Ivan PALINKAS, [1.]Eleonora DESNICA, [1.]Jasmina PEKEZ, [1.]Dusko LETIC

TYPES AND APPLICATION OF INFILL IN FDM PRINTING: REVIEW

[1.]University of Novi Sad, Technical Faculty "Mihajlo Pupin", Zrenjanin, SERBIA

Abstract: 3D printing encompasses many forms of technologies and materials as 3D printing is being used in almost all industries you could think of. It's important to see it as a cluster of diverse industries with a myriad of different applications. 3D printing is technology that today has various application in production, through mechanical industry, medicine, civil engineering, food production, etc. Through 3D printing the fabrication of complex geometrical parts using various materials had been made possible. Fused deposition modeling (FDM) is widely used 3D printing technology. It has found its place from manufacturing consumers products through industrial parts. FDM also has been popular because of low price of commercially used printers and plastic materials such as PLA or ABS. In 3D printing process there are many elements that have great influence on finished product, such as part orientation, used material, support, infill, etc. Part infill have impact on overall part functionality, printing process and material consumption. In this paper it will be discussed the infill types, printing parameters of infill and their functional role in part production for FDM 3D printing.
Keywords: 3D printing, FDM, infill

INTRODUCTION

3D printing is, relatively, new technology used for production of parts (with various purpose, from decorative like ornaments, figurines etc. to mechanical elements) from various materials. There are several parameters that influence on 3D printing production and quality. Some of these parameters are part orientation, printing speed, layer size, type and percentage of infill, thickness of printing part exterior wall etc. that can be defined in slicer software (with regards of printer capabilities), and also the characteristics and material of 3D printer (temperature of nozzle and bed, movement speed, type of materials, etc.). For example, the part orientation has influence on printing time and material consumption [1].

3D printing or additive manufacturing is a process of making three dimensional solid objects from a digital file. The creation of a 3D printed object is achieved using additive processes. In an additive process an object is created by laying down successive layers of material until the object is created [9]. Each of these layers can be seen as a thinly sliced cross-section of the object [9].

3D printing is the opposite of subtractive manufacturing which is cutting out / hollowing out a piece of metal or plastic with for instance a milling machine [9]. Adoption of 3D printing has reached critical mass as those who have yet to integrate additive manufacturing somewhere in their supply chain are now part of an ever-shrinking minority. Where 3D printing was only suitable for prototyping and one-off manufacturing in the early stages, it is now rapidly transforming into a production technology [9].

Infill is a measure of how dense the object is, i.e. how much material has been used to print its internal structure. We can also determine the shape or pattern of the internal structure in the slicer (infill pattern), and selecting the right infill settings at the time of slicing can optimize the strength, rigidity, weight, feel, appearance, cost and print time of the model.

Infill in 3D printing is "filling" that allows printed parts to be solid, hollow or in between [2]. In comparison to conventional production, infill is unique for 3D printing. In conventional production like injection molding or subtractive manufacturing the interior of part is solid without the control or possibility to change that [3]. Based on that, with appropriate infill parameters, a desired part can be printed with reduced material consumption, or with lesser weight (where weight plays significant role).

Fused deposition modeling (FDM) is one of the most widely used additive manufacturing techniques [10,11]. It has been utilized in the automobile industry, ranging from testing models, lightweight tools to final functional components. However, FDM technique faces two main obstacles to be developed as an effective processing method in the automobile industry: weak and anisotropic mechanical properties and limited variety of printing materials [10,11]. The weak interlayer bond formed in the layer-by-layer process contributes to the mechanical characteristics of FDM parts [10,11].
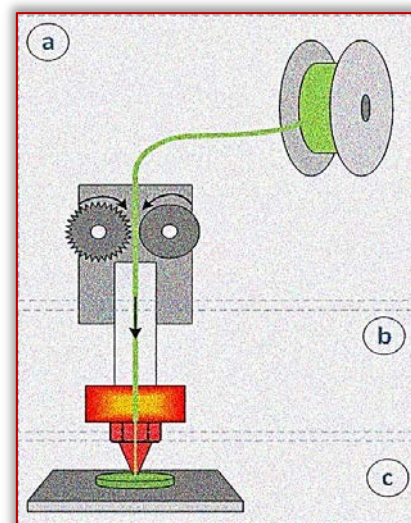

Figure 1. FDM additive manufacturing process [10,11]

Figure 1 shows schematically the FDM additive manufacturing process [10,11]:

—— A thermoplastic filament with constant diameter is feed into a heated extrusion head by motor driven feeding rollers (a).

—— The polymer melts inside the heated 3D printing head and is extruded through a thin nozzle (b).

—— During the deposition process the material cools and solidifies. In this way the head makes one layer with the desired shape and pattern of the deposited material. After the completion of the first layer the head is lifted in z-direction, and a new layer is deposited fused with the previous (c).

—— Finally, a complete part is constructed layer by layer.
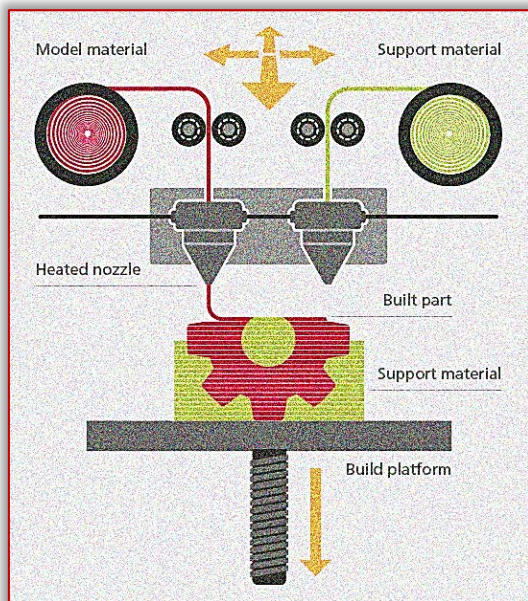
Figure 2. Fused Deposition Modelling (FDM) [10,11]

Fused Deposition Modelling (FDM) is the most accessible 3D printing process, from home hobbyists through to full production systems, with rapid turnaround times and a wide range of materials and colours aimed at functional applications and design verification [10,11].

Fused Deposition Modelling (FDM) is the most accessible 3D printing process, from home hobbyists through to full production systems, with rapid turnaround times and a wide range of materials and colours aimed at functional applications and design verification [10,11].

Fused deposition modeling parts used in the automobile industry requiring desired mechanical properties and good dimensional accuracy can be attained by either optimizing printing process or improving material properties [10,11].

Fused Deposition Modeling (FDM) is one of the widely used additive manufacturing processes due to its capability to create complex parts. One of the major research issues related to FDM process has been its ability to create components with esthetically appealing geometry. The optimum selection of FDM process parameters is playing an important role for improving the quality and the surface roughness of the manufactured components [10,11].

INFILL PATERNS AND INFILL DENSITY

The density of the infill defines how much material is going to be used on the inner structure of the print, which can go from 0% all the way up to 100% [10]. At 100%, the object will be completely solid from the inside and at 0% it will be completely hollow [10].

The amount of filament to be used during printing is highly determined by the infill density (also called infill percentage). The printed object's strength, rigidity, weight, buoyancy, cost and printing duration are all highly affected by the Infill density [10]. The weight, strength and print time of a part depend on the amount of material it has inside [10].

Different infill patterns and infill density are defined through slicing software. CURA [6], as well as most other slicers, allows you to have different infill densities, as well as patterns, within the same part [10]. This technique is also known as variable infill density. In CURA, the default infill percentage is usually 20% [6,10].

—— Infill patterns

Infill patterns can be divided in 4 (or 5) different groups, based of part usage [4]:

1. Low strength (prints that are decorative, in most cases without any functional use)
2. Medium strength (functional parts, with low durability)
3. High strength (functional parts)
4. Flexibility (patterns to use with flexible materials)
5. Vanity (patterns that look good but without application in specific cases. For example, printing the flexible pattern but with nonflexible materials)

Why 4 or 5 groups? Basically in the fifth group are the infill types that look good, but have their application in other four groups. By Ultimaker (based only on Cura software) there are 4 groups [5]:

1. Strong 2D infills are used for everyday prints
2. Quick 2D infills are used for quick, but weak models
3. 3D infills are used to make the object equally strong in all directions
4. 3D concentric infills are used for flexible materials

Different infill patterns from different softwares are shown on Figures 3–5, and printed example of different infill patterns is shown on Figure 6.
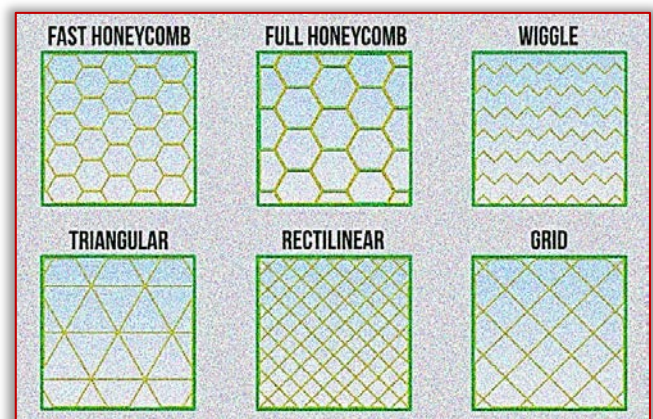
Figure 3. Infill patterns from Simplify3D software [4]
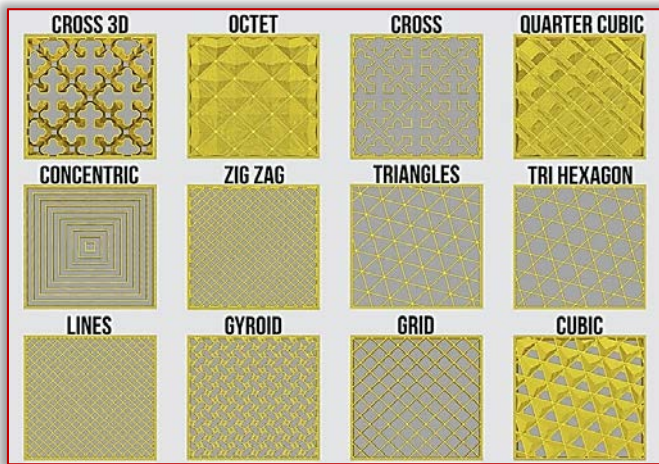
Figure 4. Infill patterns from Cura software [4]
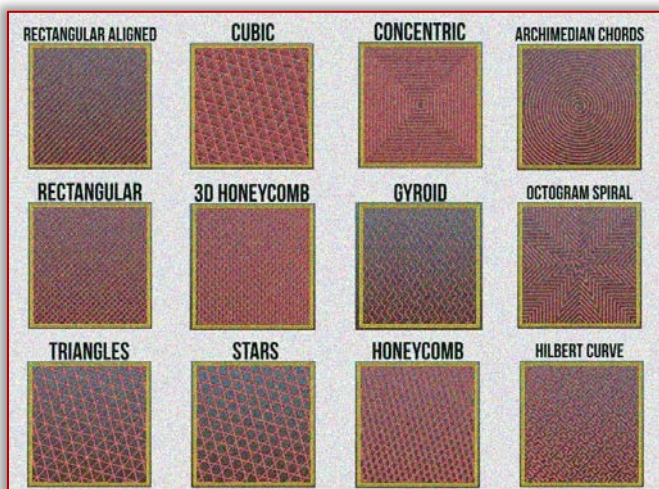
Figure 5. Infill patterns from Slic3r software [4]
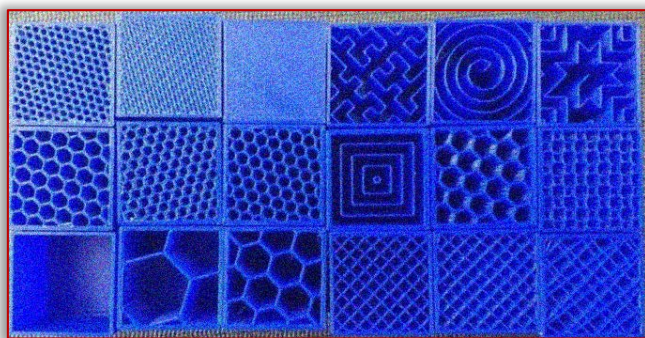
Figure 6. Different infill patterns printed [6]

In 3D printing, infill plays an important role in a part's strength, structure, and weight. Infill in 3D printing is different from other, more traditional manufacturing methods [10,13]. Infill pattern is the structure and shape of the material inside of a part [10,13]. Ranging from simple lines to more complex geometric shapes, infill patterns can affect a part's strength, weight, print time, and even flexibility [2,10,13].

3D printing involves selective extrusion of material in almost any pattern. Let's take a closer look at different options for infill density and pattern [2,10,13]. Based on groups mentioned before, Table 1 shows infill pattern by groups.

Table 1. Infill types from different softwares [4]

	Simplify3D	Cura	Slic3r
Low strength	Wiggle	Lines	Rectangular Aligned
Medium strength	Rectilinear Fast honeycomb Full honeycomb	Octet Quarter Cubic Gyroid	Honeycomb 3D Honeycomb Gyroid Grid (not included in patterns image) Archimedian Chords Octogram Spiral
High strength	Grid Triangular	Cubic Cubic Subdivision Triangles Tri-Hexagon Grid	Cubic Rectangular Triangles Stars
Flexibility	Wiggle	Concentric Cross 3D Cross Lines	Concentric Cross 3D Cross
Vanity	Wiggle	Concentric Cross 3D Gyroid Cubic Subdivision Cubic Octet	Concentric Cross 3D Gyroid Archimedian Chords Hilbert Chords Octogram Spiral

— Infill density

Infill density have impact on weight and durability of printed parts. It also can be defined through printed part application, or mentioned pattern groups. Basically [5]:

≡ for low strength parts typical infill density ranges from 0 – 15%,

≡ for medium strength parts typical infill density ranges from 15 – 50%,

≡ for high strength parts typical infill density ranges from 50 – 100%,

≡ for flexible parts typical infill density ranges from 0 – 100%,

Percentage of infill density depends on part application and used patterns. Also in some softwares the multiple infill density can be defined and printed. Different infill density percentage is shown on Figure 7.
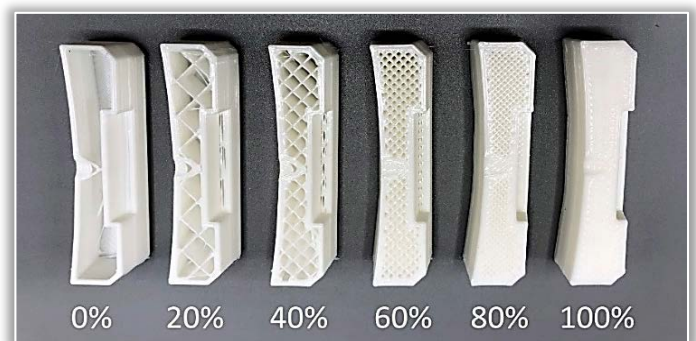
Figure 7. Different infill density percentage [7]

INFILL PATTERNS AND INFILL DENSITY APPLICATION

Infill patterns and infill density are entwined in 3D printing. As mentioned before, there are some guides to apply in 3D printing in order to obtain desired printed part (what pattern to use and what density corresponds). But there are also several other parameters to consider: printing speed, visuals, support for top layer, flexibility, filling (if used for creatin mold). For example, printing speed. If low strength infill pattern is used with higher infill density, printing time is reduced yet part durability is increased.

Also there are many papers on infill influence on mechanical strength. In paper [8] the authors give review of mechanical properties of 3D printed PLA products for various infill design. Based on that research it can be seen that infill patterns and infill density have great impact on different mechanical properties (tensile strength, flexural strength, compression strength, yield strength, stiffness etc.)

CONCLUSION

3D printing is highly used technology today. Low price of commercial FDM printers make this technology suitable for creation of unique parts (visual and functional) even in homemade conditions. When 3D printing, it is necessary to adjust printing parameters in order to obtain desired printed part, to decrease material consumption, to reduce printing time, and overall to reduce printing cost.

As shown in this paper, there are various infill patterns that can be used in 3D printing to fullfill desired goals. There are multiple guidelines that can be used to determine what is the suitable infill pattern for part to be printed based on part application. Most important, the guidelines are, in many cases, based on experience. It varies because of different printer's configurations and also because of different material characteristics.

Note: This paper was presented at ICOSTEE 2022 – International Conference on Science, Technology, Engineering and Economy, organized by University of Szeged, Faculty of Engineering (HUNGARY) and Hungarian Academy of Sciences – Regional Commettee in Szeged (HUNGARY), in Szeged, HUNGARY, in 24th of March, 2022.

References

[1] PALINKAŠ, I. & DESNICA, E. 2018. Determination of Influence of Part Orientation on Production Time in 3D Printing. Journal of Engineering Management and Competitiveness (JEMC), 8, 28-36.

[2] O'CONNELL, J. 2021. The Strongest Infill Pattern for Your 3D Prints, accessed on 20.02.2022., https://all3dp.com/2/strongest-infill-pattern/

[3] MOODY, J. 2021. PrusaSlicer Infill Patterns: All You Need to Know, accessed on 20.02.2022., https://all3dp.com/2/prusaslicer-infill-patterns/

[4] SIMMONS, J. 3D Print Infill Patterns Explained, accessed on 19.02.2022., https://the3dbros.com/3d-print-infill-patterns-explained/

[5] GOLDSCHMIDT, B. 2021. Best Cura Infill Pattern For Your Needs, accessed on 19.02.2022., https://all3dp.com/2/cura-infill-patterns-all-you-need-to-know/

[6] ISLAM, R. 2020. Cura Infill Patterns |A definitive Guide, accessed on 19.02.2022., https://iamrafiqul.medium.com/cura-infill-patterns-6dd62be22d77

[7] Choosing Infill Percentage for 3D Printed Parts, accessed on 19.02.2022., https://www.3d-pros.com/choosing-infill-for-3d-printed-parts

[8] SUTEJA, T.J. & SOESANTI, A. 2019. Mechanical Properties of 3D Printed Polylactic Acid Product for Various Infill Design Parameters: A Review. Journal of Physics: Conference Series, 1569, 042010

[9] https://3dprinting.com/what-is-3d-printing/

[10] https://rapidfab.ricoh-europe.com/technologies/fused-deposition-modelling/

[11] https://euroceram.org/en/eu/fused-deposition-modeling

[12] https://3dsolved.com/different-infill-same-print/

[13] https://all3dp.com/2/infill-3d-printing-what-it-means-and-how-to-use-it/

[1,2]Veronika VALKOVÁ, [1]Hana ĎÚRANOVÁ, [2]Lucia GALOVIČOVÁ, [2]Miroslava KAČÁNIOVÁ

BASIL ESSENTIAL OIL (*OCIMUM BASILICUM*): *IN VITRO* ANTIFUNGAL PROPERTIES AND ANTIOXIDANT ACTIVITY

[1.]AgroBioTech Research Centre, Slovak University of Agriculture, Nitra, SLOVAKIA
[2.]Institute of Horticulture, Faculty of Horticulture and Landscape Engineering, Slovak University of Agriculture, Nitra, SLOVAKIA

Abstract: The purpose of the present study was to evaluate the antioxidant and *in vitro* antifungal properties of commercial basil (*Ocimum basilicum*) essential oil (BEO). The antioxidant activity of BEO was estimated by DPPH free radical scavenging ability. The antifungal activity of the EO was tested against three pathogenic *Penicillium* (*P.*) spp. (*P. expansum*, *P. citrinum*, *P. crustosum*) using the disc diffusion method (concentrations: 12.5 µL.L⁻¹, 25 µL.L⁻¹, 50 µL.L⁻¹, and 100 µL.L⁻¹). From the results it is clearly evident that *Ocimum basilicum* EO showed a strong antioxidant activity with the value of 86.20 ± 0.15% for inhibition. The highest concentration (100 µL.L⁻¹) of BEO exhibited the strongest antifungal activity manifested by the highest diameters (5.33 ± 0.58 mm, 4.33 ± 0.58 mm, 3.33 ± 0.58 mm) of inhibition zones against all three fungi strains (*P. crustosum*, *P. citrinum* and *P. expansum*, respectively). These findings show that the BEO represents a good source of biologically active substances that could have potential applications in the food and pharmaceutical industries.
Keywords: basil, essential oil, disc diffusion method, DPPH assay

INTRODUCTION

Currently, the efforts of consumers for a healthy lifestyle and also well-known increasing resistance of microorganisms to synthetic antifungal substances has supported the search for new types of effective and non-toxic antifungal substances among natural sources (Roller et al., 2009). One of the possible solutions to this problem is the application of plant essential oils (EOs; Ba-Hambad et al., 2014).

Generally, EOs are products obtained from diverse parts of herbs, routinely isolated using the steam distillation method (Sahraoui et al., 2008). These natural substances are usually composed of secondary metabolites of aromatic plants with oxygenated structures (e.g. alcohols, ketones, aldehydes, and esters), characterized by significant biological properties, including antibacterial, antifungal and antioxidant activities (Babtista-Silva et al., 2020). In total, about 3,000 types of EOs are known, of which about 300 are also used commercially in the food, pharmaceutical and cosmetic industries (Shaaban et al., 2012).

Aromatic plants belonging to the genus *Ocimum* from the Lamiaceae family are also considered to be a rich source of EOs (Avetisyan et al., 2017), from which basil (*Ocimum basilicum* L.) is the most common species. Consumption of this herb has an anti-inflammatory, antimicrobial, antiviral (Martinec, 2012) and also strong antiseptic effect (Bozin et al., 2006) on human health. Moreover, a number of proven biological properties are dominated by its antifungal (Oxenham et al. 2005), antibacterial, repellent and high antioxidant potential (Bunrathep et al., 2007; Carović-Stanko et al., 2010).

Methyl chavicol (45.8%) and linalool (24.2%), the most abundant components in the concept of basil essential oil (BEO), are responsible for these biological effects (Bozin et al., 2006). Regarding these properties, the effect of BEO as a growth inhibitor of microorganisms in selected food models has been documented in several studies (Suppakul et al., 2003; Hemalatha et al., 2017; Amor et al., 2021).

Therefore, the aim of our study was to determine antioxidant and *in vitro* antifungal activity of BEO to assess its potential as an agent used in food or pharmaceutical industries.

MATERIALS AND METHODS

Essential oil

For all determinations, a commercial *Ocimum basilicum* essential oil (BEO) possessing methyl chavicol (≥ 65%), linalool, and eugenol as major compounds (declared by the manufacturer) was applied. The EO was obtained by the steam distillation of fresh stalks of basil growing in Vietnam (Hanus Company, Nitra, Slovakia).

Fungal strains

Three *Penicillium* (*P.*) strains (*P. crustosum*, *P. citrinum*, and *P. expansum*) were isolated from berry samples of *Vitis vinifera* and consequently classified using a reference based MALDI-TOF MS Biotyper. The obtained results were also validated by comparison with the taxonomic identification obtained by 16S rRNA sequences analysis.

DPPH assay

The antioxidant activity of the BEO was assessed on the basis of the scavenging activity of the stable radicals 2,2-diphenyl-1-picrylhydrazyl (DPPH) according to the methodology used in the study Valková et al. (2021).

Disc diffusion method

The evaluation of the antifungal activity of the BEO was performed using the agar disc diffusion method. For this purpose, there was an aliquot of 0.1 mL of fungal suspension in distilled water inoculated on Sabouraud Dextrose Agar (SDA; Merck, Gernsheim, Germany).

Subsequently, the discs of filter paper (6 mm) were impregnated with 10 µL of the analyzed BEO samples (in four

concentrations: 12.5 µL.L^{-1}, 25 µL.L^{-1}, 50 µL.L^{-1}, and 100 µL.L^{-1}), and then applied on the SDA surfaces.

The fungi were incubated aerobically at 25 °C for 5 days. The diameters of the inhibition zones were measured in mm after incubation. Each test was repeated three times (one repetition reflected one separate plate). The values for inhibitory activity increased in the following manner: weak antifungal activity (5 – 10 mm) < moderate antifungal activity (10 – 15 mm) < very strong antifungal activity (zone > 15 mm).

Statistical analysis

The data from the analyses were statistically evaluated using Prism 8.0.1 (GraphPad Software, San Diego, CA, USA). One-way analysis of variance (ANOVA) followed by Tukey's test were used to evaluate the statistical significance of differences between the analyzed groups of samples.

RESULTS AND DISCUSSIONS

Antioxidant activity of BEO

The antioxidant potential of the BEO was estimated in terms of the multiple radical scavenging abilities (Alara et al., 2019). Generally, it is known that DPPH radical is a stable free radical that can donate hydrogen when reacts with antioxidant constituents, and it is reduced to diphenyl picryl hydrazine (Thaipong et al., 2006), which has the ability to neutralize free radicals of extracts that possess unpaired electrons (Atangwho et al., 2013).

Our results showed that the BEO had a strong antioxidant activity with the value for inhibition of 86.20 ± 0.15%. In agreement with our study, Bozin et al. (2006) reported strong antioxidant activity of basil EO containing methyl chavicol (45.8%) and linalool (24.2%) as the main EO components. On the other hand, Mahmoud (2013) found that methyl chavicol had only moderate antioxidant activity.

The study by Dawidowicz and Olszowy (2014) even showed no antioxidant properties of methyl chavicol. Therefore, we assume that the main component of EO does not have to determine its antioxidant activity. Indeed, it is possible that the constituents present only in lower concentrations may contribute to some type of synergic interactions with other active compounds to enhance their antioxidant properties.

Antifungal properties of BEO

Results from the inhibitory effects of the BEO on growth of three tested *Penicillium* spp. fungi (*P. crustosum*, *P. citrinum*, and *P. expansum*) assessed by disc diffusion method are shown in Tables 1-3. Our findings showed that the growth inhibition of *Penicillium* strains depends on the concentration of the BEO applied; whereas the highest growth inhibition (P < 0.05) was recorded in all three analyzed strains in the highest BEO concentration (100 µL.L^{-1}) used.

On the other hand, the lowest concentration of the BEO (12.5 µL.L^{-1}) tested had no (*P. crustosum* and *P. expansum*) or only very weak inhibitory efficacy (*P. citrinum*) against the growth of microscopic filamentous fungi.

Table 1. Antifungal activity of BEO against P. crustosum growth.

Fungal strain	Concentration of BEO (µL.L^{-1})			
	12.5	25	50	100
P. crustosum	0.00 ± 0.00 [a]	1.00 ± 0.00 [b]	2.33 ± 0.58 [c]	5.33 ± 0.58 [d*]

Notes: Means ± standard deviation. Values followed by different superscripts within the same row are significantly different (P < 0.05). 0.00 – no efficacy. * Weak antifungal activity (5 – 10 mm).

Table 2. Antifungal activity of BEO against P. citrinum growth.

Fungal strain	Concentration of BEO (µL.L^{-1})			
	12.5	25	50	100
P. citrinum	0.67 ± 0.58 [ab]	1.33 ± 0.58 [a]	2.33 ± 0.58 [b]	4.33 ± 0.58 [c]

Notes: Means ± standard deviation. Values followed by different superscripts within the same row are significantly different (P < 0.05).

Table 3. Antifungal activity of BEO against P. expansum growth.

Fungal strain	Concentration of BEO (µL.L^{-1})			
	12.5	25	50	100
P. expansum	0.00 ± 0.00 [a]	1.67 ± 0.58 [b]	2.67 ± 0.58 [bc]	3.33 ± 0.58 [c]

Notes: Means ± standard deviation. Values followed by different superscripts within the same row are significantly different (P < 0.05). 0.00 – no efficacy.

Generally, microscopic filamentous fungi possess a great ability to colonize many kinds of substrates, and grow even under extreme conditions. Among them, *Penicillium* spp. are the most important species producing the spoilage of food products (Groot et al., 2019); therefore, these species were also selected in our research for analyses.

Our results are in agreement with the study of Saggiorato et al. (2009) who observed that BEO inhibited the growth of *Penicillium* spp. (isolated from an industrial environment), depending on the concentrations used. The weaker antifungal potential of our BEO in lower concentrations can be attributed to the lower presence of methyl chavicol (as the most abundant compound in the EO) that in earlier studies showed variable activity depending on the analyzed microorganisms (Stević et al., 2014). Tadtong et al. (2009) found a moderate to weak antimicrobial activity of EO comprising the highest amount of this substance. Our evaluation of the antifungal activity of the BEO using the disc diffusion method showed promising results. In view of this fact, the study focused on the application of BEO on selected food models in order to determine its effective concentration inhibiting the fungi growth in food products is our next challenge.

CONCLUSIONS

Findings obtained from the study have revealed the antioxidant and *in vitro* antifungal properties of the BEO. From the results it is clearly evident that the BEO showed a remarkable value (86.20 ± 0.15%) for antioxidant activity. Further, all the tested *Penicillium* spp. (*P. crustosum*, *P. citrinum*, and *P. expansum*) were the most sensitive to the BEO in the highest concentration (100 µL.L^{-1}). Thus, our data confirm the possibility of the application of the BEO in the higher

concentration (≥ 100 µL.L^{-1}) as an alternative to traditional medicine, and also as a natural agent applied for food preservation. These data also complement our previous research providing an extensive overview of the biological functions of several commercial EOs purchased from the Hanus Company.

Acknowledgements

Note: This paper was presented at ICOSTEE 2022 – International Conference on Science, Technology, Engineering and Economy, organized by University of Szeged, Faculty of Engineering (HUNGARY) and Hungarian Academy of Sciencies – Regional Commettee in Szeged (HUNGARY), in Szeged, HUNGARY, in 24th of March, 2022.

References

[1] Adams, R. P.: Identification of Essential Oil Components by Gas Chromatography/Mass Spectrometry. USA : Allured Publishing Corporation, Carol Stream, IL. 456 p. ISBN 978-1- 932633-11-4, 2007.

[2] Alara, O. R.; Abdurahman, N. H.; Mudalip, S. A.; Olalere, O. A.: Effect of drying methods on the free radicals scavenging activity of *Vernonia amygdalina* growing in Malaysia, Journal of King Saud University-Science, vol. 31(4), p. 495-499, 2019.

[3] Amor, G.; Sabbah, M.; Caputo, L.; Idbella, M.; De Feo, V.; Porta, R.; Mauriello, G.: Basil essential oil: Composition, antimicrobial properties, and microencapsulation to produce active chitosan films for food packaging, Foods, vol. 10(1), p. 121, 2021.

[4] Atangwho, I. J.; Egbung, G. E.; Ahmad, M.; Yam, M. F.; Asmawi, M. Z.: Antioxidant versus anti-diabetic properties of leaves from *Vernonia amygdalina* Del. growing in Malaysia, Food chemistry, vol. 141(4), p. 3428-3434, 2013.

[5] Avetisyan, A.; Markosian, A.; Petrosyan, M.; Sahakyan, N.; Babayan, A.; Aloyan, S.; Trchounian, A.: Chemical composition and some biological activities of the essential oils from basil *Ocimum* different cultivars, BMC complementary and alternative medicine, vol. 17(1), p. 1-8, 2017.

[6] Ba-Hamdan, A. H. A.; Aly, M. M.; Bafeel, S. O.: Antimicrobial activities and phytochemical analysis of the essential oil of *Ocimum basilicum*, collected from Jeddah Region, Saudi Arabia., Journal of Microbiological Resistance, vol. 4(6), p. 1-9, 2014.

[7] Baptista-Silva, S.; Borges, S.; Ramos, O. L.; Pintado, M.; Sarmento, B.: The progress of essential oils as potential therapeutic agents: A review, Journal of Essential Oil Research, vol. 32(4), p. 279-295, 2020.

[8] Behbahani, B. A.; Shahidi, F.; Yazdi, F. T.; Mortazavi, S. A.; Mohebbi, M.: Antioxidant activity and antimicrobial effect of tarragon (*Artemisia dracunculus*) extract and chemical composition of its essential oil, Journal of Food Measurement and Characterization, vol. 11(2), p. 847-863, 2017.

[9] Bozin, B.; Mimica-Dukic, N.; Simin, N.; Anackov, G.: Characterization of the volatile composition of essential oils of some Lamiaceae spices and the antimicrobial and antioxidant activities of the entire oils, Journal of agricultural and food chemistry, vol. 54(5), p. 1822-1828, 2006.

[10] Bunrathep, S.; Palanuvej, C.; Ruangrungsi, N.: Chemical compositions and antioxidative activities of essential oils from four *Ocimum* species endemic to Thailand, Journal of Health Research, vol. 21(3), p. 201-206, 2007.

[11] Burt, S.: Essential oils: their antibacterial properties and potential applications in foods—a review, International journal of food microbiology, vol. 94(3), p. 223-253, 2004.

[12] Carović-Stanko, K.; Orlić, S.; Politeo, O.; Strikić, F.; Kolak, I.; Milos, M.; Satovic, Z.: Composition and antibacterial activities of essential oils of seven *Ocimum* taxa, Food Chemistry, vol. 119(1), p. 196-201, 2010.

[13] Cox, S. D.; Markham, J. L.: Susceptibility and intrinsic tolerance of *Pseudomonas aeruginosa* to selected plant volatile compounds, Journal of Applied Microbiology, vol. 103(4), p. 930-936, 2007.

[14] Dawidowicz, A. L.; Olszowy, M.:Does antioxidant properties of the main component of essential oil reflect its antioxidant properties? The comparison of antioxidant properties of essential oils and their main components, Natural product research, vol. 28(22), p. 1952-1963, 2014.

[15] Djerrad, Z.; Kadik, L.; Djouahri, A. Chemical variability and antioxidant activities among *Pinus halepensis* Mill. essential oils provenances, depending on geographic variation and environmental conditions, Industrial Crops and Products, vol. 74, p. 440-449, 2015.

[16] Grayer, R. J.; Kite, G. C.; Goldstone, F. J.; Bryan, S. E.; Paton, A.; Putievsky, E.: Infraspecific taxonomy and essential oil chemotypes in sweet basil, *Ocimum basilicum*, Phytochemistry, vol. 43(5), p. 1033-1039, 1996.

[17] Groot, M. N.; Abee, T.; van Bokhorst-van de Veen, H.: Inactivation of conidia from three *Penicillium* spp. isolated from fruit juices by conventional and alternative mild preservation technologies and disinfection treatments. Food Microbiology, vol. 81, p. 108–114, 2019.

[18] Hemalatha, T.; Umamaheswari, T.; Senthil, R.; Krithiga, G.; Anbukkarasi, K.: Efficacy of chitosan films with basil essential oil: perspectives in food packaging, Journal of Food Measurement and Characterization, vol. 11(4), p. 2160-2170, 2017.

[19] Mahmoud, G. I.: Biological effects, antioxidant and anticancer activities of marigold and basil essential oils, Journal of Medicinal Plants Research, vol. 7(10), p. 561-572, 2013.

[20] Martinec, R.: Some implications of using aromatherapy as complementary method in oncology setting, Archive of Oncology, vol. 20(3-4), p. 70-74, 2012.

[21] Oxenham, S. K.; Svoboda, K. P.; Walters, D. R.: Antifungal activity of the essential oil of basil (*Ocimum basilicum*), Journal of phytopathology, vol. 153(3), p. 174-180, 2005.

[22] Roller, S.; Ernest, N.; Buckle, J.: The antimicrobial activity of high-necrodane and other lavender oils on methicillin-sensitive and-resistant *Staphylococcus aureus* (MSSA and MRSA), The journal of alternative and complementary medicine, vol. 15(3), p. 275-279, 2009.

[23] Saggiorato, A. G.; Gaio, I.; Treichel, H.; De Oliveira, D.; Cichoski, A. J.; Cansian, R. L.: Antifungal activity of basil essential oil (*Ocimum basilicum* L.): evaluation in vitro and on an Italian-type sausage surface, Food and bioprocess technology, vol. 5(1), p. 378-384, 2012.

[24] Sahraoui, N.; Vian, M. A.; Bornard, I.; Boutekedjiret, C.; Chemat, F.: Improved microwave steam distillation apparatus for isolation of essential oils: comparison with conventional steam distillation, Journal of Chromatography A, vol. 1210(2), p. 229-233, 2008.

[25] Sajjadi, S. E.: Analysis of the essential oils of two cultivated basil (*Ocimum basilicum* L.) from Iran, Journal of Pharmaceutical Sciences, vol. 14(3), p. 128-130, 2006.

[26] Shaaban, H. A.; El-Ghorab, A. H.; Shibamoto, T.: Bioactivity of essential oils and their volatile aroma components, Journal of Essential Oil Research, vol. 24(2), p. 203-212. 2012.

[27] Sikkema, J.; De Bont, J. A.; Poolman, B.: Mechanisms of membrane toxicity of hydrocarbons, Microbiological reviews, vol. 59(2), p. 201-222, 1995.

[28] Suppakul, P.; Miltz, J.; Sonneveld, K.; Bigger, S. W.: Antimicrobial properties of basil and its possible application in food packaging, Journal of agricultural and food chemistry, vol. 51(11), p. 3197-3207, 2003.

[29] Stević, T.; Berić, T.; Šavikin, K.; Soković, M.; Gođevac, D.; Dimkić, I.; Stanković, S.: Antifungal activity of selected essential oils against fungi isolated from medicinal plant, Industrial Crops and Products, vol. 55, p. 116-122, 2014.

[30] Tadtong, S.; Wannakhot, P.; Poolsawat, W.; Athikomkulchai, S.; Ruangrungsi, N.: Antimicrobial activities of essential oil from Etlingera punicea rhizome. Journal of Health Research, vol. 23(2), p. 77-79, 2009.

[31] Thaipong, K.; Boonprakob, U.; Crosby, K.; Cisneros-Zevallos, L.; Byrne, D. H.: Comparison of ABTS, DPPH, FRAP, and ORAC assays for estimating antioxidant activity from guava fruit extracts, Journal of food composition and analysis, vol. 19(6-7), p. 669-675, 2006.

[32] Valková, V.; Ďuranová, H.; Galovičová, L.; Vukovic, N. L.; Vukic, M.; Kačániová, M.: In Vitro Antimicrobial Activity of Lavender, Mint, and Rosemary Essential Oils and the Effect of Their Vapours on Growth of Penicillium spp. in a Bread Model System, Molecules, vol. 26(13), p. 3859, 2021.

[33] Van Den Dool, H.; Kratz, P. D.: A Generalization of the Retention Index System Including Linear Temperature Programmed Gas-Liquid Partition Chromatography, Journal of Chromatography A, vol. 11, p. 463-471, 1963.

[34] Vieira, R. F.; Simon, J. E.: Chemical characterization of basil (Ocimum spp.) based on volatile oils, Flavour and Fragrance Journal, vol. 21(2), p. 214-221, 2006.

[1.]H.O. GANIYU, [2.]A.G. ADEOGUN, [3.]S.B. BAKARE, [4.]A.S. AREMU

EFFECTIVENESS OF GIS–BASED APPROACH FOR FLOOD HAZARD ASSESSMENT OF ONA RIVER, IBADAN, NIGERIA

[1-3.]Department of Civil Engineering, Kwara State University, Malete, NIGERIA
[4.]Department of Water Resources and Environmental Engineering, University of Ilorin, Ilorin, NIGERIA

Abstract: Flooding is one of the most reoccurrence natural disasters globally and the plan to mitigate the effects of flood cannot be over emphasized. This study assessed the flood stage and flood extent of Ona River, Ibadan, Nigeria using Geographic Information System (GIS) in concert with Hydrologic Engineering Center-Geographic River Analysis System (HEC-GeoRAS). The results of the study revealed that the highest flood stage was predicted at 4.73 m, and 33% of the flood prone areas has a flood stage above 2 m based on the developed inundation map which implies that human and urban infrastructure are not safe. In the case of flood extent, the smallest flood extent was estimated at 694 m^2 (Mount Zion Baptist church at Oke-Ayo and its environs) while the largest flood extent was estimated at 115,329 m^2. It is recommended that an emergency rescue plan should be formulated to mitigate the effect of flooding in the affected areas such as Sweeco Foods, Tedaz Organic Home, Rehoboth Cathedral, a section of Oluyole Estate Road, Zartech Limited, 7-Up Bottling Company, Obasanjo Farm, and a section of Arapaja estate which are most prone to floods.
Keywords: Floods, Inundation Map, GIS, HEC-RAS, Ona River

INTRODUCTION

Flood has become an annual event globally particularly in Nigeria during the rainy seasons as a result of by increased precipitation due to climate change and variability (Adaku, 2020) or dam break phenomenon which may cause substantial loss of life and property damage downstream of the dams (Balogun and Ganiyu, 2017). Flood occurs in the form of coastal flood, river flood, flash flood and urban flood. In the past decades, many cities have experienced unusual and devastating flood disasters which are beyond the government's capability to prevent (Komolafe et al., 2015). In view of this, modeling of floodplain is very important because it focuses on many areas of civil and environmental engineering such as preparation of comprehensive floodplain studies, design of transportation features (such as roads, bridges and other facilities), floodwave development, and structural and non-structural solutions to flood problems (Mohammad and Parviz, 2013). Floodplain modeling predicts water surface profiles and generates floodplain maps to identify flood prone areas (Moramacro et al., 2005). The inundation/floodplain maps as explained in Ayemu et al. (2015) study can be classified as low, medium and high flood hazards.

Charles and Hamisi (2018) assessed the floodplain mapping of Bunga-Soya, Uganda. The return periods were estimated using Gringorten method, while the simulated inundated areas were mapped by incorporating HEC-RAS and HEC-GeoRAS extension of ArcMap. The result indicated that discharges of 618 m^3/s, 709 m^3/s, 850 m^3/s, 974 m^3/s, 1126 m^3/s, 1350 m^3/s and 1435 m^3/s were estimated for the return periods of 1, 2, 5, 10, 20, 50 and 60 years respectively. The 60-years return period produced maximum flood depth of 1.25 m and it was observed that HEC-RAS is an effective tool for flood inundation mapping. In the study carried out by Olasunkanmi and Dan'azumi (2018), flood inundation and

hazard mapping of River Zungur Watershed, Bauchi, Nigeria was assessed using GIS and HEC-RAS models at return periods of 2 to 100 years. Area inundated by 2, 5, 10, 25, 50 and 100-year floods were 186.71 m^3/s, 189.15 m^3/s, 193.59 m^3/s, 197.63 m^3/s, 200.09 m^3/s and 205.32 km^2 flood extent respectively with maximum inundation depths ranging from 5.37 m to 7.37 m for 2 to 100 years. Flood inundation mapping showed the areas likely to be affected by the100-year flood included agricultural land, and it can be deduced from the study that hydraulic simulation and GIS are effective tools for floodplain mapping and management.

Tolera and Fayera (2019) modeled the floodplain of Awetu River Sub-Basin, Jimma, Oromia, Ethiopia. The magnitude of the flood was determined using Log-Normal distribution function for different return periods. The 1000-year return period predicted a discharge of 783.1m^3/s. HEC-RAS was used for the simulation, and the flood extent and stage for 1000-year return period was estimated at 1.852 km^2 and 21.2 m respectively. Bikram (2010) conducted a study on flood plain analysis and risk assessment of LotharKhola watershed, Nepal using HEC-RAS and GIS. Gumbel, Log Pearson Type III, and Log Normal method were used to analyze the flood frequency. The results of flood frequency analyzed by Log Pearson Type III method showed the discharges of 286 m^3/s, 647 m^3/s, 990 m^3/s, 1347 m^3/s, and 1284 m^3/s for 2, 10, 50, 100 and 200-years return period of floods respectively. The flood extent of inundated areas by return periods of 2, 10, 50, 100 and 200-years were estimated as 230 km^2, 239 km^2, 246 km^2, 249 km^2 and 252 km^2 respectively. The flood depth showed that most of the flooding areas had water depth greater than 3m.

Nigerian cities have a history of flood disasters particularly Ibadan city in Southwestern part of the country. Floods are common occurrence in the city and have been officially recorded since 1951 but records on urban floods in Ibadan

are patchy and characterized by incomplete information. The heaviest rain on record that caused flood in the city occurred in 1980 when the city recorded 274 mm of rainfall during a single flood episode. The second heaviest recorded rainfall was 258 mm in 1963. The amount of rain that fell on 26th of August, 2011 was 187.5 mm which was the third heaviest recorded (Agboola et al., 2012). Many studies have been carried out on flood in Ibadan city with major focus on River Ogunpa which is the popular river that spread over Ibadan but with the flood of August 2011, it is apparent that other rivers in Ibadan require immediate attention. River Ona was among the water bodies that were flooded in 2011 causing several loss of lives and properties at the downstream (Jonah, 2011). This study presents the development of a comprehensive flood inundation map for River Ona which predicted the flood stage and flood extent of the identified flood prone areas. The map is a very useful tool which may be used to plan land use features in the floodplains and also, to formulate an emergency rescue plan to mitigate the effect of flooding in the affected areas.

METHODOLOGY

— Description of the Study Area

The River Ona is situated upstream of Eleyele River and continues at the downstream of the river in the city of Ibadan, Nigeria. River Ona lies within geographical coordinates of Latitude 7º20'- 7º25'N and Longitude 3º51'- 3º56'E and spans within the Ido and Ibadan North-West Local Government of Oyo State. Eleyele reservoir was formed from confluence of River Ona and River Alapata. An earth dam was constructed along the confluence at Eleyele community in 1942 for the supply of raw water for treatment at the Eleyele waterworks to provide potable water for the city of Ibadan. The dam also acts as flood control during high flow periods through its reservoir holding capacity. The River was further dammed at Nigeria Horticulture Research Institute (NIHORT) Idi-Isin and traverses many locations within Ibadan Metropolis such as Odo-Ona Apata, Oluyole Estate, Odo-Ona Elewe and New Garage Challenge (Elufioye, 2016). Figure 1 shows the map of the study area.
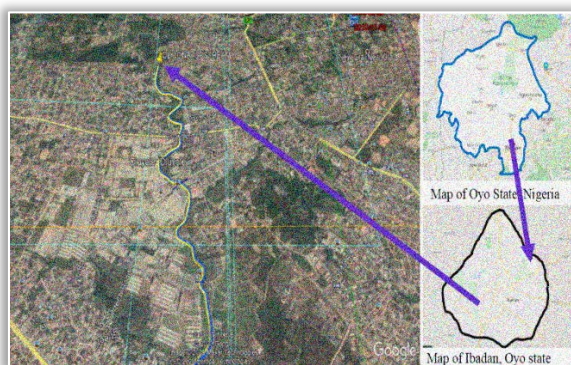
Figure 1: Map of the study area

— Model Development

The flood model for this study was developed from the combination hydrologic and hydraulic models where the spatial (DEM, Land use map and Soil map) and temporal (meteorological) data served as the model input data. The hydraulic model used for this study was Hydrologic Engineering Center's – River Analysis System (HEC-RAS) model. HEC-RAS requires two main input data which are geometric data and steady flow data. The flowchart of the modeling processes is shown in Figure 2.
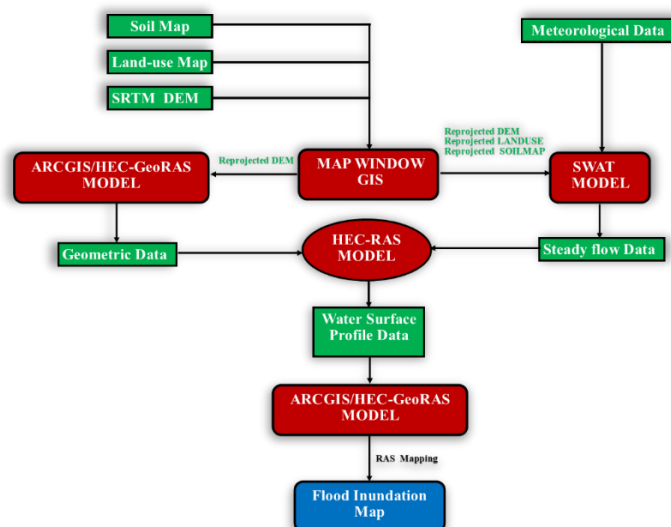
Figure 2: Flowchart of flood inundation mapping processes

In order to predict the steady flow data of the river, the spatial data (DEM, land use map and soil map) for the study area were delineated and processed in Map Window GIS. The processed spatial data were used in conjunction with temporal data which consist of 30-year daily meteorological data (precipitation, humidity, maximum and minimum temperature, solar radiation and wind speed).

Weather data from January, 2012 to December 2020 were obtained from the Nigerian Meteorological Agency (NIMET). Temporal data from January 2021 to December 2041 were forecast using Markov model. Markov model is a basic idea and concept of stochastic process or time series. It is used in modeling streamflow, rainfall, temperature, and other phenomena whose values changes with time *(Loucks and Van Beek, 2005)*. Both the spatial and temporal data were used as model inputs for the SWAT model. The model was run, and the predicted flow of 30-year return period was used as steady flow data in HEC-RAS model. Figure 3 shows the SWAT model run interface as used in the research.
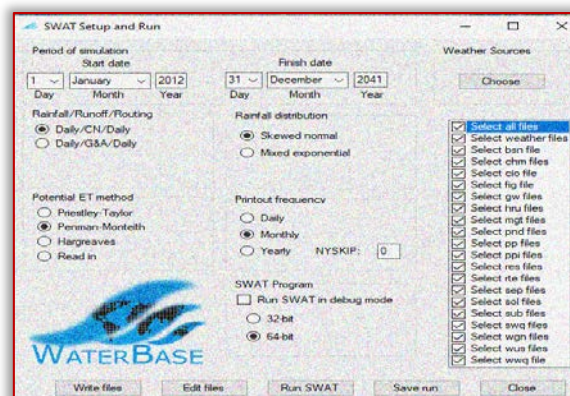
Figure 3: SWAT setup and run interface

The geometric data for this study was generated in HEC-GeoRAS (an extension of ArcMap version 10.1), where 90 m resolution Digital Elevation Model (DEM) was used as the main input data for the model. The DEM which gives a description of elevation of the area was extracted from the Shuttle Radar Topography Mission (SRTM) as shown in Fig. 4.
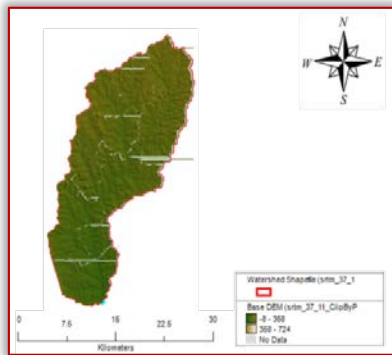
Figure 4: DEM of the study area

The DEM which was converted to Triangular Irregular Network (TIN) was used in order to set up 2D models for generating geometric data and processing the results of flood inundation. After creating all the required geometric data for hydrologic modeling, the created River Analysis System (RAS) layers containing stream centerline, main channel bank, flow path centerline, cross-sectional cut lines and bridges were exported into HEC-RAS model as presented in Figure 5. The geometric data was then imported in HEC-RAS model as presented in Figure 6. Manning's value was also inputted into the model. The characteristics of the channel and banks of the river were compared with Chow (1959) Manning's Table and the values of 0.04 and 0.045 were assigned to the channel and banks of the river respectively. Boundary conditions are also required to perform the calculations. In this study, the normal depth was used as a boundary condition. The flood model was run to compute the water surface profiles of the study area. The model result was then exported and visualized in GIS incorporated with HEC-GeoRAS.
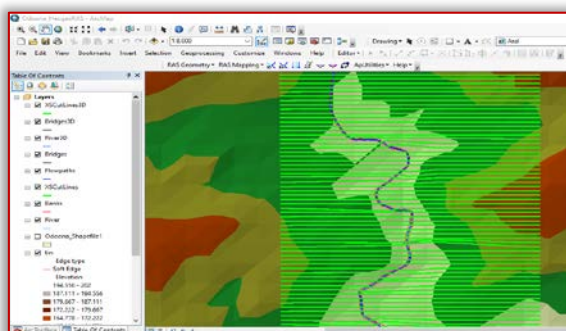
Figure 5: Graphical interface of River Analysis System (RAS) layers

In the flood mapping phase, the model results from HEC-RAS model were analyzed with HEC-GeoRAS, an extension of ArcMap 10.1 to produce the flood extent polygons (inundation map) of the study area. The inundation map was then overlaid on Google earth image to identify the affected areas.
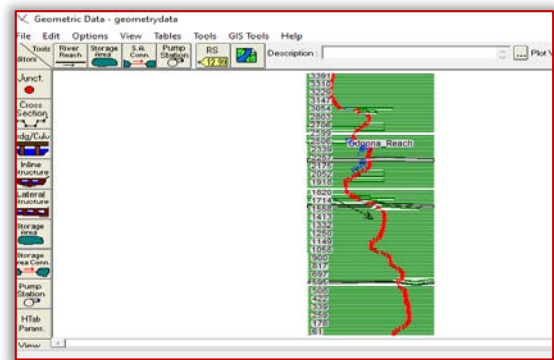
Figure 6: Graphical interface of geometric data in HEC-RAS model

RESULTS AND DISCUSSION
— Prediction of Steady Flow
The watershed of the study area was delineated and discretized into 10 sub-basins and 30 Hydrological Response Units (HRU). The predicted flow for all the sub-basins was represented with map as shown in Figure 7.
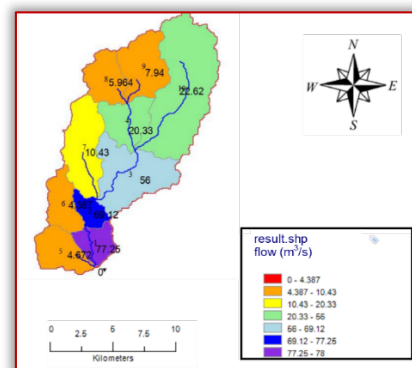
Figure 7: Spatial map of flow of the study area

It was observed from the map that sub-basin 6 has the lowest predicted flow of 4.39 m^3/s whereas, sub-basin 1 which was represented with purple colour has the highest predicted flow of 75.25 m^3/s and considered for the worst flood condition. The value was used as steady flow data in HEC-RAS model.

— Prediction of Flood Stage
It was reported in Srinivasa et al. (2019) that flood stage is classified into five hazard levels according to Japan Ministry of Land Infrastructure and Transport (Table1).

Table 1: Flood hazard classification according to MLIT

Flood hazard	Depth (m)	Hazard	Implications
H1	<0.5	Very low	Easy evacuation for human and animals
H2	0.5-1	Low	Difficult evacuation for adults, infants and animals
H3	1-2	Medium	People can get drowned but safe in their homes having plinth level to be 0.6 to 1 meter
H4	2-5	High	Not safe in their homes but may safe on their roofs
H5	>5	Extreme	Not safe even on their roofs

Source: Srinivasa et al. (2019)

The flood hazard classification was used to classify the flood stage of the study areas into various hazard levels. Figure 8 shows the flood stage of the study area. From the result, it was observed that an estimated 33% of the flood prone areas has a flood stage above 2 m (H4 classification) with the highest flood stage predicted at 4.73 m. Some landmark infrastructures (Zartech Limited, E99 Events Centre, Alaafin Avenue road, Sweeco Foods and Rehoboth Cathedral) were identified to be prone to flooding. This implies that human and urban infrastructure are not safe.
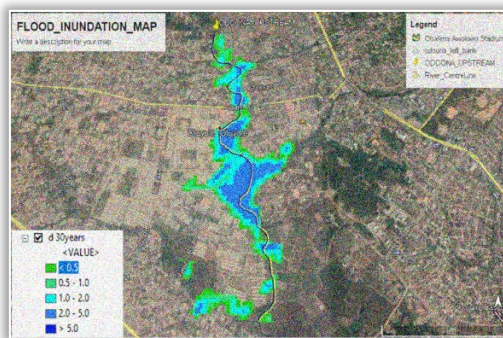
Figure 8: Inundation map showing the flood stage of the study area

— Prediction of Flood Extent

The inundation map produced shows the flood extent at peak flow as shown in Figure 9. The model revealed that the river has overflown its banks invariably causing flood to the downstream parts of the river.
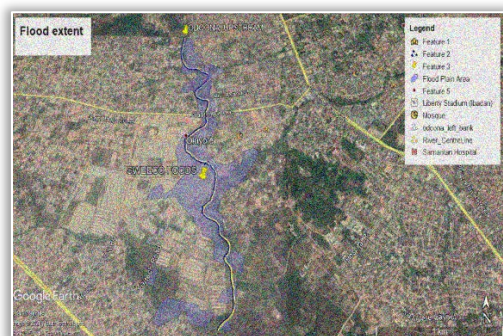
Figure 9: Inundation map showing the flood extent of the study area

The total flood extent of the study area was estimated at 0.585 km^2. The smallest flood extent was estimated at 694 m^2 (Mount Zion Babtist church, Oke-Ayo and its environs) while the largest flood extent was estimated at 115,329 m^2. Some of the identified flood prone areas are Sweeco Foods, a section of Oluyole Estate Road, Tedaz Organic Home, Rehoboth Cathedral, Zartech Limited, 7-Up Bottling Company, Obasanjo Farm, and a section of Arapaja estate.

CONCLUSION

This study presents a systematic approach to the process of flood inundation mapping. SWAT model was used to predict a 30-year simulation steady flow data. The estimated steady flow (75.25 m^3/s) served as the data for the HEC-RAS model along with geometric data which was generated using GIS in concert with HEC-GeoRAS and DEM. The HEC-RAS model was used to simulate the floods for a 30-year return period, and the flood inundation map was produced in GIS environment where the flood stage and flood extent were predicted. The model revealed that 33% of the flood prone areas had a flood stage above 2 m with the highest flood stage predicted at 4.73 m. In the case of flood extent, the smallest and largest flood extent were estimated at 694 m^2 and 115,329 m^2 respectively. It can be deduced from the study that HEC-RAS and GIS models are effective tools for floodplain mapping and the map is a very useful tool to formulate an emergency response plan of the affected areas.

References

[1] Adaku, J. E., (2020). The Impact of Flooding on Nigeria's Sustainable Development Goals (SDGs). Ecosystem Health and Sustainability, 6(1): 1-12.

[2] Agboola, S. B., Ajayi, O., Taiwo, O. J. and Wahab, B. W. (2012). The August 2011 Flood in Ibadan, Nigeria: Anthropogenic Causes and Consequences. International Journal Disaster Risk Sciences, 3(4): 207–217.

[3] Aja, G. and Olaore, A. Y. (2014). The Impact of Flooding on the Social Determinants of Health in Nigeria: A Case Study for North-South Institutional Collaboration to Address Climate Issues. Developing Country Studies, 4(22): 6-12.

[4] Ayemu, I. A., Ayoola, M., A., Ajibola, A., I. and Samuel, A. (2015). Inundation and Hazard Mapping of River Asa (Unpublished Master Thesis). LadokeAkintola University of Technology, Ogbomoso, Nigeria.

[5] Balogun, O.S. and Ganiyu, H.O. (2017). Study and Analysis of Asa River Hypothetical Dam Break Using HEC-RAS. Nigerian Journal of Technology (NIJOTECH), 36(1): 315-321.

[6] Bikram, M. (2010). Flood Plain Analysis and Risk Assessment of Lothar Khola

[7] Charles, M. and Hamisi, J. (2018). Flood Plain Mapping of Bunga-Soya (Unpublished Bachelor's Thesis). Kampala International University, Kampala, Uganda.

[8] Elufioye, A. (2016). Environmental and Social Impact Assessment (ESIA) for Emergency Rehabilitation of Eleyele Dam, Ibadan, Oyo State. (Accessed from https://documents.worldbank.org/ on December 8, 2020)

[9] Jonah, F. (2011). Nigeria floods: Ibadan Reflects on Eleyele Dam Tragedy.

[10] Komolafe, A. A., Adegboyega, S. A. and Akinluyi, F. O. (2015). A Review of Flood Risk Analysis in Nigeria. American Journal of Environmental Sciences, 11(3): 157-166.

[11] Loucks, D. P. And Van Beek, E. (2005) Water Resources Systems Planning and Management. United Nations Educational, Scientific and Cultural Organization, Ages Arti Grafiche Turin, Italy.

[12] Mohammad, H. Q. and Parviz, K. (2013). Efficiency of Hydraulic Models for Flood Zoning using GIS (Case Study: Ay-Doghmush River Basin). Science and Research Branch Islamic Azad University, Iran, 10: 915-924.

[13] Moramarco, L., Melone, F. and Sing, V. P. (2005). Assessment of Flooding in Urbanized Ungauged Basins: A Case Study in the Upper Tiber Area, Italy. Hydrological Processes, 19(10): 1909-1924.

[14] Olasunkanmi, A. B. and Dan'azumi, S. (2018). Flood Inundation and Hazard Mapping of River Zungur Watershed using GIS and HEC-RAS Models. Nigeria Journal of Technology (NIJOTECH), 37(4): 1162-1167.

[15] Srinivasa, R., G., Tushar, S., Asiya, B., Mruthyunjaya, R., K. and Jagadeeswawa, R. P. (2019). 2D Flood Simulation and Development of Flood Hazard Map by using Hydraulic Model. International Journal of Advanced Remote Sensing and GIS, 8(1): 3096-3105.

[16] Tolera, A. F. and Fayera, G. T. (2019). Floodplain Modelling of Awetu River Sub-Basin, Jimma, Oromia, Ethiopia. Journal of Material & Environmental Science, 10(11): 1030-1042.

[1.]A. KAOUKA, [1.]A. BENSALEM

MECHANICAL BEHAVIOR AND TRIBOLOGICAL PROPERTIES OF ELECTROCHEMICAL BORIDE TITANIUM ALLOY Ti-6Al-4V

[1.]Laboratoire de Sciences Appliquées et Didactiques, Ecole Normale Supérieure of Laghouat, Laghouat, ALGERIA

Abstract: Some mechanical properties and tribological properties of borided Ti-6Al-4V titanium alloy were investigated with different testing methods; tensile tests, and bending tests along with hardness measurements. In this work, boriding process based on the electrochemical boriding applied on titanium alloy at 950 °C for 30 min, this method has an electromagnetic frequency in the range of 100–500 kHz during electrolysis has been proposed and realized on Ti-6Al-4V alloy. The surface methodology was used to analyse the effects of boride. The formation of the new microstructure was examined by optical-light microscopy, scanning electron microscope inspections along with thin film X-ray diffraction analyses, and elemental dispersion spectrometry analyses, which confirmed the borided layer formations. XRD patterns confirmed the formation of titanium borides (TiB and TiB_2). The micro-hardness of the boride layer was measured using Vickers microhardness tester. Some mechanical characterization were investigated on the borided substrates such as the surface hardness of borided titanium alloy, microhardness measurements were achieved to study the consequence of the microstructure on hardness. Vickers microhardness values were around 1400 HV to 1800 HV, its exhibited excellent adhesion to the substrate as long as the boride layer, which was much higher than 260 HV hardness of Ti-6Al-4V titanium alloy.

Keywords: titanium alloy Ti-6Al-4V, electrochemical boride, mechanical behavior, tribological properties

INTRODUCTION

Titanium is lustrous transition metal with low density and high strength; it is resistant to corrosion, seawater, and chlorine. Titanium is widely distributed in the earth's crust and lithosphere and it found in almost all living things water bodies rocks and soils the metal is extracted from its principal mineral ores by the crawl and hunter processes [1–3]. The most common compound titanium dioxide is a popular vote a catalyst and it used in manufacture of white pigments other compounds include titanium tetrachloride a component of smokescreens, catalysts, and titanium tri-chloride, which is used as a catalyst in the production of polypropylene titanium, can be alloyed with iron, aluminium, vanadium, and molybdenum. Among other elements to produce strong lightweight alloys for aerospace, jet engines, missiles, and spacecraft military, industrial processes, chemicals, petrochemicals, desalination plants, medical prosthesis, orthopaedic implants dental, endodontic instruments, files dental implants, and many other applications. Titanium is as strong as some steels but less dense there are two allotropic forms and five naturally occurring isotopes of this element.

However, the hardness of titanium alloy is relative low and revealed a weak wear resistance. With a view to enhanced some properties of titanium alloy, the processes of surface hardening and diffusion of chemical elements on the surface of materials have been established, among those methods is boriding. Boriding or boronizing is a thermochemical hardening treatment, which boron can form compounds with materials, such as steels, cast iron, and titanium alloy. Boriding processes involves solid; pack or past, liquid; with or without electrolysis, gas, and plasma boriding. Among these methods, melted salt does not require special equipment to achieve the treatment.

In the literatures, some researchers reported that titanium can be treated by boriding to enhance some properties [4, 5], but these reports are very little. The aim of this work is develop the properties of titanium and study the effect of boriding on mechanical and tribological properties on titanium alloy Ti-6Al-4V. The effects of wear under dry sliding conditions on the sample were investigated.

EXPERIMENTAL

— Materials

Titanium alloy Ti-6Al-4V used as the base material in this work. The chemical composition of Inconel 600 alloy was as follows: 5.65 Al, 3.67 V, 0.30 Fe, 0.05 C, 0.05 O, 0.04 N, 0.01 H and balance Ti (wt %).

Before the boriding process, the samples should be pre-treated. The samples with the size of 50×20×5 mm were polished by grinding with emery paper using the 2000 mesh emery paper, cleaned with acetone in ultrasonic cleaner, and then washed in deionized water.

— Boriding process

The boriding was performed on titanium alloy Ti-6Al-4V after cutting. Each sample was put in an Al_2O_3 crucible and covered by the boriding componds of 20 wt% B_4C (as boron source), 60 wt% of sodium tetraborate $Na_2B_4O_7$ (as a transport medium), 10 wt% Al (as a reducing agent), and 10 wt% NaCl (as an activator) [6].

Boriding was carried out by immersing the samples in the bath at 950°C for 30 min and constant current of 200 mA/mm^2 [7]. After the treatment, the samples were taken out from the solution and water cooled, and then it was boiled and washed in water for about 1 h.

— Experimental method

Microstructural and morphological characteristics of borided titanium alloy Ti-6Al-4V were analysed band examined by a TESCAN Scanning Electron Microscope (SEM), with an Energy Dispersive X-Ray Spectro- scope (EDS). The presence of the titanium boride formed on the surface of sample and the phase composition of the samples were

confirmed by X-Ray diffractometer (XRD) with 2h varying 0° to 90°, using Cu K$_a$ radiation worked at the optimum voltage of 32 kV, anodic current of 20 mA, and the wavelength k = 1.54060 Å.

Microhardness measurements were carried out throughout the boride layers via SHIMATZOU Vickers microhardness. The results of microhardness of boride layers formed on the surface of titanium alloy Ti-6Al-4V was obtained after three times measurements.

The wear resistance of borided titanium alloy Ti-6Al-4V was estimated using the four-ball method. Furthermore, the wear mechanisms occured in the boride layers were examined during the four-ball test method. After boriding wear test at room temperature was achieved along a circular track of 10 mm diameter against ZrO$_2$ of a radius of 3/32 inch counterpart at 50 rpm under a constant normal load of 4.9 N in the atmosphere of the relative humidity of about 30% at room temperature using the pin-on-disk-type abrasion testing equipment.

The wear width obtained with a metallographic microscope to test the width of wear scar. The wear depth and wear width tested four times to get the average value. The other tribological configurations that utilize a pin-on-disk tribometer. A Mitutoyo Surft- est SJ-30 roughness meter was used to analyse the surface rough- ness, the CNs deposit thickness, and the wear profiles performed by the tribological test. The wear of both borided and non-borided titanium alloy Ti-6Al-4V was evaluated in dry and lubricant conditions under different applied loads.

The friction and wear tests of the coatings were carried out using ball-on-disk method with a CSM Tribometer. The tests were performed dry sliding a tungsten carbide (CW) ball (5 mm diameter) at a temperature of 25 °C with a relative humidity 66%, during a total sliding distance of 600 m with a sliding speed of 0.2 m/s and the covered radial distance was 5 mm under a normal load of 1 N.

RESULTS AND DISCUSSION

⎯ Structure analysis

The surface morphology of the sample was observed by SEM. Fig. 1 appearances the SEM micrographs of boride layer of titanium alloy Ti-6Al-4V. It is apparent from the micrograph that a dual boride layer consisting of monolithic TiB$_2$ and needle-like TiB whiskers form beneath the surface, but present a high roughness at higher magnifications, with a degree of porosity due to the presence of amorphous grains.

No discontinuity and lack of adhesion are observed between boride layer and substrate, which means that TiB whiskers anchor boride layer formed on the substrate.

According to the results of the line analysis, the thickness of the boride layer was 25 µm, which consists of 3 µm thick continuous and smooth monolithic TiB$_2$ and remaining TiB layers 22 µm.
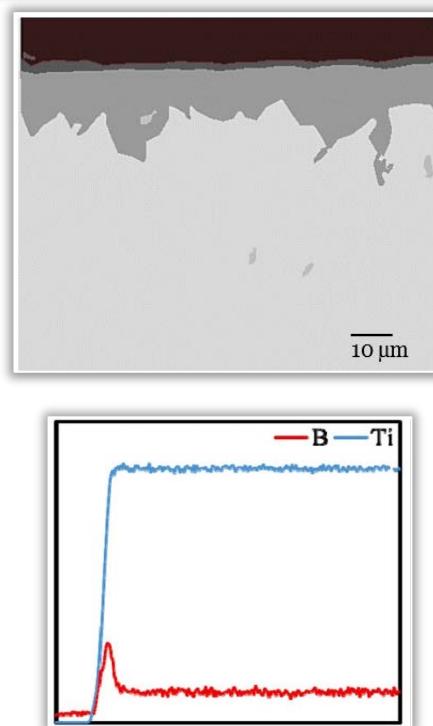
Figure 1. SEM images of the cross section of boride layer of titanium alloy Ti-6Al-4V and EDS analysis

XRD patterns of the sample analyzed is shown in Fig. 2, Fig. 2 revealed the X-ray diffraction patterns of the surface of titanium alloy Ti-6Al-4V at 950 °C. As shown in Fig. 2 as the first peak is shallow and relatively low, the degree of graphitization is low, from the X-ray diffraction measurement, it was confirmed that TiO2, TiB, and TiB$_2$ were formed. The main chemical composition of TiB$_2$ is obtained from the EDS, showing mostly B and Ti. Since neither TiB$_2$ peaks are present in the XRD, nor B is obtained in the EDS.
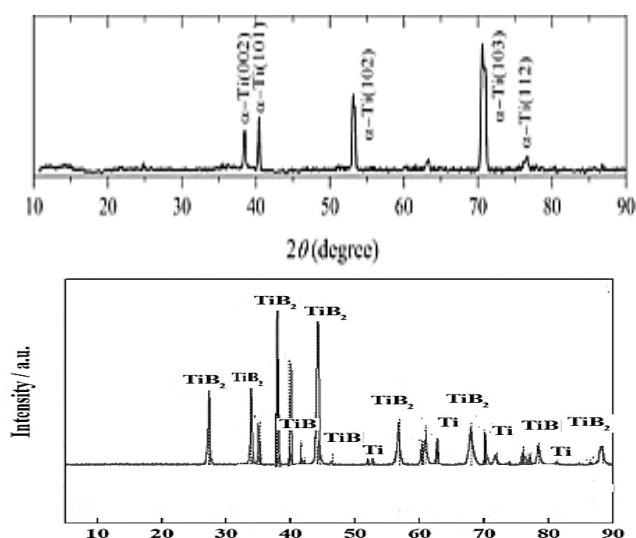
Figure 2. X-ray diffraction patterns; (a) Untreated titanium alloy Ti-6Al-4V (b) boride layer of titanium alloy Ti-6Al-4V

⎯ Mechanical property

The surface hardness of boride samples was investigated. The hardness of titanium alloy Ti-6Al-4V was about 260 HV. However, the microhardness of boride samples was about

1458 HV, it was much higher than that of the untreated specimen. The surface hardness of the hardened layers was improved significantly.

Young's modulus of boride samples reached the maximum value was about 352 GPa. Thus, the Young's modulus of boride samples was much higher than that of the untreated specimen; which was about 111 GPa.

Table 1. Some mechanical and tribological values of untreated and boride sample

Characterization	untreated	boride sample
Microhardness (HV)	260	1456
Young's modulus (GPa)	111	352
Wear width (µm)	1240.28	57.82
Wear depth (µm)	640.04	25.84

It should be noted that corrosion occurred in the surface of the ball in addition to the surface of the hard layer. The wear depth and the wear width of boride sample decreased significantly compared to untreated. It can be concluded that the reason for these differences is the transition from mechanical to abrasive wear.

Table 1 regrouped some mechanical and tribological values of untreated and boride sample such as: microhardness, Young's modulus, wear width and depth. It is noted that the higher the hardness, the lower the wear depth of the hardened layer. Therefore, the wear of boride layers is improved.

CONCLUSIONS

Mechanical and tribological properties of Ti-6Al-4V titanium alloy after boriding were estimated including the H, E, and wear. The main conclusions are as follows:

— Boriding process based on the electrochemical boriding was achieved at 950 °C for 30 min.

— The surface methodology was used to analyze the effects of boride.

— XRD patterns confirmed the formation of titanium borides (TiB and TiB_2).

— Vickers Microhardness values were around 1400 HV to 1800 HV.

Acknowledgments

References

[1] Zhao S, Hou W T, Yang R, Ti-6Al-4V lattice structures fabricated by electron beam melting for biomedical applications, Titanium in Medical and Dental Applications (2018) 277-301.

[2] Gerald Q C, McEwen D, Zhou A, Corrosion resistance of Ti–6Al–4V with nanostructured TiO_2 coating, Emerging Nanotechnologies in Dentistry (2012) 165-179.

[3] Biesiekierski A, Munir K, cang Y, Wen L C, Titanium alloys, Structural Biomaterials, (2021) 157-187.

[4] Kaouka A, Allaf H, Khamed M A, Alaoui O, A simultaneous improvement of both hardness and ductility of Ti-6Al-4V alloy by Nb addition, Journal of Physics: Conference Series 1781 (1), 012006.

[5] Das S, Kumar R, Joshi R S N, Surface Alloying of Titanium Di-boride (TiB_2) and Silicon Carbide (SiC) on Aluminium Al 5052 using Electric Discharge Processing 14 (2019) 119-126.

[6] Kulka M, Current Trends in Boriding, ISBN: 978-3-030-06782-3.

[7] Kaouka A, Benarous K, Electrochemical boriding of titanium alloy Ti-6Al-4V, Journal of Materials Research and Technology 8 (6), 6407-6412.

Fascicule 2

[April – June]

t o m e
[2022] XV

ACTA Technica CORVINIENSIS
BULLETIN OF ENGINEERING

[1.]Babatope A. OLUFEMI, [1.]A. I. BAYE

SIMULTANEOUS ADSORPTION OF LEAD AND COPPER USING MODIFIED CHICKEN EGGSHELLS

[1.] Department of Chemical and Petroleum Engineering, University of Lagos, Akoka, Lagos, NIGERIA

Abstract: Water containing heavy metals if not properly treated can lead to serious health implications for humans and animals and severely destroy the environment. The present study investigated the simultaneous adsorptive removal of lead and copper ions from aqueous solutions using modified chicken eggshells (MCE). The eggshells were calcined at 600^0C for 2 hours. Optimum conditions obtained were pH 6, adsorbent dose of 15 g and contact time of 90 minutes. Under these conditions, the percentage adsorptions attained were; 96% for lead and 86% for copper. The Langmuir isotherm model fitted the copper adsorption most with a correlation coefficient (R^2) value of 0.9992, while the pseudo second order kinetics fitted the lead and copper adsorption most with R^2 values of 0.9998 and 0.9979 respectively. The efficacy of MCE as a good adsorbent for lead and copper ions is presented as a viable low–cost adsorbent for waste water purification.
Keywords: Modified Egg Shell (MCE), Lead adsorption, Copper adsorption, Kinetics, Biosorbents

INTRODUCTION

Wastewater obtained from sources like tanneries, battery manufacturing factories, mining fields, metal processing industries and so on needs to be properly disposed of to prevent pollution of water bodies, which can in turn alter the growth and development of aquatic organisms. Most common heavy metals found are copper and lead, which when prevalent in high concentrations may be injurious to health and the surrounding environment. Copper is used for various purposes industrially due largely to its good conductive abilities. Copper is carcinogenic and toxic when ingested in large quantities resulting in headaches, vomiting, nausea, liver and kidney failure, respiratory problems and abdominal pain (Ren *et al.*, 2008; Hu *et al.*, 2013; Lan *et al.*, 2013). Lead is toxic, teratogenic and carcinogenic, posing serious health implications to life when exposed to unhealthy quantity. To maintain a safe environment, these metals disposal have to be properly taken care of in the discharged wastewater. There are a variety of methods employed to treat wastewater and extract heavy metals from it, some of these methods include ion exchange, chemical oxidation, reduction, chemical precipitation, adsorption, ultrafiltration, electrodialysis and reverse osmosis (Fu & Wang 2011). Adsorption seems to be one of the most efficient of these techniques.

Biosorbents obtained from biological substances seems cheaper compared to commercial adsorbents. They are not synthetically manufactured, thereby possessing the ability to passively adhere, concentrate and bind contaminants onto their cellular structure. This work will be considering the removal of two heavy metal ions (lead and copper) using modified chicken eggshell. The chicken eggshell is known to possess some distinct mechanical characteristics like impact resistance, excellent blend of stiffness, strength and toughness. It contains about 95% calcium carbonate and 5% organic materials. Modification of the egg shell is usually carried out by calcining at high temperatures. After calcining, the structure changes due to the development of pores as a result of the emission of carbon dioxide gas (Rohim *et al.*,

2014). Simultaneous as well as selective adsorption of lead, copper and some heavy metals onto eggshells and composite formulations had been reported in the literature. For lead adsorption alone, Vijayaraghavan and Joshi (2013) studied the use of eggshell as an additive to remove lead cations from aqueous solutions in the pH range of 2–5. They confirmed that on reducing the particle size of the eggshell from 750 to 100 microns, the removal efficiency increased from 30.7 to 99.6% using an initial lead concentration of 1045 mg/L. Soares et al., (2016) has evaluated a biosorbent derived from co–composting eggshell (CES) with other organic materials like potato peels, grass clipping, and rice husk, for removing lead (II) ions from an aqueous solution, with about 30 % w/w CES. The CES provided supplementary sites for lead sorption and an increase of about 43 % in the sorption capacity was reported. The efficacy of eggshells for adsorption of lead ions in a hybrid composite formulation with sericite as a binder had been investigated by Choi (2019) with the observation that the adsorption process of lead removal was optimal for adsorbent concentration of 1–1.5 g/L and 30 min mixing time. The removal was well fitted by the Langmuir isotherm model with a correlation coefficient of 0.9963, while the kinetic data were well fitted by the pseudo–second–order model with a correlation coefficient of 0.9982. Hen egg shells (HES) from EnShi, HuBei Province, China, with selenium as a constituent have been used as adsorbent for the adsorption of lead ion from aqueous solutions (Gong et al., 2019).

More recently, chemical surface modification of eggshells using three modifying agents of NaOH, HNO_3 and $KMnO_4$ to produce adsorbents have been investigated for lead removal from aqueous solution with a maximum adsorption capacity of 700 mg/g and removal efficiency of 98% (Basaleh et al., 2020). The development and characterization of magnetic eggshell membranes (MESM) for lead removal from wastewater had been reported by Peigneux et al., (2020). Their results suggested that MESM could be utilized as an efficient nano–remediation agent for lead removal from contaminated waters. As reported, 98.62% maximum

adsorption was obtained by Jamion et al., (2021) for the removal of lead in soil by eggshells activated carbon. The application of synthesized calcium oxide nanoparticles from hen eggshells for the removal of lead ions from aqueous solutions had been investigated (Jalu et al., 2021). The HES was found to remove about 95% of lead from its aqueous solution.

Adsorption of copper alone with eggshell and eggshells formulations had also been investigated. The sorption of copper (II) ions from aqueous solutions by eggshell was investigated by Nõlvak et al., (2013) in a batch experimental system with respect to temperature, initial Cu(II) ions concentrations, pH, and biosorbent doses. The system was best described by the pseudo second–order kinetic with a maximum adsorption capacity of 5.05 mg Cu^{2+}/g eggshell at 25 °C. Waste eggshells for adsorption of copper from synthetic and swine wastewater had been investigated by Hess et al., (2018). From their work, the adsorption of copper followed a second order kinetic model with a theoretical maximum adsorption capacity of 3.0 mgg^{-1} at 20°C. Mohammad et al., (2020) had evaluated the potential of using two types of eggshells of untreated raw eggshells (ES) and eggshells that were mechanically ball–milled into the nano–size (NES), as biosorbents for the removal of Cu(II) ions from aqueous solutions. The NES provided an advantage over ES through much rapid removal of Cu (II). The ES and NES removal efficiencies were 91.36% and 97.21% respectively. A maximum percentage copper(II) removal of about 85% had been confirmed by Madiabu et al., (2021), after Investigating the feasibility of eggshells as a potential adsorbent for copper (II) ion removal from an aqueous solution.

Simultaneous adsorption operation had also been investigated. The feasibility of using magnetic eggshell–Fe_3O_4 powder as an adsorbent for the removal of Pb(II) and Cu(II) ions from aqueous solution with optimal adsorption pH value of 5.5, equilibrium capacity value 263.2 mg/g for Pb(II) and 250.0 mg/g for Cu(II) had been reported by Ren et al., (2012). The removal of lead and copper from textile wastewater using waste egg shells in a continuous stirred tank reactor had been reported by Pandey et al., (2017). The Langmuir isotherm showed the best fitting for the isotherm equilibrium data, with a maximum adsorption capacity of 4.33 mg/g and 3.54 mg/g for lead and copper respectively. Mashangwa et al., (2017) had investigated the adsorptive removal of zinc, lead, copper, and nickel ions from synthetic aqueous solutions and various metals from three acid mine drainage (AMD) sites using chicken eggshells. The percentage adsorptions obtained were 97% for lead, 95% for copper, 94% for nickel, and 80% for zinc. In addition, aluminium, iron, potassium, nickel, and zinc ions all had percentage adsorptions above 75%. Furthermore, potassium had a 98.78% adsorption, while magnesium, strontium, and zinc had 72.33, 68.75, and 53.07% adsorption, respectively. Arsenic, chromium, copper, iron, antimony, and tellurium ions also had above 75% adsorption.

The adsorptive efficacy of eggshell on some other metals with commendable results had been reported. Sasikala et al (2021) has worked on reducing toxic compound extracted from battery waste using activated carbon from Egg shells Nano sized (ES–NP). The ES–NP recorded about 96% removal efficiency. Perchlorate removal efficiency of highly porous nano hydroxyapatite (nHA) and its magnetic composite aerogels (SPIONS@nHA) by freeze–drying technology produced from eggshell had been investigated by Prabhakaran and George (2021). Very fast removal kinetics were observed and the maximum adsorption capacity for nHA and SPIONS@nHA were 148.4 and 305.8 mgg^{-1} respectively. The removal of bismuth ion by 0.45 μm pulverized chicken eggshells had been investigated with optimal removal of 891.29 mg/g by Abbas et al., (2021).

The aim of this study is to simultaneously adsorb lead and copper ions from wastewater onto MCE. The objectives include to study the effect of pH, agitation time, adsorbent weight, adsorbate concentration, and temperature on the adsorption with MCE. Adsorption isotherms like Langmuir, Freundlich, Temkin and Dubinin–Raduskevich as wells as various kinetics will be used to fit the adsorption operation.

METHODOLOGY

All experimental data are averages of three runs. Documented methods were followed (Rajendran and Mansiya, 2011, Rohaizar et al., 2013, Kumaraswamy et al., 2015).

— Materials

These include Simulated wastewater containing copper and lead ions, adsorbent locally sourced from Jekaplay restaurant (chicken eggshells), USA Merck $CuSO_4 \geq 99.99\%$ 7758–98–7 and USA Merck $Pb(NO_3)_2 \geq 99.95\%$, 10099–74–8 required for preparation of simulated wastewater, USA Merck 37% HCl 7647–01–0 and USA Merck 97% NaOH 1310–73–2.

— Equipment

Switzerland OHAUS Model Explorer Semi micro electric balance, USA Skyray AAS 6000 Flame Atomic Absorption spectrometer, England Pyrex conical flasks (50–500 ml), Germany Witeg Microliter pipettes Witopet premium Starter–Kit 5 402 600 P, India VeeGee 20114–Series Burettes, Timer or a stop watch, United States Carson MicroBrite Plus 60x–120x Power LED Lighted Pocket Microscope (MM–300), England Surgifield Model SM 1002A Muffle Furnace for the calcination of the eggshells, United States Hanna Instruments model HI98107 pH meter, United States Perkin Elmer Fourier Transform Infrared(FTIR) Spectrophotometer Spectrum 2000 Model, Germany Merck KGaA Whatman filter paper no. 41, and Australia RATEK model SWB20D shaker.

— Preparation of simulated wastewater

The wastewater for the procedure was prepared by dissolving lead salts and copper salts in water. USA Merck $Pb(NO_3)_2 \geq 99.95\%$ salt was utilized alongside copper (II) sulphate ($CuSO_4$). This was carried out by preparing stock solution of 1000ppm, here 3.93g of copper sulphate was dissolved in 1L of deionized water. 1.598g of lead nitrate was

added in 1L deionized water to prepare the 1000ppm stock solution. From the stock solution, a 100ppm concentration of heavy metal contaminated water was prepared. To prepare 5 ppm solution, 100ml was used from 1000 ppm (for Cu & Pb) solution in a beaker and then added to deionized water to top up to 1000ml. A 0.1M HCl or 0.1M NaOH was then used to effectively adjust the pH.

— Pretreatment of eggshells

The locally sourced eggshells were first washed with clean water and then washed with distilled water severally after which, they were left to air dry and then subjected to hot air in an oven at 50 ^{0}C for 2 days. After the drying process was completed, the eggshells were grinded to fine particles with a grinder and then were mixed, it was sieved afterwards to achieve a uniform particle size.

— Calcination of the adsorbent

This modified the eggshells to open the pores thus enhancing adsorption. Different portions of cleaned and crushed powder were put into a metal container and calcined in a muffle furnace at varying temperatures and various time periods. Eggshells were calcined at temperatures ranging between 600 ^{0}C using England Surgifield Model SM 1002A Muffle Furnace with a time period 2 hours at a heating rate of 10 ^{0}C/min.

— Scanning Electron Microscope test

This test was carried out on the eggshell surface to analyze the ultrastructure of the eggshell membrane. This was done by taking up a little portion of the eggshell powder (about 0.5 cm^3) and then mounting on a specimen stub using an adhesive that is conductive in nature, and coated with gold before examination occurs in the electron microscope.

— Fourier Transforms Infrared Spectroscopic Analysis

This test was carried out to study the surface chemistry of the modified eggshells before and after adsorption using spectroscope (FTIR–2000, Perkin Elmer model). FTIR spectra was recorded between 4000 cm^{-1} and 400 cm^{-1}. This was carried out by mixing 1mg of dried eggshell powder with 500 mg of KBr in a mortar and then pressing this mixture at a certain pressure for a time period of 15 minutes. This spectra test gives information about the functional groups on the surface of the modified eggshells.

— Effects of pH on the Cu^{2+} and Pb^{2+} adsorption

The effect of pH on adsorption of Pb^{2+} and Cu^{2+} ions onto eggshell was studied by mixing a given weight of the adsorbent with 100 ml of each 100–ppm individual solution of the adsorbate at different pH values ranging from 4 – 10 at 24ºC (ambient temperature). The varied pH value was adjusted using 0.1M NaOH and/or 0.1M HCl solutions and was continually measured by United States Hanna Instruments model HI98107 pH meter. The mixtures were then put on a shaker for time periods varying between 60–90 minutes. The solutions were then filtered through Germany Merck KGaA Whatman filter paper no. 41 (diameter 125 mm) and the filtrate obtained was then analyzed for residual metal concentration. The final concentration of Pb^{2+} and Cu^{2+} after

the residence time of 90 minutes were measured with the Analyst 400 Perkin Elmer Atomic Absorption Spectrometer (AAS).

— Effects of adsorbate concentration on the adsorption of Cu^{2+} and Pb^{2+} ions

The effect of initial metal concentration on adsorption of Pb^{2+} and Cu^{2+} ions was studied by mixing 0.5 g of the adsorbent with 100 ml of the individual adsorbate (Pb^{2+} or Cu^{2+}) in varied concentrations of 100, 200, 300, 400 and 500 ppm at ambient temperature and pH 7. The individual ion mixtures were then agitated for periods ranging between 60–90 minutes. The solutions were then filtered and analyzed.

— Effects of adsorbent weight on the adsorption of Cu^{2+} and Pb^{2+} ions

The effect of adsorbent dose on the adsorption of Pb^{2+} and Cu^{2+} ions was studied by mixing different masses of the egg shell adsorbent ranging from 2 to 15 g with 100 ml of each 100–ppm individual solution of the adsorbate at ambient temperature and pH 7. The individual ion mixtures were then agitated for a time range between 60–90 minutes. The solutions were then filtered through and analyzed.

— Effects of agitation time on Cu^{2+} and Pb^{2+} adsorption

The agitation on the shaker was decided to be 150 rpm to make the process more efficient for a contact time of 60 minutes and 90 minutes after the pH adjustment and addition of a given weight of adsorbent was done. Afterwards filtration using Germany Merck KGaA Whatman filter paper no. 41 was carried out and then the samples were sent to USA Skyray AAS 6000 Flame Atomic Absorption spectrometer to check the level of adsorption.

3. RESULTS AND DISCUSSION

Figure 1 show the Fourier Transform Infrared spectroscopy of the modified adsorbent (eggshell) after adsorption. It shows sharp declines at 628 cm^{-1} which depicts effects of CaCO$_3$, while those of 1132 cm^{-1} and 1638 cm^{-1} are attributable to the C=O groups. The peak at 3436 cm^{-1} is attributable to H$_2$O molecules. For most parts of the figure, the spectra after adsorption was lower in value due to the presence of the adsorbed lead and copper ions.
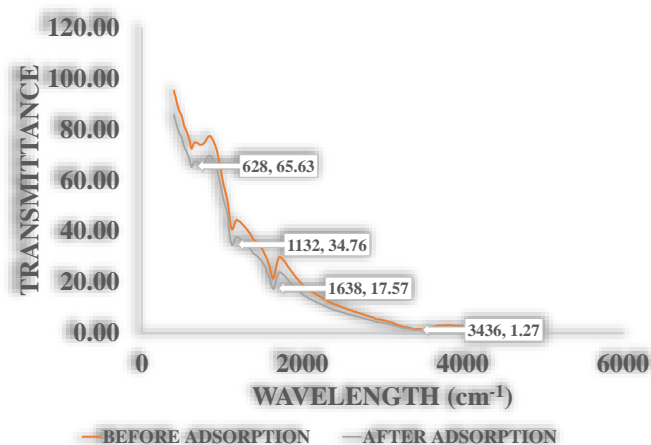

Figure 1: FTIR spectra of the MCE adsorbent before and after adsorption

Figures 2 and 3 show the Scanned Electron Microscope (SEM) image of the MCE adsorbent before and after adsorption

respectively. Figure 3 shows the reduction of the pores sizes and effective surface area after adsorption of the lead and copper ions on the adsorbent.
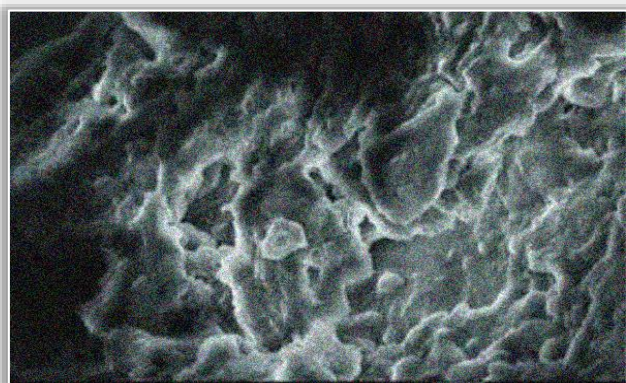

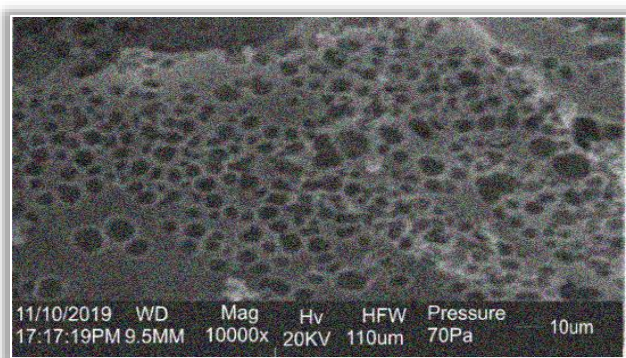Figure 2: SEM image of the MCE adsorbent before adsorption

Figure 3: SEM image of MCE after adsorption

— Effect of pH on the adsorption of Cu^{2+} and Pb^{2+} ions

The effect of pH on the adsorption capacity of MCE for lead (Pb^{2+}) and copper (Cu^{2+}) is represented in Figure 4. The solution pH was maintained within the range of 4.0 – 10.0. It was noticed that optimum adsorption in this experiment occurred at pH values around 6. At pH 6, the increase in adsorption could be attributed to the weak inhibitory effect of H_3O^+ ions. At pH levels above 6, the adsorption rates were unpredictable due to the accumulation of metal ions on the surface of the adsorbent. A fall in the rate of removal of metal ions at lower pH is due to the higher concentrations of H^+ in the solution which compete with the metal ions for the adsorption sites on the adsorbents. The effect of pH on adsorption was reported by Rohaizar et al. (2013) in a study about the removal of Cu^{2+} from water by adsorption on chicken eggshell. It was found that the adsorption of Cu^{2+} increased as the pH increased from 4 – 7. This displacement reaction creates space for the exchange of ions on the surface of eggshell. Therefore, a pH above neutral is favorable for the effective binding of heavy metals present within the solution. Park et al. (2007) in a simulated study about the removal of heavy metals using waste eggshell, predicted the presence of soluble lead species as $Pb(OH)_4^{2-}$ above pH 12.

Another study, however, reported optimum adsorption of lead ions at pH 6 after which the metal ions started to precipitate (Arunlertaree et al., 2007). This suggests that the optimum pH for the removal of metal ions is dependent on other factors than the acidity or the alkalinity of the solution, which affects the behavior of compounds formed. All metals precipitate as hydroxides by the addition of NaOH and the observed metal removal at these high pH values may also have been due to NaOH and not adsorption onto the adsorbent. Another controlling factor could be the size of eggshell used. This was demonstrated by Pettinato et al. (2015), where they obtained the best results with the smallest particles of the eggshell, owing to the increased surface area available for the adsorption. Although higher percentage adsorption was noted at higher pH values (pH of 8 upwards) for all metal ions, pH 7 was chosen as the optimum pH, as it is the point before adsorption slowed down and also due to environmental considerations where it is environmentally friendly to release neutral aqueous solutions, as opposed to acidic or basic effluents.
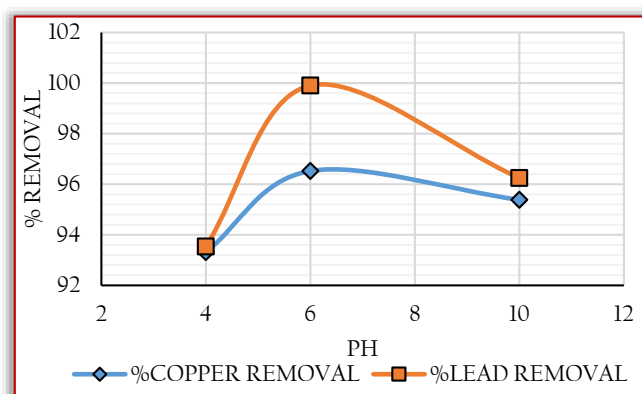

Figure 4: A plot of % metal removal with pH

— Effects of adsorbate concentration on the adsorption of Cu^{2+} and Pb^{2+} ions

The effect of adsorbate concentration on the adsorption capacity of eggshells for Cu^{2+} and Pb^{2+} is represented in Figure 5. The analysis on the effect of metal ion concentration demonstrates that an increase in the concentration of lead and copper ions led to a decrease in the percentage adsorption. Anantha and Kota (2016), noticed that the metal ion adsorption of copper increased sharply in the beginning and then decreased slowly with further increase in the initial concentration. This relationship is noted as the initial concentration of lead and copper ions increase. The decline in percentage adsorption may be ascribed to lack of sufficient surface area (1g of eggshell) to allow more metal ions have access to the solution. At lower concentrations most of the ions present can interact with the binding site and thus the percentage adsorption is higher, whereas at higher ionic concentration, the adsorption is low due to the saturation of adsorption sites which is attributed to the increasing number of ions competing for available binding sites on the eggshell. The maximum percentage adsorption of lead ions was found to be 96% at a concentration of 300 ppm. For the copper metal, adsorption was noticed to be the highest at a concentration of 100 ppm after which the adsorption percent decreased slightly but steadily.
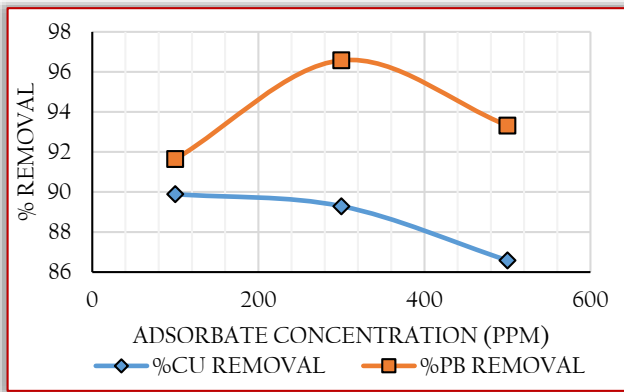
Figure 5: A plot of percentage metal removal with metal ion concentration

— Effects of adsorbent weight on the adsorption of Cu²⁺ and Pb²⁺ ions

The effect of adsorbent dose on the adsorption capacity of eggshells for Cu^{2+} and Pb^{2+} is presented in Figure 6. The results represented in the figure show that an increase in the adsorbent dose leads to an increase in adsorption percentage. This is largely due to the increased number of pores that are available for adsorption. Some previous studies reported the removal of lead to be influenced by the dose of eggshell, as the effective removal of solutes increased with increasing dose of adsorbent (Agarwal and Gupta (2014); Agarwal (2012); Arunlertaree et al. 2007). At high sorbent dosage, the available metal ions have adequate exchangeable sites on the eggshell to bind to, resulting in a higher metal ions uptake. Lead showed a very high affinity to the eggshell. It was observed that 1 g of the eggshell was able to adsorb 97.89% of the metal ions.
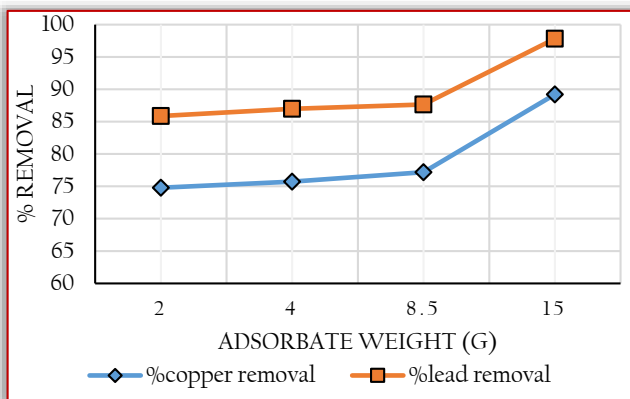

Figure 6: A plot of percentage removal with adsorbent dose

— Effects of contact time on the adsorption of Cu²⁺ and Pb²⁺ ions

The effect of contact time on the adsorption capacity of eggshells for Cu^{2+} and Pb^{2+} is represented in Figure 7. The exponential phase for lead was found to be between 60 and 120 minutes, further increase in contact time led to no significant adsorption of metal ions by the eggshell. A slight increase in the percentage adsorption for Cu^{2+} was observed as the contact time increased. Copper indicated a slightly higher increase in percentage adsorption over time. It however dipped at a contact time around 75 minutes, this was due largely to other factors affecting adsorption. The lead

ions showed a different trend, as their adsorption reduced with contact time, this can be attributed to the fact that at 60 minutes, the pores available for adsorption had already been filled up, hence any further introduction of adsorbate will only bring about a decline in the percentage metal removal. Similarly, Ipeaiyeda and Tesi (2014) obtained an optimal adsorption for 100 ppm of Pb^{2+} at a contact time between 60 – 120 minutes.
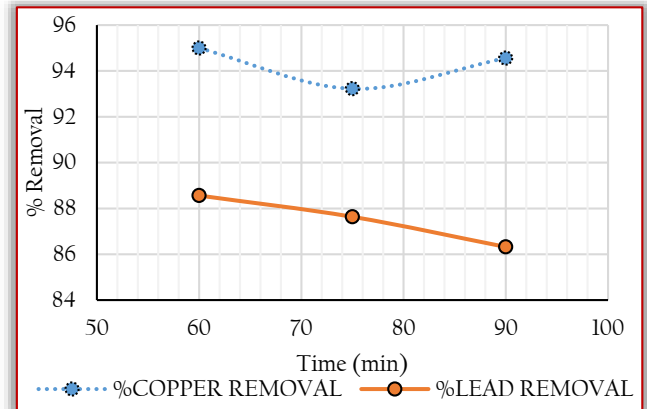
Figure 7: A plot of percentage removal with contact time

— Adsorption Isotherms

The experimental data were tested and compared with the four isotherm models.

≡ Langmuir isotherm

The Langmuir isotherm assumes that the surface of any adsorbent material contains a number of active sites where the adsorbate attaches itself. This attachment can either be physical or chemical. When the attachment is via Van der Waals interactions, it is known as physiosorption and when via covalent bond it is known as chemisorption. It says that there is not much interaction between the adsorbate molecules and once a saturation value has been reached no further adsorption would take place.

Figure 8: A plot of 1/qe with 1/ce showing the Langmuir isotherm for lead and copper

A linear plot obtained for Langmuir isotherm is shown in Figure 8 for copper and lead.

The Langmuir isotherm equation is given in Equation (1). The equation obtained for the Langmuir isotherm for the current data was obtained from the plot of $1/q_e$ against $1/c_e$.

$$\frac{c_e}{q_e} = \frac{1}{Q_0 b_L} + \frac{c_e}{Q_0} \qquad (1)$$

where q_e is the amount of dye adsorbed (mg/g), Ce is the equilibrium concentration of the adsorbate (mg/L), Q_0 is the maximum adsorption capacity (mg/g) and b is the energy of adsorption (J/mol).

≡ Freundlich Isotherm

The Freundlich model is given by Equation 2.

$$\log q_e = \log k_f + \frac{1}{n} \log C_e \qquad (2)$$

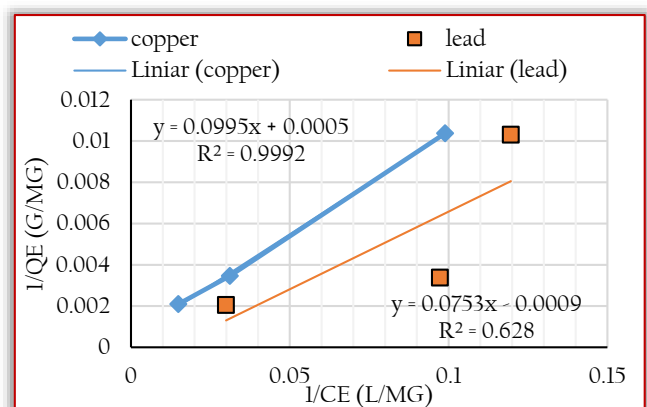where q_e is the amount adsorbed (mg/g), Ce is the equilibrium concentration of the adsorbate (mg/ L), k_f and n, the Freundlich constants are related to adsorption capacity and desorption intensity respectively. The model is based on the assumption that adsorption occurs on a heterogeneous adsorption surface having unequally available sites with different energy of adsorption.

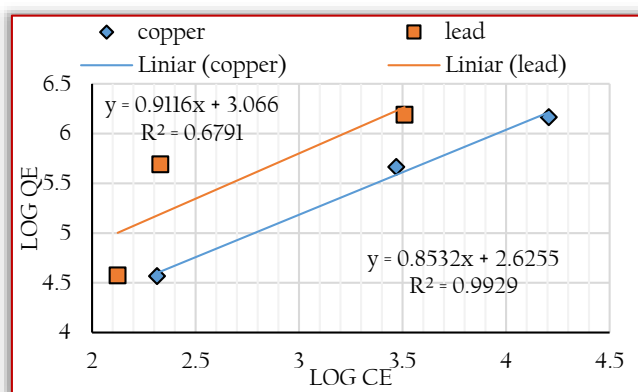The plots for the Freundlich isotherm for the metal ions (lead and coper) are given in Figure 9.

Figure 9: A Plot of log qe with log ce for Freundlich isotherm

≡ Temkin Isotherm

The Temkin isotherm assumes that the heat of adsorption of all the molecules increases linearly with coverage. The linear form of this isotherm is given in Equation (3).

$$q_e = \frac{RT}{b_T} \ln a_T + \frac{RT}{b_T} \ln C_e \qquad (3)$$

Qe is the amount adsorbed at equilibrium in mg/g, b is the Temkin isotherm energy constant, T is the temperature, R is the gas constant and a_T is the Temkin isotherm equilibrium binding constant (L/g). The slopes and intercept obtained from the graphical plot q_e against ln Ce were used to calculate the Temkin constants. Figure 10 show a plot of q_e with ln ce for the Temkin Isotherm.
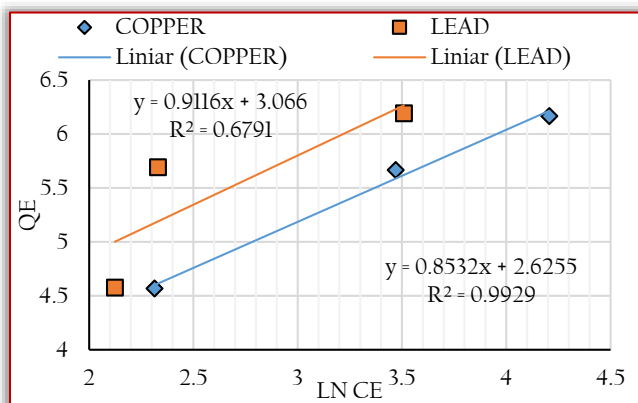
Figure 10: A plot of q with ln ce for the Temkin Isotherm

— Dubinin–Radushkevich Isotherm

The linear form of the Dubinin–Radushkevich isotherm is given in Equations (4), (5) and (6).

$$\ln q_0 = \ln q_D - B\,E^2 \qquad (4)$$

where q_D is the theoretical saturation capacity (mg/g), B is a constant related to mean free energy of adsorption per mole of the adsorbate (mol^2/J^2) and ϵ is the Polanyi potential which is related to equilibrium as follows;

$$\epsilon = RT \ln\left(1 + \frac{1}{C_e}\right) \qquad (5)$$

$$E = \frac{1}{\sqrt{2B}} \qquad (6)$$

where ϵ is Polanyi potential, β is the Dubinin–Radushkevich constant, R is gas constant (8.31 J/mol.K), T is absolute temperature, and E is mean adsorption energy.

Figure 11 shows the plot of ln q with E^2 for lead and copper.
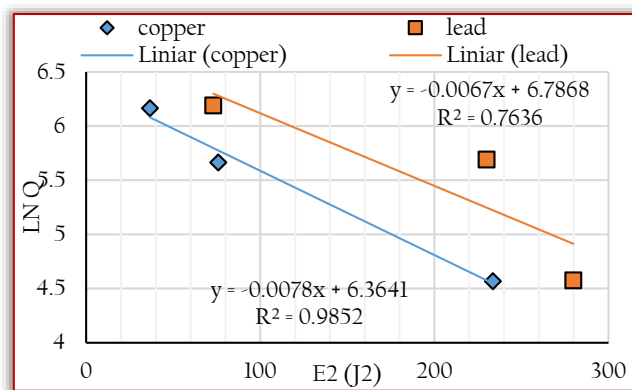
Figure 11: A plot of ln q with E^2

≡ Pseudo First Order Kinetics

This is given in Equation (7).

$$\log(q_e - q_t) = \log q_e - \frac{K_1}{2.303} t \qquad (7)$$

Where k_1 (min^{-1}) is the pseudo– first–order adsorption kinetic parameter; q_t is the amount adsorbed at time t (min); and q_e denotes the amount adsorbed at equilibrium, both in mg/g. The plot of log (q_e–q_t) as a function of t provides the k_1 and q_e values as shown in Figure 12.
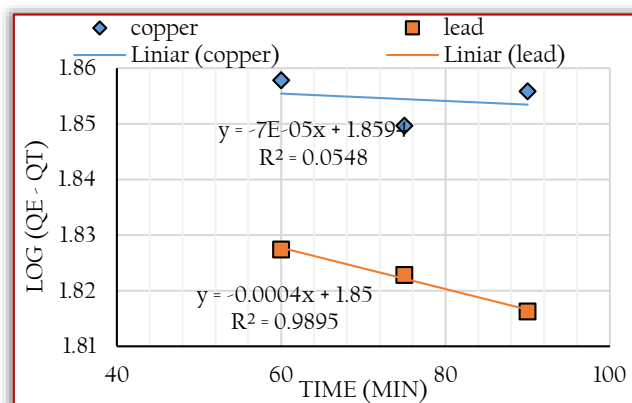
Figure 12: A plot of ln (q_e–q_t) against time

— Pseudo Second Order Kinetics

The pseudo – second–order equation based on the adsorption capacity at equilibrium is expressed in Equation (8).

$$\frac{t}{q_1} = \frac{1}{k_2 q^2_e} + \frac{t}{q_e} \qquad (8)$$

where k_2 (g/mg.min) is the pseudo–second – order adsorption kinetic parameter. From the slope and intercept of the (t/qt) as a function of t, k_2 and q_e was obtained in Figure (13). The plots according to Equation (8) provided excellent linearity as R^2 value was 0.9979 and 0.9998 for copper and lead respectively.
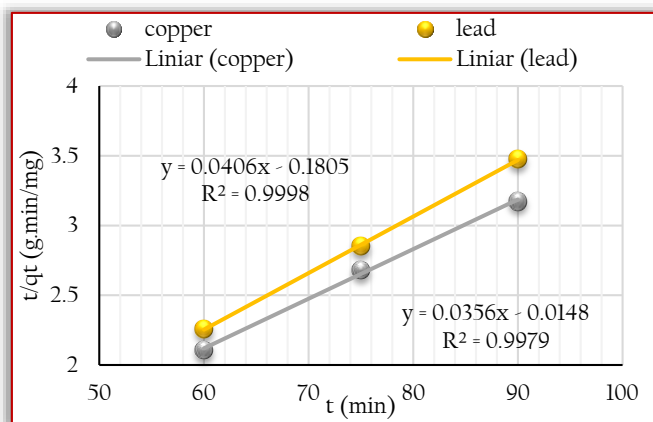
Figure 13: A plot of t/qt with time

—— Elovich Model
The Elovich model applicable for chemisorption kinetics and systems in which the adsorbing surface is heterogeneous (Namasivayam and Kavitha, 2002) is given in Equation (9).

$$\frac{dq_t}{dt} = \propto e^{-\beta qt} \qquad (9)$$

Integrating this equation for the boundary functions yields Equation (10).

$$q_t = \frac{1}{\beta}\ln(\propto \beta) + \frac{1}{\beta}\ln t \qquad (10)$$

where α is the initial adsorption rate (mg.min/ g) and β is related to the extent of surface coverage and the activation energy for chemisorption (g mg^{-1}). A plot of qt vs. ln t in Figure 14 gives a linear trace with a slope of (1/β) and an intercept of 1/β ln (α β). The plot is linear with good correlation coefficient (R^2 = 0.0852 for copper, R^2 =0.9754 for lead).
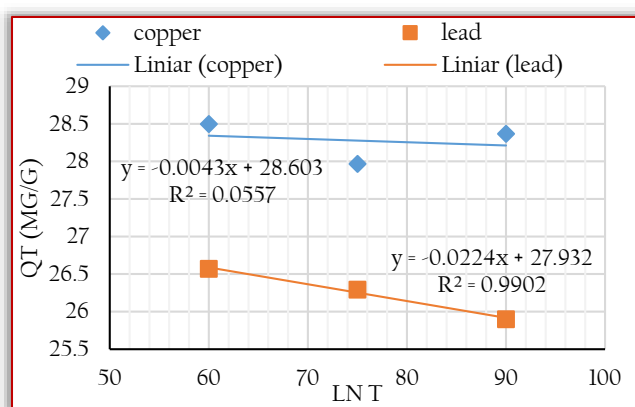

Figure 14: A plot of q_t with ln t

CONCLUSION AND RECOMMENDATIONS
Evidence provided in this study has shown that MCE have a high efficacy and have the potential to be used as an effective adsorbent for the removal of Pb^{2+} and Cu^{2+} ions aqueous solutions. The Langmuir isotherm model fitted the copper adsorption most with a correlation coefficient (R^2) value of 0.9992, better than for lead, while the pseudo second order kinetics fitted the lead and copper adsorption most with R^2 values of 0.9998 and 0.9979 respectively. A conclusion could be reached that pH, contact time, adsorbent weight/dose and initial metal concentration all played significant roles in the rate of adsorption of the metals. It was observed that adsorption of the metal ion was more pronounced with samples that had higher contact times. Adsorption was also higher in more basic solutions, as experimental runs with pH heading towards alkalinity showed greater adsorption capacities. This method of adsorption can be employed in purifying wastewater from metal mine effluents, metal refining and battery manufacturing facilities effluents.

References
[1] Abbas, A., Chen, L., Liao, Y. L., Wu, Z. Z., Yu, Y. Q., & Yang, J. Y., Removal of bismuth ion from aqueous solution by pulverized eggshells, Desalination and Water Treatment, 213, 395–405, 2021
[2] Agarwal, A., Removal of Cu and Pb from aqueous solution by using eggshell as an adsorbent. International Journal of Environmental Sciences, 3, pp.198–202, 2013.
[3] Agarwal, A. and Gupta, P.K., Removal of Cu and Fe from Aqueous Solution by Using Eggshell Powder as Low Cost Adsorbent. Advanced Applied Science Research, 5(2), pp.75–79, 2014.
[4] Arunlertaree, C., Kaewsomboon, W., Kumsopa, A., Pokethitiyook, P. and Panyawathanakit, P., Removal of lead from battery manufacturing wastewater by egg shell. Songklanakar in Journal of Science and Technology, 29(3), pp.857–868, 2007
[5] Basaleh, A. A., Al–Malack, M. H., & Saleh, T. A., Metal removal using chemically modified eggshells: preparation, characterization, and statistical analysis. Desalination and Water Treatment, 173, 313–330, 2020
[6] Choi, H. J., Assessment of the adsorption kinetics, equilibrium and thermodynamic for Pb (II) removal using a hybrid adsorbent, eggshell and sericite, in aqueous solution. Water Science and Technology, 79(10), 1922–1933, 2019
[7] Fu, F & Wang, Q., Removal of heavy metal ion from wastewater: a review, Journal of environmental management 92(3), 407–418, 2011.
[8] Gong, H. H., Li, T., Zhang, W. Y., & Liao, Z. J., A Study on Lead Adsorption by the Hen Egg Shells from EnShi, HuBei Province, China, In Solid State Phenomena, Trans Tech Publications Ltd., Vol. 294, pp. 11–16, 2019
[9] Hess, B. J., Kolar, P., Classen, J. J., Knappe, D., & Cheng, J. J., Evaluation of Waste Eggshells for Adsorption of Copper from Synthetic and Swine Wastewater, Transactions of the ASABE, 61(3), 967–976, 2018
[10] Hu, X. J., Liu, Y. G., Wang, H., Chen, A. W., Zeng, G. M., Liu, S. M., Guo, Y. M., Hu, X., Li, T. T., Wang, Y. Q., Zhou, L. & Liu, S. H., Removal of Cu(II) ions from aqueous solution using sulfonated magnetic graphene oxide composite, Separation and Purification Technology 108, 189–195, 2013
[11] Ipeaiyeda, R. and Tesi, G.O., Sorption and desorption studies on toxic metals from brewery effluent using eggshell as adsorbent. Advances in Natural Science, 7(2), pp.15–24., 2014
[12] Jalu, R. G., Chamada, T. A., & Kasirajan, R., Calcium oxide nanoparticles synthesis from hen eggshells for removal of lead (Pb (II)) from aqueous solution, Environmental Challenges, 4, 100193, 2021
[13] Jamion, N. A., Adun, M., Baharin, S. N. A., & Sambasevam, K. P., Removal of lead (Pb) in soil by eggshells activated carbon. In AIP Conference Proceedings, Vol. 2332, No. 1, p. 030003, 2021. AIP Publishing LLC
[14] Kumaraswamy, K., Dhananjaneyulu, B.V., Vijetha, P., and Kumar, Y., Kinetic and equilibrium studies for the removal of chromium using eggshell powder.

Research Journal of Pharmaceutical, Biological and Chemical Sciences, 6(1), pp.529–532, 2015.

[15] Lan, S., Wu, X., Li, L., Li, M., Guo, F. & Gan, S., Synthesis and characterization of hyaluronic acid–supported magnetic microspheres for copper ions removal. Colloids and Surfaces A: Physicochemical and Engineering Aspects 425, 42–50, 2013.

[16] Madiabu, M. J., Untung, J., Solihat, I., & Ichzan, A. M., Equilibrium and Kinetic Study of Removal Copper (II) from Aqueous Solution Using Chicken Eggshells: Low Cost Sorbent, Molekul, 16(1), 28–37, 2021

[17] Mashangwa, T. D., Tekere, M., & Sibanda, T., Determination of the efficacy of eggshell as a low–cost adsorbent for the treatment of metal laden effluents. International Journal of Environmental Research, 11(2), 175–188, 2017

[18] Mohammad, S. G., Ahmed, S. M., & El–Sayed, M. M., Removal of copper (II) ions by eco–friendly raw eggshells and nano–sized eggshells: a comparative study. Chemical Engineering Communications, 1–13, 2020

[19] Namasivayam. C and Kavitha. D., Removal of congo red from water by adsorption onto activated carbon prepared from coir pith, an agricultural solid waste, Dyes and Pigments. 54: 47–58, 2002

[20] Nõlvak, H., Truu, J., Limane, B., Truu, M., Cepurnieks, G., Bartkevičs, V., Juhanson, J. and Muter, O., Microbial community changes in TNT spiked soil bioremediation trial using biostimulation, phytoremediation and bioaugmentation. Journal of Environmental Engineering and Landscape Management, 21(3), pp.153–162, 2013

[21] Pandey, S. S., Singh, N. B., Shukla, S. P., & Tiwari, M., Removal of lead and copper from textile wastewater using egg shells. Iranian (Iranica) Journal of Energy & Environment, 8(3), 202–209, 2017

[22] Park, H.J., Jeong, S.W., Yang, J.K., Kim, B.G. and LEE, S.M., Removal of heavy metals using waste eggshell, Journal of Environmental Sciences, 19(12), pp.1436–1441, 2007

[23] Peigneux, A., Puentes–Pardo, J. D., Rodríguez–Navarro, A. B., Hincke, M. T., & Jimenez–Lopez, C., Development and characterization of magnetic eggshell membranes for lead removal from wastewater. Ecotoxicology and environmental safety, 192, 110307, 2020

[24] Pettinato, M., Chakraborty, S., Arafat, H.A. and Calabro, V., Eggshell: A green adsorbent for heavy metal removal in an MBR system, Ecotoxicology and environmental safety, 121, pp.57–62, 2015

[25] Prabhakaran, K., & George, B. K., Biogenic Magnetic Nano Hydroxyapatite: Sustainable Adsorbent for the Removal of Perchlorate from Water at Near–neutral pH. Journal of Environmental Chemical Engineering, 106316, 2021

[26] Rajendran, A. and Mansiya, C., Extraction of chromium from tannery effluents using waste egg shell material as an adsorbent, British Journal of Environment and Climate Change, 1(2), p.44, 2011

[27] Ren, J., Bopape, M. F., Setshedi, K., Kitinya, J. O., & Onyango, M. S., Sorption of Pb (II) and Cu (II) by Low–Cost magnetic eggshells–Fe3O4 powder, Chemical Industry and Chemical Engineering Quarterly, 18(2), 221–231, 2012

[28] Ren, Y., Zhang, M & Zhao, D., Synthesis and properties of magnetic Cu(II) ion imprinted composite adsorbent for selective removal of copper. Desalination 228(1), 135–149, 2008.

[29] Rohaizar, N.A.B., Hadi, N.B.A. and Sien, W.C., Removal of Cu (II) from water by adsorption on chicken eggshell. Environmental Pollution, 117(2), pp.50–57, 2013.

[30] Rohim, R., Ahmad, R., Ibrahim, N., Hamidin, N. & Abidin, C. Z. A., Characterization of calcium oxide catalyst from eggshell waste. Advances in Environmental Biology 8, 35–39

[31] Sasikala, V., Sruthi, T., & Vangalapati, M., Extraction and removal of nickel from battery waste, using nano sized activated carbon of Egg shell powder in a column, Materials Today: Proceedings, 44, 2296–2299, 2021

[32] Soares, M. A., Marto, S., Quina, M. J., Gando–Ferreira, L., & Quinta–Ferreira, R., Evaluation of eggshell–rich compost as biosorbent for removal of Pb (II) from aqueous solutions. Water, Air, & Soil Pollution, 227(5), 150, 2016

[33] Vijayaraghavan, K. and Joshi, U.M., Chicken eggshells remove Pb (II) ions from synthetic Wastewater, Environmental Engineering Science, 30(2), pp.67–73, 2013.

[1.]Mustefa JIBRIL, [1.]Messay TADESE, [2.]Eliyas Alemayehu TADESE

MODELLING AND SIMULATION OF VEHICLE WINDSHIELD WIPER SYSTEM USING H∞ LOOP SHAPING AND ROBUST POLE PLACEMENT CONTROLLERS

[1.]School of Electrical & Computer Engineering, Dire Dawa Institute of Technology, Dire Dawa, ETHIOPIA
[2.]Faculty of Electrical & Computer Engineering, Jimma Institute of Technology, Jimma, ETHIOPIA

Abstract: Vehicle windshield wiper system increases the driving safety by contributing a clear shot viewing to the driver. In this paper, modelling, designing and simulation of a vehicle windshield wiper system with robust control theory is done successfully. H∞ loop shaping and robust pole placement controllers are used to improve the wiping speed by tracking a reference speed signals. The reference speed signals used in this paper are step and sine wave signals. Comparison of the H∞ loop shaping and robust pole placement controllers based on the two reference signals is done and convincing results have been obtained. Finally the comparative results prove the effectiveness of the proposed H∞ Loop Shaping controller to improve the wiping mechanism for the given two reference signals.
Keywords: H∞ Loop Shaping, Robust Pole Placement, Windshield

INTRODUCTION

Driving a vehicle is complicated in harsh weather condition without using glass wiper system. Controlling the wiper speed based on the change in weather condition is one of the research area in automotive industries now a day. Recently, the wiper speed is adjusted manually controlled by the driver. Dc motors are used to drive the wiper system based on feed forward techniques. In this paper a separately excited Dc motor is designed and controlled using robust control method to improve the feed forward wiper system performance.

MATHEMATICAL MODELLING

Consider the electromechanical car mirror wiper system shown in Figure 1.
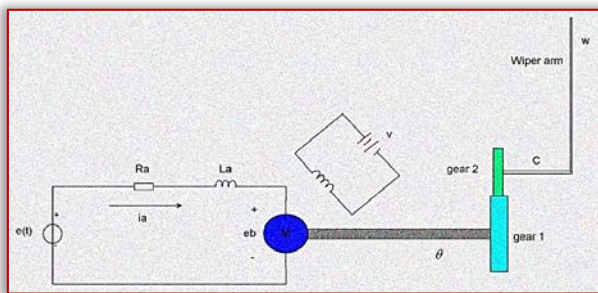

Figure 1. Electromechanical car mirror wiper system

The motor shown is a servomotor, a dc motor designed in particular for use in a control system. The operation of this device is as follows: A fixed voltage is carried out to the field winding. A voltage is implemented as an input to the servo motor and the angular position c of the wiper arm is the output of the device. The input voltage is implemented to the armature circuit of the dc motor. A constant voltage is carried out to the field winding. If an errors exists, the motor develops a torque to rotate the output load in the sort of way as to reduce the error to zero. For constant field current, the torque evolved by using the motor is

$$T = K_1 i_a \qquad (1)$$

where K1 is the motor torque constant and ia is the armature current.

When the armature is rotating, a voltage proportional to the fabricated from the flux and angular velocity is brought on within the armature. For a constant flux, the brought about voltage eb is without delay proportional to the angular velocity $\dfrac{d\theta}{dt}$ or

$$e_b = K_2 \frac{d\theta}{dt} \qquad (2)$$

Where eb is the back emf, $K2$ is the back emf constant of the motor, and θ is the angular displacement of the motor shaft. The speed of an armature-managed dc servomotor is managed via the armature voltage e(t). The differential equation for the armature circuit is

$$L_a \frac{di_a(t)}{dt} + R_a i_a(t) + e_b = e(t) \qquad (3)$$

Substituting Equation (2) in to Equation (3) yields:

$$L_a \frac{di_a(t)}{dt} + R_a i_a(t) + K_2 \frac{d\theta}{dt} = e(t) \qquad (4)$$

Taking the Laplace transform the equation will be

$$sL_a I_a(s) + R_a I_a(s) + sK_2 \Theta(s) = E(s) \qquad (5)$$

The equation for torque equilibrium is

$$J_0 \frac{d^2\theta}{dt^2} + b_0 \frac{d\theta}{dt} = T = K_1 i_a(t) \qquad (6)$$

Taking the Laplace transform the equation will be

$$s^2 J_0 \Theta(s) + b_0 \Theta(s) = K_1 I_a(s) \qquad (7)$$

Where J0 is the inertia of the combination of the motor, load, and gear train referred to the motor shaft and b0 is the viscous-friction coefficient of the aggregate of the motor, load, and gear train mentioned the motor shaft.

By eliminating $I_a(s)$ from Equations (5) and (7), we obtain

$$\frac{\Theta(s)}{E(s)} = \frac{K_1}{L_a J_0 s^3 + J_0 R_a s^2 + (L_a b_0 + K_2)s + b_0 R_a} \qquad (8)$$

We assume that the gear ratio of the gear train is such that the output shaft rotates n times for each revolution of the motor shaft. Thus,

$$C(s) = n\Theta(s) \qquad (9)$$

The wiper arm speed can be evaluated by using an integrator to the wiper arm position as

$$W(s) = \frac{1}{s} C(s) \qquad (10)$$

Substituting Equation (10) in to Equations (9) and to Equations (8) gives us the transfer function between the applied voltage and the wiper speed as

$$\frac{W(s)}{E(s)} = \frac{nK_1}{L_a J_0 s^4 + J_0 R_a s^3 + (L_a b_0 + K_2) s^2 + b_0 R_a s} \qquad (11)$$

The parameters of the system is shown in Table 1 below.

Table 2 Parameters of the system

No	Parameters	Symbol	Values
1	Inertia of the motor, load, and gear train	J_0	$10^{-2}\ Kg\ m^2$
2	Viscous–friction coefficient	b_0	$0.2\ N\ ms\ /\ rad$
3	Back emf constant	K_2	$0.8\ V\ s\ /\ rad$
4	Motor torque constant	K_1	$0.7\ N\ m\ /\ amp$
5	Motor Resistance	R_a	$1.2\ \Omega$
6	Motor Inductance	L_a	$3\times10^{-2}\ H$
7	Gear ratio	n	25

Numerically the transfer function is

$$G(s) = \frac{17500}{3s^4 + 12s^3 + 806s^2 + 240s}$$

The state space form will be

$$\dot{x} = \begin{pmatrix} -40 & -2686.7 & -800 & 0 \\ 1 & 0 & 0 & 0 \\ 0 & 1 & 0 & 0 \\ 0 & 0 & 1 & 0 \end{pmatrix} x + \begin{pmatrix} 1 \\ 0 \\ 0 \\ 0 \end{pmatrix} u$$

$$y = \begin{pmatrix} 0 & 0 & 0 & 58333 \end{pmatrix}$$

PROPOSED CONTROLLERS DESIGN

— H infinity Loop shaping using Glover-McFarlane method Controller Design

The block diagram of the car mirror wiper system with H infinity Loop shaping design using
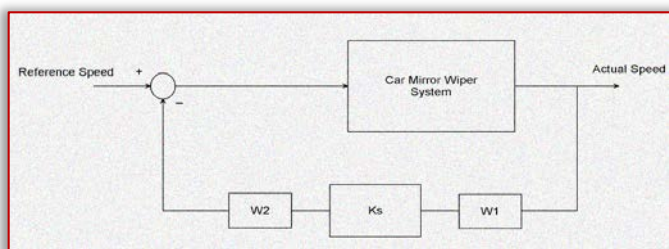Glover-McFarlane method is shown in Figure 2 below

Figure 2. Car mirror wiper system with H infinity Loop shaping design using Glover-McFarlane method

A feedback controller, KS, is synthesized that robustly stabilizes the normalized left cop rime factorization of G, with a balance margin. It may be proven that the frequency response of KsW2GW1 will be much like that of W2GW1. On the other hand, if the viable gain is simply too large, this will probable indicate an overdesigned case in appreciate of the robustness, which means that the performance of the system can also in all likelihood be progressed by the usage of a larger in computing Ks. The final feedback controller, Kfinal, is then constructed with the aid of combining the H infinity controller Ks, with the weighting functions W1 and W2 such that

$$K_{final} = W_1 K_s W_2 \qquad (12)$$

We choose a pre compensator, W1, and a post compensator, W2 transfer functions as

$$W_1 = \frac{1}{s+24} \qquad W_2 = \frac{1}{s+13}$$

The H infinity controller transfer function is

$$K_s = \frac{-1.419s^5 - 109.3s^4 - 6357s^3 - 1.6e05s^2 - 1.235e06s - 3.84e05}{s^7 + 114.3s^6 + 7678s^5 + 3.05e05s^4 + 6.536e06s^3 + 6.968e07s^2 + 3.027e08s + 1.7e08}$$

— Robust Pole Placement Controller Design

In a typical feedback manage system, the output, y, is fed back to the summing junction. It is now that the topology of the layout changes. Instead of feeding again y, what if we feed back all of the state variables? If each state variable is fed back to the manipulated, u, through a gain, ki, there might be n gains, ki that would be adjusted to yield the required closed-loop pole values. The feedback via the profits, ki, is represented by way of the feedback vector -K.

The block diagram of the car mirror wiper system with robust pole placement method is shown in Figure 3.
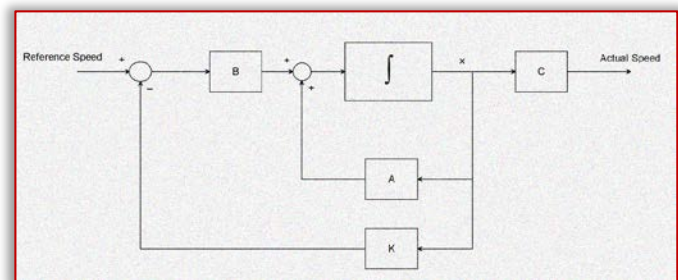
Figure 3. Car mirror wiper system with robust pole placement method

The state equations for the closed-loop system of Figure 3 can be written by inspection as

$$\dot{x} = Ax + Bu = Ax + B(-Kx) = (A - BK)x \qquad (13)$$

$$y = Cx$$

The poles for this system is chosen as

$$P = \begin{bmatrix} -1-2i, -1+2i, 4-3i, 4+3i \end{bmatrix}$$

Solving using Matlab the robust pole placement algorithm gain will be

$$K = \begin{bmatrix} -46 & -26727 & -790 & 125 \end{bmatrix}$$

RESULT AND DISCUSSION

In this section, the Simulink model design and simulation of the vehicle windshield wiper system using H infinity loop shaping and robust pole placement controllers by comparing

the two proposed controllers for tracking the step and sine wave speed references.

— **Comparison of the proposed controllers for tracking the step speed reference**

The Simulink model of the vehicle windshield wiper system using H infinity loop shaping and robust pole placement controllers for tracking the step speed reference is shown in Figure 4 below.

Figure 4. Simulink model of the vehicle windshield wiper system using H infinity Loop Shaping and Robust Pole Placement Controllers for tracking the step speed reference

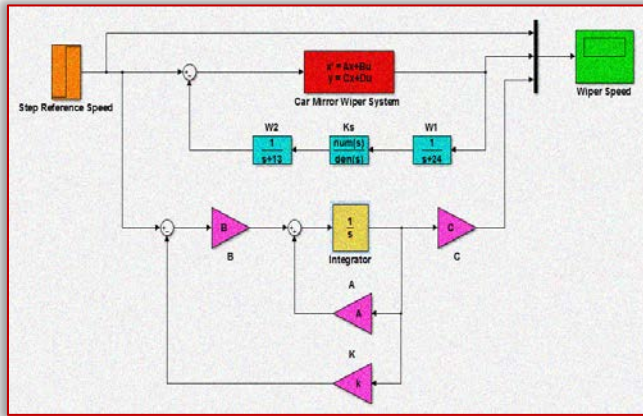The wiper system performance for the proposed controllers using a step reference (step change from 0 to 6 m/s) of the wiper speed simulation is shown in Figure 5 below.
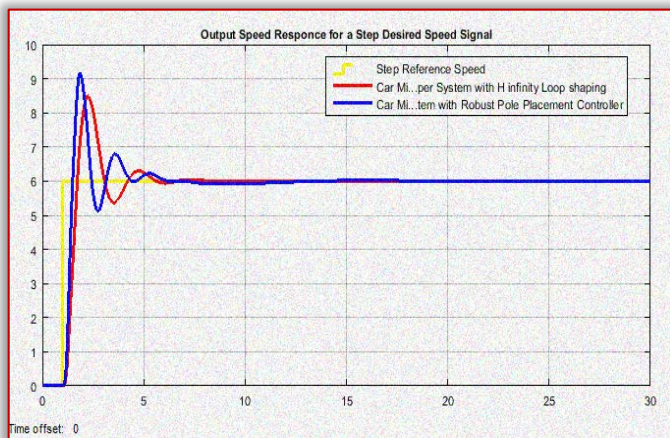

Figure 5. Simulation result for a step reference input

The data of the rise time, percentage overshoot, settling time and peak value is shown in Table 1.

Table 1. Step response data

No	Performance Data	Robust Pole Placement	H infinity Loop Shaping
1	Rise time	1.2 sec	1.22 sec
2	Per. overshoot	53.4 %	40 %
3	Settling time	8 sec	6 sec
4	Peak value	9.2 m	8.4 m

— **Comparison of the proposed controllers for tracking the Sine Wave speed reference**

The Simulink model of the vehicle windshield wiper system using H infinity loop shaping and robust pole placement controllers for tracking the sine wave speed reference is shown in Figure 6 below.
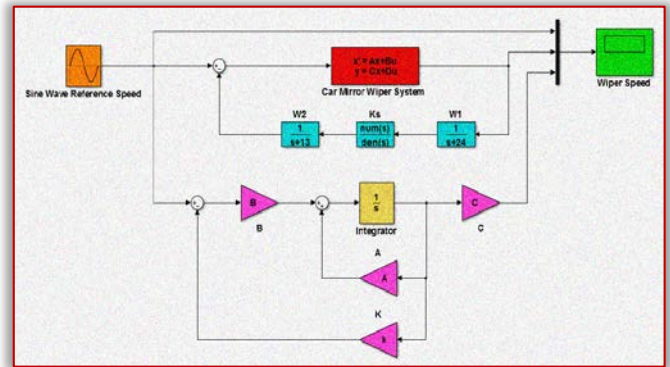

Figure 6. Simulink model of the vehicle windshield wiper system using H infinity loop shaping and robust pole placement controllers for tracking the sine speed reference

The wiper system performance for the proposed controllers using a sine wave reference (wiper moving in the forward and reverse with 6 m/s) of the wiper speed simulation is shown in Figure 7 below.
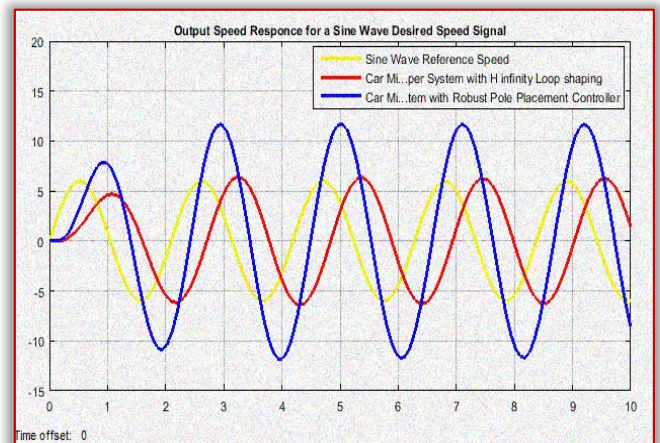
Figure 7. Simulation result for a sine wave reference input

The simulation result shows that the vehicle windshield wiper system with H infinity loop shaping controller track the reference speed better than the vehicle windshield wiper system with robust pole placement controller.

CONCLUSION

The vehicle windshield wiper system is designed and simulated based on the given control signals using Matlab/Simulink and a promising result have been analyzed. The performance of the vehicle windshield wiper system is tested for wiping speed regulation using track a signal method.

Comparison of the vehicle windshield wiper system with H infinity loop shaping and robust pole placement controllers is done for a step and sine wave reference speed signals and the vehicle windshield wiper system with H infinity loop shaping controller shows a good result in improving the wiping mechanism in almost the all performance measures taken.

Finally the comparative results prove the effectiveness of the proposed H ∞ Loop Shaping controller to improve the wiping mechanism for the given two reference signals.

References

[1] Vijay S. et al. "Automatic Rain Operated Wiper and Headlight Dim and Bright Controller" International Journal of Innovative Research in Science, Engineering and Technology, Vol. 9, Issue 2, February 2020.

[2] Punam W. et al. "An Automated Wiper System for Vehicles" International Journal for Research in Applied Science & Engineering Technology (IJRASET), Volume 7 Issue IV, Apr 2019.

[3] Matthew B. et al. "Windshield Wipers on Connected Vehicles Produce High Accuracy Rainfall Maps" Journal of Scientific Reports, Vol. 9, 2019.

[4] Varshitha P J et al. "Improvement of Auto Wiper Controller According to Rain Force" International Journal of Advanced Research in Electrical, Electronics and Instrumentation Engineering, Vol. 7, Issue 5, May 2018.

[5] Prajakta C. et al. "Automatic Rain Operated Wiper and Dimmer for Vehicle" International Research Journal of Engineering and Technology (IRJET), Volume: 03 Issue: 04, 2016.

[6] Lubna A. et al."Design and Implementation of a Reconfigurable Automatic Rain Sensitive Windshield Wiper" International Journal of Engineering & Technology Science, Vol. 8, Issue 2, pp. 73–82, 2015.

[7] Mark D. et al. "Dynamic Modelling and Experimental Validation of an Automotive Windshield Wiper System for Hardware in the Loop Simulation" Journal of Systems Science & Control Engineering, Vol. 3, Issue 1, 2015.

[8] Fazle E. et al. "Intelligent Windshield for Automotive" Conference: International Conference on Computer & Information Technology (ICCIT), Vol. 17, Issue. 2, 2014.

[1.]Olakunle ADEWEMIMO, [1.]Olumuyiwa Idowu OJO, [1.]Toyin Peter ABEGUNRIN, [1.]Jeremiah Oludele OJEDIRAN

RIVER ONA DISCHARGE MODELING USING GIS AND LOGARITHMIC TRANSFORMATION MODEL

[1.] Department of Agricultural Engineering, Ladoke Akintola University of Technology, PMB 4000, Ogbomoso, NIGERIA

Abstract: Climate unpredictability and change in climatic parameters have direct influence on environment and human existence. A negative change in the climate, always have its corresponding dysfunctional impacts on man and the ecosystem globally or locally leading to flooding, poor agricultural yields, famine, and even death at some stages. Knowledge and information on the climatic variation parameters in an environment is very vital for environmental study assessment and proper planning. Therefore, evaluating the effect of weather variability on discharge of Ona River in Ibadan cannot be under–estimated. A methodology to evaluate river discharge exclusively from remotely sensed data was developed. Water surface width and maximum channel width measured from satellite images of Ona River was coupled with channel slope data obtained from topographic maps created using Shuttle Radar Topography Mission (SRTM) were used to estimate the discharge. Landsat images were acquired for the years 1990, 2000 and 2015, which were used to determine anthropogenic activities. SRTM and Quick bird were used to model environmental changes and effects on the discharge of Ona River. The weather change effects on water discharge from Ona River in Ibadan was examined in three phases; site observation and data collection which was done in 2015 to get weather and discharge data of Ona River for each month, model simulation of temperature to determine discharge was done using regression model analysis. The rainfall distribution is being revealed to have strong effect on the discharge rate ($R^2 = 0.77$) and that of temperature on discharge rate of Ona River ($R^2 = 0.80$). In 2015, the influence of rainfall on discharge rate was stronger ($R^2 = 0.85$) while the discharge was 2.88m^3/s. The monthly temperature–discharge gives a negative relationship ($R^2 = 0.55$). There is strong negative relationship between vegetation and rainfall, −0.7. It has been projected that in 2028, the discharge rate will be reduced to about 2.17 m^3/s. There is evidence of dynamic responses of rivers to precipitation rate, which implied a significant response between rainfall and discharge and the negative effect of anthropogenic activities on rivers. This result can be used to predict the discharge of rivers given weather and environmental factors.
Keywords: River Ona; discharge; GIS; logarithmic; model

INTRODUCTION

Climate change has been discovered to be one of the biggest threats to humanity, human security in addition to producing adverse environmental conditions such as rising sea level, drought, crop failure, degradation of water/air quality, heat waves (Emmanuel et al., 2015). Climate change and its effect on river discharges has been studied in different ways, ranging from different spatial scales to time series of diversified lengths in many periods. Modeling climate change and its effect on river discharge is usually achieved either by collecting climate data such as temperature and rainfall in hydrological models or by varying climate data series with expected changes (Singh and Bengtsson, 2004). Change in weather data and weather uncertainties have direct effect on environment and human existence. A negative change in the state of weather causes a retrospective effect on man and the ecosystem both locally and globally. Weather is the condition or state of an atmosphere of a particular place at a given time (Ayoade, 2004). It may also be said to be the aspects of the atmospheric state which is visible and experienced and which affect human activities. The weather conditions of any particular can be explained and understood with the aid of some meteorological elements such as precipitation, temperature, winds, pressure, sky state and humidity, which are factors triggers and influence the process of the atmosphere (Gbadegesin et al., 2020). Climate change is an overtime change observed from either natural variability or human activities according to the United Nations of Intergovernmental Panel on Climate Change (IPCC, 2011). While weather on the other hand is the day–to–day condition of the atmosphere, and its variation over minutes to weeks,

climate can be expressed by statistical weather analysis or information that describes the abnormalities of weather for a specified interval at a given location. The weather of a certain location is usually averaged over a 30–year period to determine its climate (Gutro, 2005). Climate and have different implications on the economy because of the different phenomena they represent (Fisher et al., 2012). According to IPCC (2011), assets and people in most countries are increasingly vulnerable to extreme weather. It was observed that the nature these extreme conditions have changed over the past 50 years, and may likely remain as this century progresses. However, there is uncertainty on exactly how the frequency and strength of extreme weather events might change. Adaptation measures taken in the near future therefore need to be resilient to a broad range of future climates (Howden, 2011).

In a recent assessment, IPCC (2011) mentioned that there is possibility that Africa will be warm during this century, noting that the drier subtropical regions will be warmer than the moist tropics. There is likelihood for the decrease in annual rainfall throughout most of the region, except the eastern Africa, where annual rainfall is projected to increase. These physical changes in the environment are expected to have devastating effect on agricultural production, such as millet and maize, which are staple foods. In addition, acute soil erosion and land degradation are also effect of land climate change to be considered (Oyiga et al., 2011). The effect of climate change may be weaker or stronger, permanent or temporary, favorable or adverse, harmful, primary (direct) or secondary (indirect) impact on soil processes. Among these processes soil moisture regime plays a distinguished role

(Adeoye et al., 2018) as it influences the amount of water supply in plants, the air and heat regimes, biological activity and plant nutrient status of soil (Montgomery, 2007).The erosion process, sediment delivery and sediment transportation are important components and measures of the functioning of the earth system. Erosion and sediment redistribution processes are the primary drivers of landscape development and vital in soil development (Philippe et al., 2014; Ojo, et al., 2018). Furthermore, high sediment loads can result in pollution and habitat degradation in river system (Islam and Tanaka, 2014). For instance, reservoir capacity of Awara dam has greatly reduced due to continuous sedimentation and siltation. There have been struggles in most countries because of water stress emanating from water borne sewerage, irrigation demands and industrial pollution. These pressures will be significantly exacerbated by climate change, which in reduced rainfall and increasing temperatures for many regions, also reducing the quantity of water available for drinking, household chores, agriculture and industry purposes. The more the need for water due to climate change, the more effective balancing water demands will become so important, most especially in areas where there are pressing demands for industrial uses over other uses like drinking supplies. High temperatures affect the quantity of runoff that negatively, hereby, reducing the quantity of groundwater also which is the major source of water supply in some parts of the nation. Similarly, reduced rainfall, especially in the north would further compound the inability of the zone to meet people's water demand (Idogho et al., 2014). In Africa, several factors are responsible for the variability in weather, one of it is deforestation. In addition, the agriculture and industry that replace the forests often cause an extra problem by producing carbon emissions of their own (Chakravarty et al., 2012). Another factor is the growing population, as the population grows, there are more people who need food, livestock and energy, and this increased demand leads to increased emissions (McMichael et al., 2007). According to Heinrich (2009) the northern part of Nigeria may increase its dependence on ground water sources because of low rate of precipitation experienced unlike the south–western Nigeria.

APPLICATION OF GEOGRAPHICAL INFORMATION SYSTEM (GIS) TO WATER RESOURCES

GIS is a very important tool used to address various water resources related issues like the quality of water, ground water contamination, ground water movement, river restoration, flood prediction and management on a local, regional, national or even global scale (ESRI, 2012). GIS can analyze the current situation, model and stimulate different scenarios for predicting the future, project new information to enhance decision–making and watershed management (Yoo et. al., 2004). It can also be employed in making a suitable decision in critical scenario, evaluating the effects of land use/cover, soil type, vegetation, topography, water quality and geology. Hydrology is a common field that recently employed GIS and Remote Sensing (RS) to tackle different issues within the field. There is mainly as a result of its integration can help the hydrological cycle and all related processes. In addition, it could enhance the possibility of a three dimensional approach for distributed models. GIS has a great ability to integrate data from multiple sources as long as they all have the same spatial reference. For instance, it can combine data from sources such as boreholes and wells, subsurface isopach maps, structure contour, surface geology maps, and satellite imagery. This ability allows all of these data to be used simultaneously to develop a more comprehensive model. Such models could assist geographers to gain a deeper understanding of the movement of different surface (or subsurface) waters and their interactions (Ziliaskopoulos and Waller, 2000; Olaniyan, et al., 2015).

GIS system uses data acquired from Remote Sensing and other sources to build new geo–referenced databases in specific referable forms. Within the map conversion process, some cells might represent pits or holes. These cells should be removed before running the model otherwise; water would accumulate in these cells when drainage patterns are being extracted. The whole map forms a stream network, which will define the flow direction and ultimately determine the outlets of the basin. Simulated runoff can be compared to the measured runoff at basin level for return periods of 10 and 50 years. However, the results often indicate that the generated model is not biased in over–predicting /under–predicting the runoff. Baiyinbaoligao et. al. (2011) and Olaniyan, et al., (2015) employed GIS for modeling the rainfall–runoff process in the Kuronagi River based on two rainfall stations. Since rainfall–runoff could be modeled based on different methods, they engaged the distributed Kinematic Wave hydrological model to calculate the two rainfall–runoff events in 2005 and 2006. They used ESRI's Arc View version 8.3 and its Spatial Analyst extension module to carry out the flow direction, flow accumulation, and stream network as features. A 50 m DEM spatial data issued by Japan Geographical Survey Institute in 1996 was used to produce the digital basin of the Kuronagi River (Baiyinbaoligao et. al., 2011).The approaches vary from a simple sensitivity analysis of hydrology to the changes observed in climate inputs to the study of palaeo climatic data, spatial shifting of current climates towards polar region. Because of its physically based nature, the latter approach is arguably the most attractive. Therefore, this study aimed at determining the weather change effects on water discharge from Ona River in Ibadan in three phases; site observation and data collection between 1990 and 2000, predicted for some years and resulted into maps.

METHODOLOGY

The method used for this work involved GIS tools in the analysis and evaluation of rainfall and temperature effect on discharge of Ona River. In–situ analysis was done, alongside extraction of images through Quick bird, Landsat and DEM of the Ibadan for previous years before 2015.

─ The Study Area

Spatially, the study area has a tropical wet and dry climate and is strongly influenced by the West African monsoon climate, marked by a distinct seasonal shift in the wind pattern (Odewunmi et al, 2013). Ona River is one of the major rivers in Ibadan, South Western, Nigeria and lies between Latitude 7° 15′ 49″ and 7° 45′ 21″ N longitude 3° 57′ 58″ and 4° 08′ 20″ E (Andem, et. al., 2012; Bello et al., 2019). The river has a length of about 8 km and an area of about 28.5 Km² and it flows through the low–density western part of Ibadan. The river flows in a north–south direction from its source at Ido Local Government Area where it is dammed and flows through Apata Ganga (Ibadan South–West Local Government Area) to Oluyole Local Government (Andem, et. al., 2012). Figure 1 depicts the study area in relation to Oyo State, Nigeria.
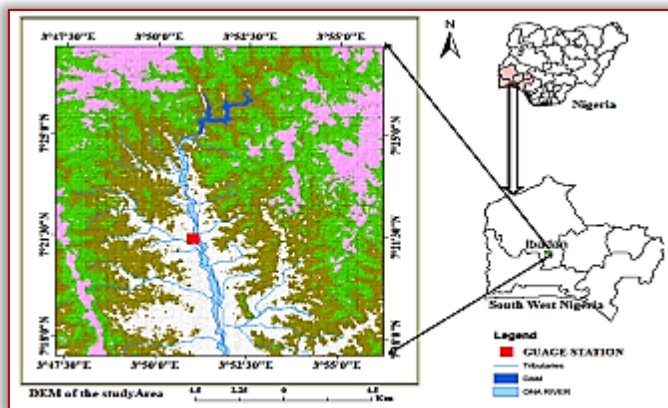

Figure 1: Map of Study Area in relation to Oyo State, Nigeria
(adapted from Andem, et. al., 2012)

─ Data Acquisition

The data used for this study are temperature, rainfall and discharge data between 1990–1999 and were obtained from meteorological station of Forestry Research Institute of Nigeria (FRIN), Ibadan office. The discharge data for 1990 to 1999 were obtained from Eleyele Dam gauge station. The River Discharge rate of 10 years (1990 to 1999) were used due to its availability, while an in–situ discharge data of 2015 were collected at a distinct point along the river course. Satellite images; Landsat, Shuttle Radar Topography Mission (STRM), and Quick bird were obtained and utilized to model environmental changes and their effects on the discharge of Ona River. The Landsat image was used to determine anthropogenic activities within the study area. The Digital Elevation Model (DEM) was used to show the slope and flow direction of the river and its distributaries, while the Quick bird image was use to delineate the study area.

─ Methods

The methods used to include data preparation, image processing, mapping, and modeling as outlined by Otieno et al., (2013).

─ Data preparation

Ona River basin was generated using Landsat images covered by path 191 and row 55. The providers; NASA have already rectified these satellite images used for this study, while the downloaded DEM and Landsat images of the study area were clipped into a shape file.

─ Image Processing

To process the images, the spectral respond pattern was first developed for easy identification of remotely sensed features using IDRISI 17.0 software. A simultaneous query of all the images included in a raster image group file, in order to obtain quantitative information from images, digital number was converted to physical quantities, radiance and brightness temperature.

$$L\lambda = \left(\frac{(L_{MAX}\lambda - L_{MIN}\lambda)}{Q_{CAL}\lambda}\right)Q_{CAL} + L_{MIN}\lambda \qquad (1)$$

where;

$L\lambda$ = Spectral radiance at the sensor's aperture [W/ (m²sr µm)]

The above expression does not consider the atmospheric effects, therefore there was need to convert images from radiance to reflectance measures, using equation 2 (Gyanesh et al, 2009).

$$\rho\lambda = \frac{\pi.TOAr.d^2}{E_{SUN}\lambda.Cos\theta_{sz}} \qquad (2)$$

where;

$\rho\lambda$ = Planetary TOA reflectance (unit less),

π = Mathematical constant approximately equal to 3.14159 (unit less),

$L\lambda$ = Spectral radiance at the sensors aperture [w/ (m²sr µm)],

d^2 = The earth–Sun distance (Astronomical unit),

E_{SUN} = Mean exoatmospheric solar irradiance [w/ (m²sr µm)],

θ_{SZ} = the solar zenith angle (degree),

The cosine of this angle is equal to the sine of the sun elevation $\theta_{SE,}$

Therefore, $\theta_{SZ} = 90 - \theta_{SE}$.

─ Prediction of Discharge using Logarithmic Transformation Model

To project temperature into the future year 2028, logarithmic transformation model of Brian Field et al, 1993 was used:

$$\log_e P((t-n)) = \log_e B + n\log(1+r) \qquad (3)$$

To project discharge into the future using equation 3.4 (Brian et al, 1993).

$$P_{(t-n)} = (1+r)^n P_{(t)} \qquad (4)$$

where;

$P_{(t-n)}$ = the discharge to be forecast at time t+n

$P_{(t)}$ = the discharge at time t – the base year,

r = annual growth rate

The ratio K was calculated using equation 5

$$k = \frac{P_{(t-n)}}{P_t} \qquad (5)$$

The mean annual rate value r is 0.00425 using the equation 3.6

$$r = antilog\{\frac{\log P_{(t+1)} - \log P_{(t)}}{n}\} - 1 \qquad (6)$$

RESULTS AND DISCUSSION

The discharge in–situ measurement of River–Ona in 2015 is as shown in Table 1. The discharge between January to March and October to December are relatively low compared to the months, but January and February remained constant because the depth is also constant due to lack or inadequate

precipitation. It was observed that the discharge reduced in August, which is meant to be one of the peak periods, this is traceable to seize in rain during the period but the discharge increased in September as the discharge measurement were affected by the depth, width area and distance. The time depends on the depth since the width (8m) and distance (3m) remained constant, the more the depth, the lesser time taken for the float to get to the 3m mark. The average discharge data and average weather data between 1990 and 1999 as displayed in Table 2. The rate of discharge measured in 1996 and 1999 were the highest due to the high rainfall observed in those years, 1990 was a drought year and the corresponding discharge (0.59) was low also, also 1998 whose discharge was 2.05 m³/s. There is an increase in the discharge as 2015 which was collected as 2.88 m³/s.

Table 1: Discharge in–situ measurement of River–Ona (2015)

Date	Depth (m)	Width (m)	Area (m²)	Distance (m)	Time (s)	Velocity(m/s)	Discharge (m³/s)
Jan	1.2	8	9.6	3	12.1	0.24	2.30
Feb	1.2	8	9.6	3	12.1	0.24	2.30
Mar	1.25	8	10	3	11.2	0.26	2.60
Apr	1.28	8	10.24	3	10.8	0.28	2.84
May	1.4	8	11.2	3	9.42	0.318	3.56
Jun	1.5	8	12	3	9.12	0.33	3.96
Jul	1.59	8	12.72	3	9.0	0.33	4.239
Aug	1.48	8	11.84	3	10.92	0.274	3.253
Sept	1.52	8	12.16	3	9.12	0.33	4.013
Oct	1.11	8	8.88	3	12.46	0.241	2.138
Nov	0.96	8	7.68	3	13.1	0.229	1.759
Dec	0.92	8	7.36	3	13.7	0.219	1.612

Table 2: Discharge and Weather Data of the study area 1990 to 1999

Date	Discharge (m³/s)	Temperature (°C)	Rainfall (mm)
1990	0.59	24.33	12.25
1991	0.71	23.12	398.77
1992	0.48	24.75	97.83
1993	0.48	24.59	131.23
1994	0.39	25.90	91.3
1995	0.78	22.59	422.6
1996	0.83	22.32	525.5
1997	0.77	22.17	413.33
1998	0.38	25.17	90.68
1999	2.05	21.83	556.71

— Modeling the Relationship between the Weather Elements and Discharge

To model the relationship between discharge and weather elements like temperature and rainfall, the variables were regressed and the discharge served as the dependent variable all through. The R^2 values of the regressions in Figures 2, 3, 4, 5 and 6 show good fits. 77% of the variation in discharge of Ona River is explained by the independent variable; rainfall as shown in Figure 2.
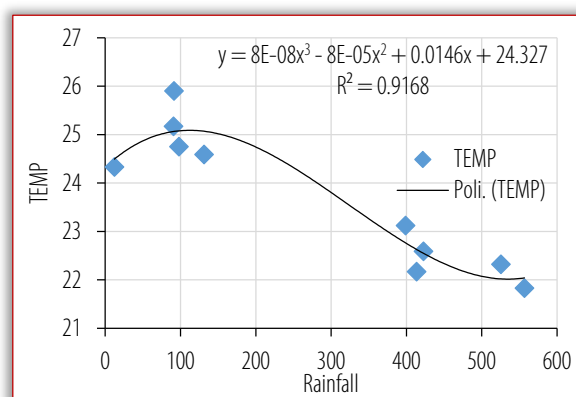

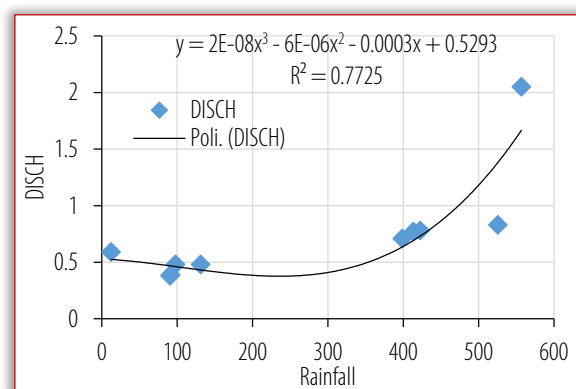Figure 2: Temperature and rainfall Relationship

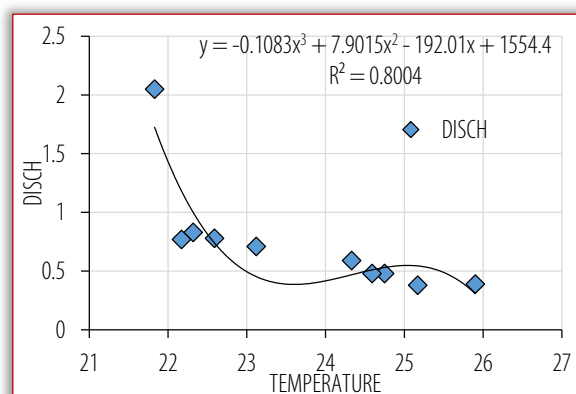Figure 3: Rainfall and Discharge Relationship
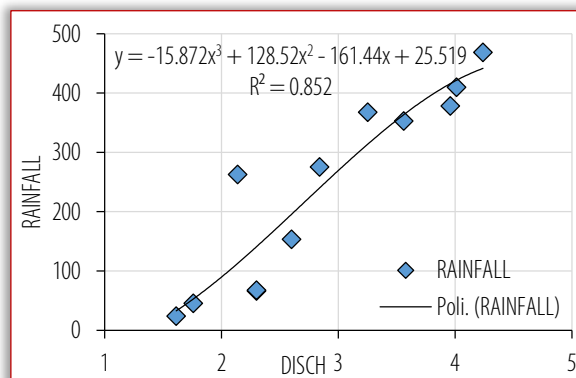

Figure 4: Temperature and Discharge Relationship

Figure 5: 2015 Monthly Rainfall–Discharges

The effect of temperature as displayed in Figure 3 is stronger with about a negative value of 80%. Result also shows that a

strong negative relationship exists between temperature and rainfall distribution.
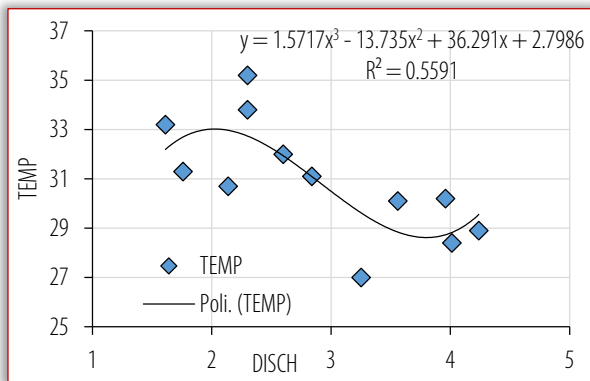

Figure 6: 2015 Twelve Months Temperature–Discharge Observations

The monthly discharge and weather parameters of 2015 regressions give strong positive relationship between rainfall and discharge, but negative relationship between temperature and discharge.

Temperature and rainfall relationship is $y = 8E{-}08x^3 - 8E{-}05x^2 + 0.0146x + 24.327$ with $R^2 = 0.9168$ as shown in Figure 2, while Figure 3 show the rainfall and discharge relationship of $y = 2E{-}08x^3 - 6E{-}06x^2 - 0.0003x + 0.5293$ with $R^2 = 0.7725$. Temperature and discharge relationship yield $y = -0.1083x^3 + 7.9015x^2 - 192.01x + 1554.4$ with $R^2 = 0.8004$ as displayed in Figure 5, while the 2015 Monthly Rainfall–Discharge gave $y = -0.1083x^3 + 7.9015x^2 - 192.01x + 1554.4$ with $R^2 = 0.8004$. 2015 Twelve Months Temperature–Discharge observations gave $y = 1.5717x3 - 13.735x2 + 36.291x + 2.7986$ with $R^2 = 0.5591$ as shown in Figure 6.

⎯ Significance F–value

In this study, the Significance F–values are 0.018697 and 0.019802 between temperature and discharge and between rainfall and discharge, respectively. Significance F shows that the results are reliable (statistically significant) since these values are less than 0.05, therefore result can be said to be good enough.

⎯ Projection of Discharge using Geometric Trend Model

The projected temperature for 2028 is as shown in the Table 3. Applying equations 4, 5 and 6, the temperature was predicted to rise up to about 35.02°C, substituting this in equation 7 as **t** it was possible to determine the future trend of Ona River discharge for another 13 years. The projection gives a discharge value of 2.17m³/s by year 2028. There is a decrease when compared with the 2015 discharge; this may not be unconnected to loss of water from the river due to higher evaporation rate that might be caused by expected increased temperature.

$$Q = 11.668 - 0.2713t \qquad (7)$$

Table 3: Projected Temperature for 2028

Date	Mean temperature	Ratio(k)	Annual Rate (r)
1989	23.33	1.3	0.002
2002	30.22	1.07	0.006
2015	32.40	1.08	0.005
2028	35.02	–	–

DISCUSSION

The effects of weather variation are obvious on River Ona and its tributaries are because of increase in the amount of rainfall and temperature thus resulting to higher annual river discharges over the years. Therefore, gradual decrease in rainfall over the years consequently leads to decrease in the mean annual river discharges, this implies that river discharges increase because of wetter climate (higher temperature and higher rainfall amount).

These results correspond with the results by Arnell (2002), Singh& Bengtsson (2004) and Olaniyan et al., (2015) stating that increment of precipitation is primarily due to discharge–runoff rather than evaporation, because the amount of evaporation is nearly constant due to the already saturated land surface condition.

The study by Arnell (2002) and Adewale et al., (2010) concluded that the effects of climate change on river discharges in the scenario period would be influenced by changes in the use of water affecting the hydrological system. This will probably increase the actual evapotranspiration, Ea and reduce river discharges from the affected areas (Brooks, 1983; Liu et al., 2005; Bello et al., 2019).

The rate of annual discharges will increase the width and depth of natural watercourses by increasing erosion according to regime theory (Ojo, et al., 2018). It could also lead to the damage the drainage networks. It could also increase the fluxes of nonpoint source pollution and sediment to the river channel and this can increase flood frequency and flood risk.

Over the years, discharge–runoff severity increases and the drainage network in River Ona is badly affected, as increase discharge will cause more floods, which would have some effect on farming along the riverbanks. Mean annual river discharge increased because of higher intensity of rainwater to the river (Otieno, et al., 2013); therefore, there is need for preventive measures to be taken to reduce flood risk.

CONCLUSIONS

This study evaluated the effect of temperature and rainfall variation on the flow of Ona River using Remote Sensing and Geographical Information System (GIS) techniques. The results revealed that the dynamic response of rivers to precipitation rate is higher during the raining season, as there is a significant relationship between rainfall and river discharge, thus affecting the discharge rate of the river. Continous data collection of discharge, temperature, rainfall, and other parameters should be carried out by all hydrological stations in order to help environmental scientists and policy makers to regulate such activities, which could affect the river course. Further studies can be carried out to establish the impact of extreme weather variations on the river discharge. The findings from this study used to predict the discharge of a particular river given the weather and environmental factors.

References

[1] Adeoye, D. O., Ajibola, E. & Ojo, O. I. (2018). Land Use Dynamics Analysis for Sustainable Development Planning Using Geo–Informatics Techniques: Case Study of Ogbomoso Town, Nigeria. LAUTECH Journal of Engineering and Technology, 12 (2), 136–148.

[2] Adewale, P.O, Sangodoyin, A.Y. & Adamowski, J, F. (2010). Use of Hec–Ras for Flood Routing in the Ogunpa River in Nigeria. Journal of Environmental Hydrology, Paper 25, Volume 18, 2010.

[3] Andem, A. B., Udofia, U., Okorafor, K. A., Okete, J. A. & Ugwumba, A.A.A, (2012). A study on some physical and chemical characteristics of Ona River, Apata, Ibadan South–west, Oyo State, Nigeria. European Journal of Zoological Research, 1 (2):37–46. (http: //scholarsresearchlibrary. com/archive.html).

[4] Arnell, N.W. (2002). The effect of climate change on hydrological regimes in Europe: a continental perspective. Global Environmental Change–Human and Policy Dimensions 9 (1): 5–23.

[5] Ayoade, J.O. (2004) Introduction to Climatology for the Tropics. 2nd Edition, Spectrum Books Limited, Ibadan, Nigeria.

[6] Baiyinbaoligao, D., W. & Xiang Y. L. (2011). Application of ArcGIS in the calculation of basins rainfall runoff, Procedia Environmental Sciences, 10: 1980–1984.

[7] Bello, H. O., Ojo, O. I., & Gbadegesin, A. S. (2019). Land Use/land cover change analysis using Markov–Based model for Eleyele Reservoir. Journal of Applied Sciences and Environmental Management, 22 (12): 1917–1924.

[8] Blench, T. (1966). Mobile–Bed Fluviology. University of Alberta Press, Edmonton, Canada.

[9] Chakravarty, S., Puri, A. & Shukla, G. 2015. Climate change vis–à–vis agriculture: Indian and global view–implications, abatement, adaptation and tradeoff. In: Climate Change Effect on Crop Productivity, eds. Sengar, R. S. and Sengar, K. CRC Press. Pp 1–88.

[10] Di Gregorio A. (2005) Land cover classification system: Classification concepts and user manual. FAO, Rome. Food and Agriculture Organization. Global Forest Resources Assessment 2005: Progress towards Sustainable Forest Management. United Nations. FAO Forestry Paper 147.

[11] Emmanuel, M. O. & Ani, C. (2015). The African State and Environmental Management: A Review of Climate and Human Security. Open Journal of Political Science, 5: 109–114.

[12] ESRI Personal Geodatabase. Map Server. Archived from the original on 2012–12–18. Retrieved 2019–02–06.

[13] Field, D. J., Hayes, A. & Hess, R. F. (1993). Contour integration by the human visual system: Evidence for a local "association field". Vision Research, 33, 173–193.

[14] Fisher, A., Hanemann, W.M., Roberts, M.J. & Schlenker, W. (2012). The Economic Impacts of Climate Change: Evidence from Agricultural Output and Random Fluctuations in Weather: Comment Forthcoming, American Economic Review.

[15] Gbadegesin, A. S., Bello, H. O. & Ojo O. I. (2020). The Hydraulically Assisted Bathymetry Modeling Of Effect Of Weather On Reservoir Water Level, Acta Technica Corviniensis–Bulletin of Engineering, 13 (1), 127–132

[16] Gutro, R. (2005). What is the Difference between Weather and Climate [Online].NASA Goddard Space Flight Center. Accessed on the 22nd January 2019 from: http://www.nasa.gov/mission_pages/noaan/climate

[17] Gyanesh, C., Brian, L. M., & Dennis, L. H. (2009). Summary of current radiometric calibration coefficients for Landsat MSS, TM, ETM+, and EO–1 ALI sensors. Remote Sensing of Environment, 113, 893–903.

[18] Heinrich, B. S. (2009). Effect of Global Warming on Rainfall and Agriculture.

[19] Howden, M. (2011). The Role of Science in Adapting to Climate Change: The Australian Experience so far. Vitro Cellular & Developmental Biology–Animal 46(35–35). Accessed on 22nd January 2019 from: http://www.nasa.gov/mission_pages/noaan/climate/climate_weather.html

[20] Idogho, P.O., Olotu, Y. & Alimi, L.O., (2014). Climate change on Discharge and Sedimentation of River Awara, Nigeria. Adv Agric. Bio, 2 (1): 25–32.

[21] Intergovernmental Panel on Climate Change (IPCC), (2001). "Working Group I Third Assessment Report." Cambridge University Press. Cambridge, UK. 881 pp.

[22] Islam M. D. & Tanaka M., (2004). Impacts of pollution on coastal and marine ecosystems including coastal and marine fisheries and approach for management: a review and synthesis, Marine Pollution Bulletin, 48: 624–649,

[23] Liu, B. Z., Yang, D. Q., Ye, B. S., & Berezovskaya, S. (2005). Long–term open–water season stream temperature variations and changes over Lena River Basin in Siberia. Global and Planetary Change 48:96–111.

[24] McMichael, A., Woodruff, R., & Hales, S (2006). Climate change and human health: present and future risks. Lancet; 367: 859–69.

[25] Montgomery, M. (2007). Multi–objective Water Resources Planning under Demand, Supply and Quality Uncertainties, Master of Science thesis, FUTA, Nigeria, 2007.

[26] Odewumi, S.G., Awoyemi, O.K., Iwara, A.I. & Ogundele, F.O. (2013). Farmer's Perception on the Effect of Climate Change and Variation on Urban Agriculture in Ibadan Metropolis, Southwestern Nigeria. Academic Journals, pp 210.

[27] Ojo, O.I., Abegunrin, T.P. & Lasisi, M. O. (2018). Application of Remote Sensing (RS) and Geographic Information System (GIS) in Erosion Risk Mapping: Case Study of Oluyole Catchment Area, Ibadan, Nigeria. Archives of Current Research International, 1–11

[28] Olaniyan, O. S., Ige, J. A., Akolade, A. S.,& Adisa, O. A. (2015). Application of GIS in Water Management of Eleyele Catchment, South–Western Nigeria. Civil and Environmental Research. ISSN 2224–5790 (Paper) ISSN 2225–0514 (Online). 7(3), 2015.

[29] Otieno, F. A., Ojo, O. I. & Ochieng, G. M. (2013). Land cover change assessment of Vaal hart's irrigation scheme using multi–temporal satellite data. Archives of Environmental Protection 39 (4)

[30] Oyiga, B.C., Mekbib, H., & Christine, W. (2011).Implication of Climate Change on Crop Yield and Food Accessibility in Sub–Saharan Africa. Center for Development Research, University of Bonn, pp 1–4.

[31] Singh, P., & Bengtsson, L., 2004. Hydrological Sensitivity of a Large Himalayan Basin to Climate Change. Hydrological Processes 18: 2363–2385.

[32] Thompson, J. A., Bell, J. C., & Butler, C. A. (2001). Digital elevation model resolution: effects on terrain attribute calculation and quantitative soil–landscape modeling. Geoderma, 100(1): 67–89.

[33] Yoo, S. H. (2004), A note on a Bayesian approach to a dichotomous–choice contingent valuation model, J. Appl. Stat., 31 (10): 1203–1209.

[34] Ziliaskopoulos, A. K. & Waller, S. T. (2000). An internet–based Geographic Information System that integrates data, models and users for transportation applications. Transportation Research Part C: Emerging Technologies 8(1–6): 427–444.

¹·Chinglung CHANG, ¹·Kuofang HUS, ¹·Bruce C.Y. LEE, ¹·Tianxing LI

DEVELOPING A SUSTAINABLE MANUFACTURING SYSTEM BASED ON THE INDIAN FDI MANUFACTURING INDUSTRY

¹· Graduate Institute of Business Administration, Fu Jen Catholic University, TAIWAN

Abstract: Sustainable development goals (SDGs) are set from the perspective of the country and industry. There is a gap between the SDGs and the corporate social responsibility (CSR) that has been implemented by industries for years. Activities from the manufacturing industry that meet the SDGs are still missing. This study surveys both academic researchers and senior managers in the manufacturing industry in India. It applies analytical hierarchy process analysis and proposes (1) a sustainable manufacturing system (SMS) that is composed of seven constructs with 55 activities that support SDG 2-12 and 41 sustainable targets, (2) ten activities as the initial stage of the SMS that support SDG 2, 3, 4, 6, 8, 9, and 12, and (3) that SMS needs to be implemented to a company's external environment first, and then within the company, in the sequence of *Local community, Enterprise welfare, Enterprise process, Enterprise performance, Enterprise policy, Enterprise human resource,* and *Enterprise product.* By implementing SMS, the gap between the SDGs and CSR can be diminished.
Keywords: Sustainable development goal, sustainable manufacturing, sustainable manufacturing system

INTRODUCTION

Manufacturing generates a significant quantity of greenhouse gases alongside the energy and transport industries [1]. Manufacturing has further a direct social impact as it produces the articles that are used by final consumers. It also has a direct impact on occupational safety and health [2]. Taken together, it is evident that manufacturing requires sustainability as a solution to meet the needs of all parties [3]. Based on the 17 sustainable development goals (SDGs) and 169 sustainable targets issued in 2015 and listed on the United Nations' website, countries around the world have begun to develop the SDGs into activities that suit their own national conditions, and implement these activities one by one. The manufacturing industry consumes a high percentage of natural resources [4] and must therefore align itself with the SDGs by implementing activities to support the sustainable targets [5].

Batterham [6] proposes that sustainable development can be categorized into five levels: global objectives, industry strategies, enterprise sustainable targets, specific projects, and individual actions/measured outcomes. Manufacturing companies often focus on internal processes and operations [7], and except for suppliers and customers, manufacturing companies rarely communicate with society and local communities [8]. Meanwhile, the requirements of the SDGs are clearly developed from the perspective of the country and industry. Activities that manufacturing companies can implement directly within the company are limited. Therefore, manufacturing companies are generally conservative in promoting sustainability. They continue to carry out corporate social responsibility (CSR) activities that were first implemented years ago [9]. Unfortunately, the scope of such CSR activities is not as broad as the triple bottom line (TBL) that SDGs comply with [10]. It shows that there is a gap between the expectation of the SDGs and the practical implementation of manufacturing companies. This study focuses on the enterprise sustainable target level within the manufacturing industry.

Many companies publish CSR reports annually. CSR is important but social responsibility is directed solely to shareholders [11]. Meanwhile, some CSR projects may do little more than promote the agenda of the corporation itself while dispelling attention from deeper economic, political, and social problems that need to be addressed [12]. It shows a gap between sustainable development and CSR. Sustainable manufacturing is expected to diminish the gap in the manufacturing industry [13].

Sustainable manufacturing is defined as the creation of manufactured products that use processes that minimize negative environmental impacts, conserve energy and natural resources, and are economically sound and safe for employees, communities, and consumers [14]. In line with this, Moldavska and Welo [15] propose that product, process, community, employees, and customers are the main domains of sustainable manufacturing. Bhatt, Ghuman, and Dhir [16] state that sustainable manufacturing deals with the conservation of energy and natural resources and ensures the safety and well-being of all stakeholders. Well-being is what employees feel as related to organizational culture [17] Kulatunga, Jayatilaka, and Jayawickrama [18] state that the supply chain, products, build environment, and processes are the industry focus when implementing sustainable manufacturing in the Sri Lankan manufacturing sector. Ocampo and Clark [19] propose a hierarchical framework for index computation in sustainable manufacturing. The framework shows that employees, customers, and community are categorized under social well-being.

In addition, Moldavska [20] states that sustainable assessments should be made not only for sustainability, but also related to competitive advantage, customer satisfaction, and competitiveness of product. Huang and Badurdeen [21] propose a framework that indicates that process and product

are two pillars of sustainable manufacturing performance measurements while philosophy is the foundation of the framework and policies are the tool by which to deliver the philosophy. The above studies show how performance, process, product, people, policy, well-being, and community are domains that enterprises should pay attention to while implementing sustainable manufacturing. This study applies these seven domains as constructs to conduct the further research.

MATERIALS AND METHODS

India, with its population of 1.4 billion, is expected to be the next major manufacturing country. This is in part due to rising manufacturing costs in China, leading many companies to move their production lines to India. Manufacturing accounts for 14% of India's GDP [22]. The importance of sustainability for India cannot be underestimated. As many foreign direct investment (FDI) manufacturing companies in India have introduced CSR and publish CSR reports to stockholders every year, these companies have a good foundation for implementing sustainable manufacturing. The purpose of this study is to establish a sustainable manufacturing system that manufacturing companies can employ to directly support sustainable targets.

The SDGs are based on a global perspective and have a broad span. To narrow the focus to the manufacturing industry in India, this study employs a two-step questionnaire to collect data. In step one, an SDG and sustainable target questionnaire is sent to Indian academic researchers through email to collect comments about which sustainable targets FDI manufacturing companies should support in India. In step two, based on the collected responses, the seven main constructs and the main activities of sustainable manufacturing are identified, and a second questionnaire is created. This questionnaire collects responses from senior managers who work in FDI manufacturing companies that have implemented CSR for more than five years. Finally, the analytical hierarchy process (AHP) is applied to build a sustainable manufacturing system and to propose the initial stage of sustainable manufacturing.

According to Wikipedia, Chennai is the fourth largest city in India. It is the automobile capital of India, and the main automobile industry base in India. Chennai produces 35% of the car parts and 30% of the vehicles in India. Global automobile companies such as Hyundai, Ford, Mitsubishi, Nissan, etc., have set up factories there. Chennai can be regarded as one of the major foreign manufacturing investment locations in India. This study sets Chennai's foreign manufacturing companies as the research scope.

Further, this study selects companies who have published annual CSR reports the past three years (2018-2020). Because these companies have implemented CSR, they have a better understanding of the terms and meanings on the questionnaire. In order to ensure that respondents have a deep enough understanding of the company's operations, organization, human resources, and local community, the respondents are required to have worked in the company for more than eight years. The collected responses are analyzed by AHP, where the consistency ratio (CR) must be less than 0.1.

RESULTS

The SDG and sustainable targets questionnaires with open ended questions were first sent by email to researchers at Indian University's management school. Twelve responses were obtained. Based on the comments from these 12 responses, a list of 11 goals (SDG 2 to 12) that FDI manufacturing companies should support was created. Under these 11 goals, a total of 41 sustainable targets that FDI manufacturing companies can directly execute activities toward to support the achievement of these goals were compiled. This study then broke down the comments of the respondents into the first 49 activities that can be executed and implemented.

Meanwhile, some respondents commented that SDG does not cover competitiveness and performance, which are two major factors companies focus on. Companies must be competitive to provide a stable environment for their employees. It was therefore necessary for this study to add four activities related to business competitiveness:
1. *Ensure the competitiveness of enterprises*,
2. *Improve customer satisfaction*,
3. *Treat suppliers fairly*, and
4. *Develop competitive products*.

In addition, some respondents commented that the impact of product life cycles on the environment is important. Companies should produce environmentally friendly products. This study thus added an activity called *Develop products with lower energy consumption and longer service life*. Some respondents commented that it would be difficult to solve the problem of sustainability with traditional methods. With the rise of new technology, digital transformation should be considered as an approach. This study therefore added *Apply digital technology to improve efficiency of end-to-end processes* [23]. There are thus six activities that do not come from SDG that also need to be addressed, resulting in a total of 55 activities explored in this study.

The main activities of the manufacturing value chain can be categorized into five dimensions: performance, product, process, people, and policy [24]. Compared with home country manufacturing companies, FDIs also face the aspect of cultural differences. Benefits or welfare are the first factors that employees compare between foreign companies and local companies [25]. To avoid the impression of being a predator, FDI companies need to communicate properly with the local community [26] to achieve the purpose of peaceful, harmonious, and common development. Thus, the issue of welfare and local communities also need to be addressed. This study uses *Enterprise performance, Enterprise product, Enterprise process, Enterprise human resource, Enterprise policy, Enterprise welfare*, and *Local community* as research constructs and then classify the above 55 activities under the seven

constructs as shown in Appendix 1. Appendix 1 presents the seven constructs, 55 activities, and the sustainable targets these activities support. It also presents that the relationship between activity and sustainable target is not one-to-one, but that multiple-to-multiple relationships exist. For example, activity 40, *Expand the scope of medical insurance to reduce the burden of family medical expenses*, supports sustainable targets 3.4 and 3.8. Activity 47, *Improve water quality and sanitation in local community to reduce malaria incidence*, supports sustainable targets 3.3, 3.9, and 6.b. Activity 43 and activity 51 both support sustainable targets 6.2.

— Analysis

This study then conducts the second survey. The questionnaire is sent to senior managers who work in the FDI manufacturing companies in Chennai that have continuously published CSR reports the past three years. Senior managers are defined as those who have worked in the company for more than eight years and hold the titles of manager, senior manager, or directors. A total of 42 response are collected. Six responses are invalid and therefore removed from the data sample, resulting in a total of 36 valid responses being used for the AHP analysis. The 36 valid responses are provided by 23 managers, eight senior managers, and five directors. These have worked in the company for an average of 9.1 years and have had direct or indirect contact with the company's CSR on an average of 3.7 years. This means that the respondents have a certain degree of understanding of the corporate culture and CSR in the FDI manufacturing companies.

This study analyses the seven constructs of the 36 responses. The CI is equal to 0.1, which means that the seven constructs are consistent. The CR is equal to 0.07, which presents that the results are acceptable. The top three rankings are *Local community*, *Enterprise welfare*, and *Enterprise process*. The rest rankings are *Enterprise performance, Enterprise policy, Enterprise human resource,* and *Enterprise product*.

The following are the analysis of each construct:

(1) *Enterprise Performance*. The CI and CR of this construct are 0.005 and 0.004, respectively. The results are thus considered consistent. The top 3 activities are *Ensure enterprise competitiveness*, *Increase salary year by year alone with productivity,* and *Improve customer satisfaction*.

(2) *Enterprise Process*. The CI and CR of this construct are 0.07 and 0.05, respectively. The results are thus considered consistent. The top three activities are *Increase the proportion of renewable energy*, *Improve productivity by diversity, technology, and innovation,* and *Adopt clean and environmental-friendly technologies to improve production processes*.

(3) *Enterprise Product*. The CI and CR of this construct are 0.07 and 0.05. The results are thus considered consistent. The top three activities are *Apply circular economy to product design to reduce the impact of product life cycle on environment, Examine the products and processes in the value chain for negative impact on ocean and land,* and *Increase number of patents for sustainable product and material*

(4) *Enterprise Human Resource*. The CI and CR of this construct are 0.03 and 0.02. The results are thus considered consistent. The top three activities are *Increase the number of young employees*, *Increase number of technicians and their skills*, and *Corporate with official school for staffs training and education degree*.

(5) *Enterprise Policy*. The CI and CR of this construct are 0.03 and 0.02. The results are thus considered consistent. The top three activities are *Put sustainable development into policy*, *Conduct training of sustainability,* and *Promote sustainable development through practical projects by staff*.

(6) *Enterprise Welfare*. The CI and CR of this construct are 0.09 and 0.06. The results are thus considered consistent. The top three important activities are *Increase the use of sustainable agricultural products in staff restaurants*, *Provide medical subsidies for pregnant employees,* and *Provide birth registration and medical and nutritional subsidies for employees' new-borns and children under five years old*.

(7) *Local Community*. The CI and CR of this construct are 0.09 and 0.06. The results are thus considered consistent. The top three activities are *Improve water quality and sanitation in local community*, *Employ a certain proportion of residents,* and *Provide awards for innovation and scientific research and development in higher education*.

— Initial Stage

According to the analysis results of the questionnaire responses collected from senior managers, the activities under the seven constructs are calculated by the Eigenvector method, and the weights of the activities at each level are calculated and ranked. The top five activities are shown in Table 1.

Table 1. Top five activities of initial stage

Construct	S.N.	Activity	Rank	Sustainable target supported
7. Local Community	47	Improve water quality and sanitation in local community to reduce malaria incidence	1	3.3, 3.9, 6.b
7. Local Community	48	Employ a certain proportion of residents	2	4.5
7. Local Community	50	Provide awards for innovation and scientific research and development in higher education	3	4.b, 9.5
6. Enterprise Welfare	37	Increase the use of sustainable agricultural products in staff restaurants	4	2.4
3. Enterprise Product	14	Apply circular economy to product design to reduce the impact of product life cycle on environment	5	8.4, 12.2

Among the top five activities, three belong to Local community. This indicates that companies can start by improving their community relationships and the local environment. Related to Enterprise welfare, Increase the use of sustainable agricultural products in staff restaurants also directly expresses the company's actions of sustainability to

employees. Many Indian FDI companies serve meals. Food fees are cheap, and the food is cleaner than roadside stands around the company where the employees usually buy their meals. At the same time, Indian vegetarians account for the majority of the population. Therefore, the simple and most direct way to educate employees regarding what sustainability is and let employees personally feel the practice of sustainability is by serving sustainable food directly to employees through company meals.

The fifth activity related to *Enterprise product* shows that company products need to also directly add sustainability. This is a further statement to employees and shareholders that the company is going to move towards sustainable manufacturing. The top four activities are related to the external environment and employee living. These activities do not yet involve the actual production process and policies that are of the major functions of manufacturing. This means that for FDI manufacturing companies, the first stage of sustainable manufacturing can be to start with communication to the community, improve employee living, and then focus on the company's products. In this way the concept of sustainable manufacturing can be introduced to all stakeholders.

To further explore the activities linked to the initial stage, the top 6-10 activities are analyzed. To officially announce a company is pursuing sustainability, it must *Put sustainable development into policy,* as this helps communicate out to all the employees how sincere the company is. Because of India's caste system, some children may not be able to complete their education. Access to clean and safe water supplies may also be an issue in certain communities. *Subsidize education for vulnerable children in local community* and *Establish public toilets in the community and supply free water and soap* are thus easy ways to enhance a company's relationship with the local community. Furthermore, the power supply in India is not as convenient or easy to access as it is in other developed countries. To reduce the impression that foreign companies plunder Indian resources, companies can *Increase the proportion of renewable energy*, which is highly supported by the government.

The medical expense of pregnant women in India is costly. It would be very helpful in the implementation of the concept of sustainability if companies help pregnant employees by providing them with company welfare plans. Welfare is not only financial support. Companies can:
(1) make contracts with high quality hospitals to provide periodic health checks during pregnancy,
(2) organize and pay for doctors to visit the company during working hours,
(3) provide postpartum leave, and
(4) relocate employees to low-labor workstations.

Among the top ten activities, five activities are related to *Local community*, two are related to *Enterprise welfare*, one is related to *Enterprise product*, and the final one is related to *Enterprise process*. This indicates that sustainable manufacturing

activities should be implemented by companies first related to outside factors then to inside factors. Companies can start with activities related to the local community so that employees are introduced to the concept of sustainable manufacturing and see that this is something the company prioritizes. It can then implement activities related to enterprise welfare. In this way employees can trust that the purpose of sustainable manufacturing is not just another public relationship activity employed by the company, but a true priority. Companies can directly put sustainable manufacturing into its product design and perform official employee training. This study considers the top ten activities to be the initial stage of sustainable manufacturing that a company can start implementing, after which the company can implement the rest of the constructs in the sequence of *Enterprise performance*, *Enterprise policy*, and *Enterprise human resource*.

Linking the first ten activities to SDG, if companies implement sustainable manufacturing according to the initial stage described above, SDG 2, 3, 4, 6, 7, 8, 9, and 12 will be supported. That is to say that four SDG 4 (*Quality education*) and three SDG 3 (*Good health and well-being*) sustainable targets will be supported. Companies can publish these activities in their CSR reports to disclosure them to the public and shareholders. The CSR reports can be used to explain the relationship between SDG and the sustainable manufacturing activities the companies implement. This strengthens the link of the companies' SDG support as well as makes it more transparent.

Sustainable Manufacturing System

Based on the above analysis, this study proposes a sustainable manufacturing system that is composed of seven constructs and the implementation sequence as shown in the following figure. The sequence is *Local community, Enterprise welfare, Enterprise process, Enterprise performance, Enterprise policy, Enterprise human resource,* and *finally Enterprise product*.

In Figure 1, one can see there is a house surrounded by Local Community. The house represents the manufacturing company itself and is composed of the six manufacturing constructs. Sustainable manufacturing can thus be seen as not only being an internal activity within companies, but also needs to be communicated out to the external environment. The most direct external environment of the company is the local community, so the sustainable manufacturing house is surrounded by the local community. Because policies are the principles and guidelines of company activities, *Enterprise policy* is placed at the bottom as a cornerstone. *Enterprise welfare* and *Enterprise process* are two of four pillars that directly communicate with the local community. These two constructs are placed on the left and right sides of the sustainable manufacturing house. *Enterprise human resource* and *Enterprise product* are placed in the middle and are thus considered the core constructs inside the enterprise. These four pillars directly influence *Enterprise performance*.
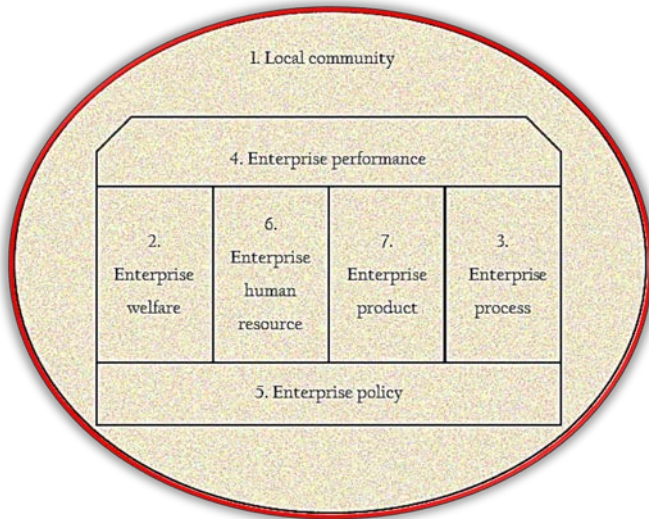
Figure 1. Sustainable manufacturing system

CONCLUSION

SDGs and sustainable targets are proposed from the perspective of the country and industry. There is a gap between the SDGs and CSR that has been carried out by the manufacturing industry for many years. This study proposes:

(1) a sustainable manufacturing system that is composed of seven constructs and 55 activities that support SDG 2-12 and 41 sustainable targets,

(2) ten activities to be implemented in the initial stage of a sustainable manufacturing system that supports SDG 2, 3, 4, 6, 7, 8, 9, and 12, and

(3) the sustainable manufacturing system needs to be implemented related to the external environment first and then internally within the company.

To sum up, by implementing the sustainable manufacturing system in the sequence of *Local community*, *Enterprise welfare*, *Enterprise process*, *Enterprise performance*, *Enterprise policy*, *Enterprise human resource*, and *Enterprise product*, SDG 2-12 will be supported and the gap between the SDGs and CSR can be diminished.

Appendix 1: AHP Results and Sustainable Targets Supported

No	S.N.	Activities	Weight within construct	Weight among all constructs	Rank	Sustainable target supported
1. Enterprise Performance (Weight: 0.120)						
1	1	Increase the recycling and utilization efficiency of both industrial and domestic water	0.14	0.02	25	6.4
2	2	Increase energy efficiency	0.16	0.02	21	7.3
3	3	Increase salary year by year along with productivity and GDP improvement	0.19	0.02	14	8.1
4	4	Ensure enterprise competitiveness	0.20	0.02	11	NA
5	5	Improve customer satisfaction	0.17	0.02	18	NA
6	6	Treat suppliers fairly	0.14	0.02	26	NA
2. Enterprise Process (Weight: 0.128)						
1	7	Increase the proportion of renewable energy	0.23	0.03	8	7.2
2	8	Improve productivity through diversity, technology, and innovation	0.18	0.02	12	8.2
3	9	Adopt clean and environmentally friendly technologies to improve production processes	0.15	0.02	20	9.4

No	S.N.	Activities	Weight within construct	Weight among all constructs	Rank	Sustainable target supported
4	10	Reduce production and emission of carbon dioxide and other gases that have a negative impact on the environment	0.14	0.02	23	11.6
5	11	Promote environmentally sound management of chemicals and wastes to reduce the negative impact on human health and the environment	0.12	0.02	31	12.4
6	12	Reduce production waste through prevention, emission reduction, and recycling	0.10	0.01	40	12.5
7	13	Apply digital technology to improve the efficiency of end-to-end processes	0.08	0.01	48	NA
3. Enterprise Product (Weight: 0.117)						
1	14	Apply circular economy to product design to reduce the impact of product life cycles on the environment	0.258	0.03	5	8.4, 12.2
2	15	Increase number of sustainable product and material patents	0.186	0.02	17	9.5
3	16	Examine products and processes in the value chain for negative impacts on ocean and land	0.190	0.02	15	11.4
4	17	Increase proportion of sustainable materials in product development	0.155	0.02	22	12.2
5	18	Develop competitive products	0.119	0.01	36	NA
6	19	Develop products with lower energy consumption and longer service life	0.092	0.01	46	NA
4. Enterprise Human Resource (Weight: 0.118)						
1	20	Cooperate with official schools for staff training and education degrees	0.067	0.01	53	4.3
2	21	Help staff receive technical training and certificates	0.078	0.01	51	4.4
3	22	Provide same education to men and women	0.080	0.01	49	4.5
4	23	Improve literacy and calculating ability of employees	0.076	0.01	52	4.6
5	24	Increase proportion of females in management	0.093	0.01	44	5.5
6	25	Increase application of information and communications technology and the technical skills of female employees	0.101	0.01	42	5.b
7	26	Offer equal pay for equal work	0.113	0.01	39	8.5
8	27	Increase hiring proportion of those with disabilities	0.123	0.01	34	8.5
9	28	Increase number of young employees	0.140	0.02	29	8.b
10	29	Increase number of technicians and their skills	0.128	0.02	32	9.5
5. Enterprise Policy (Weight: 0.119)						
1	30	Put sustainable development into policy	0.248	0.03	6	4.7
2	31	Conduct sustainability training	0.191	0.02	13	4.7
3	32	Promote sustainable development through practical projects by staff	0.142	0.02	27	4.7
4	33	Employ incentives to encourage employees to carry out sustainable development activities	0.115	0.01	38	4.7
5	34	Treat different religious beliefs fairly	0.124	0.01	33	10.2
6	35	Publish sustainable development reports periodically	0.094	0.01	43	12.6
7	36	Communicate enterprise stainability practices to the local community and society so that the public can understand the sustainability contribution of the enterprise	0.087	0.01	47	12.6
6. Enterprise Welfare (Weight: 0.150)						
1	37	Increase use of sustainable agricultural products in staff restaurants	0.205	0.03	4	2.4
2	38	Provide medical subsidies to pregnant employees	0.161	0.02	10	3.1
3	39	Provide birth registration and medical and nutritional subsidies to employees with new-borns and children under five years old	0.119	0.02	24	3.2, 16.9
4	40	Expand scope of medical insurance to reduce the burden of family medical expenses	0.111	0.02	28	3.4, 3.8
5	41	Provided transportation as a commuting option	0.093	0.01	37	3.6
6	42	Subsidize employees so their children can complete preschool, primary, and secondary education	0.083	0.01	41	4.1, 4.2

No	S.N.	Activities	Weight within construct	Weight among all constructs	Rank	Sustainable target supported
7	43	Provide indoor toilets with free soap and water for all employees	0.073	0.01	45	6.2
8	44	Create a safe working environment	0.062	0.01	50	8.8
9	45	Offer sustainable tourism to employees to promote local culture	0.053	0.01	54	8.9
10	46	Deposit salaries into bank accounts, not cash-in-hand	0.041	0.01	55	8.10
7. Local Community (Weight: 0.247)						
1	47	Improve water quality and sanitation in the local community to reduce malaria incidences	0.197	0.05	1	3.3, 3.9, 6.b
2	48	Employ a certain proportion of residents	0.166	0.04	2	4.5
3	49	Subsidize education for vulnerable children in the local community	0.118	0.03	7	4.5
4	50	Provide awards for innovation and scientific research and development in higher education	0.127	0.03	3	4.b, 9.5
5	51	Establish public toilets in the community and supply free water and soap	0.101	0.02	9	6.2
6	52	Prioritize water safety, not only meet the local government standards but require zero environment pollution	0.089	0.02	16	6.3
7	53	Adjust working days to match religious activities	0.079	0.02	19	10.2
8	54	Increase proportion of local research and development and technical personnel	0.066	0.02	30	12.a
9	55	Connect enterprises regularly to share knowledge and technology for mutual growth	0.057	0.01	35	12.a

References

[1] Choi, S.S., & Lee, J.Y. (2017). Development of a framework for the integration and management of sustainability for small- and medium-sized enterprises. International Journal of Computer Integrated Manufacturing, 30, 1190–1202.

[2] Schmidt, G., & Wilhelm, W. E. (2000). Strategic, tactical, and operational decisions in multi-national logistics networks: A review and discussion of modeling issues. International Journal of Production Research, 38(7), 1501–1523.

[3] Croson, R., & Donohue, K. (2005). Upstream versus downstream information and its impact on the bullwhip effect. System Dynamics Review, 21(3), 249–260.

[4] Roychowdhury, S. (2006). Earnings management through real activities manipulation. Journal of Accounting and Economics, 42(3), 335–370.

[5] Sutherland, J., & Bennett, B. (2007). The seven deadly wastes of logistics: Applying Toyota Production System principles to create logistics value. White Paper, 701, 40–50.

[6] Lu, J., Humphreys, P., McIvor, R., Maguire, L., & Wiengarten, F. (2012). Applying genetic algorithms to dampen the impact of price fluctuations in a supply chain. International Journal of Production Research, 50(19), 5396–5414.

[7] Christopher, M. (2005). Logistics and supply chain management: Creating value-adding networks. Pearson Education: New York, USA.

[8] Singh, S., Ramakrishna, S., & Gupta, M.K. (2017). Towards zero waste manufacturing: A multidisciplinary review. Journal of Cleaner Production, 168, 1230–1243.

[9] Abdul-Rashid, S. H., Sakundarini, N., Ariffin, R., & Ramayah, T. (2017). Drivers for the adoption of sustainable manufacturing practices: A Malaysia perspective. International Journal of Precision Engineering and Manufacturing, 18, 1619–1631.

[10] Pipatprapa, A., Huang, H. H., & Huang, C. H. (2018). Enhancing the effectiveness of AHP for environmental performance assessment of Thailand and Taiwan's food industry. Environmental Monitoring & Assessment, 190, 748.

[11] Wasserman, I.M. (1984). The influence of economic business cycles on United States suicide rates. Suicide and Life-Threatening Behavior, 14, 143-156.

[12] Drautzburg, T. (2019). Why are recessions so hard to predict? Random shocks and business cycles. Economic Insight, 4(1), 1-8.

[13] Nordhaus, W. D. (1975). The political business cycle. Review of Economic Studies, 42(2), 169-190.

[14] Barbosa-Filho, N. H., & Taylor, L. (2006). Distributive and demand cycles in the US economy – A Structuralist Goodwin Model. Metroeconomica, 57(3), 389–411.

[15] Flaschel, P., Kauermann, G., & Teuber, T. (2008). Long cycles in employment, inflation, and real wage costs. American Journal of Applied Sciences, Special Issue, 69–77.

[16] Guo, L. (2009). The benefits of downstream information acquisition. Marketing Science, 28(3), 457–471.

[17] Gaur, V., Fisher, M. L., & Raman, A. (2005). An econometric analysis of inventory turnover performance in retail services. Management Science, 51(2), 181–194.

[18] Cachon, G. P., & Lariviere, M. A. (1999). Capacity choice and allocation: Strategic behavior and supply chain performance. Management Science, 45(8), 1091–1108.

[19] Cachon, G. P. (1999). Managing supply chain demand variability with scheduled ordering policies. Management Science, 45(6), 843–856.

[20] Sogomonian, A. G., & Tang, C. S. (1993). A modeling framework for coordinating promotion and production decisions within a firm. Management Science, 39(2), 191–203.

[21] Chen, F., Drezner, Z., Ryan, J. K., & Simchi-Levi, D. (2000). Quantifying the bullwhip effect in a simple supply chain: The impact of forecasting, lead times, and information. Management Science, 46(3), 436–443.

[22] Scarano, F.R. (2019). The emergence of sustainability. In L. Wegener & U. Lüttge (Eds.), Emergence and Modularity in Life Sciences (pp. 51-71). Springer-Nature: Cham, Switzerland.

[23] Rahani, A. R., & Al-Ashraf, M. (2012). Production flow analysis through value stream mapping: A Lean production process case study. Procedia Engineering, 41, 1727–1734.

[24] Aviv, Y. (2007). On the benefits of collaborative forecasting partnerships between retailers and manufacturers. Management Science, 53(5), 777–794.

[25] Angelus, A., & Porteus, E. L. (2002). Simultaneous capacity and production management of short-lifecycle, produce-to-stock goods under stochastic demand. Management Science, 48(3), 399–413.

[26] United Nations. Sustainable development goals. http://www.un.org/sustainabledevelopment/sustainable-development-goals/

[1.]Dragos ANGHELACHE, [1.]Ana–Maria TABARASU, [1.]Catalin PERSU,
[1.]Daniel DUMITRU, [1.]Carmen BĂLŢATU, [2.]Radu RADOI

MODERN METHOD FOR OPTIMIZING TECHNOLOGICAL FLOW FOR MANUFACTURING METAL PARTS BY USING LASER CUTTING EQUIPMENT

[1.]National Institute of R&D for Machines and Installations Designed to Agriculture and Food Industry (INMA), Bucharest, ROMANIA
[2.]INOE 2000 – Subsidiary Hydraulics & Pneumatics Research Institute, ROMANIA

Abstract: Numerically controlled laser cutting (CNC) tools have been developed as an alternative to conventional cutting equipment and bring a considerable benefit due to the increased accuracy, contactless processing, higher productivity and lower energy consumption. Given the desirable need to streamline the technological flow of manufacturing to optimize production costs and minimize losses of raw materials, the use of numerically controlled equipment (CNC) for cutting metal parts is a goal of real interest. The paper presents in stages a manufacturing sequence of a metal part, with an explicit description of the necessary steps, which includes the design stage and realization of 3D and 2D models of the part, loading in the command computer and control of laser cutting equipment, positioning material on the work surface, parameterization and calibration of the equipment, proper cutting of the parts and dimensional verification of the part at the end of the process.
Keywords: optimize, CNC, process, production

INTRODUCTION

The production of laser cutting machines began fifty years ago. Progress has been rapid and laser cutting is one of the largest applications of lasers in the metalworking industry. Numerically controlled laser cutting (CNC) tools have been developed as an alternative to conventional cutting equipment and bring a considerable benefit due to the increased accuracy, contactless processing, higher productivity and lower energy consumption.

Common to all personal manufacturing tools (e.g., 3D printer, laser cutter, CNC machine) is the need for a virtual representation, diagram, drawing, or 2D / 3D model of the object to be produced. Another important aspect in the manufacture of metal parts using modern cutting equipment is the calibration and parameterization of the cutting machine. Laser cutting is a thermal process that begins by heating and focusing the laser beam (density varies around 104 Wmm-2) in combination with the gas (active or inert). The laser beam melts the metal that is being cut, and the gas with its current eliminates the liquefied metal (Ahn, D.G., et al., 2005).

MATERIALS AND METHODS

The process of laser cutting or laser cutting is done with the help of a laser beam. It is directed with a lens to the area to be cut or cut. The laser beam that passes through the lens and into the work area melts the material you want to cut or cut. In order for this activity to take place, a coaxial gas jet is pumped in order to remove the waste that occurs as a result of the melting process of the material you want to cut or cut (Barton, K.L et al., 2007).

RESULT

The necessary steps for cutting a metal part consist of a sequence of operations and parameterizations, such as: designing the part, loading into the computer the command and control of the laser cutting equipment, parameterization and calibration of the equipment, actual cutting of parts (Cheng, T. et., 2001).

— Part design

In order to cover the manufacturing flow, a side wall of a drum was selected, which was designed in the solidworks program according to predetermined dimensions (Davim, P. et al).
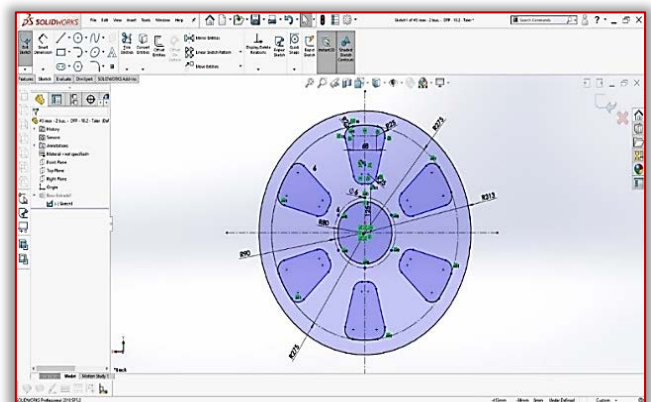
Figure 1. Design and dimensioning of the piece (Solidworks)
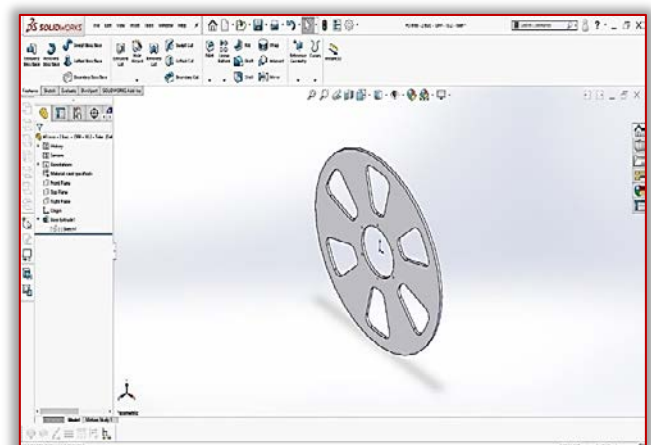
Figure 2. Previewing the piece in 3D format (Solidworks)

⎯ **Loading into the computer the command and control of the laser cutting equipment**

The project designed in solidworks has been saved in a .dxf file so that it can be loaded into the laser cutting machine program (Felix Huppert et al., 2019).
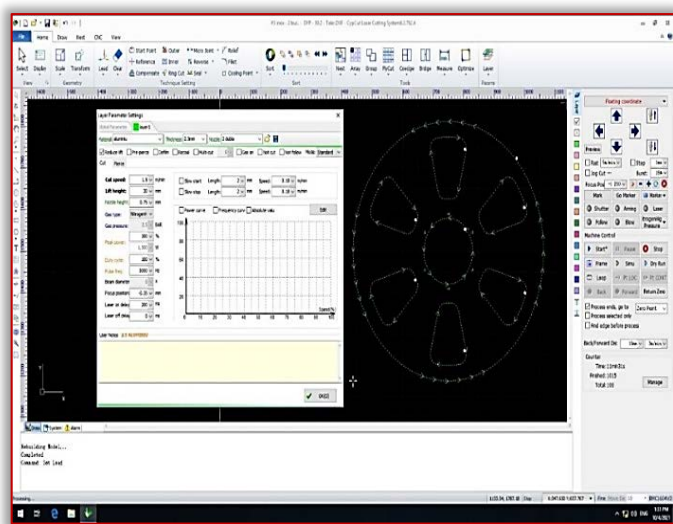
Figure 3. Loading and parameterization in the control computer of the cutting machine

⎯ **Equipment parameterization and calibration**

Depending on the material to be cut and its thickness, we choose a cutting nozzle. The size of the nozzle holes has a great influence on the quality of cutting and drilling. When the diameter of the nozzle holes is larger, its proper protection for the focusing mirror is weaker because the chances of the flying melting sparks reaching the mirror are higher (Davim, P., et al.).
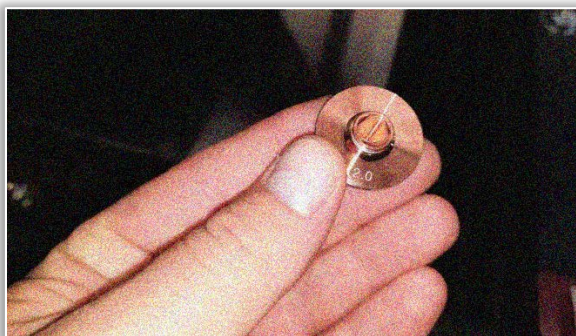
Figure 4. Cutting nozzle
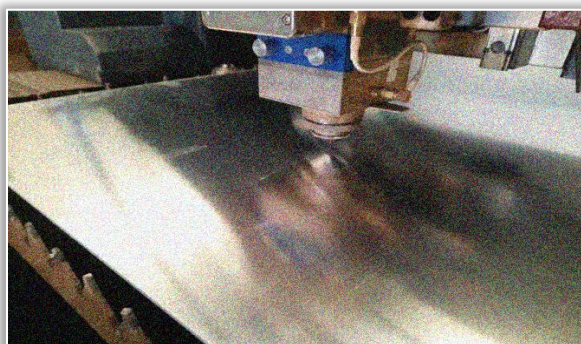
Figure 5. Calibration of sheet thickness

The calibration of the cutting machine according to the thickness of the material to be cut is done automatically, the machine having capacitive sensors.
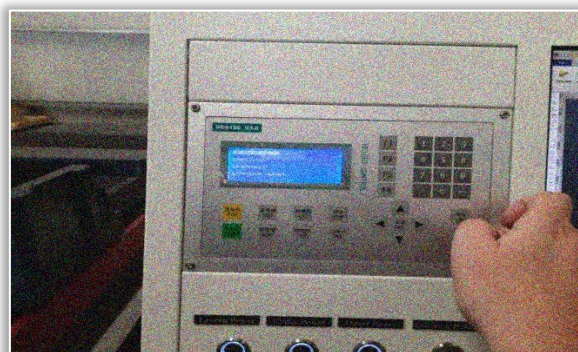
Figure 6. Calibrarea din soft

Figure 7. The results displayed on the display after calibration

The auxiliary gas used for cutting can be connected to the O2 and N2 sources at the same time. The gas can be selected as needed during cutting and the system can automatically switch the gas supply (Frederick Struckmeier et al).

Figure 8. Gas pressure adjustment

⎯ **The actual cutting of the parts**

Each workpiece has different profiles, some are easy to cut, but some are difficult to cut, such as small holes, sharp corners, etc. To ensure the cutting quality and cutting efficiency of the whole part, we will adopt the layered cutting method.

In this way, we could adopt different technological parameters to control the cutting of different profiles, thus ensuring not only the cutting quality of the hard-to-cut

profiles but also the improvement of the cutting efficiency of the easy-to-cut profiles (Miroslav Radovanovic et al., 2002).
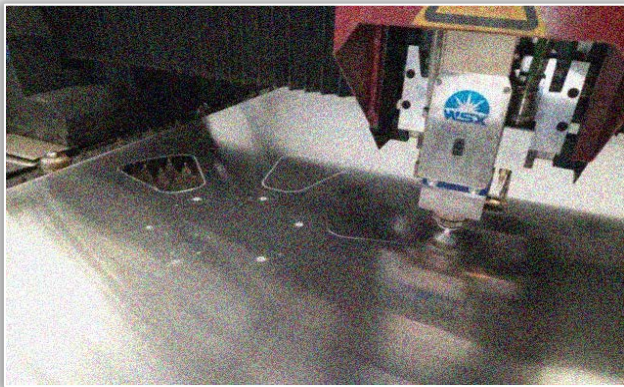
Figure 9. The debit process

After completing the above steps, the part being cut, we can measure it with the help of measuring instruments (subler) to verify compliance with the quotas in the execution drawing (Paolo Bison et al.).

Figure 10. Checking the final part

CONCLUSIONS

≡ Prototyping, an activity which normally costs a car manufacturer thousands of hours per year (the parts to be produced range from single pieces to a few dozen for experimental preproduction runs).

≡ Production in small batches, luxury or special cars, trucks and buses or parts for the aerospace industry.

≡ Production of spare parts where the robot flexibility is especially suited to following the diversified demand.

≡ For cutting and drawing dies. The process of development that precedes the die forming reaps a major advantage when laser robots are used.

≡ Cutting of large turbine blade ving contours for rotors and stators. Flexibility of the systems is often the most important reason for its purchase since in the case of production start-up or small batch production, frequent modifications will be necessary

References

[1] Ahn, D.G., Kim, M.S., Lee, S.H., Park, H., Yoo, Y.T., Influence of process parameters on the kerfwidth for the case of laser cutting of CSP 1N sheet using high power CW Nd:YAG laser, Journal of the Korean Society of Precision Engineering 22(7) pp.19–26, 2005

[2] Barton, K.L., Alleyne, A.G., Cross-Coupled ILC for Improved Precision Motion Control: Design and Implementation, American Control Conference, New York, 2007

[3] Cheng, T. et. al., Intelligent Machine Tools in a Distributed Network Manufacturing Mode Environment, International Journal of Advanced Manufacturing Technology, 17, pp. 221-231, 2001

[4] Davim, P., Barricas, N., Conceicao, M., Oliveira C., Some experimental studies on CO2 laser cutting quality of polymeric materials, Journal of Materials Processing Technology 198, pp. 99

[5] Felix Huppert, Gerold Hölzl, Matthias Kranz, Design Different: Pen and Paper for Laser Cutting, October 2019IEEE Pervasive Computing 18(4):pag. 29-37

[6] Frederick StruckmeierJim ZhaoFernando Puente León, Measuring the supporting slats of laser cutting machines using laser triangulation, June 2020The International Journal of Advanced Manufacturing Technology

[7] Miroslav Radovanovic, Laser cutting machines for 3-D thin sheet parts, "Constantin Brâncusi" University – Engineering Faculty, University's Day - 8th International Conference, Târgu Jiu, May 24-26, 2002,

[8] Paolo Bison, Giovanni Ferrarini, Gabriele Zanon, Thermographic, Monitoring of Laser Cutting Machine.

[9] Davim, P., Barricas, N., Conceicao, M., Oliveira C., Some experimental studies on CO2 laser cutting quality of polymeric materials, Journal of Materials Processing Technology 198, pp. 99

[10] ***Program Solidworks

Fascicule 2

[April – June]

t o m e [2022] XV

ACTA Technica CORVINIENSIS
BULLETIN OF ENGINEERING

1. Ionela–Mihaela BACIU, 1.Alexandru Polifron CHIRIȚĂ, 1.Radu–Iulian RĂDOI, 1.Petrin DRUMEA, 2.Iulian VOICEA

IMPROVING THE ENERGY EFFICIENCY OF WIND TURBINES USING HYDRAULIC DRIVE

1.INOE 2000 – Subsidiary Hydraulics and Pneumatics Research Institute (INOE 2000–IHP) Bucharest, ROMANIA
2.National Institute of Research – Development for Machines and Installations Designed for Agriculture and Food Industry, Bucharest, ROMANIA

Abstract: The article presents a variant of hydrostatic transmission in open circuit that replaces the classical mechanic transmission; for both variants are analyzed parameters such as energy efficiency, power, lost power, etc. Hydrostatic transmission has specific advantages that are deriving from positioning the generator on the ground such as: nacelle mass reduction that will reduce the price of the construction and the simplification of the energy transmitting chain. Energy transmitting and summing from multiple wind turbines is much easier.
Keywords: wind turbines, hydrostatic transmission, mechanical transmission, energy efficiency

INTRODUCTION

In 2020, the electricity obtained from the conversion of wind power covered 6.38% of the total consumption worldwide. Small wind turbines can produce a power of 400 watts up to 100 kW. The average wind speed from the geographical location determines how much wind power a turbine can convert (***, Small Wind Turbine & Generators to Power Your Home, 2020). Most of this energy production is obtained with horizontal axis wind turbines. For this type of turbine, the location of the electric generator in the turbine platform leads to a significant increase in the mass of the platform, and implicitly the mass of the pillar supporting the turbine. In addition, the maintenance of the turbine becomes more difficult with the increase of the rotor diameter and the height of placement.

The platform (excluding the rotor) represents between 20 … 35% of the total weight of a large turbine reaching in some cases the order of hundreds of tons. In the case of the VESTAS V90 turbine, the platform weighs 75 tons, the rotor 40 tons, and the tower 152 tons (***, Renewables 2020 Global Status Report, 2020). In August 2021, the largest offshore wind turbine with a capacity of 16 MW was launched; for this turbine, the nacelle has a weight of 37 T / MW, considered very competitive. In the case of small turbines (< 100 kW), even if we do not have such weights, the same values are kept as a percentage. Other research has shown that in offshore turbines, one of the main issues is gearbox failure, with current designs requiring replacement or capital intervention every 4 years. With the gearbox contributing to around 10% of turbine cost (Buhagiar, T. S., 2013), such frequent replacements are very detrimental to the overall viability of offshore wind energy conversion. Danop Rajabhandharaks states in his thesis (Rajabhanharaks, D., 2014) that it is not uncommon for a gearbox to fail on average every 5 years, while the designed lifetime of a wind turbine is typically about 20 years. On the other hand, there are wind turbines that have appeared in the last decades that differ from the classic solutions, and fall into the category of unconventional wind turbines; they have different shapes, are arranged vertically or horizontally at different heights, and in terms of power they usually fall into the category of low power turbines (below 100 kW).

Reducing the weight of the platform, and implicitly the weight of the support pillar, would be easy to achieve if the electric generator were located on the ground and the tower would support only the rotor and a few other auxiliary elements. Maintenance would also be much easier to achieve. As for the unconventional turbines, they are located in the most diverse places, and the reduction of the suspended mass and reduction of the gauge is likely to simplify the construction and improve the visual impact. While in the turbines with vertical axis located on the ground or near the ground, the generator has small dimensions and weight, in those placed on buildings or bridges, the location on the ground of the generator significantly simplifies the construction.
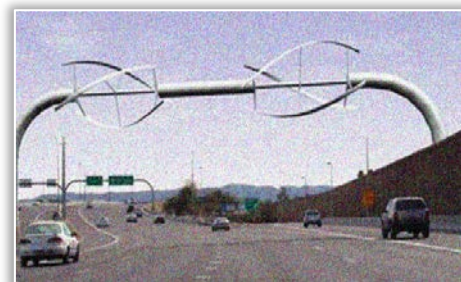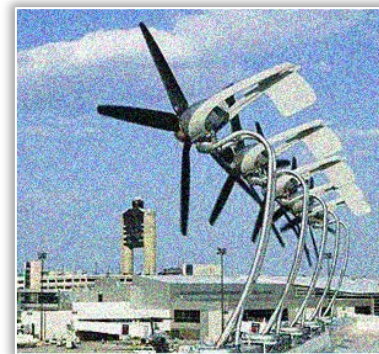

Figure 1 – Unconventional wind turbines (***, https://www.whirlopedia.com/index.php/unconventional–wind–turbines)

For all these problems the solution is the hydrostatic transmission of energy from the rotor to the generator, also giving up the gearboxes that multiply the reduced rotor speed (5...40 rpm) to make it compatible with that of the generator (1500...3000 rpm); by an intelligent use of some classic–and–modern hydraulic components, high performance hydrostatic transmission can be achieved.

MATERIALS AND METHODS

In addition to the advantages mentioned above, the research undertaken by the authors aimed to establish energy efficiency in two transmission variants: a classic variant and a hydrostatic transmission variant. Beside the main purpose of the research related to efficiency, the aim was to adjust the drive speed of the electric generator and the transmission response to the input parameter variation (wind speed mainly). In this phase, the research was performed by numerical simulation (by using Simcenter Amesim software), to reduce material costs and research time.

Hydrostatic system is consisting of a variable speed motor that represents the turbine blades, connected to a planetary speed multiplier that increases the hydrostatic pump speed up to 2000 rev/min. The hydrostatic pump is connected in an open circuit, which includes also: a hydraulic orifice that adds flow rate losses in the system; a hydraulic pressure relief valve that opens if the pressure in the system is higher than 150 bar; a hydraulic motor that drives the load pump; a hydraulic pressure relief valve. Generator is represented in this simulation by the load pump. The power sensors and the speed sensor collect the data, and then the difference between output power and input power is calculated and displayed on a chart. The same data from the sensor is divided and the result represents the efficiency of the transmission. Speed sensor measures generator speed, the data is transmitted for comparison in the comparator where the value from the sensor is compared with a reference value and then the error signal is transmitted to the PID regulator that adjusts pump displacement in such way that output speed remains constant. The reason is the necessity to maintain a constant frequency of 50 Hz.
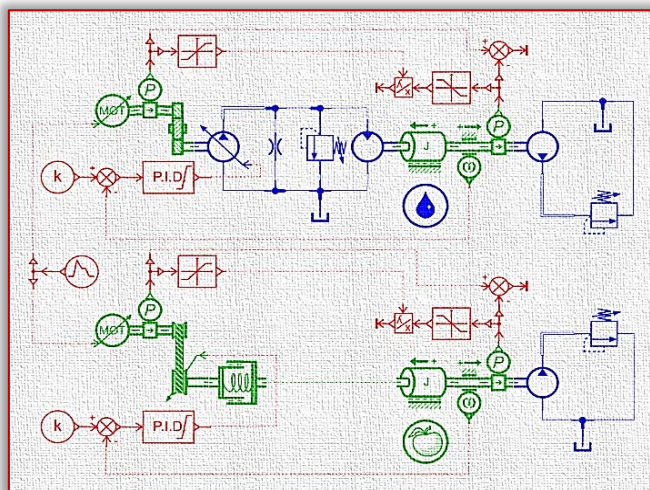
Figure 2 – Simulation Network

Mechanical transmission has in componence the same variable speed motor that is connected to a continuously variable speed multiplier that increases the speed up to 1470 rev/min. The output of the speed multiplier is connected by a flexible coupling to the load pump. The sensors from the mechanical transmission are placed in the same place as in the hydrostatic transmission, the PID regulator does the same thing as the PID regulator from the hydrostatic transmission; the difference is the parameter that is adjusted.

Table 1. Simulation parameters

Component	Hydrostatic transmission	Mechanical transmission
Variable speed motor (turbine blades)	Speed: 25...100 rev/min	
Speed multiplier	Planetary $i_R = 20$	Continuously variable $i_M = 60$
Hydraulic pump	Displacement: 112 cm³/rev Variable displacement	–
Hydraulic pressure valve	Relief valve 150 bar	
Hydraulic motor	Displacement: 35 cm³/rev Fixed displacement	–
Hydraulic oil	HEP46	–
Moment of inertia	0.1 kg·m²	
Hydraulic load pump	Displacement: 35 cm³/rev	
Hydraulic load pressure valve	Cracking pressure 120 bar	
PID regulator	$k_p = 3$ $k_i = 3750$ $k_d = 0.0016$ saturation range: 0 – 1	$k_p = 180$ $k_i = 3800$ $k_d = 0.0018$ saturation range: 0 – 60

RESULTS

The comparison between a hydrostatic transmission and a mechanical transmission by simulation leads to the following results that will be discussed next. In the following graphs, hydrostatic transmission is denoted as HT and mechanical transmission is noted as MT. The parameters have been monitored and calculated in order to ensure a fair comparison between the two transmissions.
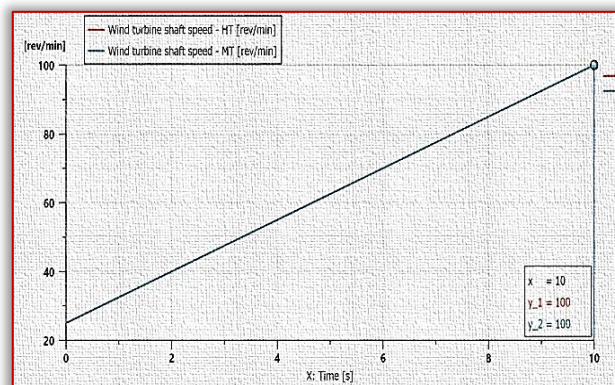

Figure 3 – Wind turbine shaft speed variation over time

Wind turbine shaft speed variation for HT and MT is shown in Figure 3. The two shafts speeds have the same variation as one can see on the graph.
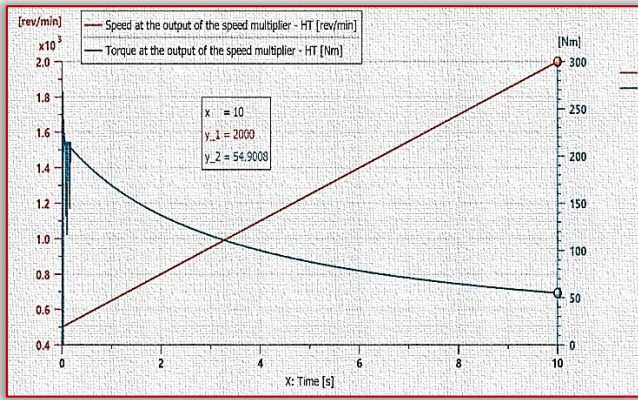
Figure 4 – Variation of the speed and torque at the output of the planetary speed multiplier (HT)

Variation of the speed and torque at the output of the planetary speed multiplier for HT, Figure 4, shows that the speed increase and simultaneously the torque decreases. The speed at the output of the multiplier increases because the input of the multiplier increases too due to the variation of the wind turbine shaft speed and because the torque decreases. The planetary multiplier provides the necessary speed for which the hydraulic pump has a good efficiency and good stability because the mass distribution of the transmission is even.

Variation of the speed and torque at the output of the continuously variable speed multiplier for MT, Figure 5, shows the output value of both parameters remains constant, the only parameter that varies is speed at the input of the multiplier. However, as is well known this type of transmission is capable to operate at a constant speed while the speed of the shaft may vary.
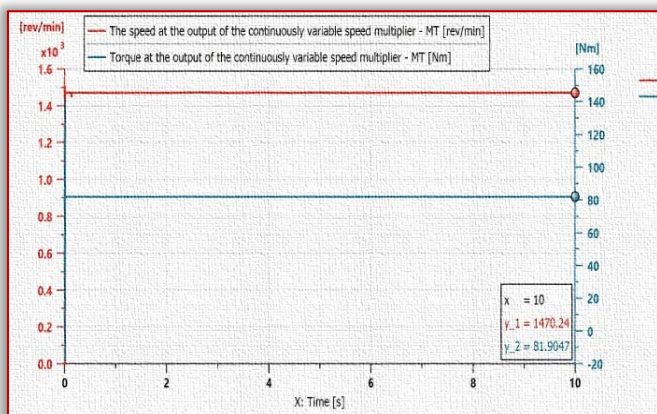
Figure 5 – Variation of the speed and torque at the output of the continuously variable speed multiplier (MT)

Variation of the pump flow rate, internal and external flow losses are shown in Figure 6, and as one can see the open circuit pump flow rate, after a short oscillation caused by the PID regulator, stabilizes. After the speed of the output multiplier shaft speed reaches 500 rev/min and the hydraulic pump enters in the speed zone where it begins to have good efficiency, the flow rate stabilizes. Of course, as in any hydraulic system, there are some internal losses in the hydraulic pump as well as in other system components and

certainly, there are external losses too; both type of losses do not exceed 5.56 L/min.
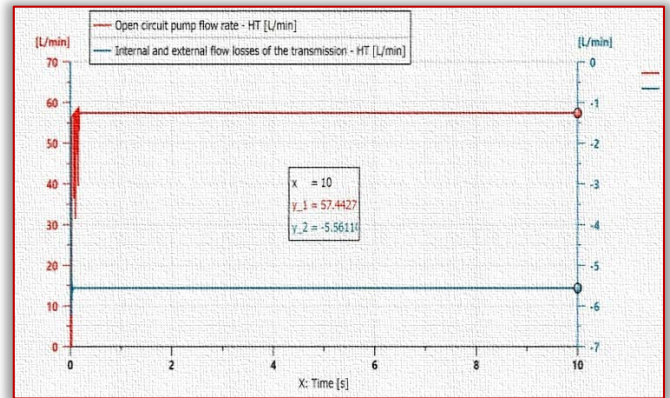
Figure 6 – Variation of the pump flow rate and internal and external flow losses (HT)
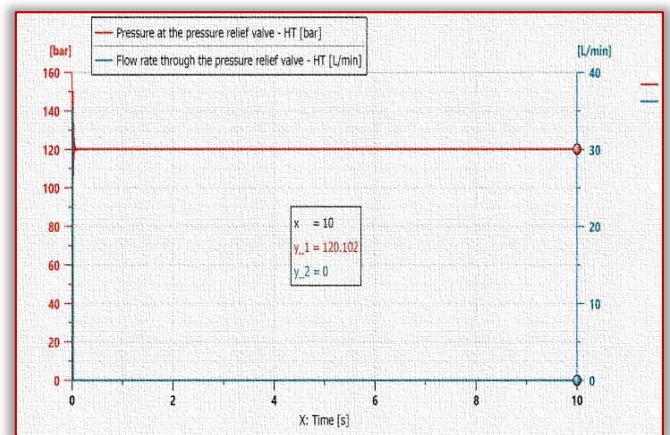
Figure 7 – Pressure and flow rate variation through the pressure relief valve (HT)

To ensure that pressure in the system has the set value and the flow rate through pressure relief valve remains zero, the values of these parameters are verified during the entire simulation. As it is shown in Figure 7, the pressure at the relief valve is 120 bar and the flow rate through the pressure relief valve is 0 L/min, meaning that it remains closed. The relief valve will open when the pressure reaches 150 bar.
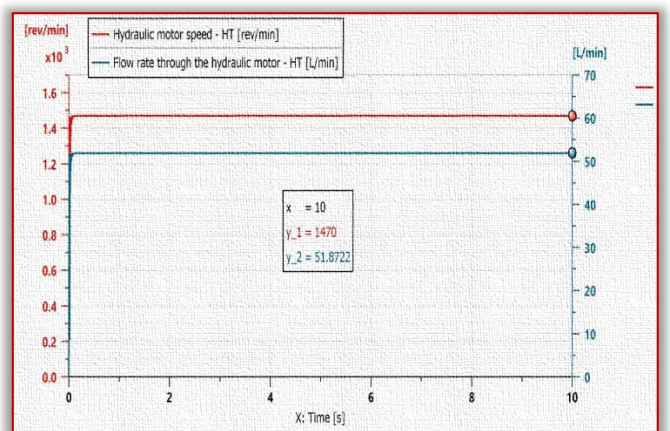

Figure 8 – Variation of the hydraulic motor speed band flow rate through the hydraulic motor (HT)

Variation of the hydraulic motor speed and flow rate is showed in graph in Figure 8; after a short period of variation in the beginning, the parameters become constant during

the rest of the simulation. Speed of the hydraulic motor is monitored with a sensor that sends the value that is measured to the comparator that compares the set value with the output value of speed from the hydraulic motor. Based on the error that the PID regulator receives, it adjusts its output according with the input and makes correction in order to obtain at the HT the desired speed.
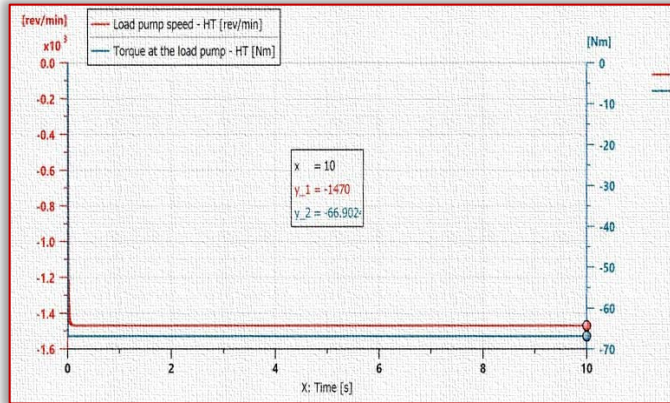

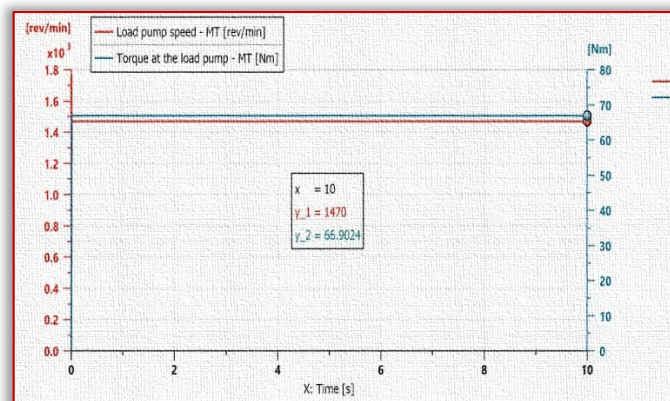Figure 9 a) – Variation of the load pump speed and torque at the load pump (HT)

Figure 9 b) – Variation of the load pump speed and torque at the load pump (MT)

Figure 9 a) is the graph for the variation of the load pump speed and torque for hydrostatic transmission and Figure 9 b) shows the graph for the variation of load pump speed and torque for mechanical transmission. The two transmissions have the same values for these two parameters that are presented in the graphs, which means that frequency is the same, and constant for both transmissions.
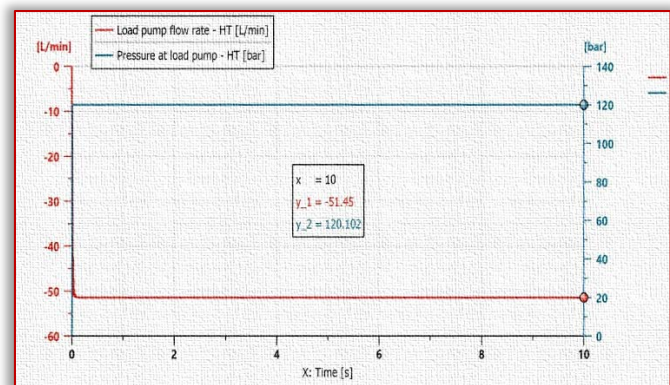
Figure 10 a) – Variation of the load pump flow rate and pressure at the load pump (HT)
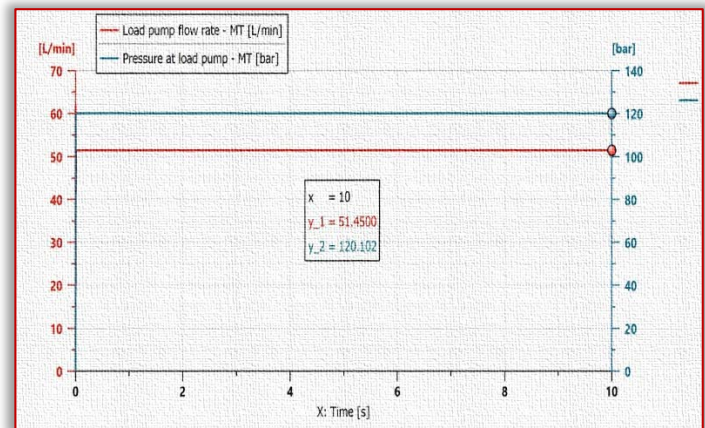
Figure 10 b) – Variation of the load pump flow rate and pressure at the load pump (MT)

Figure 10 a) shows the variation of the flow rate and pressure for the load pump of the hydrostatic transmission and Figure 10 b) shows the variation of the flow rate and pressure for the load pump of the mechanical transmission. Both pumps have the same values of the parameters during the simulation and that means that they generate the same power.
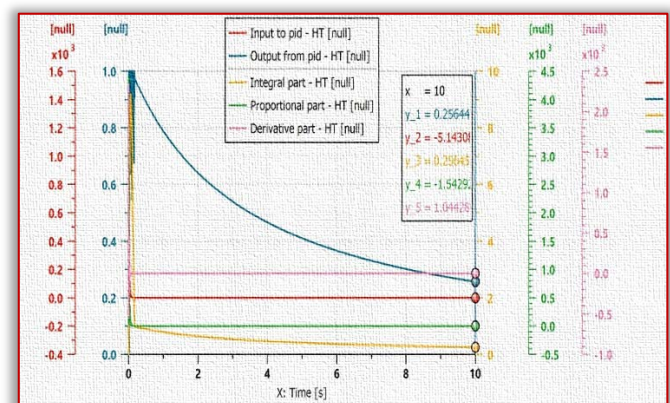
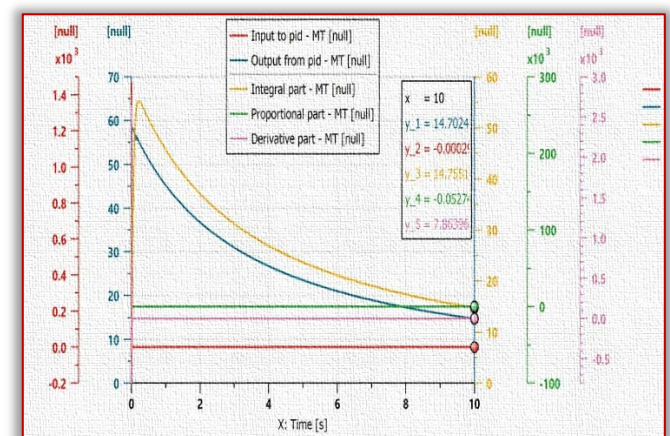Figure 11 – a) PID regulator parameters (HT)

Figure 11 – b) PID regulator parameters (MT)

The graphs in Figure 11 a) and Figure 11 b) show the PID regulator variation of the parameter for HT and MT during the simulation. The PID parameters were calculated with Ziegler – Nichols method before they were introduced in the simulation parameters. Ziegler – Nichols method consists in finding a k_u gain by increasing the proportional gain, k_p, until

output of the control loop remains stable. After finding the k_u, period, T_u, can be found too by measuring the difference between two oscillations. With those two parameters the PID regulator parameters can be calculated. For this simulation, it has been chosen Ziegler–Nichols method with no overshoot.
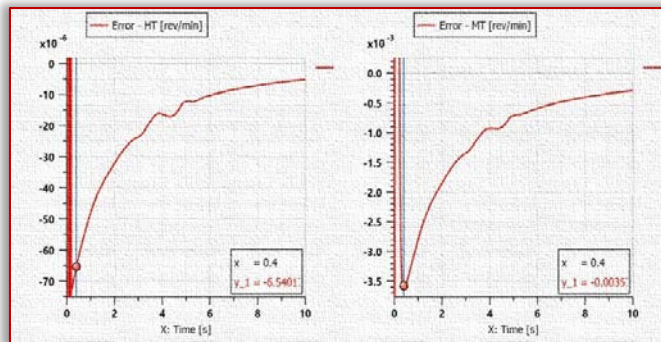

Figure 12 – Error variation for HT and MT

The speed error can be seen in Figure 12 for both transmissions. Comparing the two graphs, one can say that the hydrostatic transmission is more precise than the mechanical transmission because the speed error that enters in the PID regulator of the hydrostatic transmission is 55 times smaller than at the mechanical transmission.

Figure 13 shows the power consumption for HT and MT during the conversion of the wind power to electricity; even if the two transmissions have different power consumption the output power that is produced remains the same. Figure 14 proves that both transmissions have the same output power.
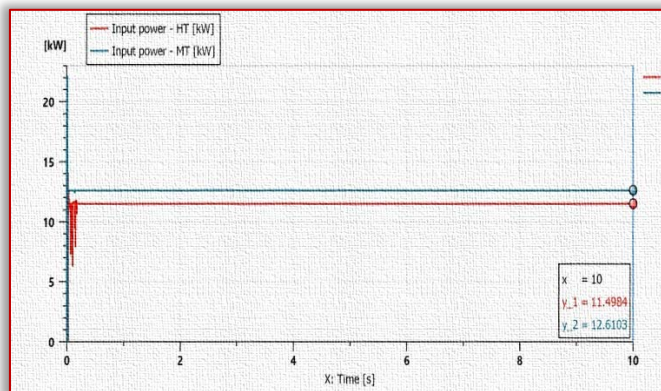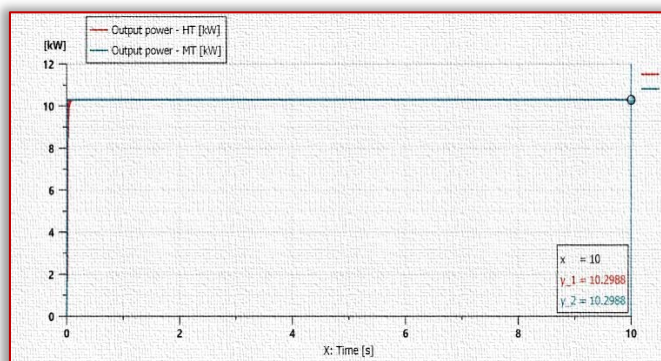

Figure 13 – Input power variation for HT and MT

Figure 14 – Output power for HT and MT

The lost power, Figure 15, is bigger for the mechanical transmission because of the friction in bearings. The friction generates heat and causes premature wear of the transmission. Hydrostatic transmission does not lose that much power because the components are permanently immersed in fluid and, as we know, the fluid has lubrication proprieties.
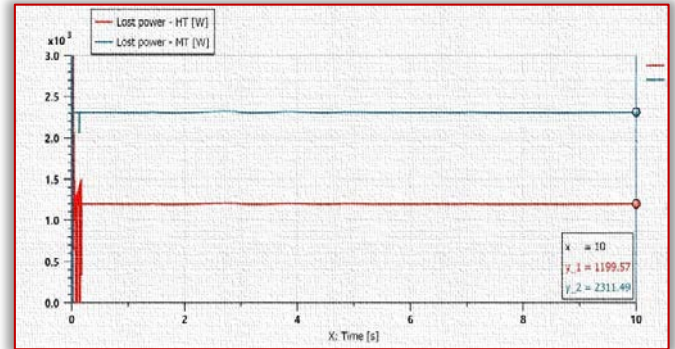

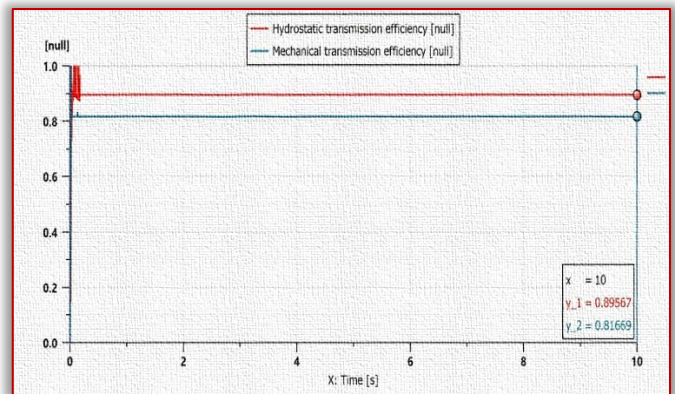Figure 15 – Lost power for HT and MT

Figure 16 – HT and MT efficiency

Figure 16 shows that HT has a higher efficiency than MT, which makes this transmission better than the other; even a small difference of efficiency means a lot in the current situation that we are today when almost everything uses energy. HTs are more reliable and more compact than MTs that need a lot of space for the gearbox to fit.

CONCLUSIONS

≡ Hydrostatic transmission is by 8% more efficient than mechanical transmission.

≡ PID regulator was introduced in the system to maintain constant the output speed for both transmissions, speed that is proportional to the frequency of the generators.

≡ The speed regulation in the hydrostatic transmission is more precise than the one in the mechanical transmission.

≡ Hydrostatic transmission is easy to control and they can perform in various weather conditions.

≡ Hydrostatic transmission adapts easy to the changes of the input parameters such as wind speed fluctuations.

≡ Hydrostatic transmissions are more reliable than mechanical transmissions.

References

[1] Al–Hamadani, H., An, T., King, M., & Long, H. (2017). System dynamic modelling of three different wind turbine gearbox designs under transient loading conditions, International Journal of Precision Engineering and Manufacturing, 18, 1659–1668

[2] Buhagiar, T., & Sant, T. (2013). Analysis of a stand–alone hydraulic offshore wind turbine coupled to a pumped water storage facility, Sustainable Energy 2013: The ISE annual conference, Malta

[3] Cai, M., Wang, Y., Jiao, Z., & Shi, Y. (2017). Review of fluid and control technology of hydraulic wind turbines, Frontiers of Mechanical Engineering, 12, 312 – 320

[4] Dulgheru, V., Dumitrescu, C., Maican, E., Ciobanu, O., & Rădoi, R. (2021). Defining the Main Parameters of a Darrieus Type Wind Turbine with a Power of 1 kW, Hidraulica Magazine, (3), 43–50

[5] Garcia – Bravo, J.M., Ayala–Garcia, I.N., & Cepeda – Aguilar, J.L. (2017). Variable Ratio Hydrostatic Transmission Simulator for Optimal Wind Power Drivetrains, Hidawi International Journal of Rotating Machinery, 5651736

[6] Jiang, Z., Yang, L., Gao, Z., & Moan, T. (2014). Numerical Simulation of a Wind Turbine with a Hydraulic Transmission System, Energy Procedia, 53, 44–55

[7] Lin, S., Qi, P., & Zhao, X. (2020). Power generation control of hydrostatic wind turbine implemented by model–free adaptative control scheme, Wind Energy, 23, 849 – 863

[8] Patriota, A.S.L., Pinheiro, R.F., & Medina – T., G.I. (2020). Harnessing Wind Energy with Hydrostatic Transmission Coupled to an Electromagnetic Frequency Regulator, Preprints, 2020110236

[9] Rajabhandharaks, D. (2014). Control of Hydrostatic Transmission Wind Turbine [Master's dissertation, San Jose State University]

[10] Rădoi, R., David, I., Chiriță, Al., & Popescu, A.–M. (2020). Considerations regarding the use of hydraulic drive systems in the construction and maintenance of wind turbines, Journal of Research and Innovation for Sustainable Society, 2(1), 5–10

[11] Schulte, H. (2014). Control–oriented description of large scale wind turbines with hydrostatic transmission using Takagi–Sugeno models, 2014 IEEE Conference on Control Applications (CCA), 664 – 668

[12] Wang, F., Chen, J., Xu, B., & Stelson, K. A. (2019). Improving the reliability and energy production of large wind turbine with a digital hydrostatic drivetrain, Applied Energy, 251, 1133092

[13] *** Small Wind Turbine & Generators to Power Your Home (2020). https://ygrene.com/blog/sustainable–living/small–wind–turbines–generators–power–your–home

[14] *** RENEWABLE 2020 GLOBAL STATUS REPORT (2020). https://www.ren21.net/wp–content/uploads/2019/05/gsr_2020_full_report_en.pdf

[15] *** https://www.whirlopedia.com/index.php/unconventional–wind–turbines

ISSN: 2067-3809

¹·Andreea–Catalina CRISTESCU, ¹·Ilie FILIP, ²·Vasilica STEFAN,
²·Lucretia POPA, ¹·George IPATE, ¹·Gheorghe VOICU

CAR BRAKING SYSTEM – GENERAL ASPECTS IN A REVIEW

¹·Faculty of Biotechnical Engineering, University Politehnica of Bucharest, ROMANIA
²·National Institute for Research–Development of Machines and Installations designed for Agriculture and Food Industry, ROMANIA

Abstract: One of the roles of the braking systems, which it has to fulfil, is to prevent the wheels from locking and keeping the sliding from falling within certain limits. Also, the primary goal is to ensure the required decelerations and progressive braking, without shocks. The safety of the vehicle, as well as the possibility of full use of speed and acceleration during its operation, is ensured by the braking capacity. Thus, the braking system must meet a number of essential criteria. The advent of automobiles has given rise to the need for the most efficient braking system that can ensure high standards of performance, reliability and safety. The braking system is indispensable for the safety of road users. The need for an efficient and efficient braking system has led to its continuous improvement, becoming more and more complex with the advent of microelectronics. Today, the braking mechanisms are assisted by complex systems such as: the anti–grip system during braking (ABS), which ensures the contact of the wheel with the surface with which it is in contact; electronic stability control system (ESP), which ensures a dynamic stability control, detecting slippage; anti–slip systems, which ensure the stability of the vehicle in different conditions.
Keywords: car breaking system, disk brakes, drum braking systems, brake pads

INTRODUCTION

As early as 5000 BC (Post W., 2019), when the first use of the wheel dates back, mankind was faced with the problem of using a braking system. Over time, it has undergone many improvements, in order to obtain a system as efficient as possible, which corresponds to current needs and technologies.

The first efficient braking system dates back to 1796, representing a wooden shoe–type braking system. It survived for several decades and was later replaced by a system that used damp textiles as a friction material, the latter being in turn replaced by tanned leather.

With the advent of motorized carriages, the need for a much more efficient braking system appeared, so that in 1880, the braking system used ferrule as a friction material. (Cimpeanu & Cimpeanu, 2019)

One of the roles of the braking systems, which it has to fulfil, is to prevent the wheels from locking and keeping the sliding from falling within certain limits. Also, the primary goal is to ensure the required decelerations and progressive braking, without shocks (Tretsiak, Kliauzovich, Augsburg, Sendler, & Ivanov) (Stefan–Ionescu, 2019).

The safety of the vehicle, as well as the possibility of full use of speed and acceleration during its operation, is ensured by the braking capacity. Thus, the braking system must meet a number of essential criteria such as:

≡ Stopping the car safely
≡ Immobilizing the car when it is on a slope
≡ Ensuring required decelerations
≡ Ensuring progressive braking
≡ Minimal effort on the part of the driver
≡ Proportionality between the effort applied to the drive mechanism and the deceleration
≡ Braking force to act in both braking directions
≡ Ensuring braking only when the driver intervenes
≡ Ensuring heat dissipation during braking
≡ Simple shrinkage, easy maintenance
≡ Prevent unwanted acceleration while driving downhill
≡ Immobilizing the vehicle when it is parked (Stefan–Ionescu, 2019, Post W., 2019).

Thus, the braking system is indispensable for the safety of road users. The need for an efficient and efficient braking system has led to its continuous improvement, becoming more and more complex with the advent of microelectronics (Post W., 2019).

MATERIALS AND METHODS

There are 2 types of braking systems to use: disc brake type braking system and clog braking system. The latter are currently used on the rear axle of cars, but their aim is to replace them with disc–type braking systems (Reif, 2019). A breaking system is presented in figure 1.
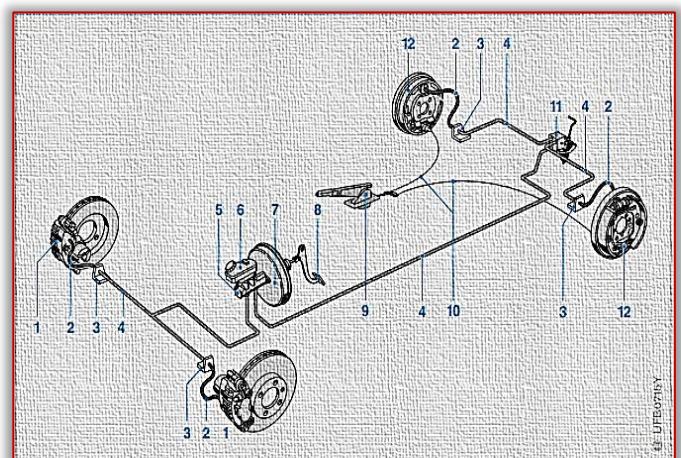

Figure 1 – Conventional braking system on both axles of the car (Reif, 2019)

In order to actuate the braking system, the driver applies force to the brake pedal (8) by moving the rod which

connects the brake pedal to the actuator piston (7). The actuator amplifies the pressing force and transmits it to the rod connected to the main cylinder (6). The main cylinder converts the mechanical force into hydraulic force. Inside the main cylinder, there are two pistons that push the hydraulic fluid from the main cylinder pressure chamber into the brake lines (4) and the brake hoses (2), thus transmitting the hydraulic pressure from the disc brakes (1) to the wheels. The front axles, and the drum brakes (12) are presented the rear axle wheels. If one of the brake circuits fails, the other remains fully functional so that braking is provided by a secondary braking system. The brake fluid container (6) is connected to the main cylinder (6), completing the fluid volume fluctuations in the brake circuits (Reif, 2019).

The parking brake system applies the rear axle brakes (12) via the lever (9) and the parking brake cable (10).

During braking, as the deceleration increases, much of the car's load is moved from the rear axle to the front axle (dynamic axle load change). Thus, the pressure regulating valve (11) lowers the brake pressure on the rear wheels to prevent overloading them. This process is called braking force balancing, unlike the ABS system, where this process involves controlling the braking force (Reif, 2019).

In unfavourable conditions, such as wet asphalt, slippery road, sudden reaction from the driver, it is possible for the vehicle's wheels to lock during braking, making the vehicle uncontrollable. To prevent such situations, the anti–lock braking system (ABS) detects if one or more wheels are gripped, ensuring a constant or reduced pressure for them, preventing wheel locking, and also ensuring the stability of the vehicle. Thus, the vehicle can be stopped safely.
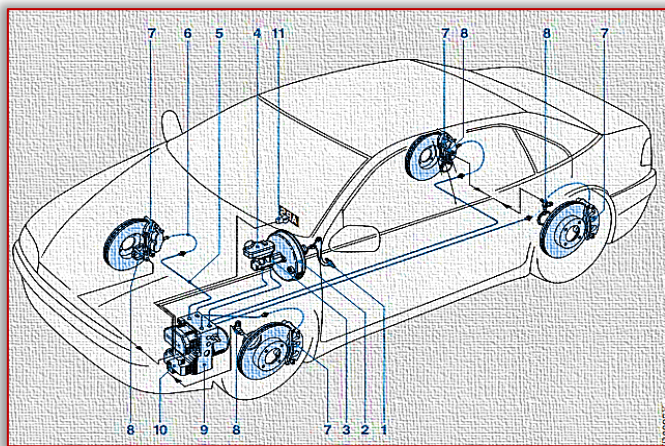

Figure 2 – ABS braking system

The ABS system is based on the components of the conventional braking system, as follows:
≡ brake pedal (1) (Figure 2)
≡ brake booster (2)
≡ main cylinder (3)
≡ Brake fluid reservoir (4)
≡ Brake fluid hoses (5)
≡ Brake fluid hoses (6)
≡ brake pads and discs (7)

In addition, there are:
≡ Wheel speed sensors (8)
≡ hydraulic modulator (9)
≡ ABS control unit (10)
≡ warning light (11) which illuminates when the ABS system does not work (Reif, 2019)

The ABS system must meet a number of requirements, characterized by safety standards associated with the braking response dynamics and braking system technology, such as stability and manoeuvrability, efficiency, timing characteristics and reliability (Reif, 2019)

Thus, the braking system of vehicles plays the main role in the safety of the driver and other road users, being composed of a series of complex elements designed for its proper operation, according to the rules.

DISK BREAK COMPONENTS

A vehicle needs a braking system to stop or adjust its speed depending on the change of road and traffic conditions. The basic principle used in braking systems is to convert the kinetic energy of a vehicle into another form of energy. During a braking operation, not all the kinetic energy is converted into the desired shape. Thus, when braking by friction, a certain energy can be dissipated in the form of vibrations.

There are two types of brakes, namely drum brakes and disc brakes. The latter are widely used. Disc and pad brakes, compared to drum brakes, cool faster, due to a larger friction surface and greater exposure to air flow, there is the ability to self–clean due to centrifugal forces (Rashid, 2014)

Studies have shown that disc brakes are the most effective at stopping cars whose mass is significant, with ever–increasing performance, and whose safety standards are becoming more demanding (Stefan–Ionescu, 2019).

The most important advantages of using disc brakes over drum brakes are the following:
≡ low sensitivity to the variation of the coefficient of friction.
≡ uniform pressure distribution on the friction surfaces and, as a result, uniform wear of the gaskets
≡ large cooling surface and good heat dissipation conditions allow them to dissipate high energy in the form of heat.
≡ stability in operation at low and high temperatures – balancing axial forces and lack of radial forces
≡ the possibility of operation with small clearances between the friction surfaces which drastically decreases the commissioning time
≡ independence of braking efficiency from the degree of wear of the friction linings
≡ ensuring the same braking moment regardless of the direction of travel – the deformations of the parts in the friction torque much more advantageous: the disc deforms in the rough axial direction unlike the radial deformation of the drum which causes change in its shape, thus affecting the play between friction surfaces;
≡ easy replacement of gaskets (Stefan–Ionescu, 2019)

In the case of the disc brake system, the pads are pressed onto a rotating disc when braking, generating heat due to friction between the pads and the disc. This is transferred to the outside environment, resulting in the cooling of the disk. (Rashid, 2014) Such a braking system consists of a caliper, fixed by screws, on the spindle port, a disc installed between the hub and the wheel. The brake pads are embedded in the caliper, which under the action of hydraulic cylinders, will press on the disc and stop its rotational movement.

DISC BREAK CALIPER

The disc brake caliper can be fixed or floating. In the case of the fixed caliper (Figure 3), it is absolutely necessary to place two pistons on each side of the disc, while in the case of the mobile caliper (Figure 4), only one piston can be arranged (Stefan–Ionescu, 2019).
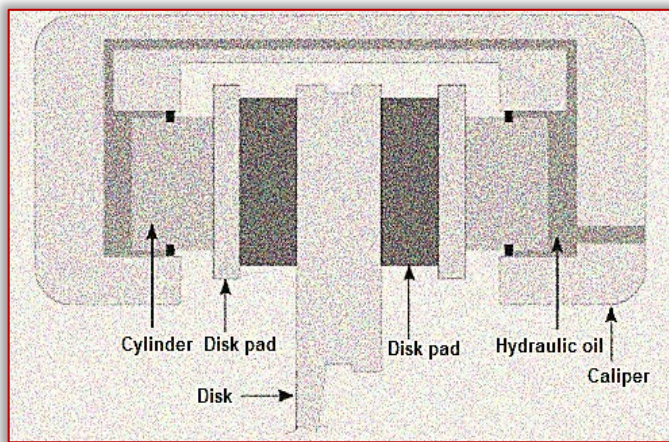

Figure 3 – Fixed caliper (Rashid, 2014)

When pressure is applied, the piston moves and pushes the inner brake pad. When it comes in contact with the surface of the disc, the stirrup moves in the opposite direction so that the outer plate comes into contact with the surface of the disc. Following this process, the rotational motion is stopped (Reif, 2019).
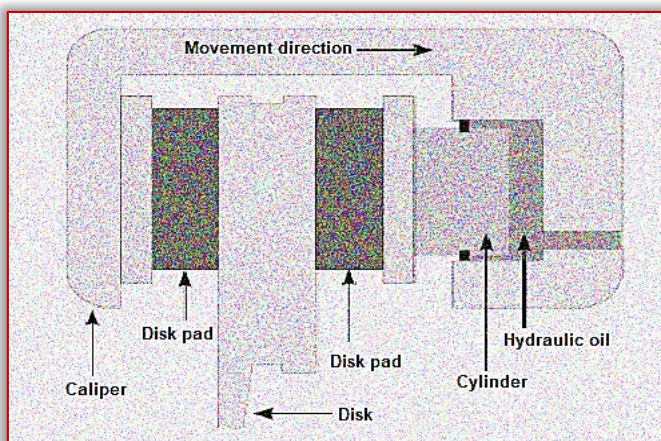

Figure 4 – Mobile disk (Rashid, 2014)

In general, inner and outer plates have different contact pressure distributions and different wear behaviors, due to the different support, drive system and the difference in thermal deformations of the internal and external surfaces of a. (Rashid, 2014)

BRAKE PADS

The brake pads are made of a rigid metal plate and a friction material as an adhesive part. The latter must withstand high temperatures, pressure and friction. The contact surface is relatively small, which means that the friction material is subjected to high pressures and forces, significant thermal loads and dynamic stresses 20 times higher than drum brakes. The friction material is the element subject to wear, which means that the brake pads require frequent replacement compared to the brake disc. They have a small surface area compared to the braking they develop (Stefan–Ionescu, 2019).

A good brake pad must meet certain thermo–mechanical requirements and develop a stable coefficient of friction. The stiffness of the friction material is relatively low, but the metal plate must be rigid to transmit the force provided by the hydraulic piston and to distribute the pressure evenly on the contact surface with the disc. This allows a uniform wear of the gasket, maintaining a constant braking and an optimal distribution of heat flow (Stefan–Ionescu, 2019).
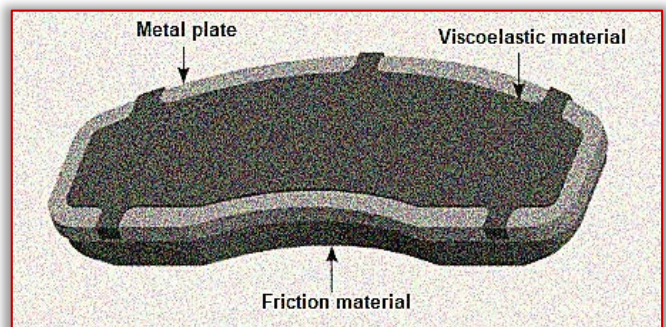

Figure 5 – Disk pad (Rashid, 2014)

In some cases, an additional layer of material, called a substrate, is added between the friction material and the metal plate, in order to absorb the vibrations resulting from the contact of the pad and the brake disc (Rashid, 2014).

The role of the metal plate is to support the friction material. They can be mounted by various methods such as adhesion, welding or clamping (Rashid, 2014).

The viscoelastic material is found between the back of the metal plate and the piston, the case of the fixed stirrup, or the metal plate and the housing of the movable stirrup. Its role is to dampen the vibrations resulting from the contact between the plate and the disc. They can be made of a steel core with a viscous coating or a viscoelastic core with a metal coating (Rashid, 2014).

BRAKE DISC

The brake disc is fixed to the wheel hub and has the same rotating motion as it. It is made mostly of gray cast iron, being very resistant to wear. In the case of high–performance vehicles, the brake disc has an aluminum or steel hub or bowl and a ceramic carbon brake pad (crown), assembled by screws (Stefan–Ionescu, 2019).

The braking power of the disc brake is determined by the speed at which the kinetic energy is converted into heat, due to the frictional forces between the plate and the disc.

The resulting heat must be removed as soon as possible, otherwise the temperature of the disc may increase and affect the braking performance (Rashid, 2014).

Thus, in order to obtain optimum performance, ventilation holes have been designed in the brake discs which increase the cooling speed.

Brake discs can be divided into two categories:

≡   solid brake disc

≡   ventilated brake discs

The solid brake disc is the most rudimentary model, while the ventilated disc has holes on the surface of the disc and / or channels between the two discs, facilitating air circulation and heat exchange with the environment. Ventilated brake discs have a higher cooling rate, so a lower surface temperature. Low temperature reduces the risk of brake fading and disc and pad wear (Rashid, 2014).

Both the solid and the ventilated disc have or do not have a mounting hub (bowl). The bowl increases the distance between the axle friction surface and the disc surface, making it easier to cool the disc and helping to protect the bearings from the high temperature wheel generated during braking operation. A schematic description of these two types of disks is shown in Figure 6. (Rashid, 2014)
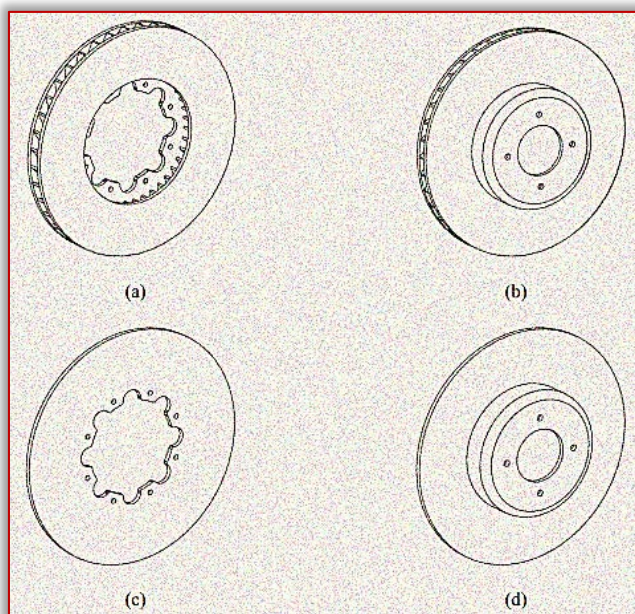

Figure 6 – Representation of different types of brake discs
a) disc with ventilation without hub b) disc with ventilation hub; b) solid disc without hub; d) solid disc with hub (Rashid, 2014)

If the bowl is not part of the brake disc, it is called a hybrid or composite brake disc.

There are different ways to mount the disc on the bowl. Figure 7 shows two methods of mounting the disc on a bowl, with a connecting element, a steel screw or a ceramic bolt. They are mounted in the radial direction of the disc (Rashid, 2014).
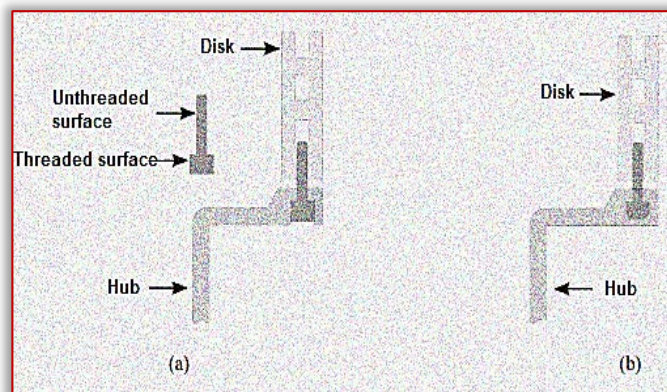

Figure 7 – Representation of the disc fixed on the hub
a) disc with ventilation without hub b) disc with ventilation hub; (Rashid, 2014)

For brake discs with ventilation, different shapes of ducts are used: radial straight, curved, diamond–shaped or teardrop, arched (Figure 8). Each configuration provides a unique airflow, but in all cases, air enters the center of the disk and is released through its outside. Due to the air circulation, high voltages can occur in the center of the brake disc, which is a disadvantage in case of heavy use (Rashid, 2014).
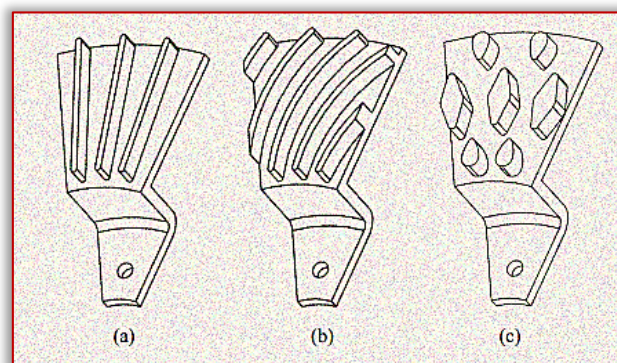

Figure 8 – Representation of brake disc ventilation ducts
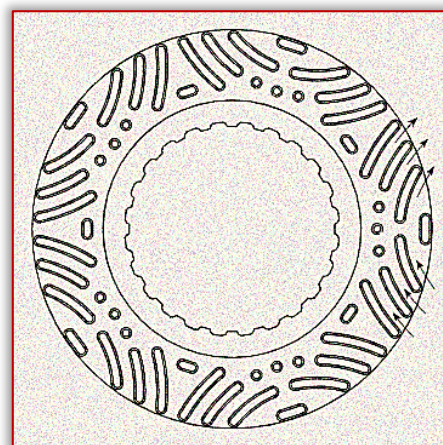a) straight; b) curved; c) diamond and tear (Rashid, 2014)

Figure 9 – Representation of airflow circulation in brake discs (Rashid, 2014)

RESULTS

Disc brakes are known to experience severe working conditions in conditions of thermal fatigue, wear and heavy mechanical loads. Among various materials, cast iron is the most widely used material in disc brakes because it has a

unique combination of excellent wear resistance and higher heat transfer coefficient.

Different parameters, including alloying elements and their morphology, affect the tribological behavior of cast irons. There are several studies on the effects of alloying elements, on the wear resistance of gray cast iron. Silicone, chromium and manganese are known to have a positive influence on the wear resistance of the brake disc (Abutu, 2018).

It is expected that higher hardness and tensile strength can be achieved, in combination with a lower wear loss, by adding silicon and chromium as an alloy to the gray cast iron. In addition to the chemistry and microstructure of the alloy, abrasion and wear test variables also have prominent attributions to the wear behavior of gray cast iron. Whether the test is performed under dry or lubricated conditions, the speed of the parts moving continuously during the test and the applied load have an effect on the wear behavior of the alloys.

For example, gray cast iron shows a much better wear resistance under lubrication conditions, obviously due to the lower coefficient of friction. It is known that gray cast iron alloys have a characteristic lubrication in themselves due to the presence of graphite particles in their microstructures. Therefore, cast iron is still by far the most widely used material in disc brakes in trains and cars (Abutu, 2018).

Given that disc brakes are an essential component of passenger safety in the vehicle, it is essential to understand the degradation mechanisms of this component.

Degradation and failure of the disc brake is very complicated due to the simultaneous contributions of mechanical loading, surface conditions and thermal stresses. The fact that the disc brakes face dynamic loading conditions makes the interpretation of the faults even more complicated. It is postulated that surface washing, formed during abrasion, creates spots that can initiate cracks. Subsequent loading causes the disk to crack and malfunction. The reason for the cracks is caused by fatigue caused by cyclic thermomechanical loading (Abutu, 2018).

As a result of the brake disc malfunction, the phenomenon of brake vibration occurs. This term refers to the uneven braking torque, resulting in fluctuations in braking force that occur during a complete rotation of the disc. These phenomena are classified into thermal trepidation and cold trepidation. Thermal shaking occurs during deceleration at high speeds, and cold shaking can occur at any speed (TEXTAR, n.d.). Thermal vibration can be defined as a resonant vibration in a frequency range between 100 and 250 Hz. Sound intensity varies throughout deceleration, but does not affect braking. These fluctuations can be felt as a vibration of the steering wheel, impulses in the brake pedal and the vibration of the chassis components.

Braking speed depends on the force applied to the pedal. Thermal vibration can usually be identified by a circular arrangement of points on the friction surface of the disk. These axles are caused by local overheating during braking, which causes the transfer of materials from the brake pad to the brake disc and / or the permanent change in the structure of the brake disc cast material. Usually, the transferred material is removed during normal braking. To prevent the risks, it would be ideal to replace the disc and not recondition it (Abutu, 2018)..

The performance of the brake depends not only on the thermal and mechanical properties of the disc friction materials, but is also affected by the topography of the contact surfaces and the third body formed as a result of wear processes (Kemmer, 2002, Österle, et al., 2008)

In addition to the causes mentioned above, there are other factors that can cause thermal shock, such as improper wheel balancing, worn wheel suspension bearing parts, steering system and incorrect front axle alignment. The trepidation is caused by multiple factors, making it difficult to identify the exact cause (TEXTAR, n.d.).

CONCLUSIONS

Disc brake is a complex system and understanding the various issues related to its design and operation requires expertise in various disciplines, e.g. tribology, materials science, fluid dynamics, vibrations, etc.

Disc brakes have evolved over the decades due to extensive research and development. There are still many phenomena that are not fully understood. For the complete and realistic analysis of disc braking systems, the further development of nonlinear finite element models, which could simulate the realistic evolution of the contact interface, is crucial.

The problems that have attracted a lot of attention from the research community are represented by the phenomena that appeared in the braking system, such as squeaking, vibrations, tremors. Due to the continuous development of disc brake systems, they have become less and less common, but the problem has not yet completely disappeared. The problem of predicting sensitivity to brake application remains a difficult task for the brake research community. (Rashid, 2014)

References

[1]   Abutu, J.–A. (2018). An overview of brake pad production using non–hazardous reinforcement materials. Acta Technica Corviniensis – Bulletin of Engineering, 3.

[2]   Cimpeanu, C. I., & Cimpeanu, I. S. (2019). Automobilul: Siguranţa Rutieră Şi Poluarea. Resita: Editura Tim.

[3]   Kemmer, H. (2002). nvestigation of the Friction Behavior of Automotive BrakesThrough Experiments and Tribological Modeling. Universitat Paderborn.

[4]   Österle, W., Dörfel, I., Prietzel, C., Rooch, H., Cristol–Bulthé, A.–H., Degallaix, G., & Desplanques, Y. (2008). A comprehensive microscopic study of third body formationat the interface between a brake pad and brake disc during thefinal stage of apin–on–disc test. Wear(268), 781–788.

[5]   Rashid, A. (2014). Overview of disc brakes and related phenomena – A review. International Journal of Vehicle Noise and Vibration, 10(4), 257.

[6]   Reif, K. (2019). Antilock braking system (ABS). În K. Reif, Car braking–system components. Function, Regulation and Components (pg. 74–93). Wiesbaden,: Springer Vieweg.

[7]   Reif, K. (2019). Car braking–system components. În K. Reif, Brakes, Brake Control and Driver Assistance Systems. Function, Regulation and Components (pg. 28–39). Wiesbaden: Springer Vieweg.

[8]   Stefan–Ionescu, R. (2019). Optimizarea constructiva si ecologica a componentelor sistemului de franare al autoturismelor. Brasov: Universitatea Transilvania din Brasov.

[9]   TEXTAR. https://textar.com/

[10]   Tretsiak, D. V., Kliauzovich, S. V., Augsburg, K., Sendler, J., & Ivanov, V. G. (fără an). Research in hyraulic components and operational factors influencing the hysteresis losses. Journal of Automobile Engineering, Procediings of the Institution of Mechanical Engineers, 1633–1645.

[11]   W., P. (2019). Car braking systems (Vol. Car braking–system components. Function, Regulation and Components). Wiesbaden: Springer Vieweg.

[1.]Iustina STANCIULESCU, [1.]Horia VLAD, [1.]Andrei GABUR, [2.]Florin NENCIU

PROOF OF CONCEPT OF AN AUTOMATED SYSTEM USED FOR PRE–COMPOSTING ORGANIC WASTE

[1.]Electronic Waste Management SRL, ROMANIA
[2.]National Institute of R&D for Machines and Installations Designed to Agriculture and Food Industry (INMA), Bucharest, ROMANIA

Abstract: A wide range of novel waste management machinery have been researched recently, due to the growing interest in composting technologies. Applying novel processing technologies for organic wastes has 2 major benefits: size and volume reduction and production of a natural fertilizer that can improve the soil quality and reestablish the properties of the soil where is needed. Due to the generation in high quantities of the organic waste, a rapid, viable solution is needed. The goal of this study was to provide a proof of concept for an urban pre–composting equipment. The advantage of using a bioreactor for the decentralized organic waste treatment is the considerable reduction of the total volume of the waste, allowing a higher quantity of processed material, in safe working conditions for both the environment and human health.
Keywords: automated composting system, organic waste management

INTRODUCTION

Food losses and food waste has become a global concern and a priority, in order to achieve the Sustainable Development Goals Target. Over the last years the interest into the food losses and food waste increased, especially due to some major management problems, which generates challenges to the environment, food security and natural resources.

At the global level the political agenda includes the reduction of the food losses and food waste. Therefore, the European Union, United States, the African Union have been taken actions to work towards the targets established of reducing food waste by 50% by 2025–2030, (Cabeza et. al. 2013; Hanson et al., 2016).

According to the Food and Agriculture Organization (FAO) of the United Nations, one third of the food production, which was meant for human consumption, is being wasted. This means a loss of USD 750 billion (FAO, 2013; Gustavsson et al., 2011). The studies revealed that the European Union generate 100 million tons of food waste and food loss every year, 45% coming especially from households (FUSIONS, 2015).

Figure 1. Food Recovery Hierarchy (epa.gov/sustainable–management–food)

The European Commission funded several projects focused towards a more resource efficient Europe focused on reducing the waste and improve the valorization of the food resources throughout the entire supply chain (Östergen et al., 2014, FUSIONS, 2016). According to the Food Recovery Hierarchy, each tier focuses on different management strategies and prioritizes actions to prevent and divert food waste and food loss.

Composting has been adopted mainly by cities in order to divert organic waste materials from landfills and create a new product which can be used for agricultural purposes at low cost. (Hargreaves, et al., 2008).

This direction of composting has attributes into the environmental factors and economic factors. Landfill capacity can decrease and also all the costs involved like transportation and materials, using the compost into the agriculture as fertilizer decreases the rate of artificial fertilizers, and the most important aspect is that the process increases the capacity of households for recycling (He et al., 1992; Otten 2001; Hansen et al., 2006; Zhang et al., 2006).

In order to obtain a good fertilizer during a short period of time through the composting process, different types of equipment emerged.

Feasible alternatives to door–to–door collection, are currently implemented in a number of European countries (Austria, Switzerland, Germany, UK, Belgium, Netherlands, Sweden and Norway) (Siebert et al., 2015). According to Sundberg et al., (2011), when organic waste is collected in classical containers, it undergoes an uncontrolled breakdown through anaerobic fermentation, resulting in odor issues and the production of leachate. While this method has no detrimental impacts on the anaerobic digestion, due to the compaction, it releases moisture in the waste, and resultant low porosity.

Sakarika et al., (2019), assessed a pre–composting technology that had the role of controlling the breakdown of organic matter, reducing time and space requirements at the final main composting stage.

Composting is the process of reducing organic substances from vast volumes of decomposable materials to smaller
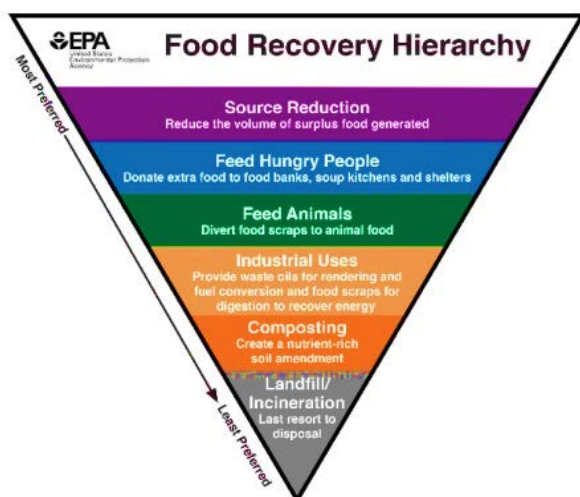
volumes of relatively stable decomposable materials. The carbon–to–other–element ratio is brought into equilibrium in this process, preventing temporary nutrient immobilization.

The classic method of composting was to pile organic materials and let them stand for a year, but the method is very long, valuable nutrients are lost during the process, and organisms, some weeds, weed seeds and insects are not properly controlled (Raabe, 2015).

New composting technologies have recently been developed that address some of the issues associated with traditional composting. Compost can be generated in 2 to 3 weeks using this method. Extra effort on the part of the composter is necessary in exchange for the time savings, but the effort is justified for people who desire big amounts of compost or who want to transform items that would otherwise be wasted into usable compost.

To achieve the correct C/N ratios, it is necessary to identify the food waste composition and define the proportion of different food waste categories before beginning the composting process. Following the assessment of physico–chemical parameters, regression analysis can be successfully utilized to determine the quantities of each type of waste in order to attain the appropriate C/N ratio.

Compostable materials should have a carbon to nitrogen ratio of 25–30 to 1 for the composting process to be most effective. This is difficult to quantify, but blending equal volumes of green plant material with equivalent volumes of naturally dried plant material, produces a carbon to nitrogen (C/N) ratio of around 30/1. Grass clippings, old flowers, green pruning, weeds, fresh rubbish, and fruit and vegetable wastes are all examples of green materials. Dead, fallen leaves, dried grass, straw, and moderately woody materials are all examples of dry material.

Salla (2016) evaluated on–farm composting of vegetable organic waste, under cold climate conditions of Eastern Canada, using bark or straw as bulking material. Feedstock was added at two–week intervals for the first six weeks, and the compost readjusted the quantities in order to have 65% water content and a C/N ratio of 30. He concluded that the mature composts have been obtained after several weeks of composting, and the analysis showed adequate physicochemical properties, being also free of E. coli. He also emphasized the importance of screening the row material in order to eliminate foreign matter before their use as soil organic matter amendment.

It's difficult to use fruit and vegetable waste as the only compost feedstock, since their moisture content is above 80% and their porosity is rapidly depleted (Sundberg et al., 2013; Chang and Chen, 2010).

Inside the composting equipment fruits and vegetables are crushed by their own weight in a short time, and the plant cells that provide structural strength and rigidity are damaged, allowing water to fill the pores of the composting mass. Plant cells decompose quickly due to microbial action in these conditions, and the pH drops, hindering the well–functioning composting microorganisms and lowering composting effectiveness (Sundberg et al., 2012). To overcome these constraints, the physical properties of composting recipes must be adjusted (Awasthi et al., 2014).

Bhave and Kulkarni (2019) researched the influence of active and passive aeration on composting of household biodegradable wastes. Their main results confirmed that both types aeration systems performed well under continuous loading, however the maturation period required for actively aerated reactor was 37.30% less efficient than the naturally aerated system.

The present paper assesses a small equipment for organic waste processing, an intelligent composting machine that can convert the organic waste into compost in a shorter period of time. The process is obtained by using a consortium of thermopile bacteria (Ecoman, Foodie user manual).

MATERIAL AND METHOD

The biological process of the FOODIE is using microorganism to transform the organic waste. By maintaining the temperature, air flow and moisture, allows the bacteria to break down the organic waste into compost within 24 hours, and reduce the volume by 85%. The tests were performed on an automatic composting equipment for organic waste management Ecoman – Foodie, and the operational mode was customized according to the type and nature of the waste (Figure 2).
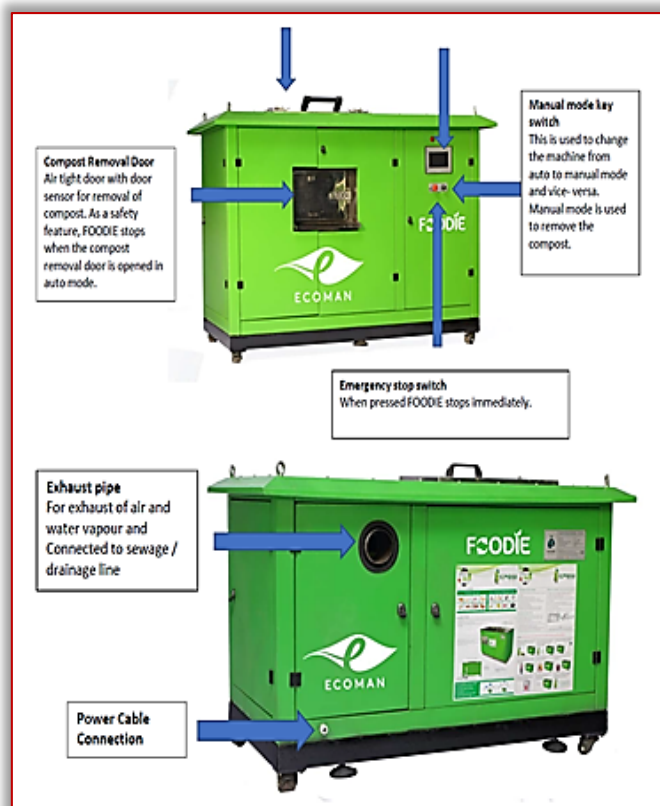

Figure 2. ECOMAN FOODIE composting equipment (Ecoman Foodie Manual, 2021)

The equipment is formed by a composting tank, with a humidity sensor, heater, mixing blades and exhaust system. Food waste from a supermarket chain was introduced into

the equipment. Previously, the waste was separated so that there was no plastic, metal and other contaminants in the mixture (Figure 3). The waste is then mixed using mixing blades, according to a predetermined schedule, depending on the nature of the introduced waste, as seen in Figure 4.

Figure 3. Adding a mixture of organic material to the composter consisting of fruits, vegetables, meat, and dairy

Figure 4. The operation of mixing and aerating the organic matter inside the equipment

When the composting tank is filled, the moisture sensor detects the humidity and the heating system starts. The parameters are controlled using a programmable logic controller, which also helps with process customization (Figure 5). The water content from the organic matter is evaporated and it is released as vapors. It is highly important the sorting stage before composting, otherwise may arise processing isues as seen in figure 6, where several small contaminants remained in the mass of processed organic matter.
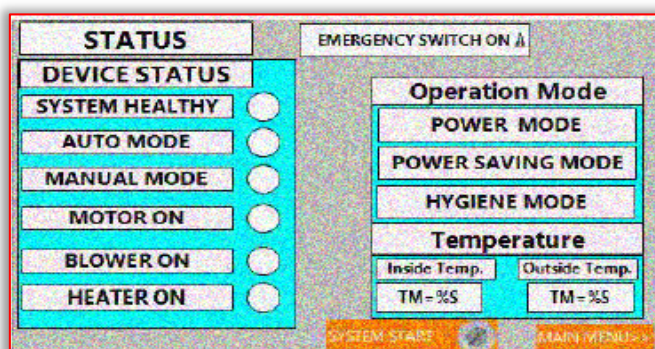

Figure 5. Parameter display and process customization

The remaining matter, after water content is released, starts to decomposed due to the microbial activity. The equipment does not emit loud or disturbing noises, as it does not use grinding or mechanical crushing processes, being equipped with internal blades that use exclusively the process of homogeneous mixing of waste. A mixture of sawdust and special cultures of microorganisms are used for organic matter decomposing. At the end of each compost extraction, a small ratio of compost ramains in the equipment to guarantee a continuity of the production of microorganisms. The equipment complies with both Romanian legislation and the European legislation, namely: REGULATION (EC) No 1069/2009 and REGULATION (EU) 142/2011.

Figure 6. Example of incorrect separation of plastic waste, leading to compost contamination

Electrical conductivity, moisture, pH, ash content are being measured every week, while nitrogen and carbon contents were determined at the beginning and the end of the composting period.

In order to kill any pathogens that could develop in the process, we introduced a sanitation phase, which involves maintaining a high temperature (70 degrees Celsius) for an hour. This stage of sanitization is necessary to ensure that there will be no pathogens at the end of the composting process (eg E–coli, Salmonella, etc.).

The composting equipment has been fed with oraganic waste for a period of 3 months. In this time it has been followed a recipe which includes: several types of organic waste such as fruits, vegetables, fruit and vegetable peels, eggs, eggshells, fish, chicken or fish bones, shells , dairy products, bakery products, meat or processed meat preparations, leaves or dried grass.

RESULTS

Samples of the compost have been tested by an authorized laboratory. Have been found that from the organic waste introduced, have been obtained 92.55% dried substance with a 4.4 pH, 93.05% and a total organic carbon of 45.62%. Also what is very important is that no Escherichia coli or salmonella spp. have been detected.

The tested working methodology envisaged a temperature increase continuously until reaching the value of 50 degrees celsius. The temperature is increased using a ceramic heater, which is mounted on the bottom of the equipment. After reaching this temperature, the heater stops, until the

temperature drops below 40 degrees Celsius, then starts again. During this time, the other mixing and steam extraction functions work without being affected. The humidity extractor has been set for a 10 minute operation with a 5 minute break.

The variation of the mixture temperature, at the surface where the temperature is homogeneous, can be observed in the graph below, for a period of 24 hours. The moment the material is introduced in the equipment generates a sudden variation of the temperature, considering that the waste is cold and humid.
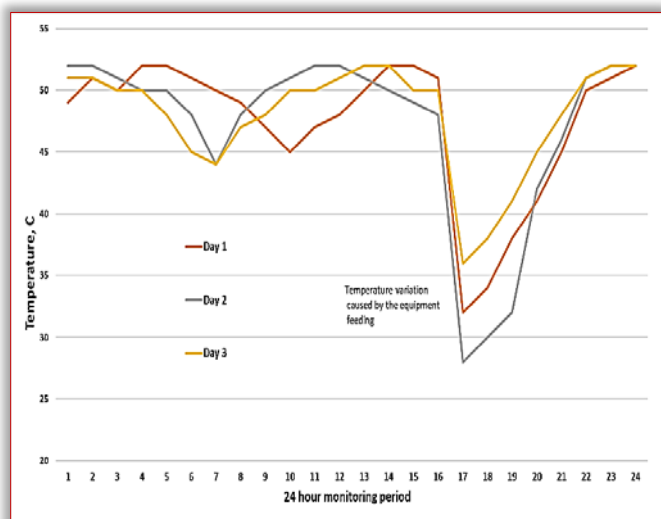

Figure 7. Temperature variation within 48 hours in the composting equipment

It can be seen that, although the upper temperature is set at 50°C, due to the heat inertia, it rises to 52°C. After the heater stops, the temperature drops gradually to 45°C, this being the temperature set for the heater to start again. At 4 pm (16^{00} on the graph), the daily supply of material takes place this explaining the sudden drop in temperature. The process then resumes, and in the period 16^{00}–19^{00} can see the increase in temperature, that returns in the range of 45–52°C.

The temperature range was chosen this way because the main objective was to reduce the volume of raw material, in order to maximize the processed waste.

The correct decomposition of organic matter have been detected by the pleasant odor of the mixture, by the heat produced (naturaley by the process), by the growth of white fungi on the decomposing organic material, by a reduction of volume, and by the change in color of the materials to dark brown. Using the equipment using the proposed processing methodology, several quality indicators were obtained, no unpleasant odors were eliminated from the process, while the presence of bacteria and fungi indicated an efficient level of processing. The color of the material changed within 24 hours, and the material became homogeneous and crumbled (Figure 8).

Insects do not survive the composting process, therefore the equipment can be placed inside production halls without disturbing the activity due to the presence of the insects. In addition, most weeds and weed seeds are killed by processing. However, the ability of the equipment to destroy highly resistant weed seeds has not been tested.

Figure 8. Depicting of the compost characteristics during processing (continuous processing for 3 weeks, adding vegetable waste every day)

After processing, the mass of compost obtained was matured, in order to obtain a quality product, without mechanically intervening on it. Therefore, at the end of the composting process using Foodie equipment and after it has been matured for another two weeks, the compost looks like in figure 9.

Figure 9. Depicting of the compost characteristics during processing (continuous processing for 3 weeks, adding vegetable waste every day)

The colour is middle brown, no plant remains or seeds have been identified. Organic matter and elemental contents are determined on dry matter basis. The analytical results on dry matter basis are used for compost quality comparison. To determine the moisture content, compost samples are dried at 103°C until constant weight is achieved. Weight loss equals moisture loss, based on which moisture content or dry matter content of the compost is calculated. A moisture content of 38% was determined (the optimal range followed being 40–45%).

The organic matter or carbon content of compost is of high importance especially if it is used to enhance soil organic matter content. Low organic matter values in compost can result from the use of purely organic waste streams while a high level of organic matter can be an indicator of an unfinished composting process or unstable compost. Continutul de substanta organica opbinut in faza de procesare utilizand echipamentul a fost de 78%, iar in urma maturarii a fost determinat un coninut de 68% (50–60 % being the desirable values for most compost uses). Total organic carbon obatined, at a pH of 5.2, was determined to be 45,62%. Major and secondary nutrient content of compost is important, in order to estimate the fertilizer value and to know how much of the compost is preferably or can be legally applied for different types of soil. Repeated applications of compost rich in certain elements can be useful to overcome an imbalance of the nutrient status of the soil.

The total nitrogen value had a very good value of 2.76 % dr. subst., total phosphorus % dr. subst., calcium 13913 mg/kg dr. subst., potasiu 13931 mg/kg dr. subst., zinc 28.60 mg/kg dr. subst., the other parameters/heavy metals being in normal parameters.

CONCLUSIONS

This study showed that food waste from supermarkets and grocery stores could be composted on local sites using high–performance composting equipment, provided with a monitoring system and sensors to control the process. The proposed process and equipment can convert organic matter into quality compost in a short a time, ranging from 14 to 21 days.

Although the performance of the equipment is high, and it manages to speed up the composting process and kill pathogens, it is recommended to be used a maturation stage, to further reduce organic matter. The higher presence of organic matter is caused by the fact that the material is added daily, while the organic material added in the last 2 days did not have time to be fully processed.

Rapid composting have proved to kill all plant diseases and the the sanitization phase proved that it can destroy pathogenic germs from meat, by maintaining a high temperature (which can vary depending on the case from 60–70°C). The compost being produced on the site can be accepted by the farmer as a soil organic amendment. However, the row material needs to be verified before use to remove potentially foreign matter and contaminants such as plastics, labels, gloves, or elastic bands.

Acknowledgment

References

[1] Awasthi, M.K., Pandey, A.K., Bundela, P.S., and Khan, J. (2015). Co–composting of organic fraction of municipal solid waste mixed with different bulking waste: Characterization of physicochemical parameters and microbial enzymatic dynamic. Bioresource Technol. 182:200–207.

[2] Bhave P.P., Kulkarni B.N., (2019). Effect of active and passive aeration on composting of household biodegradable wastes: a decentralized approach, International Journal of Recycling of Organic Waste in Agriculture, vol. 8 (Suppl 1):S335–S344

[3] Cabeza, I.O., Lopez, R., Ruiz–Montoya, M., and Diaz, M.J. (2013). Maximizing municipal solid waste—vegetable trimming residue mixture degradation in composting by control parameters optimization. J. Environ. Manage. 128:266–273.

[4] Cerda, A.; Artola, A., Font, X.; Barrena, R., Gea, T., Sánchez, (2018). A. Composting of food wastes: Status and challenges, Bioresour. Technol. vol. 248, p. 57–67.

[5] Chang, I.J, and Chen, J.Y. (2010). Effect of bulking agents on food waste composting. Bioresource Technol. 101:5917–5924.

[6] Gustavsson, J., Cederberg, C., Sonesson, U., Van Otterdijk, R. and Meybeck, A., 2011. Global food losses and food waste.

[7] Hansen, L.T., Olson, L., Kerr, J., McMellen, C., Kaplowitz, M. and Thorp, L., 2008. RECYCLING ATTITUDES AND BEHAVIORS ON A COLLEGE CAMPUS: USE OF QUALITATIVE METHODOLOGY IN A MIXED–METHODS STUDY. Journal of Ethnographic & Qualitative Research, 2(3).

[8] Hargreaves, J.C., Adl, M.S. and Warman, P.R., 2008. A review of the use of composted municipal solid waste in agriculture. Agriculture, Ecosystems & Environment, 123(1–3), pp.1–14.

[9] Ecoman food processing equipment, Foodie user manual, 2021.

[10] European Commission Food Safety Home Page, (2017). United States Department of Agriculture

[11] Galanakis, C.M. ed., 2019. Saving food: Production, supply chain, food waste and food consumption. Academic Press.

[12] Hanson, C., Lipinski, B., Robertson, K., Dias, D., Gavilan, I., Gréverath, P., Ritter, S., Fonseca, J., VanOtterdijk, R., Timmermans, T. and Lomax, J., (2016). Food loss and waste accounting and reporting standard.

[13] Raabe R.D. (2015). The Rapid Composting Method Unicersity Course, Vegetable Research and Information Center, University of California.

[14] Sakarika M., Spiller M., Baetens, Donies G., Vanderstuyf J., Vinck K., Vrancken K., Van Barel G., Du Bois E., Vlaeminck S.E., (2019). Proof of concept of high–rate decentralized pre–composting of kitchen waste: Optimizing design and operation of a novel drum reactor, Waste Management 91 (2019) p. 20–32.

[15] Salla P.M., Antounb H., Chalifoura F.–P., Beauchamp C.J., (2016). On farm composting of fruit and vegetable waste from grocery stores: a case under cold climatic conditions of eastern Canada, Proceedings SUM 2016, Third Symposium on Urban Mining and Circular Economy.

[16] Sakarika M., Spiller M., Baetens, Donies G., Vanderstuyf J., Vinck K., Vrancken K., Van Barel G., Du Bois E., Vlaeminck S.E., (2019). Proof of concept of high–

rate decentralized pre–composting of kitchen waste: Optimizing design and operation of a novel drum reactor, Waste Management 91 (2019) p. 20–32.

[17]   Siebert, S., (2015). Bio – waste recycling in Europe against the backdrop of the circular economy package. Bochum, Germany

[18]   Siebert, S., (2015). Bio – waste recycling in Europe against the backdrop of the circular economy package. Bochum, Germany.

[19]   Sundberg, C., Franke–Whittle, I.H., Kauppi, S., Yu, D., Romantschuk, M., Insam, H., Jönsson, H., 2011. Characterisation of source–separated household waste intended for composting. Bioresour. Technol. 102, 2859–2867. https://doi.org/ 10.1016/j.biortech.2010.10.075.

[20]   Sundberg, C., Yu, D., Franke–Whittle, I., Kauppi, S., Smars, S., Insam, H., Romantschuk, M., and Jönsson, H. (2013). Effects of pH and microbial composition on odour in food waste composting. Waste Manage. 33:204–211.

[21]   Stenmarck, Â., Jensen, C., Quested, T., Moates, G., Buksti, M., Cseh, B., Juul, S., Parry, A., Politano, A., Redlingshofer, B. and Scherhaufer, S., (2016). Estimates of European food waste levels. IVL Swedish Environmental Research Institute, FUSION 2016

MANUSCRIPT PREPARATION – GENERAL GUIDELINES

Manuscripts submitted for consideration to **ACTA TECHNICA CORVINIENSIS – Bulletin of Engineering** must conform to the following requirements that will facilitate preparation of the article for publication. These instructions are written in a form that satisfies all of the formatting requirements for the author manuscript. Please use them as a template in preparing your manuscript. Authors must take special care to follow these instructions concerning margins.

INVITATION

We are looking forward to a fruitful collaboration and we welcome you to publish in our **ACTA TECHNICA CORVINIENSIS – Bulletin of Engineering.** You are invited to contribute review or research papers as well as opinion in the fields of science and technology including engineering. We accept contributions (full papers) in the fields of applied sciences and technology including all branches of engineering and management.

ACTA TECHNICA CORVINIENSIS – Bulletin of Engineering publishes invited review papers covering the full spectrum of engineering and management. The reviews, both experimental and theoretical, provide general background information as well as a critical assessment on topics in a state of flux. We are primarily interested in those contributions which bring new insights, and papers will be selected on the basis of the importance of the new knowledge they provide.

Submission of a paper implies that the work described has not been published previously (except in the form of an abstract or as part of a published lecture or academic thesis) that it is not under consideration for publication elsewhere. It is not accepted to submit materials which in any way violate copyrights of third persons or law rights. An author is fully responsible ethically and legally for breaking given conditions or misleading the Editor or the Publisher.

ACTA TECHNICA CORVINIENSIS – Bulletin of Engineering is an international and interdisciplinary journal which reports on scientific and technical contributions. Every year, in four online issues (**fascicules 1–4**), **ACTA TECHNICA CORVINIENSIS – Bulletin of Engineering [e-ISSN: 2067-3809]** publishes a series of reviews covering the most exciting and developing areas of engineering. Each issue contains papers reviewed by international researchers who are experts in their fields. The result is a journal that gives the scientists and engineers the opportunity to keep informed of all the current developments in their own, and related, areas of research, ensuring the new ideas across an increasingly the interdisciplinary field. Topical reviews in materials science and engineering, each including:

— surveys of work accomplished to date
— current trends in research and applications
— future prospects.

As an open-access journal **ACTA TECHNICA CORVINIENSIS – Bulletin of Engineering** will serve the whole engineering research community, offering a stimulating combination of the following:

— Research Papers – concise, high impact original research articles,
— Scientific Papers – concise, high impact original theoretical articles,
— Perspectives – commissioned commentaries highlighting the impact and wider implications of research appearing in the journal.

ACTA TECHNICA CORVINIENSIS – Bulletin of Engineering encourages the submission of comments on papers published particularly in our journal. The journal publishes articles focused on topics of current interest within the scope of the journal and coordinated by invited guest editors. Interested authors are invited to contact one of the Editors for further details.

BASIC MANUSCRIPT REQUIREMENTS

The basic instructions and manuscript requirements are simple:

— Manuscript shall be formatted for an A4 size page.
— The all margins of page (top, bottom, left, and right) shall be 20 mm.
— The text shall have both the left and right margins justified.
— Single-spaced text, tables, and references, written with 11 or 12-point Georgia or Times New Roman typeface.
— No Line numbering on any pages and no page numbers.
— Manuscript length must not exceed 15 pages (including text and references).
— Number of the figures and tables combined must not exceed 20.
— Manuscripts that exceed these guidelines will be subject to reductions in length.

The original of the technical paper will be sent through e-mail as attached document (*.doc, Windows 95 or higher). Manuscripts should be submitted to e-mail: redactie@fih.upt.ro, with mention **"for ACTA TECHNICA CORVINIENSIS".**

STRUCTURE

The manuscript should be organized in the following order: Title of the paper, Authors' names and affiliation, Abstract, Key Words, Introduction, Body of the paper (in sequential headings), Discussion & Results, Conclusion or Concluding Remarks, Acknowledgements (where applicable), References, and Appendices (where applicable).

THE TITLE

The title is centered on the page and is CAPITALIZED AND SET IN BOLDFACE (font size 14 pt). It should adequately describe the content of the paper. An abbreviated title of less than 60 characters (including spaces) should also be suggested. Maximum length of title: 20 words.

AUTHOR'S NAME AND AFFILIATION

The author's name(s) follows the title and is also centered on the page (font size 11 pt). A blank line is required between the title and the author's name(s). Last names should be spelled out in full and succeeded by author's initials. The author's affiliation (in font size 11 pt) is provided below. Phone and fax numbers do not appear.

ABSTRACT

State the paper's purpose, methods or procedures presentation, new results, and conclusions are presented. A nonmathematical abstract, not exceeding 200 words, is required for all papers. It should be an abbreviated, accurate presentation of the contents of the paper. It should contain sufficient information to enable readers to decide whether they should obtain and read the entire paper. Do not cite references in the abstract.

KEY WORDS

The author should provide a list of three to five key words that clearly describe the subject matter of the paper.

TEXT LAYOUT

The manuscript must be typed single spacing. Use extra line spacing between equations, illustrations, figures and tables. The body of the text should be prepared using Georgia or Times New Roman. The font size used for preparation of the manuscript must be 11 or 12 points. The first paragraph following a heading should not be indented. The following paragraphs must be indented 10 mm. Note that there is no line spacing between paragraphs unless a subheading is used. Symbols for physical quantities in the text should be written in italics. Conclude the text with a summary or conclusion section. Spell out all initials, acronyms, or abbreviations (not units of measure) at first use. Put the initials or abbreviation in parentheses after the spelled-out version. The manuscript must be writing in the third person ("the author concludes… ").

FIGURES AND TABLES

Figures (diagrams and photographs) should be numbered consecutively using Arabic numbers. They should be placed in the text soon after the point where they are referenced. Figures should be centered in a column and should have a figure caption placed underneath. Captions should be centered in the column, in the format "Figure 1" and are in upper and lower case letters.

When referring to a figure in the body of the text, the abbreviation "Figure" is used Illustrations must be submitted in digital format, with a good resolution. Table captions appear centered above the table in upper and lower case letters. When referring to a table in the text, "Table" with the proper number is used. Captions should be centered in the column, in the format "Table 1" and are in upper and lower case letters. Tables are numbered consecutively and independently of any figures. All figures and tables must be incorporated into the text.

EQUATIONS & MATHEMATICAL EXPRESSIONS

Place equations on separate lines, centered, and numbered in parentheses at the right margin. Equation numbers should appear in parentheses and be numbered consecutively. All equation numbers must appear on the right-hand side of the equation and should be referred to within the text.

CONCLUSIONS

A conclusion section must be included and should indicate clearly the advantages, limitations and possible applications of the paper. Discuss about future work.

Acknowledgements

An acknowledgement section may be presented after the conclusion, if desired. Individuals or units other than authors who were of direct help in the work could be acknowledged by a brief statement following the text. The acknowledgment should give essential credits, but its length should be kept to a minimum; word count should be <100 words.

References

References should be listed together at the end of the paper in alphabetical order by author's surname. List of references indent 10 mm from the second line of each references. Personal communications and unpublished data are not acceptable references.

— *Journal Papers:* Surname 1, Initials; Surname 2, Initials and Surname 3, Initials: Title, Journal Name, volume (number), pages, year.
— *Books:* Surname 1, Initials and Surname 2, Initials: Title, Edition (if existent), Place of publication, Publisher, year.

Proceedings Papers: Surname 1, Initials; Surname 2, Initials and Surname 3, Initials: Paper title, Proceedings title, pages, year.

We are very pleased to inform that our international scientific journal ACTA TECHNICA CORVINIENSIS – Bulletin of Engineering completed its 14 years of publication successfully [2008–2021, Tome I–XIV].

In a very short period the ACTA TECHNICA CORVINIENSIS – Bulletin of Engineering has acquired global presence and scholars from all over the world have taken it with great enthusiasm.

We are extremely grateful and heartily acknowledge the kind of support and encouragement from all contributors and all collaborators!

ACTA TECHNICA CORVINIENSIS – Bulletin of Engineering is accredited and ranked in the "B+" CATEGORY Journal by CNCSIS – The National University Research Council's Classification of Romanian Journals, position no. 940 (http://cncsis.gov.ro/).

ACTA TECHNICA CORVINIENSIS – Bulletin of Engineering is a part of the ROAD, the Directory of Open Access scholarly Resources (http://road.issn.org/).

ACTA TECHNICA CORVINIENSIS – Bulletin of Engineering is also indexed in the digital libraries of the following world's universities and research centers:

WorldCat – the world's largest library catalog
https://www.worldcat.org/
National Lybrary of Australia
http://trove.nla.gov.au/
University Library of Regensburg – GIGA German Institute of Global and Area Studies
http://opac.giga-hamburg.de/ezb/
Simon Fraser University – Electronic Journals Library
http://cufts2.lib.sfu.ca/
University of Wisconsin – Madison Libraries
http://library.wisc.edu/
University of Toronto Libraries
http://search.library.utoronto.ca/
The University of Queensland
https://www.library.uq.edu.au/
The New York Public Library
http://nypl.bibliocommons.com/
State Library of New South Wales
http://library.sl.nsw.gov.au/
University of Alberta Libraries – University of Alberta
http://www.library.ualberta.ca/
The University of Hong Kong Libraries
http://sunzi.lib.hku.hk/
The University Library – The University of California
http://harvest.lib.ucdavis.edu/

ACTA TECHNICA CORVINIENSIS – Bulletin of Engineering is indexed, abstracted and covered in the world–known bibliographical databases and directories including:

INDEX COPERNICUS – JOURNAL MASTER LIST
http://journals.indexcopernicus.com/
GENAMICSJOURNALSEEK Database
http://journalseek.net/
DOAJ – Directory of Open Access Journals
http://www.doaj.org/
EVISA Database
http://www.speciation.net/
CHEMICAL ABSTRACTS SERVICE (CAS)
http://www.cas.org/
EBSCO Publishing
http://www.ebscohost.com/
GOOGLE SCHOLAR
http://scholar.google.com
SCIRUS – Elsevier
http://www.scirus.com/
ULRICHSweb – Global serials directory
http://ulrichsweb.serialssolutions.com
getCITED
http://www.getcited.org
BASE – Bielefeld Academic Search Engine
http://www.base-search.net
Electronic Journals Library
http://rzblx1.uni-regensburg.de
Open J–Gate
http://www.openj-gate.com
ProQUEST Research Library
http://www.proquest.com
Directory of Research Journals Indexing
http://www.drji.org/
Directory Indexing of International Research Journals
http://www.citefactor.org/